Chromosomal Instability in Oral Potentially Disorders

Mohamad Zaini, Zuraiza Binti

Awarding institution:
King's College London

Chromosomal Instability in Oral Potentially Malignant Disorders

A thesis presented for the degree of

Doctor of Philosophy
King's College London
August 2015

By

Zuraiza Mohamad Zaini

Dentistry - Oral Pathology - Molecular Biology

Abstract

Oral cancer is one of only four major cancers whose predicted mortality rate will significantly increase in the next 15 years. Many patients have potential precursor lesions but the methods for predicting the small number at high risk of cancer do not have sufficient predictive value or are labour intensive. The aim of this project is to investigate tests capable of predicting malignant transformation through detection of chromosomal instability.

Image-based DNA image-based cytometry ('ploidy analysis') has been used routinely in the diagnostic Oral Pathology Unit but has not been tested on lesions clinically suspected as having high risk and its predictive values are not known for targeted use. Follow up data was compiled for 252 patients with risk lesions from local databases and cancer registries and a follow up study of malignant transformation was performed. Over than half of the dysplastic lesions, which transformed into cancer were aneuploid.

Real time qPCR and QuantiGene Plex DNA assays were applied to samples of oral none dysplastic and dysplastic lesions to detect alterations in gene copy number using markers identified in previous studies in the laboratory. Discrepancies between methods were found, with inconsistent results caused by normalised to different housekeeping genes; RnaseP for qPCR, TPM1 for QGPlex and TERT in both techniques. Both these techniques were found to be insufficiently reliable for clinical use.

Fluorescence *in situ* hybridization (FISH) was applied against Cen3/TP63, Cen7/EGFR, Cen8/PTK2, Cen11/CCND1 and 20ptel/MMP9. This proved almost as effective as image based ploidy analysis but was too labour intensive and time consuming for routine use. FISH revealed previously unrecognized zones of variation within dysplastic lesions and variation in clonal structure within them.

Our data show that DNA image-based ploidy analysis combined with dysplasia assessment is the most predictive technique for use in a diagnostic setting and should be considered the reference standard.

Acknowledgements

Firstly, my deepest gratitude to Professor Edward Odell without whom this work would not have been possible. He has given me continuous support, motivation and encouragement. His immense knowledge and guidance helped me throughout the time of research and writing of this thesis. My sincere thanks go to Professor Mahvash Tavassoli for her insightful comments, suggestions and provisions. Also, Professor Henrik Muller for his help in data analysis.

I would like to thank Dr Angela Stokes and Dr Helen McParland who assisted me in the early phase of this project. I could not have learned various technical skills required without the assistance of Dr David Moyes, Mr. Robert Dunn, Mr. Michael Neat and Ms Claire Lock.

Special thanks to my labmates, Bushra, Jessica, Nina, Yae-Eun and Hersi for all the fun we had in the last four years. I also thank everybody in Head & Neck Pathology Lab for being such wonderful people to be around with.

I would like to extend my appreciation to the Ministry of Higher Education, Malaysia and University of Malaya for granting me the scholarship for my study. And, I am grateful to colleagues at Faculty of Dentistry, in particular professors in the Oral Pathology division, UM.

Finally, I thank my family and in-laws for their support and understanding. My love and gratitude goes to my beloved husband and children, to whom this is dedicated, who has provided me with tremendous support and endless love, kept me going during this study.

Table of Contents

List of Figures

List of Tables

List of abbreviations

aCGH	Array Comparative Genomic Hybridization
BAC	Bacterial Artificial Chromosomes
BL	Blocker Probe
bp	Base pairs
CCND1	Cyclin D1
CDH1	Cadherin 1
CDKN2A	Cyclin-Dependent Kinase Inhibitor 2A
CE	Capture Extender
CIN	Chromosomal Instability
CN	Copy Number
CNA	Copy Number Alterations
CNV	Copy Number Variations
COX-2	Cyclooxygenase 2
CP	Capture Probe
CV	Coefficient of Variation
CYP24A1	Cytochrome P450, Family 24, Subfamily A, Polypeptide 1
DAPK1	Death-Associated Protein Kinase 1
DI	DNA Index
DNA	Deoxyribonucleic Acid
EGFR	Epidermal Growth Factor Receptor
FCM	Flow Cytometry
FFPE	Formalin Fixed Paraffin Embedded
FHIT	Fragile Histidine Triad
FISH	Fluorescence *in situ* Hybridization
FITC	Fluorescein Isothiocyanate
GCSFR	Granulocyte Colony-Stimulating Factor Receptor
H&E	Haematoxylin & Eosin
HBV	Hepatitis B Virus

HCl	Hydrochloric Acid
HCV	Hepatitis C Virus
HER2	Human Epidermal Growth Factor Receptor 2
HIV	Human Immunodeficiency Virus
HNSCC	Head Neck Squamous Cell Carcinoma
HPV	Human Papillomavirus
HSCIC	Health and Social Care Information Centre
ICD	International Classification of Diseases
ICM	Image Cytometry
LE	Label Extender
LOD	Limit of Detection
LOH	Loss of Heterozygosity
LRP12	Low Density Lipoprotein Receptor-Related Protein 12
LY6K	Lymphocyte Antigen 6 Complex, Locus K
MET	MET Proto-Oncogene, Receptor Tyrosine Kinase
MFI	Median Fluorescence Intensity
MGMT	Methylguanine-DNA Methyltransferase
MIN	Microsatellite Instability
MMP	Matrix Metalloproteinase
MSI	Microsatellite Instability
MYC	Myc Avian Myelocytomatosis Viral Oncogene Homolog
NHS	National Health Service
NPV	Negative Predictive Value
NTC	No Template Controls
OPMD	Oral Potentially Malignant Disorders
OR	Odds Ratios
OSCC	Oral Squamous Cell Carcinoma
PBS	Phosphate Buffered Saline
PIK3CA	Phosphatidylinositol-4,5-Bisphosphate 3-Kinase, Catalytic Subunit Alpha

PPV	Positive Predictive Value
PTEN	Phosphatase And Tensin Homolog
PTK2	Protein Tyrosine Kinase 2
PTPRD	Protein Tyrosine Phosphatase, Receptor Type, D
PVL	Proliferative Verrucous Leukoplakia
QGPlex	Quanti Gene Plex
qPCR	Quantitative Polymerase Chain Reactions
RNA	Ribonucleic Acid
ROC	Receiver Operating Characteristic
SAPE	Streptavidin-conjugated R-Phycoerythrin
SD	Standard Deviation
SKY	Spectral Karyotyping
SMAD4	SMAD Family Member 4
SNP	Single Nucleotide Polymorphism
SSC	Saline Sodium Citrate
STARD	Standards for the Reporting of Diagnostic Accuracy
Tel	Telomeric
TERT	Telomerase Reverse Transcriptase
TG3	Transglutaminase 3
TNM	Tumour Node Metastasis
TP53	Tumour Protein p53
TPM1	Tropomyosin 1
TSG	Tumour Suppressor Gene
UADT	Upper Aerodigestive Tract
UK	United Kingdom
VEGF	Vascular Endothelial Growth Factor
WHO	World Health Organisation

CHAPTER 1 : General Introduction

1.1 Oral Squamous Cell Carcinoma

1.1.1 Definition

Oral cancer is a subgroup of head and neck malignant neoplasms that includes carcinomas arising from the mucosal lining of the lips, the buccal mucosa, the retromolar trigone, the alveolar ridges, the anterior two- thirds of the tongue, the floor of the mouth, and the hard palate. Although oropharynx refers to the posterior third of the tongue, the soft palate and uvula, the tonsils, and the upper part of the posterior pharyngeal wall, malignant neoplasms involving oral cavity and oropharynx have been categorized together in the codes C00-C14 in the World Health Organization (WHO) International Classification of Diseases, 10th Revision (ICD-10). Numerous types of malignant neoplasms affect the oral cavity and oropharynx, but squamous cell carcinoma that arises from the mucosal epithelial lining, accounts for more than 90% of cases (Warnakulasuriya, 2009).

1.1.2 Epidemiology

The oral cavity and oropharynx together are ranked sixth most common cancer worldwide (Warnakulasuriya, 2010). The number of new cases is projected to reach 300,000 per year for these sites (Ferlay *et al.*, 2015). It is alarming to note that the estimated number of deaths from cancer of the oral cavity was 145,000 in 2012 and this is expected to increase in the next 15 years despite easy accessibility to this site of the body for diagnosis (Ferlay *et al.*, 2010; Jemal *et al.*, 2011; Ferlay *et al.*, 2015).

Disparities between nations are evident through epidemiology, age and gender distributions, aetiology and risk factors, pathogenesis, anatomical site of lesion and socioeconomic status, reflecting differences in populations across the world.

In the United Kingdom (UK), approximately 6800 cases of oral cancer were diagnosed in 2011 accounting for 2% of all cancer cases and making it the 16th most common cancer with a male to female ratio of 2:1, the 12th commonest cancer in man and 16th in women (Cancer Research UK). Oral squamous cell carcinoma (OSCC) is diagnosed primarily between the age of 50 to 74 with the age-specific incidence rate for men peaking in the 60-64-year-old age group while for women the highest rate is in those aged 85 years (Figure 1.1). The mortality rates have risen by 10% over the last 10 years and 2.6 per 100,000 was recorded in the UK in 2012 (Table 1.1).

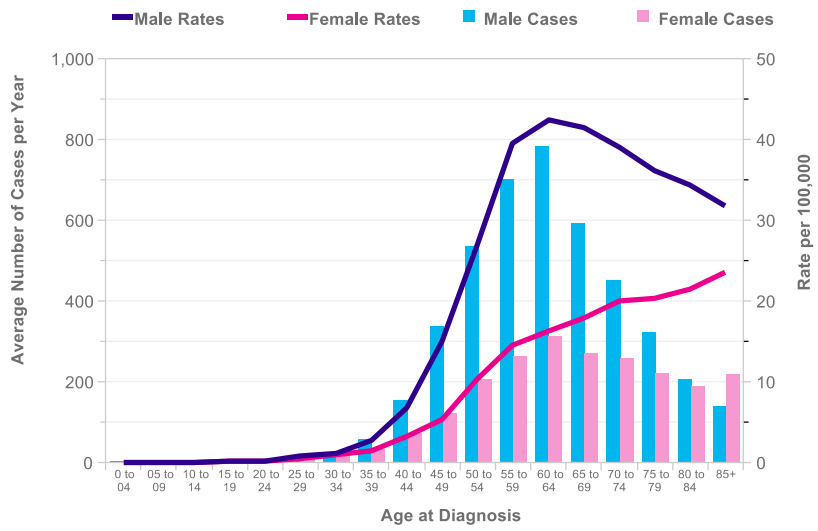

Figure 1.1 Incidence rates by gender in UK
Average number of new cases per year and age-specific incidence rates by gender in the UK 2009-2011. (source: Cancer Research UK, http://www.cancerresearchuk.org)

Table 1.1 Incidence and mortality rates in the UK
(source: Cancer Research UK)

Year	Oral cancer statistics	Males	Females	Persons
2011	Number of new cases per year	4510	2257	6767
	Incidence rate per 100,000 population	12.8	5.4	9.0
2012	Number of deaths per year	1426	693	2119
	Mortality rate per 100,000 population	3.8	1.4	2.6

There are distinctive geographical differences in incidence across the world reaching 20-fold the mean incidence in high incidence countries such as India, Sri Lanka, Pakistan and Bangladesh in the South Asia region (Warnakulasuriya, 2010). India has annual registration of more than 100,000 cases and the majority occur in individuals who chew tobacco and areca nut in betel quid (Warnakulasuriya, 2010). The age-standardised rate of mortality from mouth cancer in south Central Asia was calculated at 6.3 in men and 3.0 for woman per 100,000 individuals (Ferlay *et al.*, 2015).

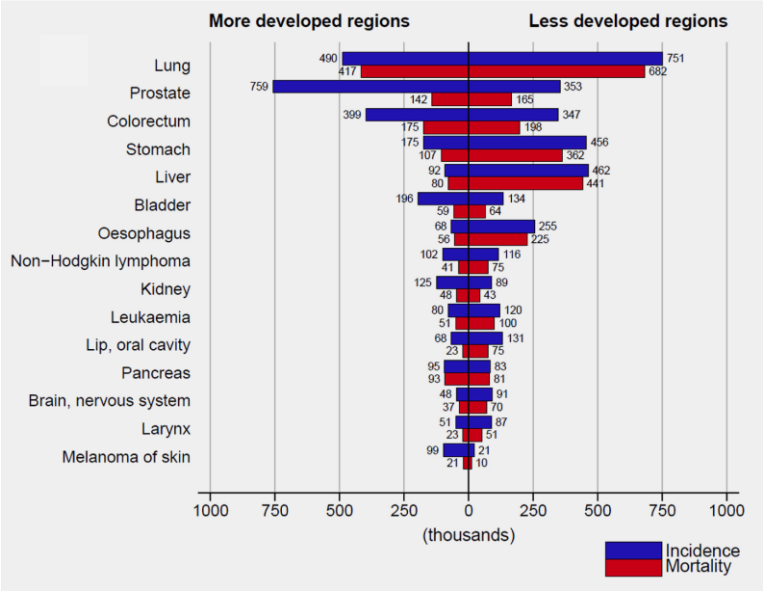

Figure 1.2 Estimated number of new cancer cases and deaths in more and less developed world in 2012
(source: Ferlay J *et al.* 2015)

1.1.3 Clinical and histopathological features

Long-standing lumps, ulcers, speckled white, red or mixed red-white oral mucosa that persists for more than 3 weeks should prompt suspicion of squamous carcinoma. There may or may not be symptoms. Risk of these presentations being carcinoma increases when lesions are hard or firm to palpation. Other signs include post-extraction non-healing tooth socket, inexplicable tooth loss and numbness. Particular sites at risk are floor of mouth, ventral tongue, lateral tongue, soft palate and the retromolar areas but the buccal mucosa and gingiva are more frequently affected in those who chew betel quid.

The key histological feature is epithelial cells with squamous differentiation that invade the underlying connective tissue. Carcinoma grading into well-, moderately- and poorly-differentiated cancers is based on the degree of resemblance to normal squamous epithelium but is a poor predictor of outcome. Other histologic parameters that taken together have more prognostic significance include nuclear pleomorphism, mitotic figures, pattern of invasive front and vascular and perineural invasion. These features are not specific to carcinoma, other than the features of invasion, and may be seen in potentially malignant lesions.

1.1.4 Risk factors

Tobacco smoking and alcohol abuse, consumed either alone or together, and betel quid chewing with or without tobacco are the major, well-recognised risk factors for oral cancer. Recently, attention has been drawn to Human Papillomavirus (HPV) infection as the most important aetiological factor for oropharyngeal squamous cell carcinoma (Gillison *et al.*, 2000) and also possibly for a small proportion of oral carcinomas. This group of HPV-associated carcinomas exhibits different patterns of

clinical presentation, age distribution, risk factors and prognosis in comparison with conventional OSCC. Affected individuals are slightly younger, and often non-smokers and it is of note that this group of patients' respond well to treatment and have a much better prognosis (Gillison, 2007; Syrjanen *et al.*, 2011).

Other risk factors include genetic predisposition, radiation exposure, immunocompromise, poor nutrition and low socioeconomic status. A family history of head and neck cancer, suggesting a hereditary genetic basis, has been shown to increase individuals' susceptibility to developing cancer. Both developed and developing regions showed higher cancer risk in individuals of low educational level and income.

1.1.5 Treatment and Prognosis

Surgery with or without post-operative chemotherapy and radiation remain the standard treatment approaches, although several factors including the site, size, depth of infiltration and proximity to bone would determine final treatment choice. In general, late diagnosis at advanced stage in the majority of patients requires a combination of surgery, radiotherapy or chemotherapy. Early stage tumours are often treated with either surgery or radiation alone, depending on site, or combined surgery and/or chemotherapy followed by close monitoring post-operatively for recurrences and second primary tumours. Concurrent chemoradiation or induction chemotherapy prior to local treatment is employed for locally advanced disease whilst in recurrent and/or metastasis, radiotherapy or chemotherapy can be administered as palliative treatment. The emergence of targeted molecular treatment towards specific molecules involved in cell growth control, angiogenesis and apoptosis, is beneficial when used in combination with chemotherapy agents and/or radiation but at present is reserved primarily for adjuvant or palliative therapy (Lorch *et al.*, 2009; da Silva *et al.*, 2011).

Advances in surgical and chemoradiotherapeutic techniques in addition to recent organ-preservation protocols have been reported to increase the quality of life after treatment (Vergeer *et al.*, 2009). However, there is a disproportion between improvement in quality of life and 5-year survival rate, which remains relatively stable at 40-50% of cases, predominantly due to development of loco-regional recurrence, distant metastases and second primary tumours (Leemans *et al.*, 2011). Well-defined prognostic indicators are tumour size, nodal and distant metastases, collectively forming the TNM cancer staging system. Advanced presentation at time of detection and diagnosis with lymph node metastases carries a poor prognosis. In contrast, approximately one third of patients seek treatment at early stage of disease allowing effective management and have a favourable prognosis (Leemans *et al.*, 2011). Because size and stage at diagnosis are so critical to outcome, detection at an early stage is the most effective method to control oral cancer and the best outcome would result if oral cancer could be detected at a preinvasive stage. Like many other cancer types, oral cancer may be preceded by a long-standing preinvasive stage termed oral potentially malignant disorders.

1.2 Oral Potentially Malignant Disorders

1.2.1 Terminology

Oral potentially malignant disorders (OPMD) form a family of clinical or histological morphological alterations of epithelium that indicate a risk of transformation into squamous cell carcinoma (Speight, 2007). Some oral cancers, the exact number is unclear, are preceded by a potentially malignant disorder.

Several nomenclatures including precancerous, premalignant and precursor lesions have been used interchangeably to signify a tissue that has undergone histologically detectable changes and may be capable of progressing into cancer. The term 'oral potentially malignant disorders' was recommended following a workshop coordinated by the WHO Collaborating Centre for Oral Cancer and Precancer held in London in May 2005 to replace various designations formerly used (Warnakulasuriya *et al.*, 2007). This term was considered better than those used previously because it indicates that not all cases will transform, allowing for the majority to either remain unchanged or even regress. It is also preferred because the distinction between potentially malignant lesions and conditions is no longer thought to be useful, accepting that all such disorders reflect field change (van der Waal, 2009).

Table 1.2 Oral disorders with increased potential for malignant transformation

Oral Potentially Malignant Disorders
Leukoplakia
Erythroplakia
Palatal lesions in reverse smokers
Proliferative verrucous leukoplakia
Submucous fibrosis
Actinic cheilitis
Lichen planus
Discoid lupus erythematosus

Source: van der Waal 2009

1.2.2 Epidemiology

Among the OPMDs, leukoplakia and erythroplakia are the commonest and have been most frequently associated with cancer progression. Although the others may also present as red or white patches, the majority of studies and reports on OPMD have been based on these two conditions, after exclusion of other causes. House-to-house surveys conducted in India, reported annual incidence rates of leukoplakia ranging from 5.2 to 30.2 per 1000 person per year in tobacco users, 0.6/1000 to 5.8/100 in non-users (Mehta *et al.*, 1972; Bhargava *et al.*, 1975), 1.1–2.4/1000 in males and 0.2–1.3/1000 in females (Gupta *et al.*, 1980).

The estimated prevalence of OPMD varies from 1% to 5% dependent upon region studied with a global prevalence of 2.6% determined in a 2003 systematic review by Petti (Petti, 2003). India showed a high range from 9% to 14.6% (Smith *et al.*, 1975) while in the developed countries the prevalence was lower; 4.2% in England (Lim *et al.*, 2003), 2.9% in the United States (Bouquot and Gorlin, 1986), 1.4% in Amsterdam (Hogewind and van der Waal, 1988) and 1.3% in Hungary (Banoczy and Rigo, 1991). In most of the world these conditions are more common in males from middle age to the seventh decade of life, and in tobacco smokers. Conversely, the habit of areca nut and tobacco chewing popular in India and East Asia shows female dominance and development of changes between the ages of 30 to 50 (Barnes *et al.*, 2005).

1.2.3 Aetiology

Even though the causative role of tobacco in OSCC is well documented, its association with oral leukoplakia has been relatively weak in epidemiological studies. This may be attributable to study design, as the majority of studies have been cross-sectional, often lacked a clear definition of leukoplakia and other risk factors were

overlooked (Arduino *et al.*, 2013). However, a positive association has been demonstrated by the habit of smokeless tobacco (Winn, 2001). Higher prevalence (Mehta *et al.*, 1972; Roed-Petersen, 1982; Banoczy and Rigo, 1991), anatomical distribution of oral leukoplakia (Schepman *et al.*, 2001) and dose-response relationship have been demonstrated among smokeless tobacco users (Gupta, 1984b; Banoczy and Rigo, 1991; Tomar *et al.*, 1997). Regression and/or disappearance of oral leukoplakia in individuals who ceased smoking also support the causative role of tobacco (Roed-Petersen, 1982; Silverman *et al.*, 1984; Gupta *et al.*, 1995; Roosaar *et al.*, 2007).

Studies on the role of alcohol in development of OPMDs have produced conflicting results; some finding a strong causal relationship while others refute the link. Controlled for tobacco use, a prospective study of 41,458 participants has suggested that alcohol was an independent risk factor even in non-tobacco users (Maserejian *et al.*, 2006). However, the link was weak compared with tobacco and would only have a noticeable effects when associated with other risk factors (Gupta, 1984a). While Jaber (Jaber, 2010) reported that the notion of alcohol as an independent risk factor was at best unproven, others were more definitive in finding alcohol alone to have no role in development of OPMD (Lee *et al.*, 2003; Dietrich *et al.*, 2004; Cebeci *et al.*, 2009).

It was noted above in section 1.1.4 that HPV is an aetiological factor for most oropharyngeal and some oral carcinomas. Whether HPV-associated carcinomas go through a long precancerous phase is not yet known, but high risk HPV subtypes, usually 16 and 18, can occasionally be found in oral mucosa. These zones of epithelium that can be recognised histologically are termed koilocytic dysplasia and the risk of transformation is unclear (Fornatora *et al.*, 1996; Woo *et al.*, 2013). Because this potential

aetiological feature is of uncertain significance, lesions of koilocytic dysplasia have been excluded from the lesions studied in this work.

1.2.4 Clinical appearances of OPMD

OPMD appear clinically as areas of white or red mucosa, sometimes in combination forming a 'speckled' lesion. Oral leukoplakia is defined as 'white plaque of questionable risk having excluded (other) known diseases or disorders that carry no increased risk for cancer'. Erythroplakia is the designation for the equivalent red patch and combined red and white lesions are termed erythroleukoplakia (Warnakulasuriya *et al.*, 2007). Other disorders that appear white and/or red should be excluded before the diagnosis of leukoplakia, erythroplakia or erythroplakia can be made (Table 1.3).

Table 1.3 Differential diagnoses of white and red oral lesions

White lesions	Red lesions
Frictional keratosis	Desquamative gingivitis
Morsicatio buccarum	Pemphigoid
Leukoedema	Hypersensitivity reaction
Linea alba	Candidosis, erythematous
Candidosis, pseudomembranous	Lupus erythematosus
Chemical burn	
Hairy leukoplakia	
Lichenoid reaction	
Lupus erythematosus	
White sponge naevus	

Clinical presentation gives some information about the degree of risk of transformation (Silverman *et al.*, 1976; Gupta *et al.*, 1980). Non-homogenous leukoplakia and erythroplakia, meaning those associated with both red and white, or lesions with nodularity or a verrucous surface are reported to progress to carcinoma more frequently (Pindborg *et al.*, 1963; Silverman *et al.*, 1984; Holmstrup *et al.*, 2006). However, these

features are not specific and the resemblance of clinical presentations of OPMD to other reactive or inflammatory mucosal lesions restricts the predictive value of the clinical descriptions and often prevents confident diagnosis on clinical examination alone.

Adjunct tools for detection of genuine risk lesions have been developed with the intention of aiding the clinician to distinguish abnormal or dysplastic mucosa from other innocuous lesions. Such devices often do not necessarily have a defined plausible scientific basis for their claimed effect. Examples include light-based (optical) technology that measure the tissue autofluorescence, marketed as VELscope (Lane *et al.*, 2006; Awan *et al.*, 2011) or chemiluminescence, available commercially as ViziLite, ViziLite Plus, MicroLux/DL (Ram and Siar, 2005; Kerr *et al.*, 2006) and vital staining with toluidine blue, TBlue and OraBlu (Epstein and Guneri, 2009; Awan *et al.*, 2012). Absorbance and reflectance properties of neoplastic and pre-neoplastic tissues following abnormal metabolic and structural changes that may differ from normal cells form the claimed basis of light-based technology. Toluidine blue is a metachromatic dye preferentially binds to nuclear DNA and is claimed to reflect cell division. However, none of these adjunctive tests has been assessed in a well-controlled clinical trial and the low specificity of these tests currently precludes their use in routine clinical applications (Lingen *et al.*, 2008; McIntosh *et al.*, 2009; Mehrotra *et al.*, 2010; Farah *et al.*, 2012; Rashid and Warnakulasuriya, 2015).

1.2.5 Histopathology

Microscopic examination to identify the presence of epithelial dysplasia in a biopsy sample is currently the reference standard in the assessment of OPMD to assess the risk of the patient developing squamous carcinoma.

1.2.5.1 Dysplasia

Dysplasia, meaning abnormal growth, is the term given to the histopathological changes associated with an increased risk of malignant transformation. Oral mucosal dysplastic changes are characterised by disturbance to the epithelial stratification and maturation (architectural features) accompanied by cellular atypia (cytological features). Diagnosis of oral epithelial dysplasia is made base on the presence, degree and significance of individual criteria of these two broad categories detailed in Table 1.4.

Atypical cytology or architectural changes can also be seen in reactive, regenerative or reparative epithelium in response to trauma, inflammation, irradiation or ulceration (Macdonald and Rennie, 1975) and can be difficult to distinguish from true dysplasia. However, cellular changes in those conditions are less prominent and may be more easily recognised in conjunction with the clinical history.

Table 1.4: Features used for diagnosis of dysplasia
(source: WHO Classification Head and Neck Tumours 2005)

Architecture	Cytology
Irregular epithelial stratification	Abnormal variation in nuclear size (anisonucleosis)
Loss of polarity of basal cells	Abnormal variation in nuclear shape (nuclear pleomorphism)
Drop-shaped rete ridges	Abnormal variation in cell size (anisocytosis)
Increased number of mitotic figures	Abnormal variation in cell shape (cellular pleomorphism)
Abnormal superficial mitoses	Increased nuclear-cytoplasmic ratio
Premature keratinization in single cells (dyskeratosis)	Increased nuclear size
Keratin pearls within rete ridges	Atypical mitotic figures
	Increased number and size of nucleoli
	Hyperchromasia

1.2.5.2 Dysplasia grading

A number of grading systems have been described that divide dysplasia into mild, moderate and severe changes, of which the WHO classification system is the most commonly applied. (Barnes *et al.*, 2005). According to this system, oral dysplasia is graded based on the degree of architectural and cytological atypia. The severity of dysplastic changes is dependent on how many of those features could be observed in a given lesion (Table 1.5). Mild cases are those in which cytological atypia is minimal and only the lower third of the epithelium is involved; moderate cases are those with between one and two thirds of the epithelial thickness affected; and severe cases are those in which marked atypia is evident with or without architectural disturbances to more than two-thirds of the epithelial thickness. Despite consensus on the features, the use of a third-based grading system is new in this classification and the system is based on little experimental data, despite its widespread use in clinical practice. Though frequently cited, the WHO classification is not a defined scoring system. The list of features has no formal evidence base and there is no guidance on how the various features should be recognised and combined. The pathologist remains able to compensate up or down the grading scale without defined criteria.

Recently, a two-tier categorization has been suggested to reduce interobserver and intraobserver disagreement and this is claimed to improve prediction of malignant transformation (Kujan *et al.*, 2006b). However, the prognostic ability of this system was found to be only on a par with the WHO classification and could only be minimally improved by refining the diagnostic threshold (Nankivell *et al.*, 2013).

Table 1.5: Criteria used for dysplasia grading
(source: Dionne *et al.,* 2015)

Architecture	Cellular atypia	Dysplasia grading
No changes	None	No dysplasia
Lower third	Mild	Mild
Middle third	Moderate	Moderate
Upper third	Prominent	Severe
Upper third	Moderate	Moderate
Middle third	Prominent	Severe
Full thickness	Prominent	Carcinoma in situ

1.2.6 Prognosis of OPMD

Despite intense focus on the clinical importance of OPMD, the great majority are never followed by development of OSCC. The lesion may persist but remain unchanged in size and appearance throughout a patient's lifetime; it may persist showing mucosal alterations that look suspicious with or without any changes in size; it may expand to involve more of the oral mucosa with or without changes in clinical appearance. On the other hand, a lesion may spontaneously reduce in size or entirely disappear (Banoczy and Sugar, 1972; Mehta *et al.*, 1972; Gupta *et al.*, 1980).

The largest epidemiological outcome study has a 10-year follow-up and was conducted by Gupta and co-workers in 3 districts of India. In that study 42% of leukoplakias had reduced in size or disappeared, 47% of lesions persisted while 4% progressed to cancer over 10 years (Gupta *et al.*, 1980). The findings must be taken in the context of the very high oral cancer rates in India and the high prevalence of risk habits. In Hungary, of the 520 patients that were treated by eliminating the causative factors and followed up for 25 years, lesions disappeared in 176 patients (33.8%),

improved in 131 patients (25.3%), remained unchanged in 135 (26%) and only 47 patients (9%) had increased in lesion size (Banoczy and Sugar, 1975). Progressive changes in clinical features were seen in 19 out of 66 leukoplakias (3.7%) and changes from more worrying to less worrying type occurred in 47 cases (9%) (Banoczy and Sugar, 1975). Lesions that appeared red, located on the tongue or floor of the mouth were more likely to progress (Banoczy and Sugar, 1975).

From the histopathological standpoint, dysplasia may behave correspondingly; it may persist at the same grade; it may advance to a higher grade, regress or even completely resolve regardless of clinical progression or resolution. However, interpretation of these changes must take into account sampling error. The excised specimen cannot undergo transformation and may or may not be representative of the surrounding tissue that remains in the patient.

1.2.7 Malignant transformation

The majority of reports regarding annual malignant transformation rates for OPMD have been derived from study of leukoplakia, and the rates reported vary widely from 0.13% to 36.4% over a period ranging from 1 to 30 years (Table 1.6). Higher rates were found in smaller series of hospital referral cases with higher degrees of dysplasia, in studies primarily performed in the developed nations.

Rates of malignant transformation in India were relatively low ranging from 0.13% to 2.2% per year, in studies carried out in large-scale community-based surveys and with long follow-up periods (Mehta *et al.*, 1972; Pindborg *et al.*, 1977; Gupta *et al.*, 1980). However, there remain slight variations between studies due to differences in tobacco habits, geographical distribution within India and follow-up times.

Table 1.6: Selected studies on malignant transformation of OPMDs

References	Country	Malignant transformation (%)		Follow-up (Years)
		Dysplastic Cases	Non-Dysplastic Cases	
Mincer *et al*, 1972	USA	11	-	Up to 8
Mehta *et al*, 1972	India	-	0.8	10
Silverman *et al*, 1976	India	0	0.13	2
Banoczy, 1977	Hungary	13.2	4.7	1-30
Pindborg *et al*, 1977	India	6.6	-	Up to 7
Gupta *et al*, 1980	India	-	0.3	1-10
Silverman *et al*, 1984	USA	36.4	15.7	Mean 8.1
Lumerman *et al,* 1995	USA	16	-	Up to 9
Cowan *et al*, 2001	UK	15	1	20
Saito *et al*, 2001	Japan	7.7	7.8	Mean 4
Holmstrup *et al*, 2006	Denmark	9	4	1-20
Amagasa *et al*, 2006	Japan	13.3	3.0	1-29
Liu *et al*, 2010	China	17.9	-	Mean 5.3
Warnakulasuriya *et al*, 2011	UK	11.8	1	Mean 9.04
Dost *et al*, 2014	Australia	4.7	-	More than 17

A recent meta-analysis (Mehanna *et al.*, 2009) has shown significant heterogeneity between the 14 follow-up studies included in the analysis indicating bias in the studies. When the 3 outliers, Silverman *et al.* 1976, Silverman *et al.* 1984 and Lee *et al.* 2000, were excluded (Figure 1.3), the pooled estimate for the mean malignant transformation rate for all studies decreased slightly from 12.1% (CI: 8.1%, 17.9%) to 11.3% (CI: 8.4%, 15.1%). Notably, referral to a single-centre and short follow up contribute to the biases in those studies. A lack of high quality studies and differences in the design, inclusion

criteria, population studied, length of follow up and risk factors further complicate systematic reviews and meta-analysis (Mehanna *et al.*, 2009).

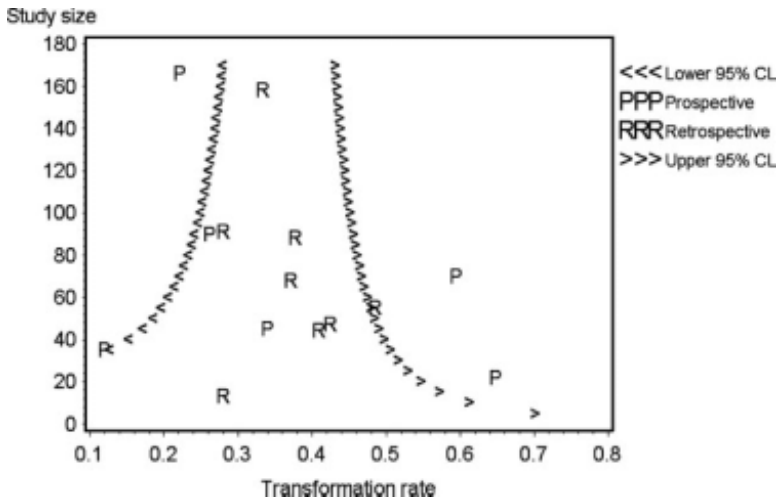

Figure 1.3 Meta-analysis of oral dysplasia studies
Funnel plot showing 3 studies (outliers) located outside the 95% confidence interval lines and an overall mean transformation rate around 0.3-0.4%. Source Mehanna *et al.*, 2009.

1.2.8 Treatment

Consensus on management of premalignant lesions has so far not been achieved and there are differences in approach between treatment centres. In general, surgical excision based on the severity of dysplasia is the common practice despite sparse clinical evidence on the success of this modality at preventing cancer developing. Surgical margin with inclusion of 3-5mm clinically adjacent normal mucosa is recommended for the surgical treatment of moderate to severely dysplastic lesions, but without good experimental support. Other surgical interventions include laser surgery (van der Waal, 2009, 2010). Leukoplakia with mild dysplasia or non-dysplastic but clinically suspicious lesions are usually managed by regular 6-month follow up.

Other treatment modalities are non-surgical; topical or systemic retinoids, mouthwash-delivered therapy containing an attenuated adenovirus, photodynamic therapy and change of lifestyle risk habits such as tobacco cessation and alcohol moderation (van der Waal, 2010). Molecular based chemopreventative trials are currently in progress, targeting COX-2 (Mulshine *et al.*, 2004; Papadimitrakopoulou *et al.*, 2008) and EGFR upregulation in dysplasia (EPOC, NCT00402779), but these treatments remain unproven.

1.3 Progression from OPMD to OSCC

1.3.1 Clinical manifestations

The currently accepted concept of progression is evolution through dysplasia to carcinoma through a sequence of dynamic stepwise alterations evident at phenotypic level with underlying cumulative molecular changes. In the field of head and neck cancer, Califano *et al.* proposed a genetic progression model linked to a series of histological stages with increasing severity from dysplasia to invasive state based on the earlier theory of multiphase pathogenesis for colorectal adenocarcinoma (Califano *et al.*, 1996). This has been proposed to be evident clinically as changes on mucosal colouration and appearance.

However, there is little evidence to support the idea that progression is always evident clinically. A high proportion of erythroplakia are already presentations of carcinoma on first biopsy as are a much smaller proportion of white lesions. The features described as features of progression may simply reflect development of carcinoma rather than worsening of dysplasia and, in addition, the features are not specific and can resemble other oral mucosal lesions. One significant defect in the progression concept as shown in Figure 1.4 is that it fails to take into account that the great majority of risk lesions, including dysplastic lesions, do not progress and may often resolve (Banoczy and Sugar, 1975; Gupta *et al.*, 1980). The only OPMD in which there is evidence of a long-term progression in clinical appearance culminating in carcinoma is proliferative verrucous leukoplakia (PVL) (Silverman and Gorsky, 1997) and in this condition, dysplasia is often not evident.

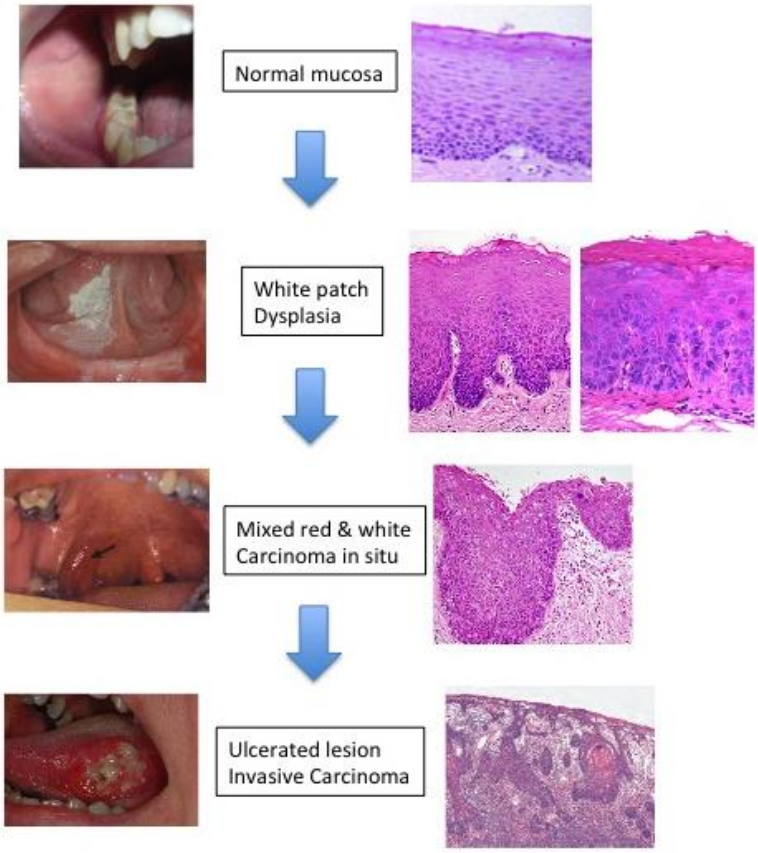

Figure 1.4 Model of progression of oral squamous cell carcinoma
Progression evident clinically as changes in mucosal colouration and appearances whilst microscopically with increasing severity of cellular morphology.

1.3.2 Genetic alterations

Dysplastic and non-dysplastic OPMDs are known to harbour a variety of genetic changes. Genetic alterations result in inactivation of tumour suppressor genes by mutations or deletions and activation of proto-oncogenes by mutations, chromosomal translocations or gene amplifications (Choi and Myers, 2008). Accumulation of these alterations is proposed to lead to dysregulation of cell division, cellular differentiation, proliferation and death, DNA repair and cellular immunity (da Silva *et al.*, 2011; Shen, 2011). Frequent observations of loss of heterozygosity at 3p, 9p and 17p in dysplasia appear to be early cytogenetic changes in oral carcinogenesis whereas chromosomal alterations at 11q, 4q and chromosome 8 are late events (Califano *et al.*, 1996). Loss of

9p21 chromosomal region is the most common genetic event, and this locus contains the gene CDKN2A that encodes p16 and p14 responsible for G_1 cell cycle regulation (van der Riet *et al.*, 1994; Mao *et al.*, 1996).

Studies on gene expression profiles have defined sets of genes that may contribute to conversion from normal to malignant cells, in particular activation of oncogenes that promote cell proliferation or inactivation of tumour suppressor gene (TSG) that typically transduce negative growth-regulatory signals. Based on level of evidence in association with aetiological factors, those genes are divided into established and candidate cancer genes for head and neck carcinoma (Leemans *et al.*, 2011). The established oncogenes are EGFR, PIK3CA, MET and CCND1 whereas CDKN2A, PTEN, TP53 and SMAD4 are established tumour suppressor genes (Leemans *et al.*, 2011). EGFR overexpression increases progressively from oral potentially malignant lesions to invasive OSCC and is overexpressed in 80-100% of HNSCC (Shin *et al.*, 1994; Kalyankrishna and Grandis, 2006; Reuter *et al.*, 2007). The p53 tumour suppressor gene that is located at chromosome 17p13 is found mutated in 25-69% of oral cancer and has been claimed to be a marker of late stage in the progression from a non-invasive to invasive phenotype. However, this is probably incorrect because in OPMD samples it appears to be an early and non-critical change (Boyle *et al.*, 1993).

Other events implicated in carcinogenesis are gene methylation, tumour-stroma interactions, angiogenesis and expression of microRNA. Gene methylation is an epigenetic alteration resulting in gene inactivation has been seen involving CDKN2A/p16, CDH1, MGMT and DAPK1 (López *et al.*, 2003; Ha and Califano, 2006). Matrix metalloproteinase family members, MMP2, MMP3 and MMP9 have been related to tumour invasion in OSCC (Campo-Trapero *et al.*, 2008). Angiogenic growth

factors play role in development of the new blood vessels and neoangiogenesis may also contribute. Many studies have shown that VEGF (vascular endothelial growth factor) expression is an unfavourable prognostic factor for patient survival in oral cancer (Kyzas *et al.*, 2005).

Despite considerable data on the molecular changes associated with dysplasia, there is no consensus on a stepwise progression model as has been validated in colorectal and some other cancer types. Different research groups have proposed different specific changes as predictive. Over the last few years it has become apparent that a simple stepwise progression model is probably not correct and its basis in cancer biology has been questioned. All such models are based on the somatic mutation theory of carcinogenesis, as summarised and promoted by Hanahan and Weinberg's seminal reviews (Hanahan and Weinberg, 2000). However, recently the validity of this theory has been questioned and a competing theory based on evolutionary theory and relationship to normal developmental or wound healing functions has been proposed (Sonnenschein and Soto, 2013). This theory is more compatible with the apparently random patterns of genetic changes in OPMDs generated by chromosomal instability and provides a better biological framework to explain field change, clonal selection and progression of a minority of lesions

Recently, a revised version of the stepwise progression model has been proposed in which HPV related tumour carcinogenesis and discrimination between high and low numerical genetic changes of HPV negative tumour were incorporated (Leemans *et al.*, 2011). Though this model is widely quoted, the evidence for the order and specificity of genetic changes at each stage of dysplasia remains sparse and it appears that HPV is very infrequently found in OPMDs (Jayaprakash *et al.*, 2011).

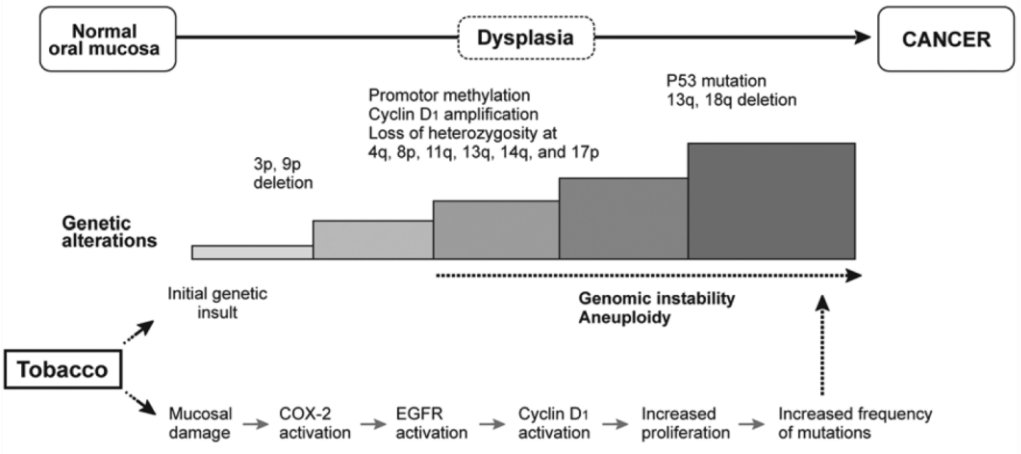

Figure 1.5 Genetic progression model of multistep oral carcinogenesis.
The accumulated genetic changes that occur in oral carcinogenesis include activation of EGFR, alterations of tumor suppressors p53 and p16, and cyclin D1 overexpression. Source: Choi and Myers 2008.

1.3.3 Predictors of progression

1.3.3.1 Clinical factors

Factors that have been related to the likelihood of developing carcinoma, regardless of OPMD, include patients' age, gender and risk habit(s), along with lesion-related predictors including grade of dysplasia, clinical appearance, duration, anatomical site and size of lesions (van der Waal, 2009; Warnakulasuriya *et al.*, 2011). It is generally accepted that these risk factors apply to those with OPMD as well as those who develop carcinoma without OPMDs.

Factors specifically associated with increase in risk in OPMD are female gender, older age, duration of a lesion, non-smokers, intraoral sub-site, size of more than 200mm^2, non-homogenous clinical appearance and higher grade of epithelial dysplasia (Schepman *et al.*, 1998; Napier *et al.*, 2003; Holmstrup *et al.*, 2006; Warnakulasuriya *et al.*, 2011).

Although many reports from Europe, United States and Japan (Banoczy, 1977; Silverman *et al.*, 1984; Schepman *et al.*, 1998; Amagasa *et al.*, 2006) have shown that transformation occurred more frequently in females, studies in India found the contrary (Mehta *et al.*, 1972; Gupta *et al.*, 1980). This may have been due to sex differences in risk habits that influence the outcomes.

The incidence of OSCC arising from leukoplakia has been shown to be greater in those aged 70-89 years (Banoczy and Sugar, 1972; Mehta *et al.*, 1972; Amagasa *et al.*, 2006). An age group of over 65 years was reported showing higher rate of transformation (Warnakulasuriya *et al.*, 2011). Long follow-up studies reported higher number of transformed lesions (Schepman *et al.*, 1998) suggesting that longer period of exposure or period of persistence might increase the risk of malignant change.

Size of lesion is thought to have an effect on malignant development to some degree. Increased risk of transition was 5.4 times greater for lesions exceeding 200 mm^2 in size in a study from Denmark (Holmstrup *et al.*, 2006). In a study of 50 patients from Northern Ireland (Napier *et al.*, 2003), large lesions indicated by the extension over more than one anatomical site were the only factor associated with conversion to cancer when other significant factors on their own (duration and clinical appearance) were controlled.

Intraoral sub-site, particularly the tongue, floor of the mouth and soft palate are believed to carry a particularly high risk of malignant transformation (Banoczy, 1977; Silverman *et al.*, 1984). Although site on the tongue has been shown to be associated with malignant progression in a meta-analysis by Mehanna *et al.* (2009), no definite association has been identified in several individual studies (Schepman *et al.*, 1998; Holmstrup *et al.*, 2006; Liu *et al.*, 2011; Brouns *et al.*, 2014).

Several recent studies have assessed the above-mentioned risk factors with conflicting results. An extensive study evaluating all risk factors has been carried out in the Regional Oral Dysplastic Clinic, Liverpool with 2 and 5 year followed-up (Ho *et al.*, 2012). In order of the most statistically significant factors, smoking status (non-smoker), clinical appearance (non-homogenous), site (lateral tongue), size of lesion (≥ 200 mm^2) and severity of dysplasia were shown to be strong predictors in that study. Gender, age, number of lesions and alcohol consumption did not predict malignant transformation. In the Netherlands, only size of the lesion of ≥ 4cm diameter was a significant predictor while gender, age, tobacco, alcohol, clinical appearance, oral subsite and presence of dysplasia were not associated with malignant transformation (Brouns *et al.*, 2014).

Unfortunately such studies may not reflect the situation in the population, because all such referral series are biased by inclusion of high-risk cases, particularly the inclusion of disproportionate numbers of patients with PVL who are often elderly female non-smokers and who may have extensive lesions, minimal dysplasia but develop several separate primary carcinomas (van der Waal and Reichart, 2008). This may account for the counterintuitive results generated in some studies. There are no epidemiological studies outside the Indian subcontinent, which as noted above has different risk factors from developed countries (Cabay *et al.*, 2007) .

1.3.3.2 Histopathology

There are many reports on the relationship between malignant transformation and OPMD with or without dysplasia. Silverman *et al* reported 36% of leukoplakia with dysplasia and 15.7% without dysplasia had transformed into carcinoma (Silverman *et al.*, 1984). A retrospective study in Northern Ireland found that 15% of dysplastic lesions

(n=165) subsequently developed carcinoma compared with only 1% of non-dysplastic lesions (n=1182) (Cowan *et al.*, 2001).

Cancer risk in different grades of dysplasia has also been evaluated in several studies (Mincer *et al.*, 1972; Banoczy and Csiba, 1976; Pindborg *et al.*, 1977; Lumerman *et al.*, 1995). Severely dysplastic lesions are generally considered to have a higher propensity for malignant transformation, although this finding was not consistent. This notion may have originated from the documented transformation rate that increased with the grade of dysplasia; mild, moderate and severe/carcinoma *in situ* being less than 5%, 3-15%, and 7-50%, respectively (Jaber *et al.*, 2003; Bouquot *et al.*, 2006; Napier and Speight, 2008). The cancer risk in moderate or severe dysplasia was reported to be double (OR 2.3) relative to mild or non-dysplastic lesions (Lee *et al.*, 2000). In a study of 1357 OPMDs patients from South East England of which 204 had dysplastic epithelium, patients with severe grade had a higher risk of transition to oral cancer (HR 35.95% CI 14.2-88.3) and a significant trend between dysplasia grades was evident (Warnakulasuriya *et al.*, 2011).

When dysplasia was assessed in a binary system, in an attempt to increase reproducibility, the prognostic value of the binary system was found to be similar to that of the three-tier WHO system (Nankivell *et al.*, 2013). That study found similar percentages of patients who developed cancer in both the high-risk (36%) and the low risk (31%) groups. In contrast, Kujan *et al.* who introduced the 2-tier system showed that 80% of transformed cases were from high-risk lesions with positive predictive value of 80% and negative predictive value of 85% (Kujan *et al.*, 2006b). This finding is supported by a study in China, which reported that high-risk dysplasia was associated with a 2.78 fold increased risk of transformation compared to the low-risk group (Liu *et*

al., 2011). However, in these studies on referral populations the low risk dysplasia group often have a relatively high risk of transformation rate, reducing the clinical value of the low-grade diagnosis for planning treatment.

Somewhat surprisingly, there are several studies that have found no correlation at all between malignant transformation and degree of dysplasia. A similar proportion of cases that progressed to cancer from all grades was demonstrated in a study from Denmark (Holmstrup *et al.*, 2006) where non-dysplastic (11% transformed) mild dysplasia (11%-14% transformed), moderate dysplasia (9% transformed) and severe dysplasia (9% transformed) showed no statistical difference in transformation, indicating that dysplasia grading was not a good predictor. In an attempt to assess the 'real-world' situation, Dost *et al.* evaluated patients with 368 dysplastic lesions retrospectively without reinterpretation of the original diagnosis reported by the pathologist and found no association between severity of oral dysplasia and risk of progression to cancer (Dost *et al.*, 2014).

Inherent subjectivity in the grading system of dysplasia with substantial interobserver and intraobserver variability in the interpretation of presence, degree and significance of the individual cytological and architectural criteria may contribute to the conflicting correlation between dysplasia grade and transformation rates or risk of cancer (Abbey *et al.*, 1995; Karabulut *et al.*, 1995; Fischer *et al.*, 2004). Lack of reproducibility is frequently blamed for the failure of dysplasia detection and grading to be an accurate predictor of transformation. However, reproducibility, while an important factor in any histological grading system, is not the critical factor it is often assumed to be. Outcome studies on large series are required to assess properly the value

of grading systems and there are only a few of these (Warnakulasuriya *et al.*, 2011; Sperandio *et al.*, 2013; Dost *et al.*, 2014).

Recently, a large outcome study performed in our department showed that dysplasia grading was predictive and that each grade of a three grade system was statistically significantly different. It also illustrated the importance of the negative predictive value of the 'no dysplasia' and mild dysplasia grades in producing a clinically useful result (Sperandio *et al.*, 2013).

Overall, it remains generally accepted that the presence of dysplasia, regardless of grade, is the most accurate predictive factor, though the evidence to support this remains incomplete.

1.3.4 Molecular biomarkers

An appealing approach to circumvent the limitations of clinical and histopathological prediction of malignant transformation in OPMD is the use of molecular biological markers. Many markers have been proposed to indicate risk for disease progression and these have been reported at the DNA, RNA and protein levels. A very large number of studies and reviews including meta-analyses have assessed the predictive ability of molecular markers to determine those lesions at highest risk of malignant transformation (Reibel, 2003; Brennan *et al.*, 2007; Pitiyage *et al.*, 2009; Smith *et al.*, 2009; Lingen *et al.*, 2011; Nankivell and Mehanna, 2011) and not all can be discussed here. It is clear that numerous biomarkers claimed to possess predictive ability for malignant transformation in oral dysplasia have been reported to date; none of these have proved useful in clinical practice (Reibel, 2003; Pitiyage *et al.*, 2009; Smith *et al.*, 2009; Lingen *et al.*, 2011).

1.3.4.1 Tumour suppressor genes

1.3.4.1.1 p53 and family

p53 is a tumour suppressor gene located on 17p13 that regulates cell cycle arrest, senescence and apoptosis. Its loss results in cells losing their response to stress such as hypoxia or DNA damage, subsequently leading to genomic instability. p53 is the most common genetic alteration found in human cancer through mutations, loss of heterozygosity or interaction with oncogenic viral proteins (Vousden and Lane, 2007).

A few investigators have found a positive correlation between p53 mutation or stabilisation detected by immunohistochemistry with the distribution, percentage, intensity of positive cells and dysplasia grades (Schoelch *et al.*, 1999; Brennan *et al.*, 2000; Vered *et al.*, 2009). Others suggest otherwise (Cruz *et al.*, 1998; Murti *et al.*, 1998). Although Cruz *et al.* (1998) found no correlation between p53 expression and grade of dysplasia, they showed that suprabasal expression of p53 could serve as a predictor of malignant transformation (p = 0.002). p53 'overexpression' (often mistaken for stabilisation) has been associated with increased risk of progression to cancer (OR = 6.63; p = 0.0001) in dysplastic lesions (Shah *et al.*, 2007). However, a meta-analysis of reported studies on biomarkers in oral dysplasia has shown that the pooled relative risk for cancer progression in p53 immunopositive cases was 0.96 (CI 0.65, 1.42) indicating lack of prognostic ability for p53 expression assessed by immunostaining (Smith *et al.*, 2009).

Contradictory results on the role of p53 in the prognosis of oral dysplasia probably arise because of the complexity of p53 function with multiple redundancies in its cellular pathways, making it difficult to interpret the biological significance of

immunocytochemical stains. Many studies have simplistic designs and insufficient cases to provide the necessary statistical power.

Investigators have extended their studies to assess the diagnostic utility of p63 and p73, other members of p53 family (Bortoluzzi *et al.*, 2004; Chen *et al.*, 2004). p63 has 6 isoforms divided into two types, TAp63 and ΔNp63 that function similar to p53 and as an oncoprotein respectively. ΔNp63 isoform is primarily expressed in the skin and oral epithelial basal layer (Romano *et al.*, 2009) while TAp63 is normally restricted to the oocytes of ovary (Laurikkala *et al.*, 2006). Expression of ΔNp63 was significantly higher ($P < 0.01$) in oral leukoplakia that progressed to carcinoma compared to the group that did not (Matsubara *et al.*, 2011). Oral cancer risk was increased with hazard ratio of 3.31 (CI 1.66-6.58; $P = 0.0007$) for dysplastic lesions that expressed ΔNp63 protein (Saintigny *et al.*, 2009).

1.3.4.2 Oncogenes

1.3.4.2.1 Cyclin D1

Cyclin D1, encode by CCND1, gene, regulates the cell cycle transition from G1 to S phase through formation of complexes with cyclin dependent kinases (CDKs). Overexpression of cyclin D1 via gene rearrangement or amplification accelerates the G1 phase transition. Several reports have demonstrated that Cyclin D1 expression increased with the degree of severity of dysplasia to OSCC (Raju *et al.*, 2005; Kovesi and Szende, 2006). Amplification of this oncogene has been associated with an eightfold risk of malignant progression from OPMD (Poh *et al.*, 2012).

1.3.4.2.2 EGFR

Epidermal growth factor receptor (EGFR), a member of the ErbB/HERs family of transmembrane receptor kinases, plays roles in cell proliferation and differentiation, apoptosis, invasion and metastasis. EGFR copy number gain and amplification were shown to associate with, and have statistically significant ability to predict, malignant transformation (Taoudi Benchekroun *et al.*, 2010; Poh *et al.*, 2012). Increased protein expression of both EGFR and transforming growth factor-α (TGFα), a growth factor binds and activates ErbB receptors, have been observed in dysplasia that increased with the histologic grade (Srinivasan and Jewell, 2001). This was supported by Grandis *et al.* who found increased mRNA expression of TGFα and EGFR in dysplasia and OSCC and suggested that these may provide early markers for oral carcinogenesis (Grandis and Tweardy, 1993). However, more studies are required to validate its usefulness as biomarker and the high levels of expression in normal oral mucosa and dysplasia are different from the expression seen in other carcinomas arising at other body sites, so that it is unclear whether EGFR alterations will have the value seen in studies of other cancer types.

1.3.4.3 Loss of heterozygosity

Loss of heterozygosity (LOH) refers to loss of one of allele pairs at a constitutional (germline) heterozygous locus. LOH that involved regions containing tumour suppressor genes has been shown to be useful as an early predictor of cancer transition from oral premalignant lesions (Partridge *et al.*, 1998; Zhang and Rosin, 2001). LOH on chromosomes 3p, specifically at 3p13-21.1, 3p21.3-25 and 3p25 (Roz *et al.*, 1996) as well as chromosomes 9p, 13q and 17p were frequent early cytogenetic changes detected in oral dysplasia (Califano *et al.*, 1996; Partridge *et al.*, 2000). Mao *et al.* have demonstrated

that 37% of patients with precancerous lesions showing loss of heterozygosity on 9p21 and 3p14 at either one or both loci were subsequently diagnosed with carcinoma in contrast to only one of 18 cases without (Mao *et al.*, 1996). The association of risk of progression with LOH at chromosome arms 3p and 9p has been further supported by several other studies (Partridge *et al.*, 1998; Jiang *et al.*, 2001; Zhang *et al.*, 2001).

A study on 116 dysplastic lesions of all grades obtained from patients without prior history of cancer further supports that LOH at 3p and/or 9p is a prerequisite for progression (Rosin *et al.*, 2000). In that study, 97% of lesions that progressed had LOH in those two regions, however a significant number of non-progressing lesions also harboured LOH on 3p (25%) and 9p (46%), reducing the predictive value. Additional LOH at other chromosomal arms increased the cancer risk; 3p and/or 9p had a 3.8-fold relative risk for developing cancer while additional LOH on 4q, 8p, 11q, or 17p increased in relative cancer risk 33-fold (Rosin *et al.*, 2000). By classifying patients according to progression, the same group of patients has been recently reviewed and showed that the high-risk lesions (3p and/or 9p LOH) had a 21.1-fold increase in risk ($p = 0.003$) compared to the low-risk group (3p and 9p retention) (Zhang *et al.*, 2012).

A new classification model has been developed by Zhang *et al.* using 9p, 17p and 4q as covariates. Lesions that retained chromosome arm 9p were designated as low-risk lesion, intermediate-risk lesions had 9p LOH only or with either 17p LOH or 4q LOH but not both while high-risk lesion had LOH on all chromosomes 9p and 4q and 17p (Zhang *et al.*, 2012). Based on this model, the hazard ratios (HR) for intermediate- and high-risk categories were 3.4 (95% CI, 1.4–8.2; $P = 0.006$) and 11.2 (95% CI, 3.3–38.6; $P<0.001$) over the low-risk lesions, respectively (Zhang *et al.*, 2012). Additionally, Zhang *et al.* (2012) have also included another prospective cohort (n=296) in that study. The

prospective cohort validated that the high-risk lesions (3p and/or 9p LOH) had a 22.6-fold increase in risk (P = 0.002) relative to the low-risk lesions (3p and 9p retention). Using the new classification model, the intermediate- and high-risk groups had 11.6-fold and 52.1-fold increase in risk (P < 0.001) respectively, compared to the low risk group (Zhang *et al.*, 2012).

1.3.4.4 DNA ploidy

Evaluation of individual cell DNA content (DNA ploidy) allows a gross measurement of chromosomal instability, as abnormal DNA content must indicate whole or part chromosome copy number changes. DNA ploidy has been shown to be a predictor of cancer transition with 53% aneuploid dysplasia transformed to OSCC within 5 years versus 25% of diploid cases (Torres-Rendon *et al.*, 2009; Bradley *et al.*, 2010). Further details are described in DNA ploidy chapter.

1.3.4.5 Podoplanin

Podoplanin is a mucin-type transmembrane glycoprotein that has multiple roles in development as well as in the initiation and progression of neoplasms (Swain *et al.*, 2014). It is specifically expressed in lymphatic but not vascular endothelial cells and by keratinocytes in epithelial dysplasia, and further overexpressed in OSCC (Inoue *et al.*, 2012). To date, podoplanin is among the most studied markers in oral dysplasia and has been shown to be a significant predictor of malignant transformation in a recent meta-analysis (Nankivell and Mehanna, 2011). Several studies have shown that expression of podoplanin was strongly associated with risk of progression to oral cancer (Kawaguchi *et al.*, 2008; Inoue *et al.*, 2012; Kreppel *et al.*, 2012). In one Japanese study, podoplanin was an independent factor for predicting oral cancer progression from oral leukoplakia (HR = 3.09; CI 1.5-6.2; P = 0.002) (Kawaguchi *et al.*, 2008). A group from Spain has

shown that positive immunoexpression of podoplanin in oral dysplasia indicated an 8.7 times ($P = 0.007$) increased risk of developing cancer (de Vicente *et al.*, 2013).

1.3.4.6 microRNA

MicroRNAs are non-protein-coding RNA molecules of 20–25 nucleotides. To date, more than 1000 microRNAs have been identified, with each playing a role as gene regulators by targeting mRNA. They have been extensively investigated in human neoplasms including oral squamous cell carcinoma but the number of studies on oral dysplasia is limited. Increased expressions of miR-21, miR-181b and miR-345 has been associated with the increasing degree of dysplasia during progression to OSCC suggesting potential use to identify leukoplakia at risk of malignant transformation (Cervigne *et al.*, 2009).

1.3.4.7 Other markers

MMP11 and VEGF in combination were commonly seen in dysplastic lesions that transformed into cancer in one study (Arora *et al.*, 2005). The pattern of expression of cytokeratin gene family members has also been evaluated as a potential marker for dysplastic progression to SCC. Expressions of cytokeratin-4 (K4), K13 and transglutaminase 3 (TG3) have been found to be suppressed while K14 and K17 were elevated in SCC and severe dysplasia (Ohkura *et al.*, 2005). Poorer prognosis of dysplasia has also been linked to the loss of expression of CD44v7-8, which belongs to the CD44 cell surface glycoproteins family (Kuo *et al.*, 1998). Expression of granulocyte colony-stimulating factor receptor (GCSFR) was higher in dysplasia and SCC than normal and hyperplastic tissue (Sunaga *et al.*, 2001). However, none of these markers have proved promising enough to merit large scale outcome studies and their value remains

speculative. Other markers that have been suggested as reliable predictors have been reviewed recently by Nankivell *et al.* (2011) and are listed in Table 1.7.

Table 1.7 Potential predictive markers of malignant transformation
(adapted from Nankivell *et al.* 2011)

Marker	RR	OR	95% CI	*P* value	Reference
Survivin	30.00	-	4.25-197.73	< 0.001	Lo Muzio *et al.*, 03
MMP9 mRNA	19.00	-	1.56-209.38	0.02	Jordan *et al.*, 04
p16 methylation	-	3.73	1.72-8.10	0.002	Hall *et al.*, 08
EGFR copy no.	HR 3.62	-	1.44-9.10	0.006	Taoudi Benchekroun *et al.*, 10
ΔNp63	HR 3.31	-	1.66-6.58	0.0007	Saintigny *et al.*, 09
Podoplanin	HR 3.09	-	1.53-6.23	0.02	Kawaguchi *et al.*, 08
LOH 3p ± 9p (pooled)	3.92	-	1.50-10.25	0.006	Rosin *et al.*, 00 Zhou *et al.*, 05
LOH 11q (pooled)	2.86	-	1.11-7.39	0.02	Rosin *et al.*, 00 Zhou *et al.*, 05
Allelic index (>2)	3.20	-	1.49-6.33	0.004	Partridge *et al.*, 98
DNA content	12.00	-	1.17-82.10	0.03	Hogmo *et al.*, 98
DNA ploidy	3.90	-	1.30-11.62	0.01	Torres-Rendon *et al.*, 09

RR relative risk; OR odds ratios

1.4 Chromosomal Instability

1.4.1 Chromosomal instability as an early change in carcinoma

Genomic instability is a hallmark of cancer (Hanahan and Weinberg, 2011) characterised by gross genetic alterations resulting from a series of mutations that facilitate acquisition of adaptive traits to drive tumourigenesis. Though this mutation centred view of carcinogenesis has been challenged (Sonnenschein and Soto, 2013), it remains the currently accepted model of carcinogenesis. Evidence for the role of genetic alterations in tumour initiation has been demonstrated by the detection of genomic changes in precancerous lesions reviewed above. There are various forms of genotypic aberrations leading to disturbances of genome integrity and the main categories studied are chromosomal and microsatellite instabilities (Negrini *et al.*, 2010).

Chromosomal instability (CIN) is loss of cells' control of their chromosomal complement, which is normally tightly regulated. A cell with chromosomal instability will exhibit gain and/or loss of chromosomal segments or whole chromosomes and this is a common feature of many solid cancers. The state of having an abnormal cell chromosomal complement is termed aneuploidy; this results from chromosomal instability and the two usually occur together.

Microsatellite instability (MIN or MSI) cause DNA base changes, of which defects in base excision repair, mismatch repair and nucleotide repair genes result in expansion and contraction of short nucleotide repeats present in microsatellite sequences (Pikor *et al.*, 2013), a smaller scale change in the genome than chromosomal instability. Both CIN and MIN often co-exist in the initial phase of tumorigenesis and increase with cancer progression. However, though MIN can be a route to carcinoma, notably in colon, CIN

is the dominant instability phenotype in cancers compared to MIN (Lengauer *et al.*, 1997; Pikor *et al.*, 2013).

The main mechanism that causes aneuploidy is missegregation of chromosomes during cell division, generating an unequal number of chromosomes in the daughter cells. These may be whole chromosomes if the parent cell had a normal chromosome complement, but structural rearrangements including deletions, duplications, translocation, inversions, and isochromosomes can also be transferred to daughter cells mitosis when the normal complement of chromosomes is not present in the parent cell. This happens after deregulation of DNA damage checkpoints and/or DNA repair pathways (Gollin, 2005). Several studies have generated evidence that the chromosomal instability signature predicts the clinical course of multiple human tumours, including breast carcinomas, soft tissue sarcoma, colorectal, lung and ovarian cancer (Carter *et al.*, 2006; Chibon *et al.*, 2010; Mettu *et al.*, 2010). In early cancer, aneuploidy probably results first from mutations in genes controlling cell division and DNA repair, and once established, chromosomal instability is progressive, self-amplifying and affected cells show increasing alterations in gene copy number at multiple loci as whole chromosomes or parts of them are amplified or deleted (Negrini *et al.*, 2010).

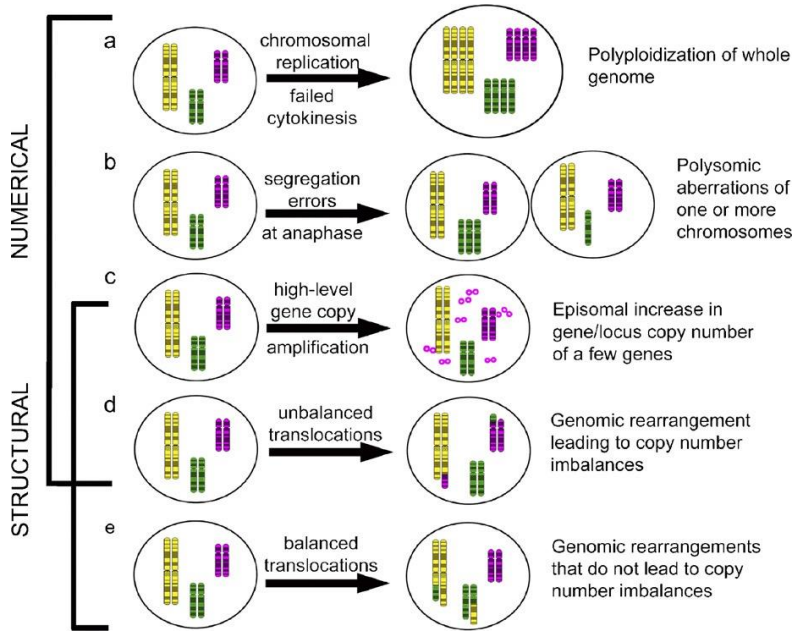

Figure 1.6 The two types of CIN, numerical and structural.
To illustrate mechanisms causing CIN, a normal cell with 3 pairs of chromosomes (left panel) undergo certain errors (labelled arrows) to generate various types of genetic alterations (right panel). Source: (Bayani *et al.*, 2007).

1.4.2 Methods of detection

Numerous sensitive, high-resolution genomic and molecular methods are available to detect CIN at a single or multicellular level. However, measuring the actual rate of chromosomal alterations that occur throughout the cancer progression is not straightforward because this would require repeated measurement over time (McGranahan *et al.*, 2012). Hence, to determine CIN on a static tumour cell population obtained from clinical tumour tissue, variation in number and structure of chromosomes is taken as evidence of progressive chromosomal instability (McGranahan *et al.*, 2012). Work is in progress to improve existing methods further and only selected methods will be discussed here.

1.4.3 Single cell based methods

Aneuploidy and intra-tumour heterogeneity detected by measuring cell-to-cell variability in chromosome number and structure has been used to describe CIN. Such methods usually depend on culture and karyotypic analysis, either using conventional banding or chromosome painting.

1.4.3.1 Fluorescence *in situ* hybridisation (FISH)

FISH is a method that has the ability to determine copy number in individual cells within tissue sections or larger cultured populations and allowing quantification of rate inferred from variation of chromosome changes from one cell to DNA or RNA hybridisation in situ allows spatial analysis of tissues. This is discussed further in chapter 3 on FISH.

1.4.3.2 Spectral Karyotyping (SKY)

SKY is a FISH-based technique that utilises multiple fluorescent colour painting to visualise all 24 chromosomes at once by a single hybridization with a probe cocktail. This technique is capable of identifying a subtle, complex interchromosomal rearrangement such as a single translocation. However, the need for metaphase spreads to perform SKY renders it unsuitable for fixed tissue tumour specimens.

1.4.4 Cell population methods

Whole genome analyses of tissues or cell populations allow screening of the complete set of genomic aberrations present in a tumour sample in a single experiment. These techniques require a population with uniform genetic changes and convey no direct evidence of cell-to-cell heterogeneity or rates of chromosome alterations. They provide an overview of the genetic complexity in cancer.

1.4.4.1 Array Comparative Genomic Hybridization (CGH)

Array-CGH measures gains and losses at specific chromosomal loci on a population of cells relative to a control. The array contains DNA fragments either cloned (for example bacterial artificial chromosomes [BACs]) or synthesized (such as oligonucleotides ['oligos']) complementary to specific chromosomal loci distributed across the genome (Gresham *et al.*, 2008). Genomic DNA from a lesion and normal control are labelled with either green or red fluorochrome respectively, which are then co-hybridized onto a microarray. Differences in fluorescence intensity between the test and reference indicate copy number changes. The spatial resolution of array-CGH is determined by the density and size of the clones and this is a limiting factor for the technique. Although the array design can be customized, array-CGH is of little use for detecting balanced chromosomal rearrangement such as translocations or inversions. Array CGH can be performed on paraffin embedded tissue but with reduced accuracy and the requirement for a normal control from the same patient further limits its applicability to assessing CIN in OPMD.

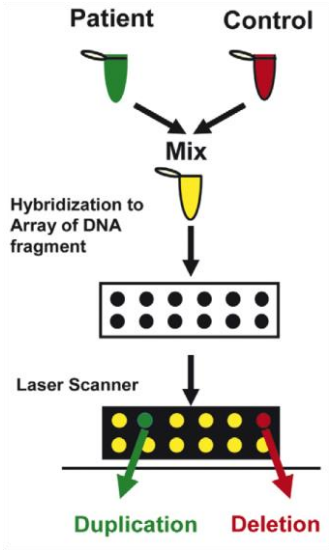

Figure 1.7 Principles of array-CGH.
Sample and control genomic DNA are differently labelled; patient with a green fluorescence dye while the reference DNA is labelled with red fluorochrome. The two samples are mixed and competitively co-hybridized to an array containing genomic DNA targets that have been spotted on a glass slide. The resulting ratio of the fluorescence intensities is proportional to the ratio of the copy numbers of DNA sequences in the test and reference genomes. Green indicates extra chromosomal material (duplication) in the test sample at that particular region. Red indicates relatively less test DNA (deletion) in the sample at that specific spot. Adapted from (Shinawi and Cheung, 2008).

1.4.4.2 Single Nucleotide Polymorphism (SNP) arrays

SNPs are a form of genetic variation in the human genome characterised by a single base polymorphism in the DNA, with population frequency of >1% (Dutt and Beroukhim, 2007). SNPs almost always have only two alleles and tend to be found in microsatellite DNA. Detection of the presence or absence of SNPs between lesional tissue and control can be used to measure copy number and thus CIN.

In comparison with array-CGH, SNP arrays offer greater resolution delivered by high density of markers ranging from 500,000 to >2.5 million SNP loci across the genome, all of which can be hybridized on one chip (Chen *et al.*, 2013). The principle of this method is based on the fact that the signal intensity depends on the amount of the sample target DNA and the affinity of a single base that mismatched between target and

probe will result in decrease fluorescence signal (Gresham *et al.*, 2008; LaFramboise, 2009). Only tumour DNA is labelled with fluorochrome and hybridized to an array that consists of small oligonucleotides of 20-60 base pairs (bp) in size. Prior to hybridization, genomic DNA is digested by restriction enzymes to generate PCR products of specific sizes that are then ligated to adaptors, amplified and fragmented before being labelled with fluorescent dye (Affymetrix SNP 6.0 method). Copy number changes are established by comparing signal intensities of each SNP locus with corresponding signal intensities from normal genome. This method also detects loss of heterozygosity (LOH) including copy-neutral LOH and allele genotype for each SNP.

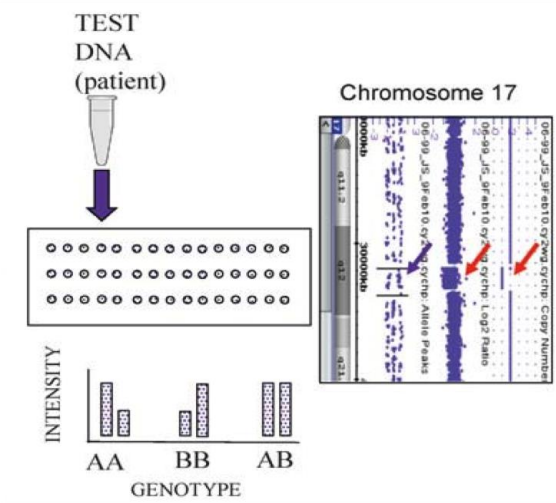

Figure 1.8 Principles of SNP array
In SNP array, only patient DNA is labeled and hybridized to the array of oligonucleotides (purple dots) each represented by its two alleles. To obtain copy number information, the intensity of each oligonucleotide on the patient array is compared with the intensity of the same oligonucleotide in a set of standard controls. In addition to copy number analysis based on fluorescence intensity, individual oligonucleotide-genotyping calls are obtained (homozygous for one or the other allele or heterozygous). Adapted from (Rajcan-Separovic, 2012).

1.4.4.3 DNA Flow and Image Cytometry

Cell ploidy determined by flow and image cytometry is based on total cell DNA content and the cell cycle stage measured by fluorescence dyes or Feulgen-Schiff stain that bind stoichometrically to DNA respectively. Flow cytometry (FCM) can only be applied to cells or nuclei in suspension whereas image cytometry assesses either tissue sections, cultured cells in monolayer or separated nuclei on a glass slide. CIN can be inferred from an aneuploid histogram stemline or other abnormalities (Pentenero *et al.*, 2012). This method is further discussed in Chapter 4.

1.5 Aims of study

1.5.1 Rationale

Early detection or prevention of carcinoma are the most effective interventions to reduce mortality and morbidity from oral squamous carcinoma. No biomarker can yet predict malignant transformation in oral potentially malignant diseases. A reliable method is required for routine clinical application, which almost always must be applicable to formalin-fixed and paraffin wax-embedded tissue.

Previous studies in our group have established that ICM DNA ploidy analysis shows promise as a predictive test. Alone it has proved as good as the best reported dysplasia grading and in combination with dysplasia grading it adds diagnostic value. Ploidy abnormalities indicate chromosomal instability and a molecular marker of this could prove more sensitive and be more economical, cost effective and feasible to perform in an automated high throughput fashion.

1.5.2 General aim

To investigate alternative tests of copy number variation for routine application to oral dysplasia and non-dysplastic oral mucosa and compare them with DNA ploidy analysis.

1.5.3 Specific objectives

i. To identify potential candidate chromosomal loci as markers for copy number variation associated with the transition from dysplasia to carcinoma using data already obtained in the laboratory and from published studies.

ii. To identify a patient group with OPMD and obtain and validate follow up data on cancer development and death registrations from the NHS Information Centre and cancer registries.

iii. To test TaqMan Copy Number Assays (Applied Biosystems) and QuantiGene Plex DNA (Affymetrix) assays to detect copy number variation

iv. To test fluorescence *in situ* hybridization to detect copy number variation

v. To test DNA image-based ploidy analysis on a series of oral potentially malignant tissue as the reference standard

vi. To compare and evaluate each test against DNA image-based ploidy analysis and outcome

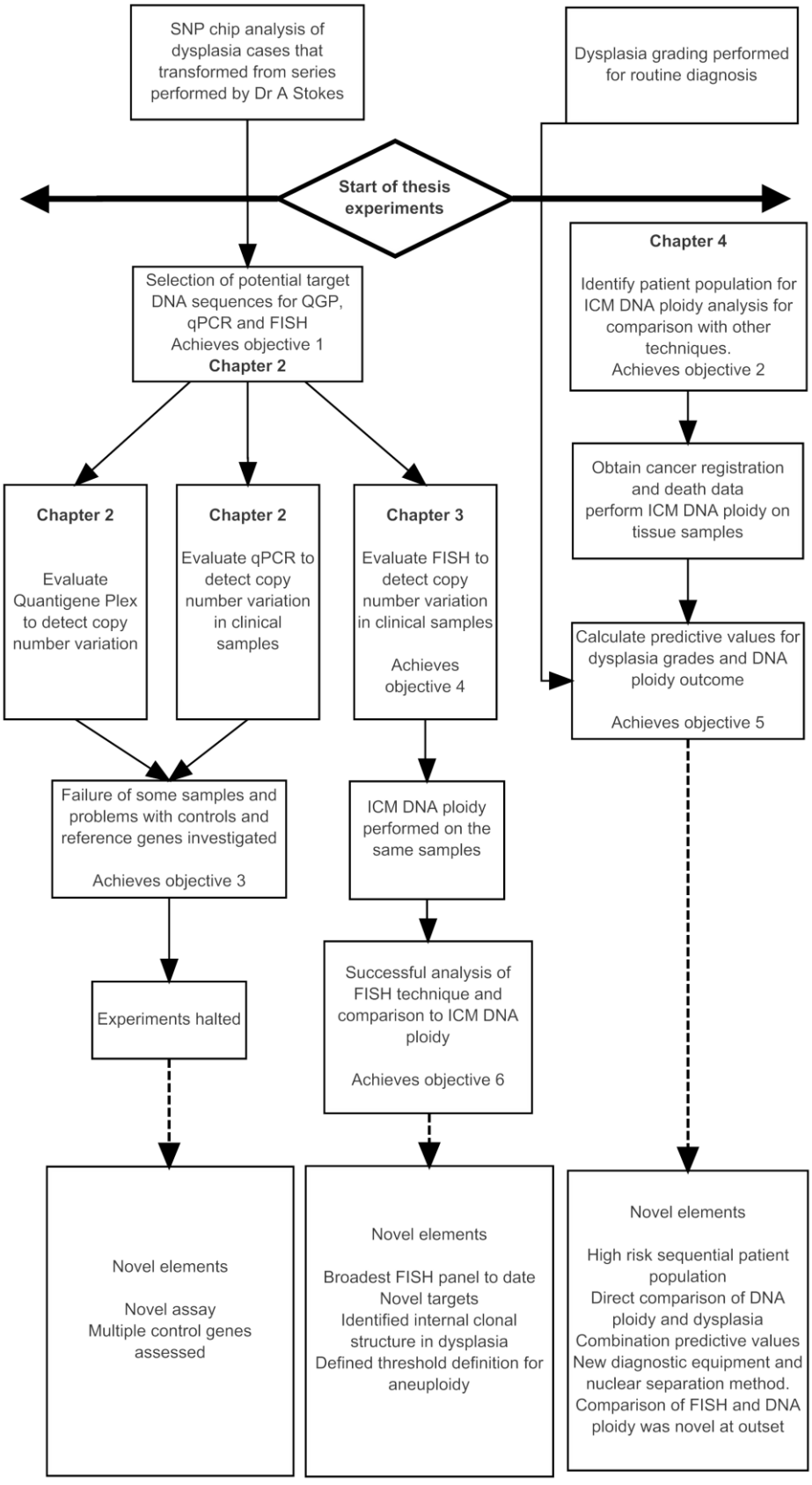

Figure 1.9 Overall experimental plan

CHAPTER 2 : QuantiGene Plex and Real Time PCR

2.1 Investigative plan for QGPlex and qPCR experiments

To investigate QuantiGene Plex (QGPlex) (section 2.2.3.1) and real time quantitative PCR (qPCR) (section 2.2.3.2) as alternative tests of copy number variation, an initial group of 10 chromosomal loci (Table 2.5 and 2.6) was selected from a list of 26 target markers generated based on previous SNP array data, loci that have been most frequently associated with aberrations in OPMD in the literature and availability of the target gene in the QuantiGene Plex DNA assay (section 2.3.1). QGPlex and TaqMan qPCR assays were designed to detect these targets.

Samples of dysplastic epithelium and a range of control tissues, two cell lines and blood were selected for analysis (section 2.3.2) and DNA extracted from each (section 2.3.4) and checked for quality. The samples were run in the two assays QGPlex (section 2.3.6.2) and qPCR (section 2.3.6.3) and results were normalised against three reference genes RNaseP, Tert and TPM1 to reduce single control normalisation error.

The results are shown in section 2.4. It was immediately apparent that both assays showed considerable variation (summarised in table 2.11) and had not performed as expected. Reasons for this were explored including reference genes, calibrators and sample quality and these are discussed in section 2.5. The high cost of the QGPlex assay and conclusion that the variation in both assays could not be reduced quickly, led us to halt these experiments and move to FISH-based assays and these more successful experiments are reported in chapter 3.

2.2 Background

2.2.1 DNA copy number terminology

Many terms referring to change in chromosome copy number have been used interchangeably. Multiplication of the entire set of homologous chromosomes is termed polyploidy. Aneuploidy refers to an unbalanced number of chromosomes, either more or less than the diploid number. When gain or loss involves entire chromosomes, it is known as whole chromosome aneuploidy. Partial or segmental aneuploidy denotes copy number changes in subchromosomal regions that are visible under light microscopy. Copy number alterations (CNA) of 1 Kbp to 1 Mbp in length are referred to as copy number variations (CNV) while those ranging from 1 bp to 1 kbp in size are called insertions or deletions when the segments are amplified or deleted respectively (Feuk *et al.*, 2006; Lupski, 2007).

Changes in copy number generally result in changes of gene expression and individual genes that may generate new or modified functions and phenotypes (Tang and Amon, 2013). In many instances, a change in gene copy number leads to genomic disorders (Lupski, 1998). Aberrations in the number of chromosomes and the significance of gaining or losing whole chromosomes vary between species and cell types. Human cells can be polyploid physiologically, as in osteoclasts or myocytes, but changes in copy number usually result from genome instability, a dominant feature and a hallmark of cancer.

2.2.2 Copy number aberrations in OPMDs

Studies on copy number aberrations in OPMDs have been evaluated either alone but mostly in comparison with oral squamous cell carcinoma using various methods. Array CGH is the most frequently applied technique, giving an overview of all genomic

alterations, usually with the intention of discovering new markers for early detection, predictors of malignant transformation or therapy. Other methods were discussed in section 1.4.2.

The most common copy number alterations detected in OPMDs have been gains on 3q, 7p, 8q, 11q and both arms of chromosome 20 whilst losses have been reported most frequently on 3p, 8p and 9p (Noutomi *et al.*, 2006; Tsui *et al.*, 2009; Bhattacharya *et al.*, 2011; Cha *et al.*, 2011; Giaretti *et al.*, 2012). Sequential increment in genetic alterations from dysplasia to invasive carcinoma were evident by the size of the alteration, affecting the whole chromosome arm in advanced stages of disease compared to smaller regions or loci in dysplasia (Garnis *et al.*, 2009; Tsui *et al.*, 2009).

Deletion of the chromosome 3 short arm is the most frequently reported alteration both in dysplastic epithelium and OSCC (Mao *et al.*, 1996; Tsui *et al.*, 2008; Zhang *et al.*, 2012). A comprehensive study of chromosome 3p has identified recurrent losses at 3p25.3-p26.1, 3p25.1-p25.3, 3p24.1, 3p21.31-p22.3, 3p14.2, and 3p14.1 in dysplastic lesions that underwent malignant transformation (Tsui *et al.*, 2008). Loss of chromosomal region 3p14 and 9p21, which both harbour tumour suppressor genes, has been claimed to be an early event in dysplasia and oral squamous cancer (Mao *et al.*, 1996). The *FHIT* (Fragile Histidine Triad) that resides in 3p14.2, influences control of apoptosis and is commonly deleted in epithelial cancers including oral carcinoma and its precursor lesions (Tanimoto *et al.*, 2000; Kujan *et al.*, 2006a). Chromosome 3q contains other cancer related genes, among which TP63 located on 3q26 was found to be highly expressed in transition from epithelial dysplasia to carcinoma, most likely as a result of a chromosomal gain (Saintigny *et al.*, 2009; Matsubara *et al.*, 2011).

Gains on multiple loci of chromosome 8 including 8q11-q21, 8q24-qter and 8q22.3 are often observed in mild dysplasia. This has been interpreted as suggestive of an early event in oral carcinogenesis (Garnis *et al.*, 2004a) though this assumes a sequential progression through grades of dysplasia that is now thought unlikely to occur. Other candidate genes that may have roles in oral carcinogenesis in 8q24 are PTK2, LY6K, MYC and LRP12 in 8q22 (Garnis *et al.*, 2004a; Garnis *et al.*, 2004b).

Using various methods other than CGH, such as FISH and real-time PCR, EGFR, which resides in 7p11.2 and CCND1 in 11q13.2 were shown to be amplified in high-grade dysplasia and were significantly associated with the progression to OSCC (Taoudi Benchekroun *et al.*, 2010; Poh *et al.*, 2012). Whole chromosome gain on both arms of chromosome 20 was frequently observed in dysplastic lesions that progress to cancer (Garnis *et al.*, 2009; Bhattacharya *et al.*, 2011).

Information on genomic alterations gathered by array CGH has provided the basis for specific chromosomal analyses that might be used to predict outcome in OPMDs. The number of studies attempting to predict malignant transformation in OPMDs based on cytogenetic profile and suitable for routine application is very limited. Further research employing methods suitable for diagnostic pathology such as fluorescence *in situ* hybridization and real time PCR or new multiplexing techniques is required to assess these and other chromosomal loci as markers of cancer development.

Table 2.1 The main studies reporting gains and losses in OPMDs

Studies	Platform	Samples	Gain*	Loss*
Weber *et al.*, 1998	CGH	8 OED, 4 CIS, 14 OSCC	8q24, 16p	3p25–p26, 4q, 5q11.2–q23, 8p, 9p21–pter, 13q21-q31
Noutomi *et al.*, 2006	CGH	35 OED adjacent to OSCCs	3q26-qter, 5p15, 8q11–q21, 8q22–23, 8q24-qter, 11q13, 17q11–22, 14q, 20q	18q22-qter, 9p
Tsui *et al.*, 2008	aCGH	2 hyperplasia, 47 OED, 22 CIS, 23 OSCC	Not available	3p25.3-p26.1, 3p25.1-p25.3, 3p24.1, 3p21.31-p22.3, 3p14.2, 3p14.1
Tsui *et al.*, 2009	aCGH	64 OED, 23 OSCC	2q11.2; 4q12; 7p11.2; 8q11.21; 8q22.3; 9p13.3; 11q13.2-q13.4	9p22.3, 9p21.1-p21.2, 9q33.1, 9q33.1-q33.2, 15q15.1, 16q23.1
Bhattacharya *et al.*, 2011	aCGH	39 OED, 152 OSCC	3q24-qter, 8q12-q24.2, chromosome 20	8pter-p23.1
Giaretti *et al.*, 2012	aCGH	8 OED, 11 non-dysplastic OL	5p13.33-pter, 16q24.2-qter, 20q13.31–q13.33	9p21.3
Cha *et al.*, 2011	aCGH	OED from the margins of 7 OSCC	3q, 5p, 6p, 7p, 8q, Xq. Amplified: 1q24.1-q25.3, 3q25.31, 3q26.3, 3q26.31, 5p13-p12, 7p21.1, 7q21.1-q21.2, 8q24.1-q24.2, 12p12.3, 12q23.1, 13q22, 15q21.1, Xq22.3, Xq24	1p, 2p, 3p, 5q, 9q, 12q, 17q, 22q Deleted: 1p34.3, 1p13.2, 2p13-p12, 2q13, 3p21.3, 3p14, 4q22, 11p13, 12q13.2, 17q24.3
	MLPA		Amplified=1p22, 2q24, 3q26.3, 6q22, 8q24, 9p21, 11q13, 13q14.3, 13q32, 17p13.3, 17q21.2, 21q11	Deleted: 6p21.3, 15q13, 15q26, 16q22.1, 20q13.12, Yq11.21
Cervigne *et al.*, 2014	aCGH	16 OED, 9 non-dysplastic OL, 5 OSCC	1q32, 1p35–36, 2p14, 5q31, 6p21, 6q25, 7p13, 10q24, 11q13.4, 12p13, 14q22, 19q13 and 22q12.3	3p26.2, 8p23.2, 9q33.1–9q33.2, 17q11.2 and 18q21

*Results included in this table were from dysplastic samples including carcinoma in situ only

CGH: comparative genomic hybridization; aCGH: array CGH; MLPA: multiplex ligation-dependent probe amplification

OED: oral epithelial dysplasia; CIS: carcinoma in situ; OSCC: oral squamous cell carcinoma

2.2.3 Methods used to detect copy number changes

Methods that are used to identify copy number changes were discussed in section 1.4.2. In this study, two methods were evaluated, a new proprietary multiplexing method of branched DNA assay and real time quantitative polymerase chain reaction. As both techniques detected the same targets and should produce comparable results, these two sets of experiments are reported together.

2.2.3.1 Multiplex Branched DNA Assay

This novel assay was released just before the start of the work reported in this thesis and only a few publications and a technical note were available for its use as a copy number variation assay. It is based on a combination of branched DNA signal amplification and bead-based multiplexing, xMAP technology developed by Luminex and is marketed commercially as the QuantiGene Plex DNA assay by Affymetrix. The manufacturers claim advantages for the measurement of copy number direct from tissue homogenates and only a small sample is required. This method appeared ideal for this study and potentially for future clinical use (Flagella *et al.*, 2006).

The power of branched DNA resides in the omission of DNA extraction or a reverse transcription step. It is therefore less labour-intensive and avoids biases associated with DNA isolation and PCR amplification by augmenting the reporter signal through "sandwich" cooperative hybridization of multiple probes that generate strong chemiluminescence signals (Collins *et al.*, 1997; Horn *et al.*, 1997; Tsongalis, 2006). The branched DNA assay has been used successfully in clinical applications including monitoring the viral load in HBV, HCV and HIV patients' and has been adapted for drug discovery research (Tsongalis, 2006).

The xMAP technology allows simultaneous analyses of several targets by utilizing discrete fluorescent-labelled beads that can be coupled with a capture reagent including antigens, oligonucleotides, antibodies, enzyme substrates or receptors. The multiple beads can be quantified in a mixture using multicolour fluorescence by the Luminex platform (Dunbar, 2006).

In the QuantiGene Plex DNA Assay, outlined in Figure 2.1, a series of beads is used, each coupled to a specific oligonucleotide capture probe (CP) that provides the binding site for the second probe (capture extender, CE) complementary to a sequence extending across both the capture probe and the target nucleic acid. The third set of probes, label extenders (LE), hybridize to contiguous regions on the target of interest and concurrently provide sites for hybridization of the branched DNA preamplifier oligonucleotide, on which multiple branched DNA molecules hybridise, forming the branched structure that gives the assay its name. The resulting branched tree-like structure offers numerous binding sites and allows capture of multiple biotinylated label probes that amplify the intensity of light generated after binding of Streptavidin-conjugated R-Phycoerythrin (SAPE) to it. The blocker probes (BL) play a vital role in maintaining an intact and stable hybridization product. The Luminex flow cytometer is used to measure the resulting fluorescence signal associated with individual capture beads and reports median fluorescence intensity (MFI), which is proportional to the number of target DNA molecules present in the sample. Target chromosomal sites can thus be quantitated direct from a cell or tissue lysate.

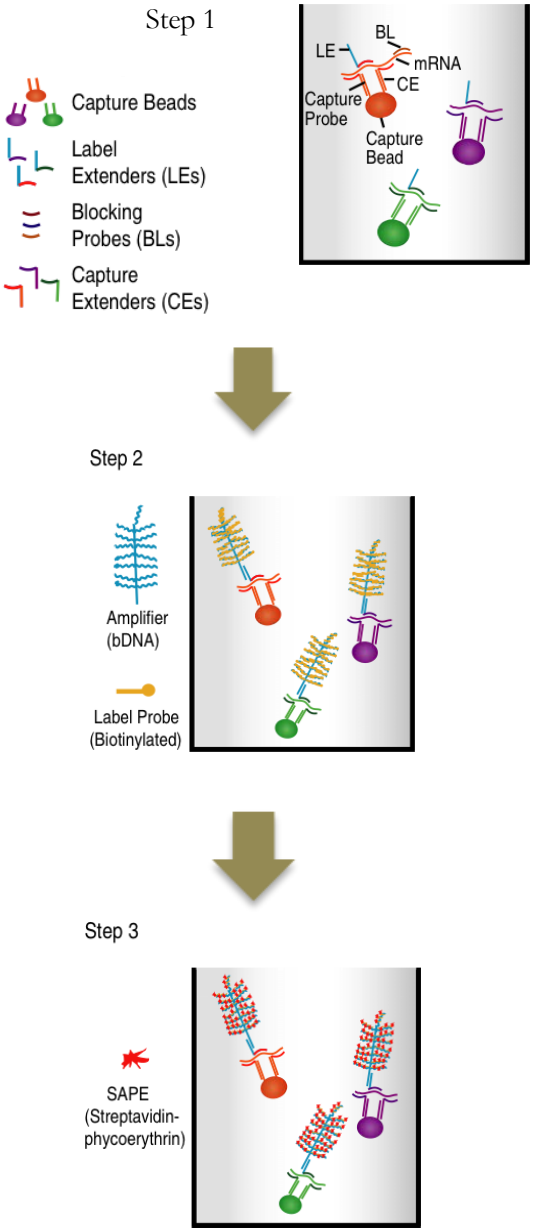

Figure 2.1 Overview of the multiplex branched DNA assay
(1) capture of the specific DNA molecules to their corresponding beads through CP–CE hybridization interactions, (ii) three serial hybridizations that capture the DNA preamplifier, DNA amplifier with biotinylated label probe molecules, and (iii) binding of SAPE to biotinylated label probe. The SAPE fluorescence signal measured by Luminex from each bead is proportional to the number of captured DNA molecules. Adapted from Flagella *et al.* 2006.

2.2.3.2 Real time quantitative PCR

Over the last decade, real time quantitative polymerase chain reactions (qPCR) has become the most commonly used technique for analysis of gene expression and quantitation. It is frequently employed as a validation assay for findings obtained from array-based or other high-throughput genotyping platforms (Ginzinger, 2002). The ability to accurately quantify the amount of amplicon accumulates at every cycle in real time using fluorescence, and is responsible for its superiority in quantitation over other methods. Quantitation, either absolute or relative, is calculated using information extracted from the rate of amplification in a time course plot of amplification constructed from detection of the fluorescence probes incorporated into PCR product. The most frequently used are SYBR Green and TaqMan probes (Ginzinger, 2002; Kubista *et al.*, 2006).

TaqMan Copy Number Assays (Applied Biosystems) are based on the use of the 5' nuclease activity of DNA polymerase to hydrolyse a target-specific, fluorogenic hybridization probe. The application of FAM dye-labelled TaqMan probe for detection of target and VIC dye-labelled TaqMan probes for detection of reference genes allows these assays to be run in duplex. The copy number of each target sequence is determined by relative quantification of the gene of interest by extrapolation from the results for a reference gene of known copy number, usually determined from a diploid sample. The highly specific hybridization of TaqMan probes to the target sequence provides a level of discrimination that is better than conventional qPCR with SYBR Green. The main weakness of SYBR Green is that it binds to any double-stranded DNA in the reaction including primer-dimers and other spurious products, hence being unsuitable for DNA obtained from formalin-fixed paraffin-embedded tissues. In

addition, the specificity of TaqMan probes requires less optimization and allows multiple DNA sequences to be measured in the same sample by designing each probe with a spectrally unique fluor/quench pair. This permits co-amplification of internal controls in single-tube.

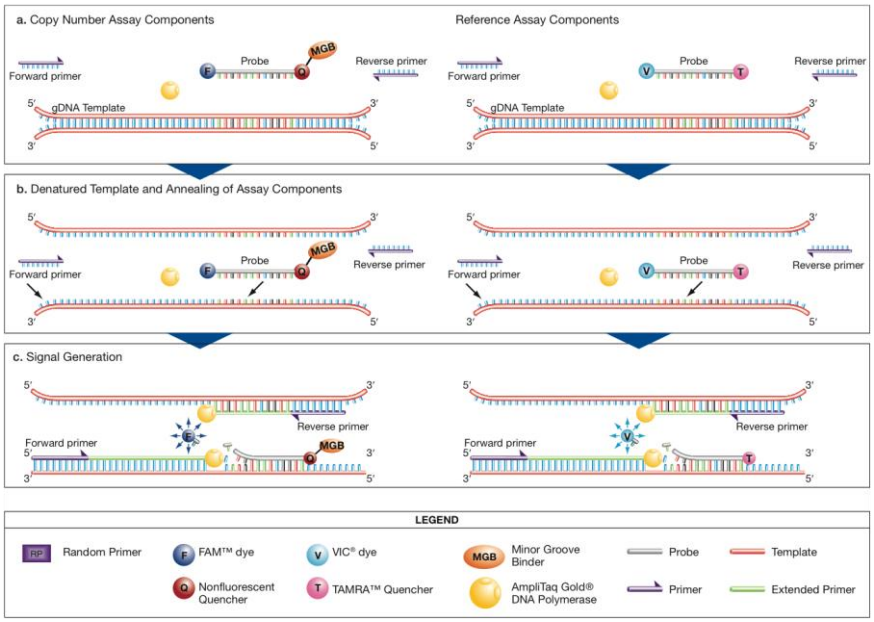

Figure 2.2 TaqMan copy number and reference assays in duplex reactions
Assays are run together in a duplex PCR reaction, which utilise FAM and VIC reporter dyes for detection of target and reference genes, respectively. Minor groove binder (MGB), a component of copy number assay probe increases the melting temperature without increasing probe length, allowing the design of a short probe. Each set of assay primers anneals to its specific target sequences when the genomic DNA denatures. During each PCR cycle, the target and reference sequences are simultaneously amplified by AmpliTaq Gold DNA Polymerase. As this polymerase enzyme extends the primers, it cleaves the 5' end of the probe releasing free reporter dye into solution. The reporter starts to fluoresce when it separates from the quencher. Accumulation of PCR products is detected in real time by monitoring the increase in fluorescence of each reporter dye at each PCR cycle. Adapted from TaqMan Copy Number assays protocol (Figure by Applied Biosystems)

2.3 Materials and Methods

2.3.1 Selection of candidate chromosomal loci and genes

Selection of the chromosomal regions for assessment of amplifications and deletions was based on previous data obtained from a series of multiple samples from individual patients with up to 15 year histories of dysplastic lesions prior to development of cancer that were obtained in our laboratory prior to the start of this work (Stokes *et al.*, 2011). In this previous study, dysplastic epithelia were laser capture microdissected (LCM) and screened for amplifications, deletions and loss of heterozygosity using whole genome Affymetrix single nucleotide polymorphism (SNP) 6.0 array. Data showed that more than 5 years prior to cancer (defined in that study as 'early' dysplasia), the epithelium had limited genomic changes, and that the number of abnormalities increased with time (unpublished). Using this SNP array data in combination with published genetic biomarkers of transformation in the literature, a total of 26 chromosomal locations were selected for further studies in conjunction with Dr A Stokes (Table 2.2).

Almost all studies of this type focus on specific genes, but because this data was SNP based, it identified chromosomal regions of copy number variation by demonstrating sequential strings of SNPs that were deleted or amplified and not specific genes. Within these sometimes large stretches of copy number-altered DNA, genes were selected for probe design based on their implication in the literature for oral premalignant lesions or the development of oral or head and neck squamous cell carcinoma. Gene sequences were selected, as they were better characterised than non-coding DNA. As sometimes no gene had been characterised corresponding to the selected region, an immediately adjacent locus that contained a gene related to cancer

development was included as alternative. Though the experiments that follow use these specific gene targets, they are used only a markers of the target loci and not because their gene products are considered important for carcinogenesis.

Only genes previously found to be amplified were selected, for several reasons. Firstly, detecting deletions can result in a maximum copy number variation of -2 but amplified genes can produce much higher number variation, providing a higher signal to noise ratio. Secondly, DNA ploidy analysis shows that malignant transformation and dysplasia is almost exclusively associated with gain of DNA. While this is a combination of gains and losses, amplification is the more appropriate change to detect overall.

Table 2.2 Initial DNA target list
Markers of changes in OPMD associated with malignant transformation

Chromosome Location	Gene Markers	Genomic changes	References
1p33	MKNK1	Del or LOH	Saintigny *et al.*, 2011
1q25.2	FAM163a	Amp or Del	Saintigny *et al.*, 2011 Cha *et al.*, 2011
3p15	FHIT (3p14.2)	Del	Tsui *et al.*, 2008
3p20	RASSF1A (p21.3)	Del	Leemans *et al.*, 2011
3p25	EMC3, FANCD2 IL17RC, CRELD1 PRRT3, CIDECP	Del or CNLOH	Tsui *et al.*, 2008
3q22	PIK3R4	Amp	Stokes *et al.*, 2011
3q25	CCNL1	Amp	Leemans *et al.*, 2011
3q27-9	deltaNp63	Amp	Saintigny *et al.*, 2011
4p16.1	CNO	Del	Saintigny *et al.*, 2011 Cha *et al.*, 2011
4q13.3	CSN1S2A	Del	Saintigny *et al.*, 2011
4q21.1	DSPP or SPP1	Del or CNLOH	Saintigny *et al.*, 2011
4q32	MAP9, MFAP3L	Del or CNLOH	Stokes *et al.*, 2011
5q23.2	LOX	Del	Stokes *et al.*, 2011
7p12	EGFR	Amp	Benchekroun *et al.*, 2010
8p23	CSMD1, CUB	Del	Partridge *et al.*, 1998 Ma *et al.*, 2009
8q23-24	DDEF1 or PTK2	Amp	Saintigny *et al.*, 2011 Leemans *et al.*, 2011
9p23	PTPRD	Del	Ambatipudi *et al.*, 2011
9q34	USP20	Amp	Cha *et al.*, 2011
11p13	FBXO3	Amp	Cha *et al.*, 2011
12q13.2	NEUROD4, GLS2, CDK2	CNLOH	Stokes *et al.*, l 2011
13q12.3	BRCA2	Del	Stokes *et al.*, 2011
14q12	PAX9	Amp	Stokes *et al.*, 2011
18q23	GALR1	Del	Kanazawa *et al.*, 2009
20q13.12	MMP9	Amp	Jordan *et al.*, 2004
21q21.1	SYNJ1 (21q22.2)	Del	Cha *et al.*, 2011
22q13.2	DIA1	Del	Stokes *et al.*, 2011

Amp: amplified; Del: deleted; LOH: loss of heterozygosity
CNLOH: copy neutral LOH

2.3.2 Selection of tissue samples and cell lines

Oral epithelial dysplasia and normal tissues diagnosed between 2004 and 2007 were identified from pathology reports issued by the Department of Oral Pathology, King's College London. Haematoxylin and eosin (H&E) stained slides were retrieved and re-examined for histological diagnosis whilst simultaneously assessed to ensure sufficient amount of tissue remained in the block specimens and suitable for this study. A total of 86 cases were screened encompassing all grades of dysplasia with priority given to moderate and severe dysplasia. 21 cases were excluded due to an insufficient amount of tissue left and/or because formalin fixed paraffin embedded (FFPE) blocks were unobtainable. A final total of 20 dysplastic samples were selected for study. 10 normal tissues were evaluated as controls, of which 6 were selected for further use on the same basis. In addition, 2 samples of oral squamous cell carcinoma paired with normal matched tissues, 4 blood samples obtained from normal subjects and 2 cancer cell lines (HSC3 and MCF7) were used to compare results (Table 2.3).

Table 2.3 Samples selected to evaluate copy number variation assays

			Number (n=36)
FFPE samples	Dysplasia	Mild	3
		Moderate	4
		Severe	13
	OSCC		2
	Normal matched - OSCC		2
	Histologically normal tissue		6
Cell lines	HSC3		1
	MCF7		1
Normal blood samples			4

To select control cell lines of known copy number variation at our targeted chromosomal loci (Table 2.2), we accessed a published data set (Rothenberg *et al.*, 2010) for which copy number measurements were available (NCBI GEO accession number GSE20306 250K SNP array data) on six cancer cell lines available in our laboratory (Table 2.4). MCF7 and HSC3 cell lines were included in this study following data analysis of copy number changes using Partek software with the aid of Dr A Stokes.

Cell lines were obtained from department stocks, having originally been obtained from Dr K Tominaga, Department of Oral Pathology, Osaka Dental University, Japan (HSC3) and The American Type Culture Collection (MCF7). These cell lines were in use for other studies in our laboratory and had been confirmed as epithelial and mycoplasma free by other workers and identity confirmed by SNP chip analysis [data published in (Suh *et al.*, 2014)]. MCF7 is known to be a previously misidentified cell line, actually of ovarian origin rather than breast, as originally described. Origin was not crucial for the purposes of these experiments and this line was selected because is well characterised karyotypically. Lines were checked against the Public Health England list of misidentified and contaminated cell lines (Public Health England).

Table 2.4 Copy number present in selected control cell lines
(Rothenberg *et al.* 2010)

Chromo-somal loci	Expected HNSCC change	MCF7 Breast cancer	HCT116C olon cancer	A431 Skin SCC	HSC3 Tongue SCC	OSC20To ngue SCC	SCC4 Tongue SCC
1p33	Del/LOH	Del 1.46	None 2.09	Amp 2.49	Amp 2.56	None 2.39	None 2.39
1q25.2	Amp or Del	Amp 3.63	None 2.01	Amp 2.48	None 2.51	None 2.41	Amp 2.98
3p15	Del	Partial gene deletion	Partial gene deletion	Del 1.48	Del 1.58	Del 1.69	Del 1.63

3p21.3	Del	Del 1.47	None 2.01	Del 1.48	Del 1.58	Del 1.69	Del 1.63
3p25.3	Del or CNLOH	Amp 2.67	None 2.0	Del 1.48	Del 1.58	Del 1.69	Del 1.63
3q22	Amp	None 2.06	None 2.03	Amp 2.99	None 2.52	Amp 2.96	Amp 2.69
3q25	Amp	Amp 2.72	None 2.03	Amp 2.99	None 2.52	Amp 2.96	Amp 2.69
3q27-9	Amp	None 2.11	None 2.01	Amp 3.07	None 2.52	None 2.44	Amp 3.35
4p16.1	Del	None 2.03	None 2.05	Del 1.49	Del 1.72	Del 1.63	None 2.18
4q13.3	Del	None 2.03	None 1.97	None 1.93	Del 1.74	Del 1.63	None 2.18
4q21.1	Del or CNLOH	None 2.05	None 2.04	None 1.93	Del 1.75	Del 1.63	None 2.18
4q32	Del or CNLOH	None 2.05	None 2.01	None 1.90	Del 1.72	Del 1.63	None 2.18
5q23.2		Amp 2.42	None 2.01	None 1.89	None 2.48	None 2.44	Del 1.62
7p12	Amp	Del 1.47	None 1.99	Amp 6.33	Amp 4.54	Amp 5.16	Amp 3.83
8q23	Del	Del 1.50	None 2.03	Del 1.47	Del 1.72	None 2.26	None 2.15
8q23-24	Amp	Amp 3.44	Amp 2.85	Amp 3.09	Amp 2.60	Amp 3.14	Amp 2.88
9p23	Del	Del 1.45	None 1.96	Del 0.72	Amp 2.94	None 2.21	Del 1.62
9q34	NA	None 2.05	None 2.05	Amp 2.59	Amp 3.19	Amp 3.26	None 2.29
11p13	NA	Del 1.50	None 2.05	Amp 2.68	Amp 3.22	None 2.46	None 2.31
12q13.2	Amp CNLOH	None 2.03	None 2.04	None 2.01	None 2.50	None 2.38	None 2.30
12p13.32	NA	None 1.97	None 2.06	None 1.98	None 2.5	None 2.43	None 2.20
13q12.3	NA	Amp 2.70	None 2.00	Del 1.45	None 2.46	Del 1.72	None 2.27
14q12	NA	Amp 2.74	None 2.02	None 1.98	Amp 3.20	Del 1.70	None 2.74
18q23	NA	Del 1.31	None 1.94	None 1.84	Del 1.00	Del 1.27	None 2.26
20q13.12	Amp	None 2.15	None 2.01	Amp 2.79	Amp 2.56	Amp 3.18	Amp 3.03
21q21.1	Del	Del 1.62	None 1.94	Del 1.49	Del 1.71	None 2.30	Del 1.62
22q13.2	NA	Del 1.47	None 2.05	Amp 2.43	Del 1.72	Del 1.65	None 2.31

Chrom: chromosome; Del: deletion; Amp: amplification
CNLOH: copy neutral loss of heterozygosity

2.3.3 Tissue and cell line sample preparation

2.3.3.1 Epithelium and matched control tissue

To ensure minimum contamination of the targeted epithelium by connective tissue, which could dilute the copy number variations in the epithelium with additional diploid cells, samples were pre-processed by melting the paraffin blocks at 56°C for 40 minutes. Epithelium from areas of interest (dysplasia) was macro-dissected using a scalpel to separate the epithelial layer from the underlying connective tissue portion, guided by H&E stained slides and the appearance of the tissue, epithelium appearing whiter and more opaque after processing. Epithelium and connective tissue were re-embedded separately in paraffin wax, generating 2 blocks, one of each different tissue type from each sample. Paraffin blocks consisting of connective tissue component were sectioned and stained with H&E to verify correct dissection, conserving the small amount of epithelial tissue for analysis. When complete separation of epithelium was uncertain from the section of the connective tissue alone, H&E slides were prepared and examined from the blocks containing the dissected epithelium to verify the presence of the least 80% lesional epithelium. Connective tissue was used as matched known diploid control for comparison with the epithelial sample.

2.3.3.2 Cell lines

HSC3 and MCF7 cells were thawed and cultured using 75cm^2 flasks in Dulbecco's modified Eagle's medium (DMEM) containing 10% foetal bovine serum (FBS) and 100 μg/ml penicillin/streptomycin and 5ml sodium pyruvate at 37 °C in humidified 5% CO_2 incubator. Cell pellets were prepared when cell growth was 70-80% confluent. After removing the medium, cells were washed with 5ml Versene and incubated with 1x trypsin at 37 °C in humidified 5% CO_2 incubator for 5 to 10 minutes. When cells

appeared round and detached from the plates, they were re-suspended in fresh medium and transferred to a 20ml centrifuge tube, spun at 900*x g* for 5 minutes, and the supernatant was then discarded. Cell pellets were either frozen or stored at -20°C or DNA extraction was done immediately.

2.3.4 Extraction of genomic DNA

2.3.4.1 FFPE tissues

For real time PCR assays, total DNA was extracted from FFPE samples with the Qiagen DNeasy blood and tissue kit (Qiagen, Valencia, CA), using a modified protocol developed in our laboratory. Four to five 15μm thick sections were cut from each paraffin block and collected in an autoclaved 1.5ml microtube. Deparaffinization was performed by vigorously vortexing the sample in 1200μl xylene before 5 minutes centrifugation at 13,000 rpm. This was followed by rehydration through 2 sequential washes in 1200μl of 100% ethanol that were spun in a microcentrifuge at 13,000 rpm for 5 minutes after each wash. At each step of centrifugation, supernatant was removed by pipetting prudently so as not to disturb the pellet. After removal of the final ethanol wash, the tubes containing the tissue samples were incubated at 37°C for 15 minutes using an Eppendorf ThermoStat Plus Incubator to evaporate the ethanol. The tissue pellet in each tube was resuspended in 180μl Buffer ATL and 20μl of prediluted kit proteinase K was added, vortexed to mix and were then incubated at 56°C for 3 days with daily addition of a further 20μl of prediluted kit proteinase K. On the fourth day, all tubes were vortexed prior to adding 200μl of kit Buffer AL, and again vortexed for 15 seconds followed by addition of 200μl of 100% ethanol. The mixture was transferred into the mini spin column provided by the manufacturer, centrifuged at 8000rpm for 1 minute and the flow through discarded. Sequential wash steps with kit solutions AW1

and AW2 of 500µl each were carried out in accordance with the standard manufacturer's protocol and tubes centrifuged at 8000rpm for 1 minute and 13000rpm for 5 minutes respectively. After placing the spin column in a new collecting tube, samples were incubated in 100µl kit Buffer AE for 5 minutes at room temperature and then spun for 1 minute at 8000rpm. To increase the overall DNA yield, the first elute of DNA collected in the tube was transferred back into the spin column and spun again in the same manner as the first centrifugation.

2.3.4.2 Cell lines

Genomic DNA extracted from cell lines was used in both QuantiGene Plex and real time PCR assays. Extraction from HSC3 and MCF7 cell lines was carried out on frozen cell pellets that were thawed at room temperature in accordance with the standard Qiagen DNeasy blood and tissue protocol. After resuspension in 200µl phosphate buffered saline (PBS), 20µl of kit Proteinase K and 200µl kit Buffer AL solutions were added, vortexed to mix and incubated for 10 minutes at 56°C using an Eppendorf ThermoStat Plus heating block. 200µl ethanol was added before the mix was transferred into DNeasy mini spin columns, which were centrifuged at 8000rpm for 1 minute. Sequential wash steps with kit buffers AW1 and AW2 of 500µl each were carried out in accordance to standard manufacturer's protocol and centrifuged at 8000rpm for 1 minute and 14000rpm for 3 minutes respectively. Final elution was carried out by adding 200µl Buffer AE into the mini spin column, incubated for 1 minute at room temperature and spun at 8000rpm for 1 minute. This step was repeated to increase overall DNA yield.

2.3.4.3 Control Blood

Using a 2.5ml microcentifuge tube, 20µl proteinase K was added to 50µl blood followed by PBS that was adjusted to reach a final volume 220µl. After mixing by vortex with 200µl kit Buffer AL, tubes were placed in a thermoblock (Eppendorf ThermoStat Plus) and incubated at 56°C for 10 minutes. 200µl ethanol was added before the mixture was transferred into mini spin columns placed in a 2ml collection tube and centrifuged for 1 minute at 8000rpm. The flow through was discarded and a new collection tube placed. The mini spin column centrifugation step for 1 minute at 8000rpm was repeated twice by first adding 500µl kit buffer AW1 followed by 500µl kit buffer AW2 and the flow through was discarded. The mini spin columns were then placed in new 2 ml collection tubes, 200µl kit buffer AE was pipetted directly onto the spin column membrane and left at room temperature for 1 minute and columns were then centrifuged for 1 minute at 8000rpm. The eluate was transferred back into the spin column and centrifuged again for 1 minute at 8000rpm to increase overall DNA yield.

2.3.4.4 Quality assessment

Nucleic acid quantity, quality and purity obtained from FFPE tissues, cell lines and blood samples were determined using a NanoDrop ND-1000 spectrophotometer (NanoDrop Technologies, Wilmington, DE).

To conserve DNA, only samples that failed to amplify or were available in the largest quantity were tested for degradation, using a 2100 Bioanalyzer (Agilent Technologies, Palo Alto, CA) and these experiments were run as a service by the Genomic Centre, King's College London Core Facility. 11 samples were tested.

2.3.5 Experimental design

From the potential target list shown in Table 1.2, an initial group of 10 markers was selected for assessment in a preliminary study as shown in Table 2.5. This selection was based on loci that have been most frequently associated with aberrations in oral premalignancy and was also subject to the availability of the target gene in the QuantiGene Plex DNA assay and the maximum number of samples that could be analysed in one experiment. When the selected chromosomal regions and/or genes were not readily available from the manufacturer, a gene at an adjacent chromosomal location within the target amplification was selected as alternative (Table 2.5).

Three reference genes were included in this set of markers to reduce single control normalisation error, RNaseP, Tert and TPM1. Reference genes were selected based on recommendation and availability from the manufacturer. RNaseP and Tert were commercially available with TaqMan Copy Number Reference assays (Applied Biosystem) while TPM1 was the recommended housekeeping gene for the QuantiGene Plex assay (Affymetrix). For these initial assays, and to compare the results generated by the QuantiGene technique, real-time PCR (qPCR) was run concurrently assessing six genes out of the ten markers (Table 2.6) on HSC3, MCF7, one squamous cell carcinoma with its normal matched and one normal tissue.

Table 2.5 Reduced 10 target probe set for QuantiGene Plex assay

Target List	Alternative target[b]	Chromosome Region[c]	Bead Number
FHIT - 3p15		59710075-61212163	25
TP63/dNp63 - 3q27-9	PIK3CA - 3q26.3	180349004-180435193	56
EGFR - 7p12		55054218-55242524	48
PTPRD - 9p23		8304245-10602508	44
BRCA2 - 13q12.3	FGF9 - 13q11-q12	21143874-21174186	34
PAX9 - 14q12	MYH7 - 14q12	22951786-22974709	30
MMP9 - 20q13.12	CYP24A1 - 20q13	52203394-52223930	43
DIA1 - 22q13.2	CYP2D6 - 22q13.1	40852444-40856826	20
TPM1[a] - 15q22.1		61121890-61151166	33
TERT[a] - 5p15.3		1306281-1348161	21

[a] Reference gene
[b] Alternative gene from the selected chromosomal locus when the primary target was unavailable
[c] Manufacturer provided genome location. Sequences omitted because of length.

Table 2.6 Reduced 7 target set for for TaqMan Copy Number Assay

Gene Symbol	Cyto Band	Location on NCBI Genome Assembly	Sequence
FHIT	3p14.2	59713630	TTCCTGAGTTATGCCTTTCAGAGAC
PIK3CA	3q26.3	178878315	GAGAAACTGCTGTTTGGGCTTGCTG
TP63	3q28	189349409	AAAACTTAATTGAAGTGCCTTGTGT
EGFR	7p11.2	55088177	TTCTCCTCAAAACCCGGAGACTTTC
PTPRD	9p24.1	8314554	AAGCCACATAACGGATGGATAGAAT
CYP24A1	20q13.2	52770529	CACAGATCCTAAATCAAGTACTGCA
TPM1	15q22.2	63334936	CTGGGAGAAGCAGGCGGCTCCGCGC

2.3.6 QuantiGene Plex DNA Assays

2.3.6.1 Tissue homogenates

Following manufacturer's instructions to perform QGPlex assays, between two and four 15µm thick sections were cut from each paraffin block to achieve a tissue area of 25-100mm^2 or 100-225mm^2 and a combined thickness of 50-60µm. Cut sections were collected into an autoclaved 1.5ml microtube. A combination of 300µl homogenizing solution (Affymetrix) and 3µl of Proteinase K or 600µl of homogenizing solution with 6µl Proteinase K were added to the tissue sizes of 25-100mm^2 or 100-225mm^2 respectively. This was followed by incubation of the samples at 65°C for 30 minutes to 1 hour with occasional brief vortex mixing and samples were then left in the incubator overnight at 65°C (16–20 hours). The samples were then centrifuged at 13,000 rpm for 5 minutes at room temperature in a microfuge to pellet the cellular debris and the homogenate was transferred using a pipette to a fresh microfuge tube, avoiding any residual paraffin and debris. Centrifugation at 13,000 rpm for 5 minutes at room temperature was repeated at least one to three times to ensure that debris was completely removed. Tissue homogenates were stored at -20°C for later use with QGPlex assays.

2.3.6.2 Assays procedures

QGPlex DNA assays were performed according to the QuantiGene Reagent System instruction manual. Procedures carried out on the first day involved capturing target DNA to the probe set on the magnetic beads in each well of a 96-well plate. Frozen tissue homogenates were thawed at room temperature followed by incubation at 37 °C for 30 minutes, vortexed and left at room temperature until use. Concurrently, total extracted DNA from MCF7 and HSC3 cell lines were thawed on ice, vortexed

briefly before dilution to 150ng with nuclease free water to produce sufficient DNA to be run in triplicate at 40µl /assay per well. In a 1.5ml microtube, each sample was sheared to an average size of 500 base pairs using a Misonix 4000 sonicator with a 1/8 inch probe tip immersed approximately 5mm below the solution level applying power output of 6, and sonicated for 10 seconds. Shearing was performed to increase the sensitivity of the assays. The tip was washed in between samples by sonicating the tip in sterile distilled water for 10 seconds. 40µl of each sonicated sample was dispensed into individual wells of hybridization plates and mixed with 18µl Lysis Mixture, 5µl Probe Set and 5µl of 2.5 M NaOH solution. Triplicate samples for background control were prepared by replacing tissue homogenate with homogenizing solution. After 30 minutes incubation at room temperature, 12µl Neutralization Buffer was added to each well followed by 20µl Working Bead Mix that had been prepared earlier by combining 1.8µl nuclease-free water, 15µl Lysis Mixture, 2µl Blocking Reagent, 0.2µl prediluted kit proteinase K and 1µl Capture Beads, mixed by vortex for 30 seconds. The assay plate was then sealed with a pressure seal and left overnight in the shaking incubator at 54°C ± 1°C (18-22 hours) at 180 shaking rpm.

On the following day, signals were developed by sequential hybridizations prior to detection of target DNA. To remove the unbound DNA, the overnight hybridization mixture was washed three times with freshly prepared kit wash buffer by mixing 0.3ml wash buffer component 1, 5ml was buffer component 2 with 75ml nuclease free water, after being transferred into a fresh magnetic separation plate. This was followed by sequential hybridization with DNA pre-amplifier, DNA amplifier and biotinylated Label Probe. Each hybridization was performed by adding 100µl hybridizing solutions into each well and the plate was then sealed with a foil plate sealer before incubation for one

hour in a 600rpm shaking incubator at 50°C ± 1°C. Unbound material was removed using three 160µl kit buffer washes before carrying on to the next hybridization. After a final wash, 100µl of Streptavidin-conjugated R-Phycoerythrin (SAPE) was dispensed into each well, sealed with aluminium foil and incubated on the shaking platform at room temperature for 30 minutes. Removal of unbound SAPE was done using three washes in 130µl SAPE wash buffer, the plate was then covered tightly with foil plate sealer and left on the shaking platform for 2-3 minutes. Bead discrimination and signal detection were performed on a Bio-Plex 200 (Bio-Rad Laboratories, Hercules, CA, USA).

By determining the amount of fluorescence signal and the identity of the beads, the amount of each target DNA present in a sample was evaluated. A cut-off value was calculated as the average background signal plus three times the standard deviation. Fluorescence signals reported as median fluorescence intensity (MFI) were exported to Excel. To calculate DNA copy number for each marker in a sample, the background signal was first subtracted from the average MFI and then normalised to signals generated by housekeeping genes (TPM1 and TERT).

2.3.6.3 TaqMan quantitative PCR

Total DNA was used for all TaqMan assays. Primers with size not more than 90bp were selected from the predesigned Applied Biosystems Copy Number Variation Assays to ensure efficient amplification by qPCR in the fragmented DNA extracted from formalin fixed tissues. Each TaqMan assay was run as a duplex real-time PCR reaction, utilizing a FAM dye-based assay targeted to gene of interest and a VIC dye-based assay for the reference gene, RNaseP (PN 4316844 from Applied Biosystems, Foster City, CA) and TERT (PN4403316). The assays were performed in triplicate and each tube

contained 2µl of 5 ng sample genomic DNA, 5µl of 2xTaqMan Universal Master Mix, 0.5µl of TaqMan® Copy Number Assay, 0.5µl of TaqMan® Copy Number Reference Assay and 2µl nuclease free water forming a 10µl final volume reaction. All PCR reactions were prepared as master mixes and transferred to tubes before adding the sample genomic DNA. No template controls (NTC) were set up in parallel but without target DNA. PCR amplification was carried out in a Corbett Rotor-Gene 6000 (Corbett, Lifescience) instrument implementing hot start for 10 mins at 95°C, followed by 40 cycles of 15 secs at 95°C and 60 secs at 60°C. Real time fluorescence data were collected and cycle threshold (Ct) values were calculated using the automatic setting provided by the instrument software (Corbett, Lifescience).

Relative concentration was obtained employing the $2^{-\Delta\Delta Ct}$ method (Livak and Schmittgen, 2001), according to the manufacturers recommendation in which:

$\Delta\Delta Ct$ = (Ct target gene – Ct reference gene) – (Ct sample – Ct calibrator)

Gene copy number was estimated by doubling the relative concentration to give a double-stranded equivalent value ($2 \times 2^{-\Delta\Delta Ct}$).

2.4 Results

2.4.1 QuantiGene Plex DNA Assays

The Quantigene assay has no intermediate steps at which correct progression of the assay can be tested and its start material is tissue. However, as part of each sample was taken for qPCR analysis, the quality of DNA present in the samples is reflected in the data shown in section 2.4.2.1. and other than this, no assessment of sample quality is possible.

The sensitivity of the assay was evaluated by determining the limit of detection (LOD), a minimal signal for detection of each target at which the signal is 3 standard deviations above the background. This was performed on HSC3, MCF7 and 2 FFPE samples. Assay precision indicated by coefficient of variation (CV) ranged from 0 to 18% (Table 2.7) for all targets.

Results obtained from un-sonicated versus sonicated samples were determined separately (Table 2.8 and Figure 2.3) in an attempt to explain early negative or uninterpretable results. Although one of the samples, S20, failed to give signals above background, others that were sheared produced higher signals. Thus, subsequent QuantiGene Plex assays were carried out on all samples using sonicated homogenates and genomic DNA.

Table 2.7 The sensitivity and precision of the QGP assays

The sensitivity and precision are indicated by limit of detection (LOD) and coefficient of variation (CV) for each gene of interest. Signals reported in MFI units

	CYP2D6	TERT	FHIT	MYH7	TPM1	FGF9	CYP24A1	PTPRD	EGFR	PIK3A
Average background (MFI)[a]	10.5	15.5	14.75	11.75	20	13.5	13	15.25	21.25	12.5
Standard deviation[b]	0.0	2.1	1.8	1.8	2.8	2.1	0.0	1.8	3.9	1.4
Limit of detection[c]	10.5	21.9	20.1	17.1	28.5	19.9	13.0	20.6	32.9	16.7
Coefficient variation (%)	0	13.7	12.0	15.0	14.1	15.7	0	11.6	18.3	11.3

[a] Average background was determined from replicates that contain all assay components except for the sample.

[b] Standard deviation of signals obtained from assay background replicates for each target gene

[c] Limit of detection (LOD) of a target is the concentration at which the signals exceed 3 standard deviation above the background signals

Table 2.8 Net MFI for each gene target detected in samples by QGP with and without shearing

	CYP2D6	TERT	FHIT	MYH7	TPM1	FGF9	CYP24A1	PTPRD	EGFR	PIK3A
HSC3	54.5	20.5	20.25	14.25	11.5	16.5	17	6.75	6.75	19.5
HSC3 sheared	123.5	78.5	60.75	86.75	56	89	62	73.75	84.75	93.5
MCF7	8.5	29.5	9.25	16.25	31.5	15.5	251	13.25	-2.25	48
MCF7 sheared	90.5	186.5	75.25	136.75	196	130	1322	88.25	100.25	131.5
S2	111.5	64	77.25	32.75	91.5	112	91	35.25	6.75	43.5
S2 sheared	114	44.5	74.75	40.75	102	82	59	46.75	26.75	54
S20	27	14.5	5.75	2.75	6	3	4	4.75	2.75	6.5
S20 sheared	16	9.5	-2.25	2.25	5	14.5	9	4.25	-0.25	13.5

Net MFI = values after subtraction from the 'no template' background signals

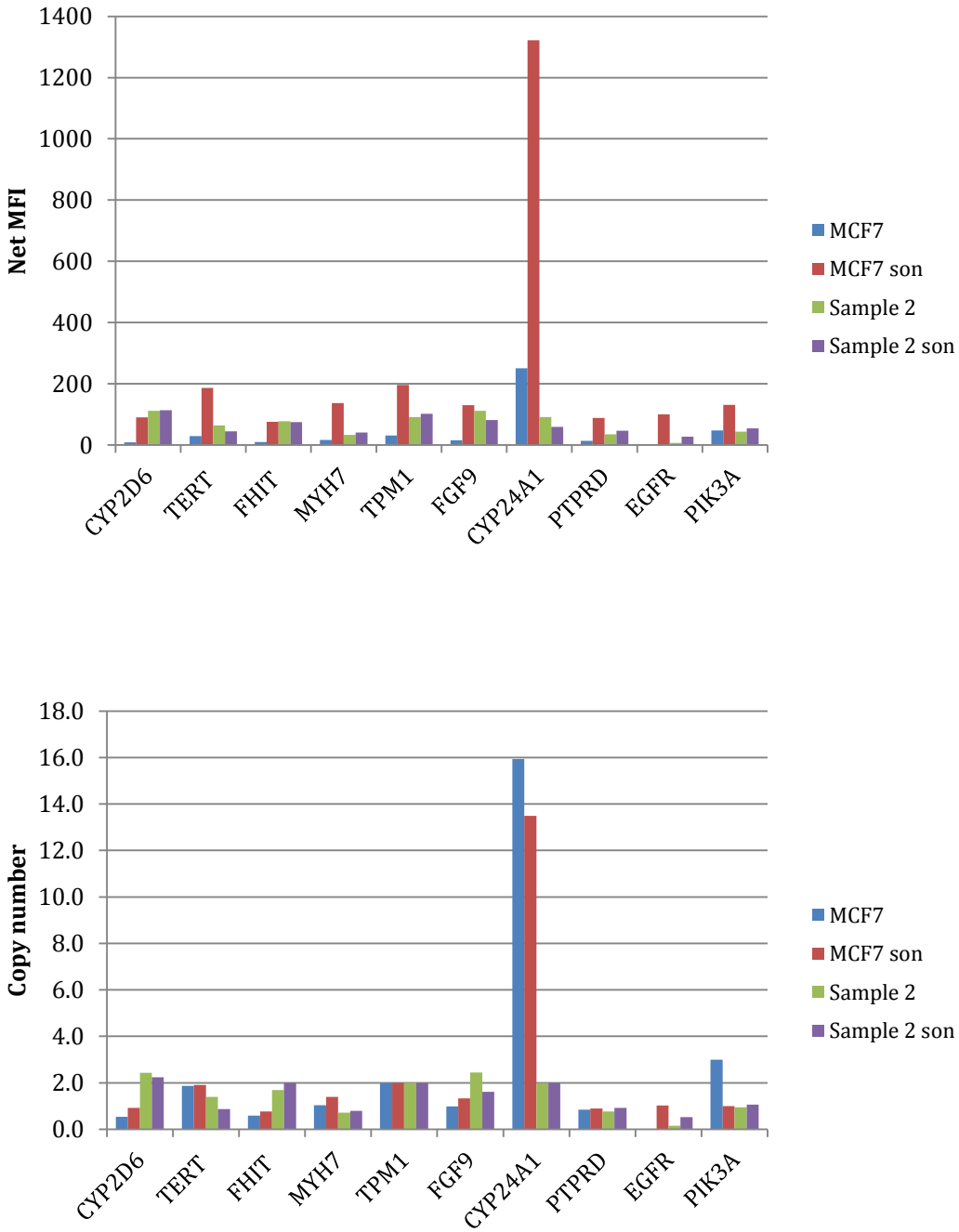

Figure 2.3 Comparison of copy number detected between sheared and unsheared samples for each target in QGP assays
Upper panel shows higher signals produced by sheared samples. Bottom panel shows estimated copy number using data obtained from upper panel. Son, sonicated sample.

Nine samples failed to give results above background; 4 dysplasia, 1 normal tissue matched to carcinoma, 3 normal tissues and 1 normal blood sample. For the samples for which the assay produced valid data, summaries of gene copy number normalised to 2 reference genes, TERT and TPM1 are shown in Table 2.9 and 2.10. There were considerable discrepancies between the gene copy number reported between samples normalised to TERT and to TPM1. This data is shown graphically in Table 2.11 in which it can be seen that non-concordance between results with the two reference genes was more frequent with tissue samples. There was agreement between copy number assessed against both reference genes in 7 out of 8 loci for only 6 samples, two dysplasias (S1 and S12), one carcinoma (S21), one normal tissue (S31), one blood sample (B4) and the MCF7 cell line.

Table 2.9 Number of cases and compiled copy number aberrations by QGP
Results for FHIT, PIK3CA and EGFR by QuantiGene Plex assays normalised to two reference genes, TERT and TPM1

Target genes	FHIT (3p14.2)		PIK3CA (3q26.3)		EGFR (7p12)	
Reference genes	TERT	TPM1	TERT	TPM1	TERT	TPM1
Severe dysplasia (n=11)	Dip 4; Gain 3; Loss 4	Dip 4; Gain 4; Loss 3	Dip 3; Gain 3; Loss 5	Dip 4; Gain 4; Loss 3	Dip 6; Gain 3; Loss 2	Dip 6; Gain 3; Loss 2
Moderate dysplasia (n= 3)	Dip 2; Loss 1	Dip 1; Gain 2	Dip 2; Gain 1	Gain 3	Dip 3	Dip 1; Gain 2
Mild dysplasia (n=2)	Dip 1; Loss 1	Gain 2	Dip 1; Gain 1	Dip 1; Gain 1	Loss 2	Gain 2
SCC (n=2)	Dip 1; Gain 1	Dip 1; Loss 1	Dip 1; Gain 1	Dip 2	Dip 1; Loss 1	Loss 2
Normal tissue matched to SCC (n=1)	Gain	Dip	Gain	Dip	Dip	Loss
Normal tissue (n=3)	Loss 3	Dip 1; Loss 2	Gain 3	Gain 3	Dip 2; Loss 1	Gain 2; Loss 1
HSC3	Loss	Loss	Dip	Gain	Gain	Gain
MCF7	Loss	Loss	Dip	Dip	Loss	Loss
Normal blood (n=3)	Gain 2; Loss 1	Gain 2; Loss 1	Dip 2; Gain 1	Dip 2; Gain 1	Dip 3	Dip 1; Gain 1; Loss 1

Dip: diploid

Table 2.10 Number of cases and compiled copy number aberrations by QGP
Results for PTPRD, FGF9 and CYP24A1 by QuantiGene Plex assays normalised to two reference genes, TERT and TPM1

Target genes	PTPRD (9p23)		FGF9 (13q11-q12)		CYP24A1 (20q13)	
Reference genes	TERT	TPM1	TERT	TPM1	TERT	TPM1
Severe dysplasia (n=11)	Dip 5; Gain 4; Loss 2	Dip 6; Gain 5	Dip 6; Gain 2; Loss 3	Dip 4; Gain 3; Loss 4	Dip 6; Loss 5	Dip 3; Gain 2; Loss 6
Moderate dysplasia (n= 3)	Dip 1; Gain 1; Loss 1	Dip 1; Gain 2	Dip 1; Loss 2	Dip 1; Loss 2	Dip 2; Loss 1	Dip 2; Gain 1
Mild dysplasia (n=2)	Dip 2	Gain 2	Loss 2	Dip 1; Gain 1	Loss 2	Dip 1; Gain 1
SCC (n=2)	Gain 1; Loss 1	Dip 1; Loss 1	Gain 1; Loss 1	Loss 2	Dip 1; Loss 1	Loss 2
Normal tissue matched to SCC (n=1)	Gain	Loss	Dip	Loss	Dip	Loss
Normal tissue (n=3)	Dip 3	Gain 2; Loss 1	Loss 3	Gain 1; Loss 2	Gain 1; Loss 2	Dip 1; Gain 2
HSC3	Loss	Gain	Loss	Loss	Loss	Dip
MCF7	Loss	Loss	Dip	Dip	Gain	Gain
Normal blood (n=3)	Dip 2; Loss 1	Dip 1; Gain 1; Loss 1	Dip 1; Gain 1; Loss 1	Gain 1; Loss 2	Dip 2; Loss 1	Dip 1; Gain 1; Loss 1

Dip: diploid

Table 2.11 Concordance between copy number in QGPlex by reference gene
Concordance using reference genes TERT and TPM1 shown by sample. Compiled data was shown in Tables 2.9 and 2.10 above. Text indicates G gain, D diploid, L loss. First character normalised to TERT, second to TPM1. Red no concordance, green concordance

Sample	Dysplasia grade	FHIT 3p14.2	PIK3CA 3q26.3	EGFR 7p12	PTPRD 9p23	FGF9 13q11-q12	MYH7 14q12	CYP24A1 20q13	CYP2D6 22q13.1
S1	Severe	GD	GG	GG	GG	GG	DD	DD	DD
S2	Moderate	DG	DG	DG	DD	LL	LD	DD	DG
S3	Severe	LD	LL	LL	LD	LL	LL	LL	DD
S4	Severe	LL	DG	DD	GG	LD	DD	DG	DG
S6	Moderate	DG	GG	DD	GG	GD	LL	DG	LL
S7	Severe	DG	LD	DD	DD	GD	LD	DD	DD
S9	Moderate	LD	DG	DG	LG	LL	DG	LD	LD
S10	Severe	GD	GD	DL	GD	DL	LL	DL	GD
S11	Severe	DG	DG	LD	DG	DG	GG	DG	LD
S12	Severe	DD	LL	GG	DD	DD	DD	LL	GG
S14	Severe	GG	GG	GD	DD	DL	LL	LL	GG
S15	Severe	DL	LL	DD	GD	DL	LL	DD	GD
S16	Severe	LL	LD	DD	DG	LD	LL	LL	LL
S17	Mild	LG	LD	LG	DG	LG	LD	LG	LG
S18	Mild	DG	DG	LG	DG	LD	LL	LD	DG
S19	Severe	LG	DG	DG	LG	GG	LL	LL	LG
S21	OSCC	DL	DD	LL	LL	LL	LL	LL	DD
S23	OSCC	GD	GD	DL	GD	GL	DL	DL	GL
S24	N-matched[a]	GD	GD	DL	GL	DL	DL	DL	GD
S25	Normal[b]	LD	GG	DG	DG	LL	LL	LD	DD
S30	Normal[b]	LL	GG	DG	DG	LG	DG	LG	GG
S31	Normal[b]	LL	GG	LL	DL	LL	LL	GG	GG
B1	Blood	LL	GD	DL	LL	DL	LL	DL	DL
B2	Blood	GG	DG	DG	DG	GG	DG	LG	GG
B4	Blood	GG	DD	DD	DD	LL	LL	DD	GD
HSC3	Cell line	LL	DG	GG	LG	LL	DG	LD	GG
MCF7	Cell line	LL	DD	LL	LL	DD	LL	GG	LL

[a] OSCC Normal matched to S23
[b] Histologically confirmed normal tissue

2.4.2 TaqMan Copy Number Assays

2.4.2.1 Sample quality

All samples showed 260/280 ratios above 1.8, which met the manufacturer's recommendation for further analysis. An example of qPCR duplex reactions is shown in Figure 2.4 below.

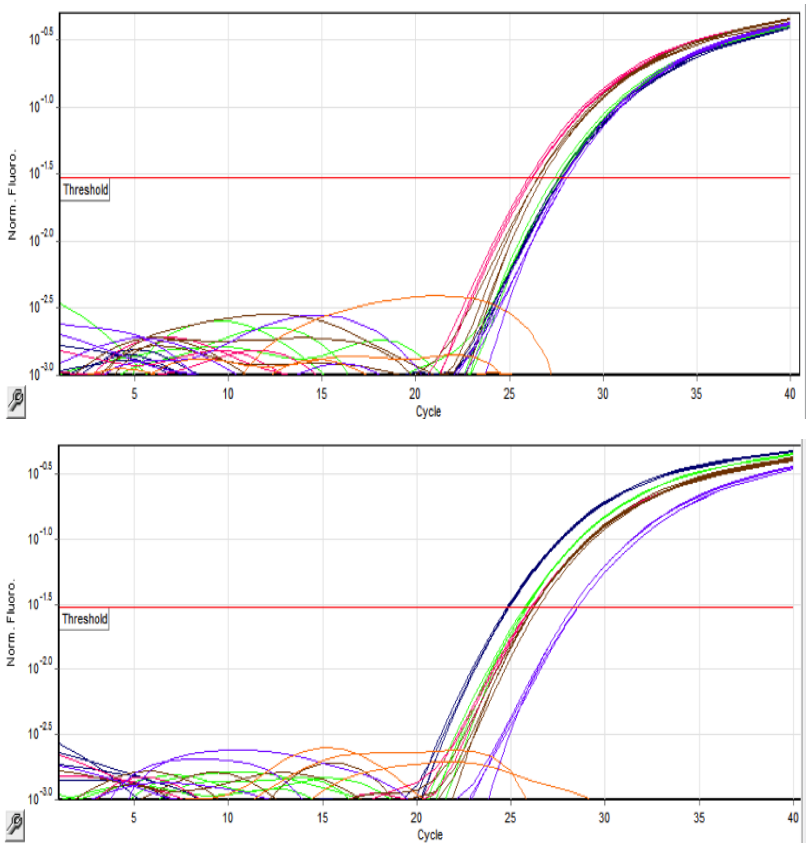

Figure 2.4 Amplification curves
Graphs show successful duplex reactions for target gene EGFR (top panel) and reference gene, RNaseP (bottom panel). The number of PCR cycle is plotted on the *x*-axis against the fluorescence emitted by fluorochrome for each reaction on the y-axis. The cycle threshold (red line) is the PCR cycle in which the reporter fluorescence reaches above the background fluorescence. Each colour represents one sample performed in triplicate.

Bioanalyser (Agilent 2100) results for DNA used in qPCR experiments that matched samples that failed QGPlex assays reported in section 2.4.1 are shown in Figure 2.5 below. These samples amplified successfully in qPCR.

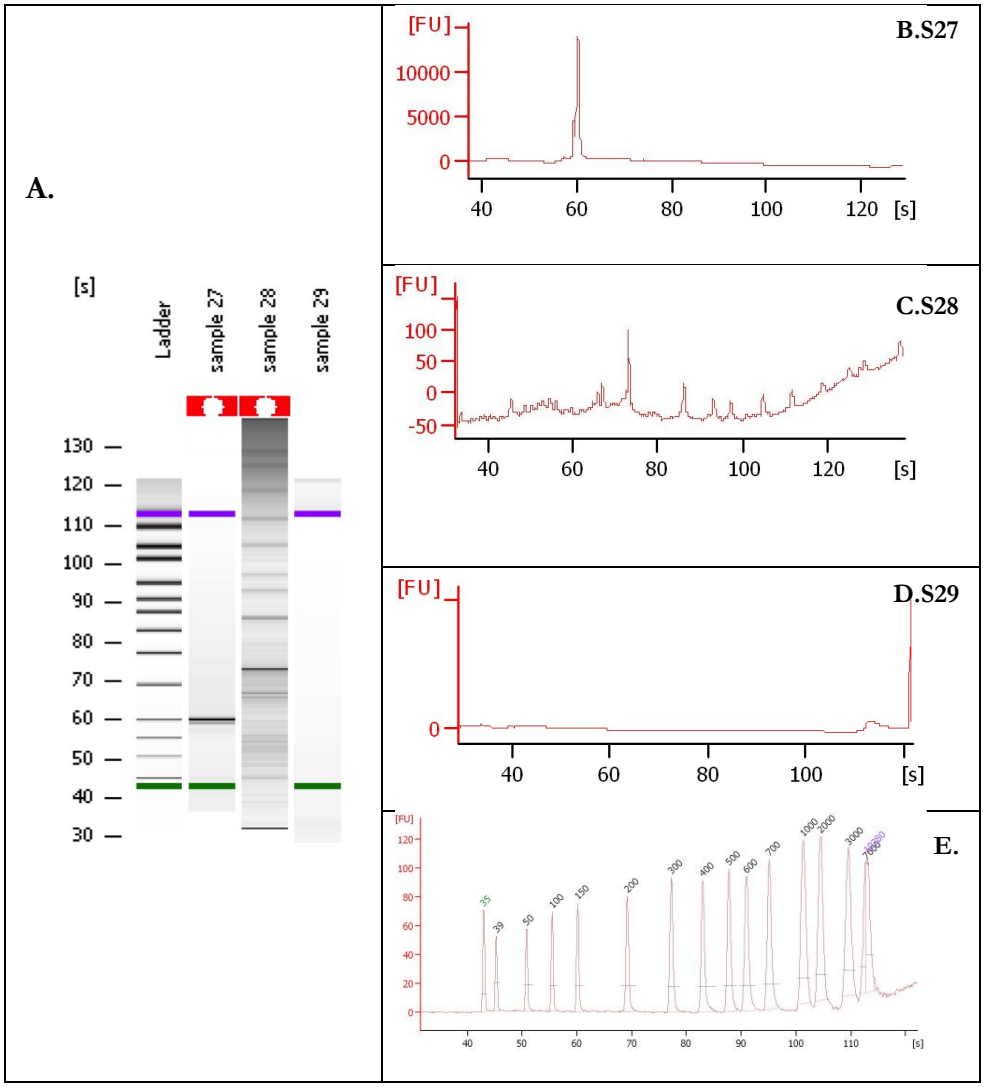

Figure 2.5. Quality of DNA in QGP failed samples
Quality of DNA isolated from samples S27, S28, S29 FFPE tissues that were failed in the QGP experiment. Gel image (A) shows sample 28 is highly fragmented but sample S27 and S29 are of good quality. The DNA size for sample S27 is 200bp and over 17kbp for sample S29. Electropherograms (B-D) show degraded DNA for sample S28 (C) and no degradation products before the major peaks (B, D). The same Agilent size markers (E) are shown on both scales, original Bioanalyser traces in seconds

2.4.2.2 Copy number changes in HSC3, MCF7, and OSCC with its normal matched and control normal tissue

Due to the limited amount of genomic DNA obtainable from dysplasia samples, TaqMan copy number assays were initially performed on a reduced panel of samples that were also used in the QGPlex assay, HSC3 and MCF7 cell lines, one oral squamous cell carcinoma with its paired normal matched tissue and one normal tissue.

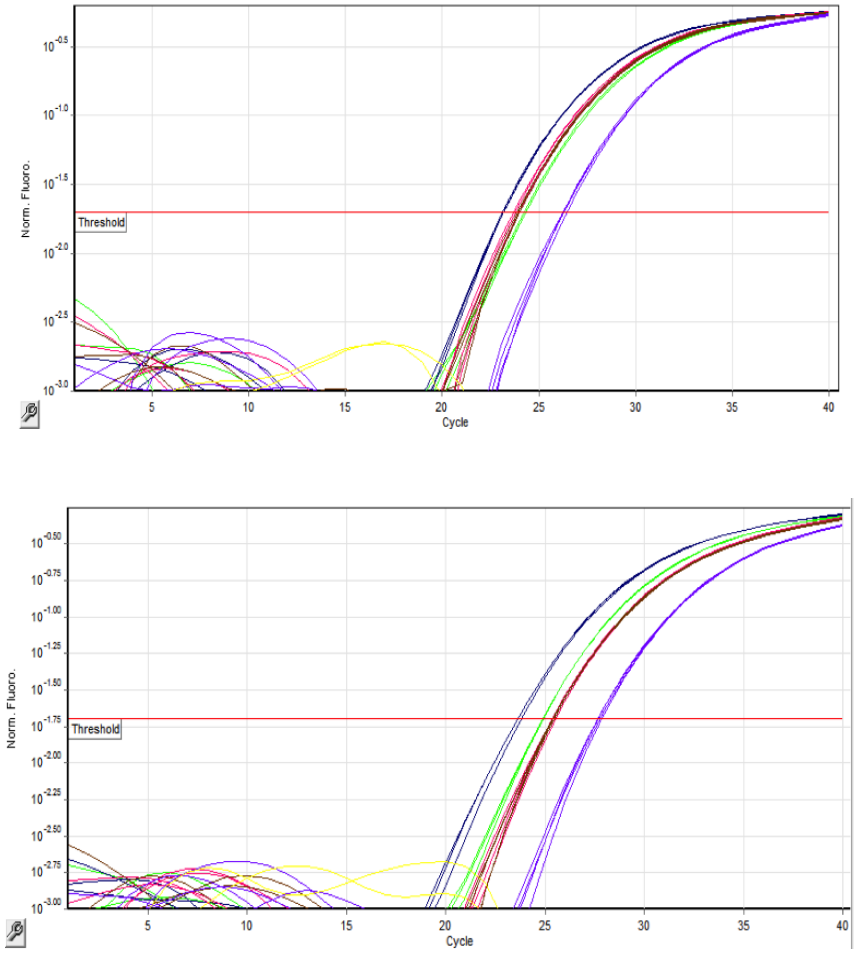

Figure 2.6 Example of amplification curves
Graphs show successful duplex reactions for PTPRD as the target gene on the upper panel and RNaseP as the reference gene (lower panel). The cycle threshold (red line) is the PCR cycle in which the reporter fluorescence reaches above the background that is used as Ct values. Each colour represents one sample performed in triplicate.

Copy number for each target gene (FHIT, EGFR, PTPRD, CYP24A1 and TP63) was normalised independently to 3 reference genes; RNaseP, TERT and TPM1. The calibrator sample used for determination of copy number was histologically confirmed normal tissue. Inconsistencies of the estimated gene copy number for OSCC and its normal matched sample were observed when different normalisation genes were used in the calculation as shown in the Table 2.12 to 2.17. In contrast, gene copy number results for both cell lines, HSC3 and MCF7 were relatively consistent.

Table 2.12 Gene copy number for FHIT by qPCR
Results when normalised to 3 reference genes; RNaseP, TERT and TPM1. Normal tissue (S30) was used as a calibrator.

Target gene	FHIT (3p14.2)		
Reference genes	RnaseP	TERT	TPM1
HSC3 (deletion)*	1.0	0.9	1.0
MCF7 (deletion)*	1.0	0.7	0.6
SCC	2.2	2.6	2.2
SCC normal matched	2.5	2.8	2.7
Normal tissue (S30)	2.0	2.0	2.0

*expected chromosome change

Table 2.13 Gene copy number for PIK3CA by qPCR
Results when normalised to 3 reference genes; RNaseP, TERT and TPM1. Normal tissue (S30) was used as calibrator.

Target gene	PIK3CA (3q26.3)		
Reference gene	RnaseP	TERT	TPM1
HSC3 (no change)*	1.0	1.0	2.1
MCF7 (amplification)*	1.2	1.0	1.7
SCC	2.2	3.0	3.6
SCC normal matched	2.1	3.1	3.5
Normal tissue (S30)	2.0	2.0	2.0

*expected chromosome change

Table 2.14 Gene copy number for TP63 by qPCR
Results when normalised to 3 reference genes; RNaseP, TERT and TPM1. Normal tissue (S30) was used as calibrator.

Target gene	TP63 (3q28)		
Reference gene	RnaseP	TERT	TPM1
HSC3 (no change)*	1.4	1.6	1.8
MCF7 (amplification)*	1.7	1.7	1.5
SCC	2.3	3.8	2.4
SCC normal matched	2.3	4.3	2.6
Normal tissue (S30)	2.0	2.0	2.0

*expected chromosome change

Table 2.15 Gene copy number for EGFR by qPCR
Results when normalised to 3 reference genes; RNaseP, TERT and TPM1. Normal tissue (S30) was used as calibrator.

Target gene	EGFR (7p11.2)		
Reference genes	RnaseP	TERT	TPM1
HSC3 (amplification)*	0.4	0.6	0.8
MCF7 (amplification)	0.2	0.2	0.2
SCC	1.4	2.2	1.9
SCC normal matched	1.2	2.0	1.2
Normal tissue (S30)	2.0	2.0	2.0

*expected chromosome change

Table 2.16 Gene copy number for PTPRD by qPCR
Results when normalised to 3 reference genes; RNaseP, TERT and TPM1. Normal tissue (S30) was used as calibrator.

Target gene	PTPRD (9p24.1)		
Reference genes	RnaseP	TERT	TPM1
HSC3 (deletion)*	1.1	1.2	2.3
MCF7 (deletion)*	1.1	1.2	1.3
SCC	2.1	3.3	2.6
SCC normal matched	2.0	3.2	2.4
Normal tissue (S30)	2.0	2.0	2.0

*expected chromosome change

Table 2.17 Gene copy number for CYP24A1 by qPCR
Results when normalised to 3 reference genes; RNaseP, TERT and TPM1. Normal tissue (S30) was used as calibrator.

Target gene	CYP24A1 (20q13.2)		
Reference gene	RnaseP	TERT	TPM1
HSC3 (amplification)*	1.1	1.9	1.0
MCF7 (amplification)*	13.3	17.0	10.9
SCC	1.8	3.0	2.1
SCC normal matched	1.6	3.1	1.7
Normal tissue (S30)	2.0	2.0	2.0

*expected chromosome change

To determine the cause of inconsistency in the results, the concentration of genomic DNA used for this qPCR was re-evaluated by NanoDrop and found that samples were at the recommended concentration of 10ng/µl. When evaluated on Bioanalyzer 1200, the genomic DNA samples isolated from OSCC, its normal matched and control normal tissue were of acceptable quality (see Figure 2.7).

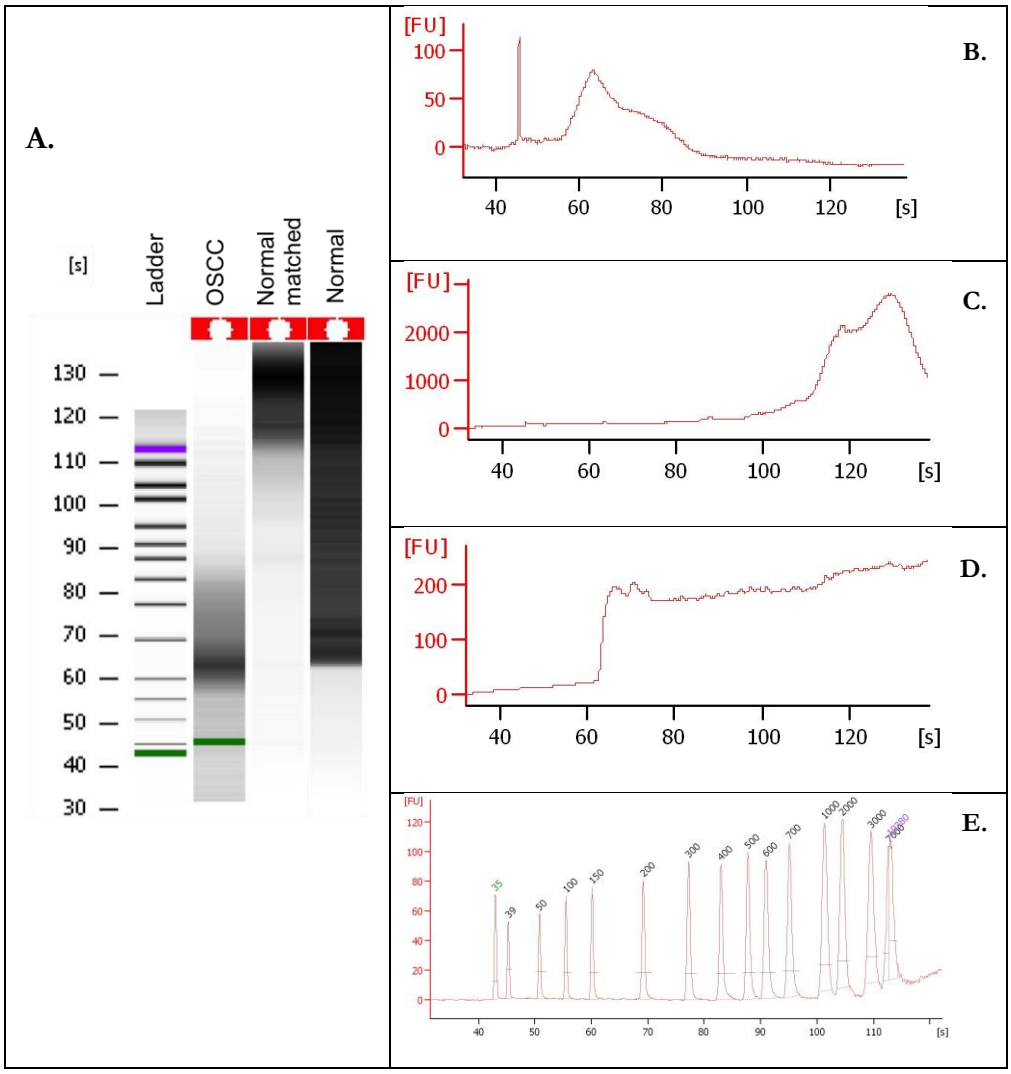

Figure 2.7 DNA isolated from OSCC, its normal matched and normal tissues FFPE samples
Samples run on the Agilent 2100 Bioanalyzer. Gel image (A) shows the size of DNA was 200bp for OSCC, over 2,000bp for OSCC normal matched and 250bp for normal tissue. Electropherograms (B-D) show patially degraded DNA for OSCC (B) and no degradation products before the major peaks (C-D). The same Agilent size markers (E) are shown on both scales, original Bioanalyser trace in seconds.

2.4.2.3 Copy number detected in blood and normal tissue

Because inconsistency in copy number estimate was observed when normalised to different reference genes and appeared likely to be caused by DNA degradation, the performance of qPCR on genomic DNA extracted from FFPE versus unprocessed samples was evaluated. In addition, we attempted to identify the most appropriate reference gene (control gene) to be used for normalisation and to investigate the influence of reference sample (calibrator) on the estimation of copy number.

Copy number changes determined in 4 normal blood samples and 6 samples of histologically confirmed normal tissue including the one (S30) used in the experiment described in section 2.4.2.2 above, were evaluated against different reference genes and calibrators.

As in the experiments in tissue samples reported in section 2.4.2.2, the copy numbers obtained varied between the reference gene and calibrator used in the calculation of copy number. Discrepancies observed when different reference genes were used for normalisation were similar to results obtained in the experiments on OSCC and cell lines. Variation was clearly demonstrated in results for EGFR. It was highly amplified in all normal tissues and all the blood samples were diploid when calibrated to blood (Table 2.21 & Figure 2.8). Conversely, EGFR copy numbers were found to be duplicated and diploid in normal tissues but showed deletion in all blood samples when calculation included normal tissue as the calibrator, despite adequate sample quality. In general, copy numbers for all blood samples were relatively consistent using either blood (B1) or normal tissue (S30) as calibrator (see Table 2.18 to 2.23).

Table 2.18 FHIT gene copy number in normal tissue and normal blood samples using qPCR

Calibrator	Sample B1			Sample S30		
Reference gene	RnaseP	TERT	TPM1	RnaseP	TERT	TPM1
B1	2.0	2.0	2.0	2.1	1.8	2.0
B2	1.9	2.2	2.1	2.0	1.9	2.1
B3	1.9	2.0	2.1	2.0	1.8	2.1
B4	1.9	2.1	2.2	2.0	1.8	2.2
S25	1.6	3.2	2.4	1.7	2.8	2.4
S27	1.0	1.6	5.2	1.1	1.4	5.1
S28	1.4	1.8	2.9	1.4	1.6	2.8
S29	0.6	2.0	1.5	0.6	1.8	1.5
S30	1.9	2.3	2.0	2.0	2.0	2.0
S31	1.4	2.4	1.8	1.5	2.1	1.8

B1-B4: normal blood samples
S25-S31: histologically normal tissue samples

Table 2.19 PIK3CA gene copy number in normal tissue and normal blood samples using qPCR.

Calibrator	Sample B1			Sample S30		
Reference gene	RnaseP	TERT	TPM1	RnaseP	TERT	TPM1
B1	2.0	2.0	2.0	1.3	1.5	1.4
B2	1.9	2.1	2.4	1.2	1.5	1.7
B3	1.9	2.1	2.4	1.2	1.5	1.8
B4	1.9	2.1	2.5	1.2	1.5	1.8
S25	2.5	5.5	3.2	1.6	4.0	2.3
S27	1.1	5.1	12.5	0.7	3.7	9.0
S28	2.2	2.8	2.8	1.4	2.0	2.0
S29	1.5	2.7	3.0	1.0	2.0	2.1
S30	3.1	2.8	2.8	2.0	2.0	2.0
S31	2.4	2.8	3.1	1.5	2.1	2.2

Table 2.20 TP63 gene copy number in normal tissue and normal blood samples using qPCR.

Calibrator	Sample B1			Sample S30		
Reference gene	RnaseP	TERT	TPM1	RnaseP	TERT	TPM1
B1	2.0	2.0	2.0	2.0	1.2	1.6
B2	1.9	2.4	1.9	1.9	1.4	1.5
B3	2.0	2.1	1.8	1.9	1.3	1.4
B4	1.9	2.4	2.1	1.9	1.4	1.7
S25	2.0	6.8	3.1	2.0	4.1	2.5
S27	0.8	7.5	6.6	0.8	4.5	5.3
S28	1.4	3.4	2.1	1.3	2.0	1.7
S29	0.0	2.6	2.6	0.0	1.6	2.1
S30	2.0	3.3	2.5	2.0	2.0	2.0
S31	1.7	4.1	2.1	1.6	2.5	1.7

B1-B4: normal blood samples
S25-S31: histologically normal tissue samples

Table 2.21 EGFR gene copy number in normal tissue and normal blood samples using qPCR.

Calibrator	Sample B1			Sample S30		
Reference gene	RnaseP	TERT	TPM1	RnaseP	TERT	TPM1
B1	2.0	2.0	2.0	0.4	0.5	0.4
B2	2.0	2.1	2.2	0.4	0.5	0.4
B3	2.1	2.2	2.4	0.4	0.5	0.5
B4	1.9	1.8	2.4	0.4	0.5	0.5
S25	8.2	16.6	11.4	1.5	4.0	2.3
S27	13.8	19.5	24.4	2.6	4.7	4.9
S28	16.6	11.1	23.6	3.1	2.7	4.8
S29	12.7	18.4	28.8	2.4	4.5	5.8
S30	10.6	8.3	9.9	2.0	2.0	2.0
S31	10.9	11.4	13.4	2.1	2.8	2.7

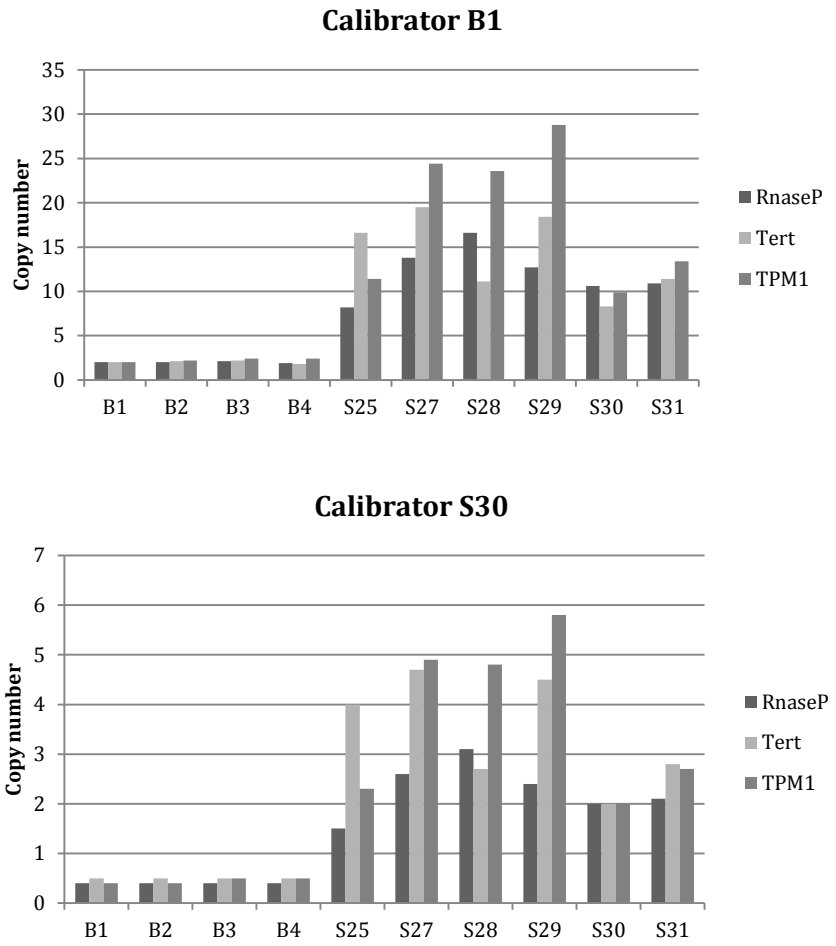

Figure 2.8 EGFR copy number estimate using blood (upper panel) and normal tissue samples (lower panel) as calibrator.
Blood samples show relatively consistent copy number compared to formalin fixed tissues (S25-31).

Table 2.22 PTPRD gene copy number in normal tissue and normal blood samples.

Calibrator	Sample B1			Sample S30		
Reference gene	RnaseP	TERT	TPM1	RnaseP	TERT	TPM1
B1	2.0	2.0	2.0	1.4	1.4	1.7
B2	1.9	2.1	2.1	1.3	1.5	1.8
B3	2.0	1.8	2.2	1.4	1.3	1.9
B4	1.9	2.1	2.6	1.3	1.5	2.2
S25	3.3	5.2	3.8	2.3	3.7	3.2
S27	1.8	4.0	4.6	1.3	2.9	3.9
S28	2.5	2.7	3.2	1.8	2.0	2.7
S29	1.8	2.2	2.7	1.3	1.6	2.3
S30	2.9	2.8	2.4	2.0	2.0	2.0
S31	2.0	2.5	2.3	1.4	1.8	1.9

B1-B4: normal blood samples
S25-S31: histologically normal tissue samples

Table 2.23 CYP24A1 gene copy number in normal tissue and normal blood samples.

Calibrator	Sample B1			Sample S30		
Reference gene	RnaseP	TERT	TPM1	RnaseP	TERT	TPM1
B1	2.0	2.0	2.0	1.2	1.6	1.2
B2	2.0	2.1	2.3	1.2	1.7	1.4
B3	2.1	2.3	2.4	1.3	1.8	1.5
B4	2.2	2.3	3.0	1.4	1.8	1.8
S25	3.6	6.0	5.4	2.2	4.8	3.3
S27	1.8	4.9	6.1	1.1	3.9	3.7
S28	2.7	2.4	3.9	1.7	2.0	2.4
S29	0.1	3.4	3.7	0.0	2.7	2.3
S30	3.2	2.5	3.3	2.0	2.0	2.0
S31	3.0	2.7	2.8	1.8	2.2	1.7

2.4.3 Comparison of QuantiGene Plex DNA and TaqMan copy number results

Tables 2.24 to 2.28 show that the copy number results generated from QuantiGene and TaqMan are generally discordant as well as internally inconsistent. Control experiments for both techniques have demonstrated that control genes and tissue type were the major influence on copy number determination.

Table 2.24 QuantiGene and TaqMan qPCR copy number analyses for FHIT

Methods	QuantiGene Plex		TaqMan qPCR	
Reference genes	TERT	TPM1	TERT	TPM1
HSC3 (deletion)*	0.7	1.2	0.9	1.0
MCF7 (deletion)*	0.8	0.9	0.7	0.6
SCC	4.3	1.9	2.6	2.2
SCC normal matched	3.5	1.8	2.8	2.7
Normal tissue (S30)	0.4	1.0	2.0	2.0

* expected chromosomal change

Table 2.25 QuantiGene and TaqMan qPCR copy number analyses for PIK3CA

Methods	QuantiGene Plex		TaqMan	
Reference genes	TERT	TPM1	TERT	TPM1
HSC3 (no change)*	2.1	3.8	1.0	2.1
MCF7 (amplification)*	2.0	2.1	1.0	1.7
SCC	4.0	1.7	3.0	3.6
SCC normal matched	3.3	1.7	3.1	3.5
Normal tissue (S30)	2.7	6.8	2.0	2.0

*expected chromosomal change

Table 2.26 QuantiGene and TaqMan qPCR copy number analyses for EGFR

Methods	QuantiGene Plex		TaqMan	
Reference genes	TERT	TPM1	TERT	TPM1
HSC3 (amplification)*	2.6	4.8	0.6	0.8
MCF7 (amplification)*	1.4	1.5	0.2	0.2
SCC	2.1	0.9	2.2	1.9
SCC normal matched	1.8	1.0	2.0	1.2
Normal tissue (S30)	1.5	3.9	2.0	2.0

*expected chromosomal change

Table 2.27 QuantiGene and TaqMan qPCR copy number analyses for PTPRD

Methods	QuantiGene Plex		TaqMan	
Reference genes	TERT	TPM1	TERT	TPM1
HSC3 (deletion)*	1.5	2.7	1.2	2.3
MCF7 (deletion)*	1.3	1.3	1.2	1.3
SCC	4.0	1.7	3.3	2.6
SCC normal matched	2.8	1.5	3.2	2.4
Normal tissue (S30)	1.6	4.0	2.0	2.0

*expected chromosomal change

Table 2.28 QuantiGene and TaqMan qPCR copy number analyses for CYP24A1

Methods	QuantiGene Plex		TaqMan	
Reference genes	TERT	TPM1	TERT	TPM1
HSC3 (amplification)*	1.3	2.3	1.9	1.0
MCF7 (amplification)*	18.1	19	17.0	10.9
SCC	2.5	1.1	3.0	2.1
SCC normal matched	2.1	1.1	3.1	1.7
Normal tissue (S30)	1.3	3.2	2.0	2.0

*expected chromosomal change

2.5 Discussion

2.5.1 Sample quality

As noted in the introduction, any test designed for routine pathology practice must be able to use FFPE tissue but nucleic acids isolated from formalin fixed specimens are not ideal for molecular analysis. In the experiments reported in this chapter, the techniques essentially failed to produce reliable copy number estimates and the quality and suitability of the clinical material must be considered.

DNA fragmentation is one possible cause but this effect has been reduced by selecting PCR primers that produce PCR products that are as short as possible (Lehmann and Kreipe, 2001). In our study utilizing TaqMan Copy Number Assays, all primers used were of less than 90 bp in length. Fragmentation results from crosslinking of DNA, DNA-to-protein and protein-to-protein caused by formaldehyde (Chaw *et al.*, 1980; Crisan and Mattson, 1993) and the average fragment size range isolated from formalin fixed tissues in reports in the literature is between 300-400 bp dependent upon fixation conditions, particularly pH of fixation and type of tissue (Lehmann and Kreipe, 2001). In our studies the fragment sizes obtained were between 150 to 500 bp. Despite some fragmentation the samples were suitable for both qPCR and QGPlex assays (Yang *et al.*, 2006; Cukier *et al.*, 2009). Further evidence that fragmentation was not responsible for failure of at least some of the QGPlex assays is seen in the comparison on sonicated and unsonicated DNA samples (Table 2.8).

In this experiment (section 2.4.1), manually shearing the samples resulted in significantly higher signals in genomic DNA samples (Table 2.8) but only slightly higher for FFPE samples. This indicates that shearing was not necessary for FFPE samples as the DNA was already fragmented resulted from formalin fixation. Nevertheless,

shearing has relatively increased MFI signals and thus was applied to all samples and we conclude that fragmentation, though present, did not reduce DNA fragment size below that required for the assay.

A second potential sample defect is the presence of cross-links, even at as low a level as 2.5%. This leads to errors in DNA production by polymerase enzymes in fragments larger than 200 bp. Lehmann and Kreipe have shown that a 300 bp fragment was not detectable whereas an 80 bp fragment generated strong signal on real-time PCR (Lehmann and Kreipe, 2001). Neither of these two sample defects appears significant as all reactions amplified successfully and subsequent control stages indicated that amplification was successful (Figure 2.4 and 2.6).

DNA degradation is a third unfavourable consequence of fixation that inhibits PCR amplification (Crisan and Mattson, 1993; Wu *et al.*, 2002). We carried out genomic DNA purification using Qiagen DNeasy Blood & Tissue Kit, a well-established method, with slight modification to the protocols for QGPlex, as recommended by Affymetrix using a prolonged 3-day treatment with Proteinase K. As a result, all our FFPE samples gave a reasonably good 260/280 ratio above 1.8 considered sufficient for analysis by the manufacturer.

Branched DNA methods used in the QGPlex assays have been shown to be less affected by formalin fixation and DNA degradation, contributing to the assay being more sensitive than real time PCR (Yang *et al.*, 2006). Strong signal generated by sandwich nucleic acid hybridization allows detection of low concentrations of target molecules that are not amplifiable by normal PCR. Despite these advantages, we could

not determine whether branched DNA was more sensitive due to difficulties in identifying suitable reference gene for estimation of copy number.

The limited amount of tissue obtained in a biopsy of OPMD also hinders analysis. The characteristics of the QuantiGene Plex assay should make it ideal for limited tissues such as OPMD. Despite some initial difficulties with this novel assay and with the help of the manufacturer, we were able to obtain a signal from a total of 36 samples and simultaneously assessed 10 genes in one experiment.

2.5.2 Internal assay validation

In QGPlex, as noted in the methods, there are no intermediate validation steps to demonstrate correct progression of the assay. The manufacturer does not recommend any sample quality assessment because the assay sample is whole tissue. However, experiments with cell lines and some tissue samples produced apparently valid results that could not have been produced had any of the intermediate stages failed completely. As shown in Table 2.8, 2 cell lines (HSC3, MCF7) and 2 FFPE samples (S2 and S20) worked sufficiently well to give a coefficient of variation within manufacturer's limits and it was possible to detect the effect of sonication of samples in three cases. We therefore conclude that the assay was performing as expected and that the 9 failed samples are most likely to have failed because of inadequate or insufficient sample. The latter seems likely because repeated failed assays in the early pilot stages consumed much of the sample available.

The samples of normal tissue selected for qPCR were also used in QGPlex and extraction of DNA of good quality (section 2.4.2.1) suggests that the tissue quality in at least these samples was adequate.

No data from the QGPlex or qPCR can be compared with the FISH results discussed in the subsequent chapter, as the samples were independent. It was intended to analyse the same samples but the high variation in the QGPlex and qPCR made further use of the limited tissue impractical.

2.5.3 Normalisation and calibration of results

In both qPCR and QGPlex the estimated gene copy number in our experiments was very dependent on the reference gene used for normalisation. The inclusion of a reference gene for normalisation serves as a method to correct for differing amount of DNA from each sample. Nevertheless, it has been shown here that no single gene can be reliably used as the internal control in either qPCR or QGPlex. This is a well recognised problem (Radonic *et al.*, 2004). Vandesompele *et al.* have recommended the use of multiple reference genes for accurate normalisation (Vandesompele *et al.*, 2002).

In our experiments the measurement of copy number for gene of interest was performed relative to control genes that were specifically recommended by the manufacturers and commercially available for both methods. We found significant differences of copy number when data were normalised independently to RNaseP, TERT and TPM1 suggesting that none of those genes were suitable to be used as a control gene in our material. One possible cause is that these genes are themselves amplified or deleted in the dysplasia and cancer samples. Several studies have shown that TERT and TPM1 can be upregulated in OSCC and may play role in the progression of OPMDs to carcinoma (Toruner *et al.*, 2004; Cervigne *et al.*, 2009; Cheong *et al.*, 2009). However, these reference genes also failed to perform effectively in normal samples so, while this cannot be excluded, it does not appear to be the cause of our variable results.

In the determination of the gene copy number by qPCR, a reference sample with known diploid copy number is included in the calculation as a reference point, also known as calibrator (Livak and Schmittgen, 2001). The use of more than 2 calibrator samples provides results that are more accurate (D'Haene *et al.*, 2010). Accordingly, to address the problem, we formed a group of normal samples comprising 6 FFPE samples of oral mucosa that were histologically confirmed as normal tissue and 4 blood samples from healthy individuals and determined the copy number for all samples using different calibrators (Table 2.18 – 2. 23). The analyses of copy number were performed using 3 reference genes (RNaseP, TERT and TPM1) for normalisation and 2 calibrators; the normal tissue S30 used in the experiment in section 2.4.2.2 and one of the blood samples. The gene copy numbers were most consistent when using blood sample as calibrator. Cukier *et al.* demonstrated that notwithstanding normalisation with an internal control gene run concurrently in a duplex qPCR reaction, the errors of CNV calls were significant and this has been corroborated in other studies (McSherry *et al.*, 2007; Bediaga *et al.*, 2008; Cukier *et al.*, 2009). This may be due to the difference in the quality of genomic DNA derived from blood samples compared to archival tissues, as the blood has not been fixed in formalin (Cukier *et al.*, 2009). A reference sample was not a critical element in the estimation of copy number by the QuantiGene method, which gives it a theoretical advantage over qPCR.

Results obtained from QuantiGene and real-time PCR were compared and the copy numbers were discordant between the two techniques. Both methods showed inconsistencies in gene copy number of one gene when normalised to different housekeeping genes and it was considered that neither analysis could be used in our study, in which a change of copy number from 2 to 3 would be expected. It appears that

the final copy number differences were caused in part by methodological differences and in part by failure of reference gene and calibrator, probably to a degree related to formalin fixation and processing.

One final further control would be to perform sequencing to confirm the qPCR for target and reference products as homogeneous and the expected product. While this control was previously considered essential, the consistency of qPCR using modern methods has made this control less important. As all primers and probes were commercially available and have published confirmation, this was not performed in these pilot experiments but might have been considered if the experiments had progressed.

2.5.4 Sample homogeneity

One cause for error in copy number calculation would be differing degrees of dilution of the epithelial different samples by diploid connective tissue. To ensure evaluation of copy number was restricted to epithelial tissues, all samples were macro-dissected. Having a known pure diploid control sample was the most critical factor. A small amount of contamination by connective tissue in each epithelial sample was inevitable because of the presence of dermal papillae and the need to ensure a pure connective tissue sample. Microdissection was checked for larger samples but a minimum of 80% epithelium was our target and an estimate of 20% contamination by volume seems likely.

Final copy number estimates must be whole integers, but the assay outputs in our experiments have been reported to one place of decimals and if can be seen that the

results are often close to half integers, so that small errors in the assays could alter rounding to whole numbers.

2.5.5 Conclusion

Neither qPCR nor QGPlex produced reproducible copy number estimates in our experiments. Tissue and DNA quality were adequate despite tissue processing and small size of samples. The major contributors to the variability were lack of a reliable control gene and failure of calibrator samples. The possible contribution of microdissection and small sample size cannot be assessed from our data.

CHAPTER 3 : Fluorescence *in situ* hybridization

3.1 Investigative plan for ICM DNA ploidy analysis experiments

To evaluate FISH as a measure of copy number variation in OPMD and compare it to ICM DNA ploidy, a panel of 10 FISH probes was tested on a series of dysplastic tissue samples from OPMD. Sample selection was undertaken to ensure a representative range of dysplasia (section 3.3.1) because only a small number of cases could be assessed with this labour intensive technique. From the same list of potential targets described for QGPlex and qPCR (section 2.3.1) a reduced set of 5 targets and 5 matched chromosome specific probes were selected (section 3.3.2) and applied to the tissues (section 3.3.3 and 3.3.4).

FISH proved reproducible (section 3.3.6) and accurate at identifying control diploid samples and low copy number gain in samples considered diploid by ICM DNA ploidy (section 3.4.2) and to identify aneuploidy in almost all known aneuploid samples (3.4.4). The borderline areas between diploid and aneuploid status, low copy number gain, were explored by analysis to determine a threshold for definition of aneuploidy by FISH to apply in future experiments (section 3.4.3 and 3.4.7). FISH also revealed small foci of gene amplification for some targets (section 3.4.5) and there was good concordance between this novel FISH panel and DNA ICM ploidy analysis (section 3.4.6) but poor concordance with dysplasia grade (section 3.4.8).

3.2 Background

In situ hybridization (ISH) has the ability to detect copy number in individual cells on morphologically preserved tissue sections. This allows selection of specific cells for analysis and direct comparison with dysplasia assessment. It provides information on both the number of sequences present and their localisation, the latter depending on the technique used to demonstrate hybridisation. Fluorescence *in situ* hybridization (FISH) has been the preferred method in cytogenetics because it generates bright fluorescent signals facilitating enumeration of chromosomal aberrations.

Evaluation of total nuclear DNA content by image-based ploidy analysis has been shown to correlate with dysplasia and malignant transformation in oral potentially malignant diseases (Torres-Rendon *et al.*, 2009; Bradley *et al.*, 2010; van Zyl *et al.*, 2012; Sperandio *et al.*, 2013). Image-based analysis is currently preferred for routine clinical analysis because it can be performed on archival paraffin embedded samples, allows control of which areas of epithelium are analysed and provides the ability to separate and compare epithelial nuclei against internal control nuclei. However, the process is relatively slow and an automated high throughput analysis would have advantages. *In situ* hybridisation with multicolour visualisation agents is now an automated process available on several different laboratory platforms. We therefore undertook an investigation of a multiplex FISH and compared it with DNA image-based cytometry (ICM) ploidy analysis.

3.2.1 Fluorescence *in situ* hybridization

FISH is a robust technique that can be applied to metaphase or interphase nuclei allowing visualisation of chromosomes, genes and other specific DNA sequences at a single cell level. Its high sensitivity and specificity has made FISH a useful tool in the

clinical setting for screening of genetic aberrations in prenatal, paediatric and adults, to diagnose and monitor disease progression and to predict prognosis. In research, it has been widely used for gene mapping, the study of chromosome evolution and a second technique to confirm the findings of other molecular screening assays.

The principle of *in situ* hybridization is the specific annealing of labelled DNA or RNA probes to complementary sequences of interest in the target tissue (Figure 3.1). Depending on the application, the probes may target unique or repetitive DNA sequences, entire chromosome arms, or whole chromosomes. Attached to the probes are reporter molecules, either a fluorochrome for fluorescence *in situ* hybridization (FISH) or a hapten for chromogenic *in situ* hybridization (CISH), which generate coloured signals viewed under fluorescence or bright field microscope, respectively. Using different colours, multiple sequences or genes can be recognised simultaneously.

One appealing aspect of FISH when performed on interphase cells in cytological preparations or tissue sections is the ability to measure cell-to-cell variability, such as in intra-tumoural heterogeneity and to locate areas bearing a specific sequence in tissue sections. Disadvantages include background normal tissue autofluorescence that may cause difficulties in analysis and relatively rapid fading of fluorescence signals, rendering it unsuitable for prolonged retention of the original stained samples.

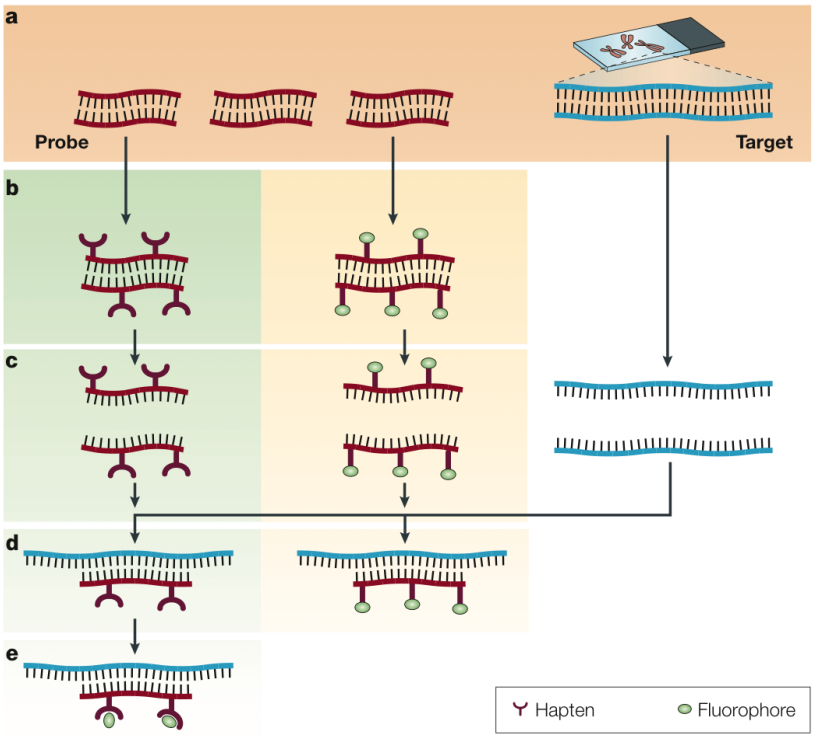

a. Basic elements are DNA probe and a target sequence
b. DNA probe is either labelled directly with modified nucleotides that contain a fluorophore (right) or indirectly labelled with nucleotides containing hapten for CISH (left)
c. The probe and the target DNA are denatured to yield single strandedDNA
d. During hybridization, the probe anneals to complementary sequence in the target tissue
e. An extra step is required for visualization of the non-fluorescent hapten that uses an enzymatic or immunological detection system.

Adapted from Speicher and Carter, 2005

Figure 3.1 Principles of DNA in situ hybridisation.

3.3 Materials and Methods

3.3.1 Patients and tissue samples

A sample consisting of twenty cases was selected from diagnostic histopathology reports on the basis of ploidy status determined by routine diagnostic DNA image-based cytometry (ICM) and inclusion of all grades of dysplasia (Table 3.1). 9 samples had been diagnosed between the years 1990 to 1999 and had been used in a previous ploidy study from the department (Sperandio *et al.*, 2013). 11 additional cases were retrieved from the year 2008 to allow at least five years outcome data of malignant transformation to be included. This series of samples was independent of the samples used for ICM DNA ploidy analysis in the present work. Haematoxylin and eosin (H&E) stained slides were re-examined to confirm histological diagnosis, to select and mark areas of representative dysplasia to be scored and to confirm that sufficient tissue suitable for this study was available.

Table 3.1 Dysplasia grades and DNA ploidy status of samples for FISH (n=20)

	DNA Ploidy status	
Dysplasia grade	Diploid	Aneuploid
Mild	2	5
Moderate	4	6
Severe	0	3

3.3.2 Selection and construction of DNA probes

The chromosomal loci selected for assessment of amplifications were based on previous SNPs data that was also referred to for qPCR work (Table 3.2), in combination with published genetic biomarkers of transformation in the literature as discussed in section 2.1.2. A total of the 5 most frequently amplified chromosomal regions were selected for further study. By utilizing pairs of probes labelled with two fluorochromes, 2 loci could be evaluated simultaneously on each tissue section, and we selected two sequences on the same chromosome including one chromosome specific probe for the centromere/ telomere.

EGFR and CCND1 are among the established oncogenes involved in the head and neck carcinogenesis whereas oncogenic trait of TP63 and PTK2 has been recently reported in multiple studies. Besides its main role of degrading extracellular matrix, MMP9 also involves in the epithelial to mesenchymal transition and angiogenesis during tumorigenesis and its expression was associated with dysplastic grading (Fraga *et al.*, 2012; de Carvalho Fraga *et al.*, 2014).

Dual coloured FISH probes were purchased from Cytocell, Cambridge UK. This was the only company that offered custom design probes compatible with our microscope filter sets for FITC/DAPI/Texas Red triple filter. The probe set for chromosome 7 was commercially available while the others, chromosome 3, 8, 11 and 20 were of customized design (myProbes, Cytocell). Development of these probes involved close communication, meetings and documentations of the probes specification in particular, nucleotide locations, signal colour and suitability for formalin fixed tissue embedded in paraffin (Table 3.2).

All probes were generated by the company using multiple bacterial artificial clones (BAC) mapped to the Ensemble genome browser version 69 (http://www.ensembl.org/index.html). DNA probes were labelled directly with Texas Red fluorochrome and fluorescein isothiocyanate (FITC)-labelled peptide nucleic acid was employed for the centromere and telomeric regions, viewed as red and green signals respectively. To confirm that each custom probe pair hybridized specifically to intended targets and without interference between target and chromosome-specific probes, the company performed hybridization to normal metaphase slides confirming specific binding to the same chromosome at the expected location (Figure 3.2).

Table 3.2 Details on the cytogenetic band and BACs clones used to produce probes

Cytoband	Gene	Start base	End base	Clone Length (bp)	Probe Size (kb)
3q28	TP63	189289309	189647536	A=140218 B=155847	358
7p11.2	EGFR	54988969	55283917	A=174060 B=140036	295
8q24.3	PTK2	141622027	142119601	A=133107 B=163598 C=110681 D=138554	497
11q13.3	CCND1	69449043	69676750	A=125866 B=126113	228
20q13.12	MMP9	44427553	44808231	A=122174 B=140036 C=113945	381

TP63 (Red) / 8cen (Green)

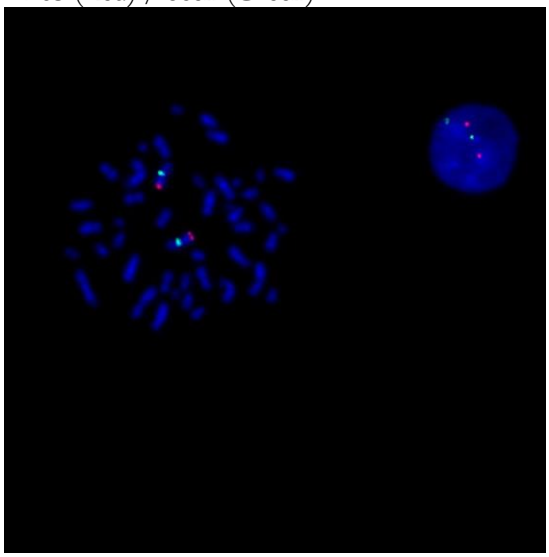

PTK2 (Red) / 8cen (Green)

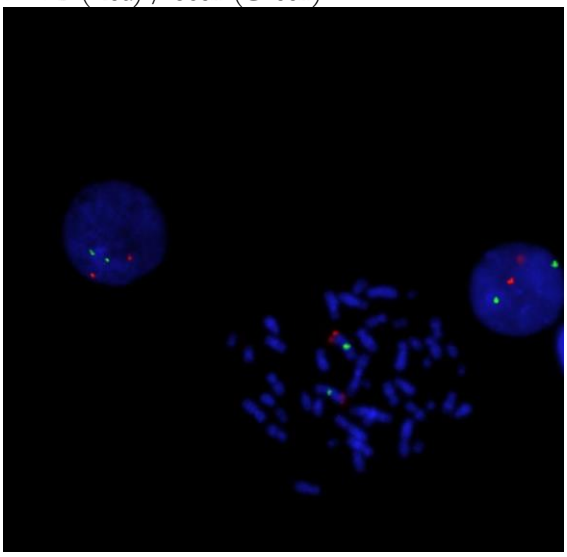

CCND1(Red) / 11cen (Green)

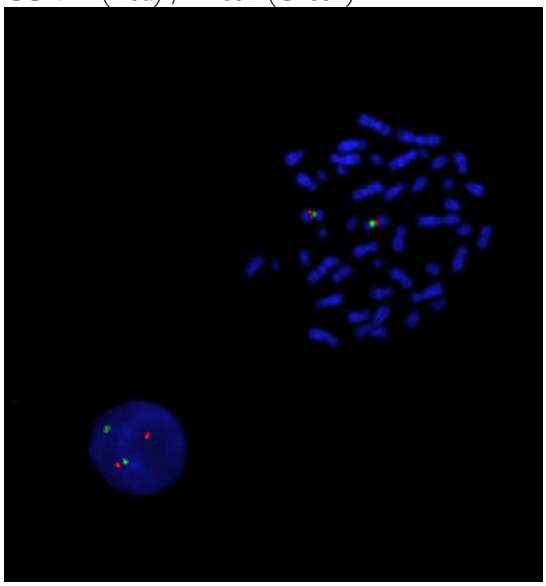

MMP9 (Red) / 20ptel (Green)

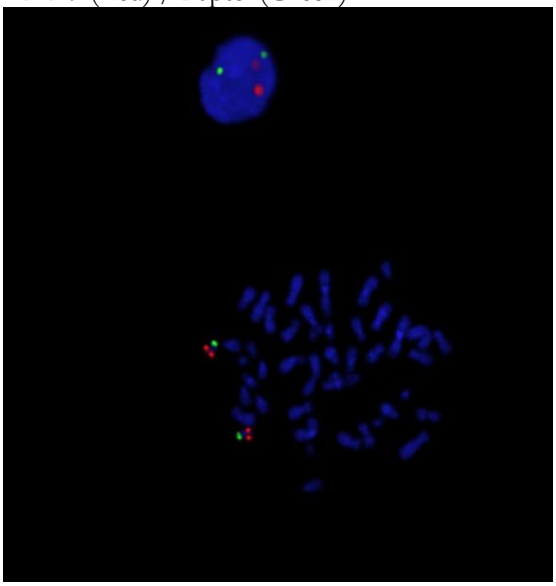

Figure 3.2 Confirmation of probe targets on metaphase and interphase nuclei

3.3.3 Procedure

FISH was performed according to the manufacturer's protocol (Cytocell, Cambridge, UK) with some minor modifications on 5μm paraffin-embedded tissue sections placed on charged slides. To facilitate removal of paraffin, the slides were incubated first in an oven for 15 minutes at 57°C. After deparaffinization in two 5 minutes xylene washes and rehydration in a series of graded ethanols of 100%, 90% and 70% of 2 minutes each, pretreatment was carried out using the Aquarious tissue pretreatment kit to permit probe penetration and binding to the target DNA whilst reducing autofluorescence. This step entailed treatment with Reagent 1 from the kit, in a 95°C waterbath using a Coplin jar for 30 minutes, and enzyme digestion with Reagent 2 on a hot plate at 35°C for 15 minutes, followed by prompt washing with sterile distilled water three times, each wash for 2 minutes.

The specimens were dehydrated consecutively in 70%, 90% and 100% ethanol for 2 minutes each before application of 10ul of undiluted probe (concentration not specified) to the tissue and sealing of the coverslip with rubber solution to prevent drying during overnight hybridization. Denaturation and hybridisation were performed using the Thermobrite StatSpin hybridiser (Abbott Molecular, US) pre-programed for a sequence of 85°C for 5 minutes and then 37°C for 20 hours in a humid environment maintained by dampened humidity control cards inside the lid. After incubation, to remove excess probe, post-hybridization washes were performed sequentially in 0.4xSSC (pH 7.0) followed by a stringent wash at 72°C, 2xSSC/0.05% Tween and PBS both at room temperature, each for 2 minutes. Slides were air-dried and mounted with 10ul of DAPI containing premixed antifade. Slides were stored in boxes in the dark at 4°C until image acquisition within 14 days from the day staining was completed.

3.3.4 Scoring and analysis

Probe signals and nuclear counterstain were viewed using an Olympus BX61 microscope equipped with 4,6-diamidino-2-phenylindole (DAPI), Spectrum Green and Spectrum Red filters. Images were captured at 600x magnification using an Olympus XM10 camera and Olympus Image Cell software. The entire length of epithelium on the section was scanned and a preliminary assessment undertaken to analyse areas showing the greatest copy number changes for each probe pair. Depending on the size and the number of tissue sections per slide, one or more areas were scored. Each area was a consecutive length of basal and parabasal cells. In each case these were also the areas pre-selected to show the most severe morphological changes in routine stains. Nuclei in the underlying connective tissue acted as a methodological and diploid control.

Each area scored comprised 200 consecutive non-overlapping intact nuclei in the basal cell layer and parabasal cell layers up to 5 cell layers superficial to the basement membrane and the same area was scored for each probe in each pair. The number of red and green signals for individual nuclei was counted during the same pass, blind to the histological diagnosis and ploidy status. Nuclei without any signals were excluded.

Counting of signals conformed to conventional cytogenetic practice. Signals that appeared doublet or triplet spots and appeared in contact with each other were counted as one signal only. Adjacent spots had to be at least one signal spot size apart to be counted as separate signals (Figure 3.3). Precise enumeration of clustered signals was not possible, thus each clusters were estimated to comprise of 15 signals per cell for statistical analysis according to the guidelines for EGFR FISH lung cancer and HER2 breast cancer (Hicks and Tubbs, 2005; Varella-Garcia *et al.*, 2009).

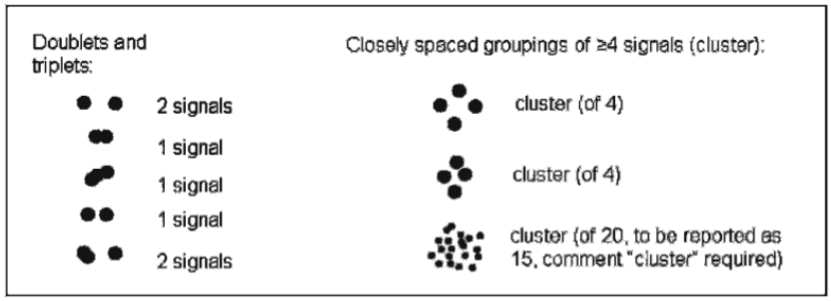

Figure 3.3 Guide for signal enumeration of FISH
(source: Varella-Garcia M *et al.* 2009)

When numerous signals clustered together as a result of gene amplification, the nucleus was classified as aneuploid. Variability in copy number between areas of tissue section in one sample was evaluated when present and the worst copy number aberration was selected as the sample final status. Samples were classified as aneuploid when at least one of the 10-targeted sequences was aneuploid.

3.3.5 Evaluation of possible FISH copy number thresholds to define aneuploidy

For initial analysis, all counts were analysed as absolute counts. To determine whether a cut-off value could be defined to classify borderline cases with possible low copy number gain, threshold values were calculated subsequently as shown in the FISH results, section 3.4.3.

3.3.6 Intraobserver variability

All counts were performed by one operator (ZZ). Duplicate counts were performed using one chromosome specific and one targeted probe on 400 cells from 2 areas in 2 samples, a total of 4% of the total nuclei counted in all experiments. For sample S3 a total of 649 signals were entered into the experimental data and 629 were counted in the duplicate assessment. For sample S5 a total of 630 signals were entered into the

experimental data and 639 were counted in the duplicate assessment, making an overall difference of 29 signals from 2547, a percentage error of 1.14%. How these discrepancies were distributed between copy number are shown in Table 3.3.

Table 3.3 Data from duplicate counting shown as copy number (CN) as a percentage of total cells counted (n=200)

Sample	Count	Tel20p CN %			MMP9 CN %			Mean difference %
		1	2	3	1	2	3	
S3	Test	29.0	61.5	9.5	56.0	44.0	0	2.65
	Duplicate	32.0	60.5	7.5	61.0	39.0	0	
S5	Test	42.0	53.5	4.5	51.0	45.5	3.5	
	Duplicate	40.0	53.5	6.5	52.0	43.0	5.0	

3.3.7 Statistical analysis

The percentage of nuclei containing each copy number was calculated using Excel. SPSS version 21 (SPSS Inc., Chicago, USA) was used to calculate the mean percentage of nuclei with respective copy number for each target and perform receiver-operating characteristic analysis. Power calculation and probability estimates for receiver operating characteristic (ROC) analysis were performed using MedCalc version 15.6.1 (MedCalc Ostend, Belgium). The agreement between ICM DNA ploidy and FISH ploidy results was determined by calculating the κ-statistic.

3.4 Results

3.4.1 Patterns of FISH signals

One tissue sample was excluded after the failure of *in situ* hybridization. A total of 47 tissue areas from 19 samples were evaluated in this study (3 cases with one area assessed, 8 cases with 2 areas, 7 cases with 3 areas and 1 case with 6 areas as size of tissue allowed). 1 additional area was scored for CCND1 only when amplification was found. In every case, all connective tissue cell nuclei were diploid. Detailed counts can be found in the appendix.

3.4.2 Copy number in ICM diploid samples

All samples that had been identified as diploid by DNA image-based cytometry (ICM) (n=7) had FISH results compatible with diploid status, usually with only two signals per nucleus for each probe. Proportion of cells presumed to be in S phase, G2 or mitosis, showed signal counts of three ranging from 0.5% to 14.5% of the total. Only 2 samples (S6 and S7) showed four signals per nucleus of 1% of total cells (appendix). No variations were seen between areas assessed in each case for all probes and these patterns were consistent between all probes, whether centromeric, telomeric or at the specific target chromosomal loci.

The mean percentage of nuclei with two signals or less for all 5 chromosomes specific (centromeric or telomeric) probes ranged from 98.3% to 99.5%. The ranges of mean percentage for nuclei with three and four signals were 0.5% to 1.7% and 0% to 0.13% respectively. For all *in situ* probes, the mean percentage of nuclei with respective copy number and the standard deviation (SD) are shown in Table 3.4.

Table 3.4 Mean percentage nuclei positive for each FISH probe in the ICM DNA diploid dysplasia samples

Mean percentage nuclei positive for each probe in the ICM diploid dysplasia samples and standard deviation with copy number of 2, 3 and 4 on each targeted probe for diploid samples (n=7). A total of 16 areas were evaluated on all samples.

Locus	Copy number ≤ 2		Copy number 3		Copy number 4	
	Mean	SD	Mean	SD	Mean	SD
Cen 3	99.03	1.12	0.84	1.01	0.13	0.29
3q28	99.44	0.54	0.50	0.49	0.06	0.17
Cen 7	98.28	3.63	1.66	3.51	0.06	0.17
7p11.2	98.73	3.06	1.24	2.94	0.03	0.13
Cen 8	98.34	1.01	1.63	0.99	0.03	0.13
8q24.3	98.66	1.17	1.34	1.17	0	0
Cen 11	98.56	1.90	1.41	1.82	0.03	0.13
11q13.3	99.41	0.55	0.59	0.55	0	0
Tel 20p	98.28	2.54	1.63	2.41	0.09	0.27
20q13.12	99.47	1.01	0.47	1.02	0.06	0.17

Means are given in percentage Cen: centromeric; Tel: telomeric; SD: standard deviation

FISH copy number counts of 3 and 4, which might represent low copy number gain, were distributed unequally between samples. All probes identified some nuclei with copy number of 3 and all samples contained some nuclei with copy number 3 with multiple probes (data in appendix). Probes against PTK2 and CCND1 produced no nuclei with 4 signals. The distribution of copy number 4 for each probe and sample is shown in Table 3.5.

Table 3.5 Distribution of nuclei with copy number 4 by FISH probe.

The left two-column shows number of lesions for each target. The right two-column shows the number of probes producing a copy number of 4 for each sample

Locus	Number of samples with copy number 4	Sample	Number of probes showing copy number 4
Cen 3	3	S1	5
3q28	2	S2	2
Cen 7	2	S3	2
7p11.2	1	S4	0
Cen 8	1	S5	0
8q24.3	0	S6	3
Cen 11	1	S7	4
11q13.3	0	-	-
Tel 20p	2	-	-
20q13.12	2	-	-

3.4.3 Calculation of FISH threshold to define aneuploidy

To set a threshold value for aneuploidy based on copy number counts of 3 and 4 (which might represent either diploid or low copy number gain) two methods were used.

Initially, according to a standard method (Kearney, 2001), a percentage limit was set of nuclei with signal counts of 3 or more at 15%. This was derived by calculating the mean percentage cells with counts of 3 or 4 and adding 3x the standard deviation for all ICM DNA diploid samples (original data shown in Table 3.4) and the calculated threshold for each probe is shown in table 3.6 below.

Table 3.6 The total mean percentage nuclei plus three the standard deviation of copy number 3, 4 and 3 & 4 for each probe target

	Mean percentage nuclei + 3SD		
Locus	Copy number 3	Copy number 4	Copy number 3 and 4
Cen 3	3.88	0.99	4.87
3q28	1.97	0.57	2.54
Cen 7	12.18	0.58	12.76
7p11.2	10.06	0.41	10.47
Cen 8	4.60	0.41	5.01
8q24.3	4.84	0.00	4.84
Cen 11	6.86	0.41	7.27
11q13.3	2.26	0.00	2.26
Tel 20p	8.86	0.91	9.77
20q13.12	3.54	0.57	4.12

The final selected threshold was set at the highest percentage found, which was for probe centromeric 7 at 12.8 plus 2.7 estimate of intraobserver error as detailed in section 3.3.6 above, rounded to nearest whole percent.

The second method used to define a threshold was ROC analysis. This was performed by taking the signal counts from all individual areas for the analysis and also by sample using data from the area with highest total count.

Calculation of sample size required for ROC analysis showed that in order to achieve type 1 error rate of 0.05 (incorrect rejection of the null hypothesis) and type 2 error at 0.2 (incorrect acceptance of the null hypothesis), a total of 105 aneuploid and 62 diploid results would have been required. The number of samples available can only achieve a probability of distinguishing diploid from aneuploid of 0.75. Analysis by area provides 46 samples and has equivalent probability of 0.8. This calculated threshold was therefore used for initial analysis.

ROC analysis revealed an area under the curve of 0.988 (insufficient data to calculate confidence interval) based on sample data and 0.951 (95%CI 0.89-1.00) based on area data. The minimum distance value to identify the optimum threshold (balancing sensitivity and specificity) was 0.032, providing a sensitivity of 0.833 (95%CI: 0.73-0.94) and specificity of 0.938 (95%CI: 0.87-1.00).

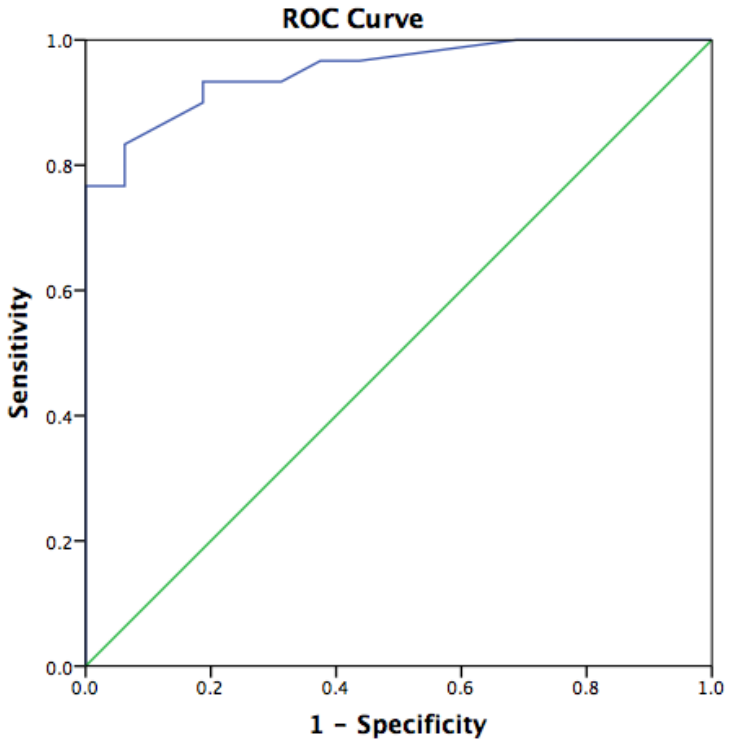

Figure 3.4 Receiver operating characteristic curve (blue line) for 3 or more signals data of all sample areas scored on FISH.

Table 3.7 The possible cut-off points obtained from ROC analysis to be used as a threshold to define FISH aneuploidy.

Cut off points	Sensitivity	Specificity
3.50	0.96	0.62
4.25	0.93	0.68
5.25	0.93	0.75
6.50	0.93	0.81
7.25	0.90	0.81
10.25	0.83	0.93
13.75	0.80	0.93
14.75	0.76	0.93
17.50	0.76	1.00
20.50	0.73	1.00

3.4.4 Copy number in ICM aneuploid samples

In contrast to ICM DNA diploid samples, heterogeneous patterns of copy number change were evident in ICM DNA aneuploid dysplasia samples as demonstrated by variation in copy number for individual probes, centromeric chromosomal probes and differences in the proportion of nuclei displaying them (detailed count data in the appendix). Compiled data is shown in Figure 3.5.

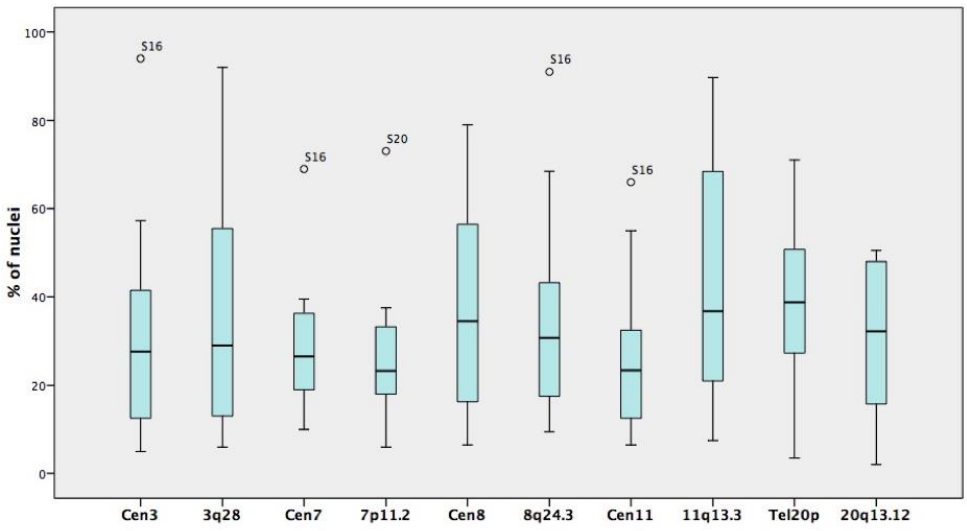

Figure 3.5 Percentage of nuclei with copy number of 3 or more in the ICM DNA aneuploid dysplasias.
Boxplot (horizontal line: median; box length: interquartile range; whisker: smallest and largest values; o; outlier). n=12.

FISH against centromeric loci on chromosomes 3, 7, 8, 11 and telomeric loci on chromosome 20p revealed relatively frequent copy number changes of three and four copies, found in between 10% and 30% of cells in all samples. Cells containing 2 copies were predominant (Figure 3.6 and 3.7). This pattern was also seen on the corresponding specific target loci on all chromosomes. Signal counts of five and more per nucleus were found in most cases but were detected at only low frequency, with a percentage of less than 5%. The highest copy number for any locus per nucleus was 12 but this was a rare

occurrence and cells with only one or two copies of each locus were predominant in most samples (Figure 3.6 to 3.9). Mean copy number per nucleus ranged from 1.32 to 11.54 (appendix). Figure 3.8 and 3.9 show example of aneuploid samples.

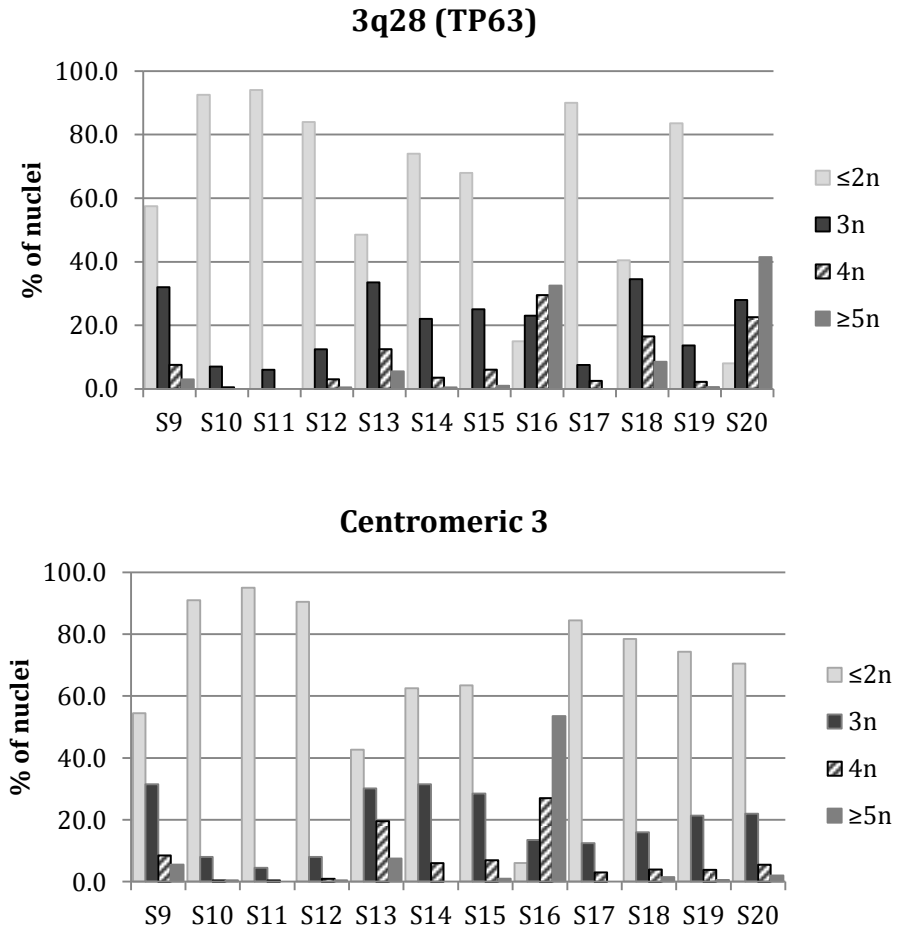

Figure 3.6: Example of compiled data for copy number (n) detected by FISH for chromosome 3
The probes against 3q28 (upper panel) and the corresponding centromeric 3 probe (lower panel) on ICM DNA aneuploid samples (n=12) showing the percentage of nuclei with different copy numbers.

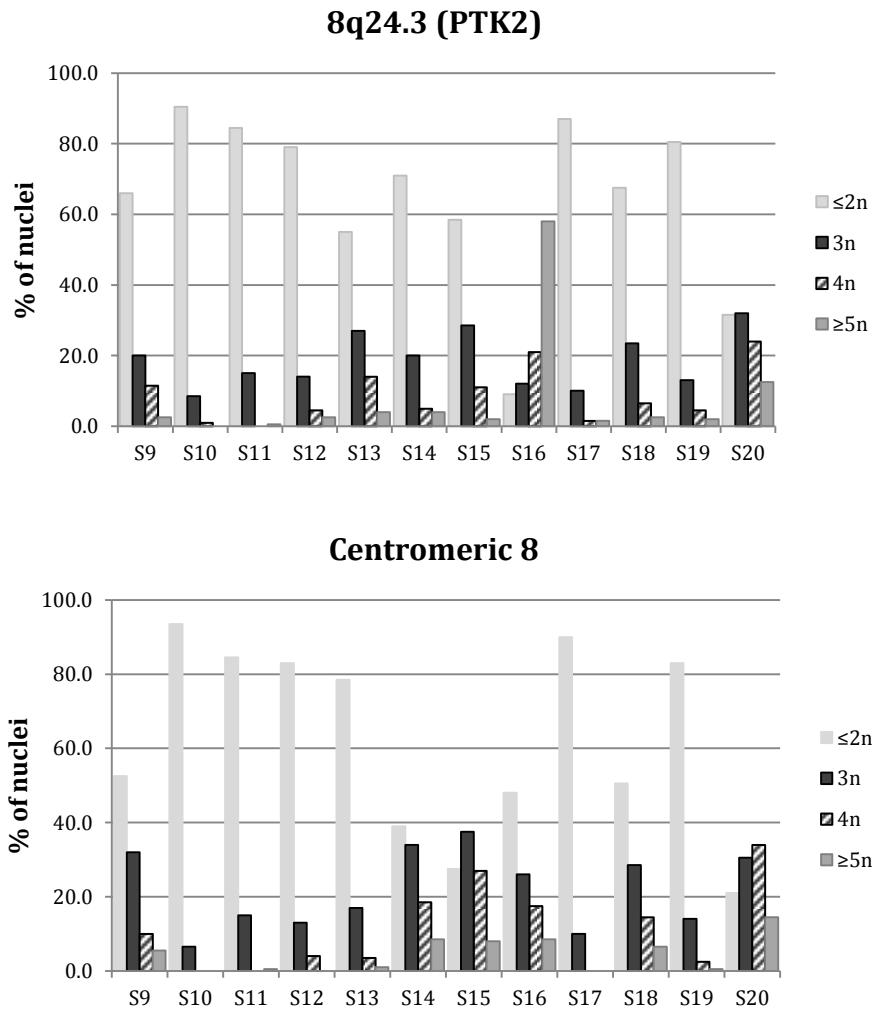

Figure 3.7: Further example of compiled data for copy number (n) detected by FISH for chromosome 8

The probes against 8q24.3 (upper panel) and the corresponding centromeric 8 probe (lower panel) on ICM DNA aneuploid samples (n=12) showing the percentage of nuclei with different copy numbers..

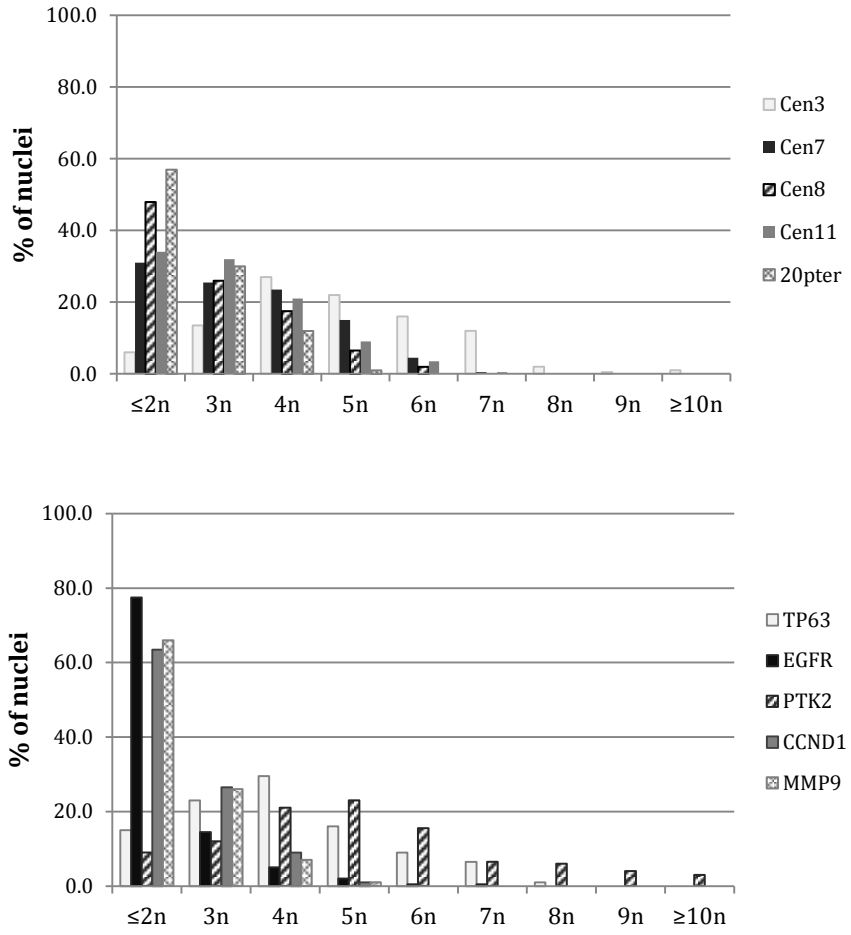

Figure 3.8: Example of FISH copy number assessment for a single dysplastic lesion. Results for all 10 FISH probes on sampleS16, an ICM DNA aneuploid sample showing the main aberrations to be copy number 3 and 4. Nuclei with signals of more than 5 per nucleus detected mainly on chromosomes 3, 7, and 8. Centromeric or telomeric probes (upper panel), gene specific probes (lower panel).

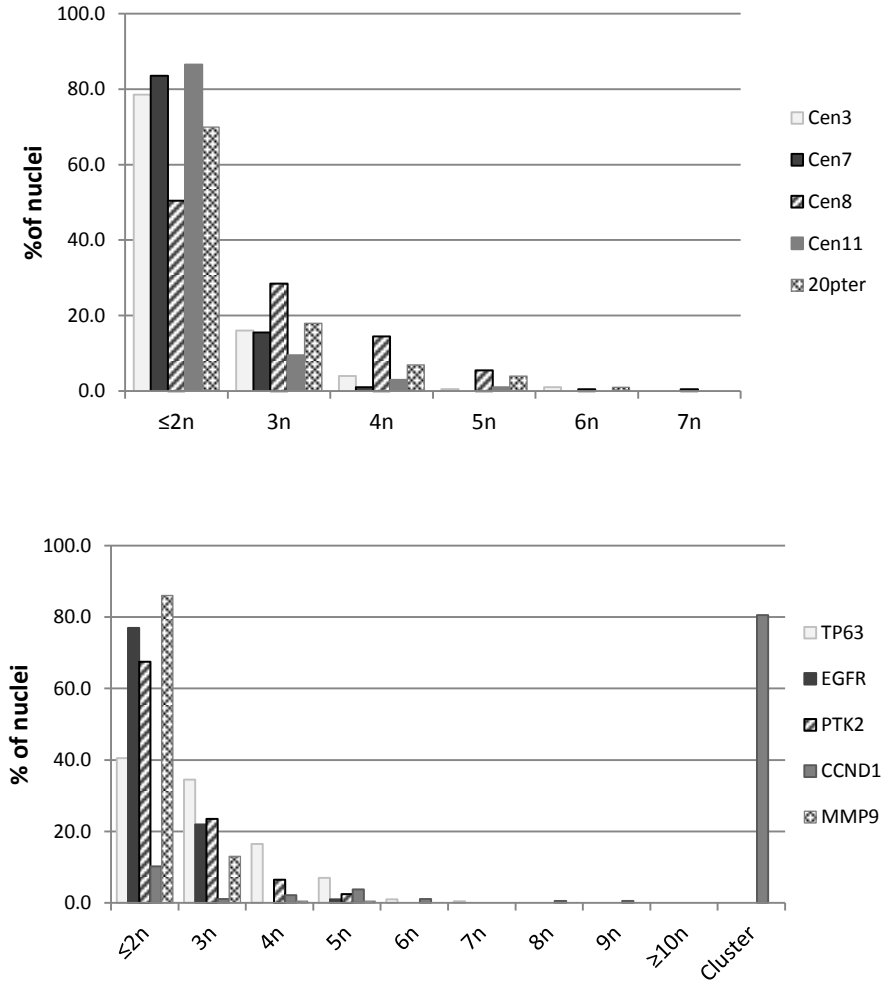

Figure 3.9: Second example of FISH copy number assessment for a single dysplastic lesion.
Sample S18, an ICM DNA aneuploid sample showing aneuploidy defined by FISH signals of three and more per nucleus detected on chromosomes 8, 20 and gene amplification for CCND1. Centromeric or telomeric probes (upper panel), gene specific probes (lower panel).

3.4.5 Gene amplification

Gene amplification was seen as tight clusters of overlapping signals, too many to count accurately. This was a relatively infrequent change seen only with EGFR and CCND1. Of the 12 dysplastic lesions, one contained a single area that demonstrated amplification of EGFR that was sharply demarcated and not seen in adjacent epithelium, was not present in separate tissue slices on the same slide and was not in the area showing the most severe dysplasia in routine stains (Figure 3.10).

CCND1 amplification was found in four lesions of which one was the same lesion that showed EGFR amplification. Amplification was found in all three areas scored in one case (S18), five out of six areas in the second case (S20), two of four areas in the third case (S17) and only one of three areas assessed in the fourth case (S13). A sharp demarcation between areas of amplification and adjacent areas without gene amplification was observed in two cases. CCND1 amplification was more frequent in the single sample (S20) that showed both EGFR and CCND1 amplification, where clustered signals were detected in five areas compared to only one area in which EGFR amplification was found (Figure 3.11).

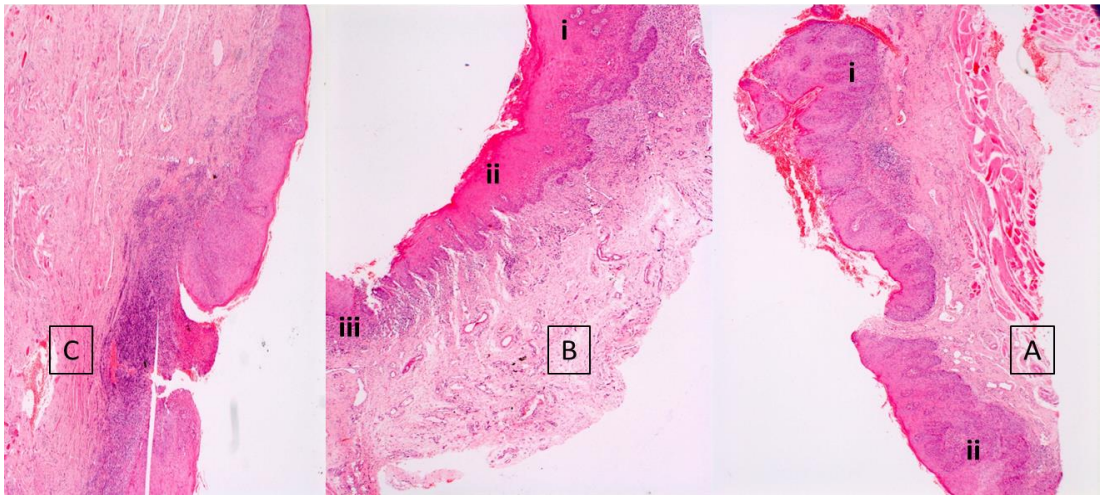

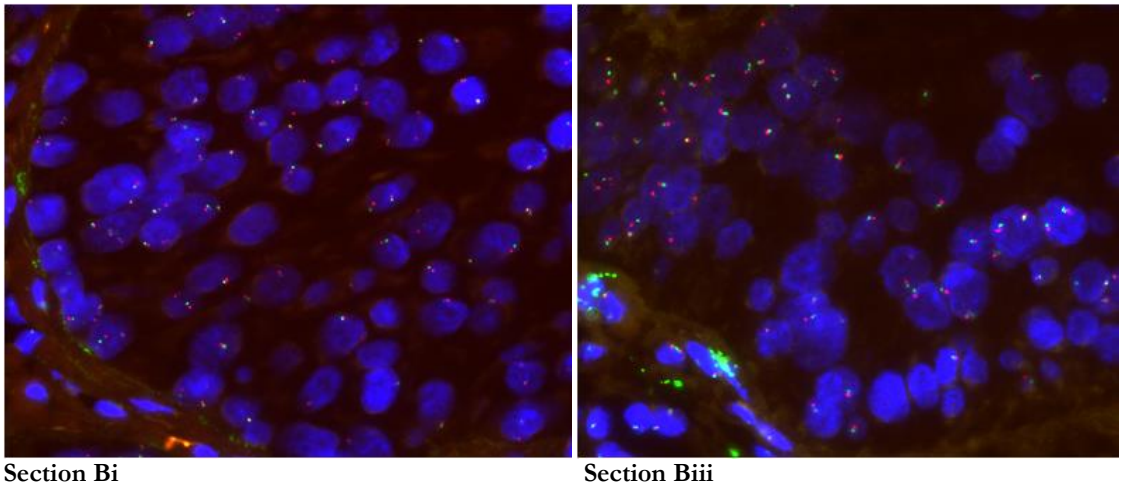

Section Bi Section Biii

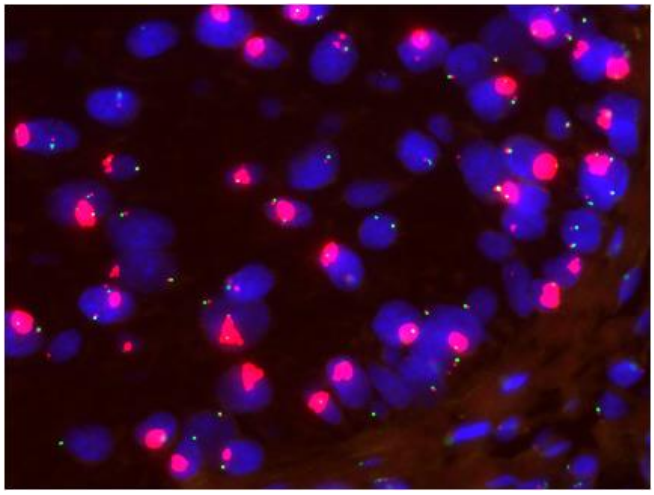

Section Bii

Figure 3.10 The single lesion showing EGFR amplification.
Upper panel: H&E of S20 showing the six areas for scoring. EGFR amplification was observed in section Bii only and on each sidet issue in Bi and Biii were FISH diploid.

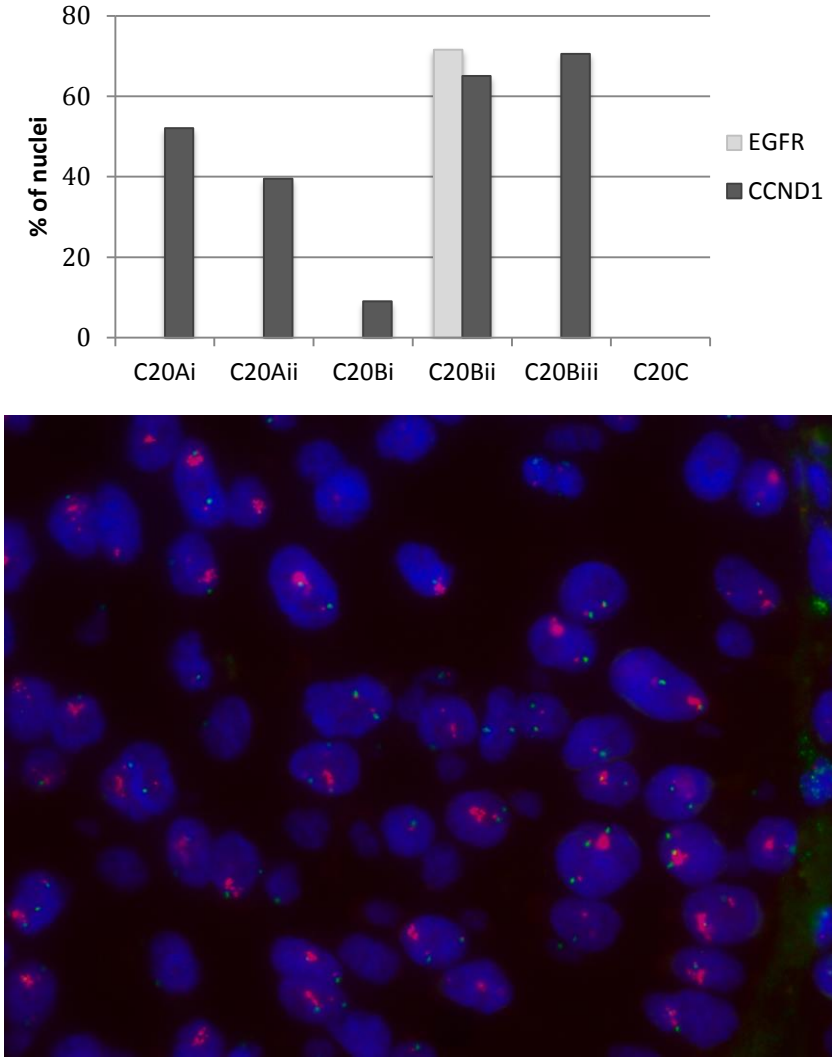

Figure 3.11 The sample showing amplification of EGFR and CCND1

Upper panel shows that sample S20 was the only sample that showed amplifications of both EGFR and CCND1. Lower panel shows example of CCND1 amplification seen by clustered FISH signals for CCND1 in section Aii of sample 20. This area was FISH diploid as assessed by the probe against EGFR. Red signals CCND1, green signal centromeric C11.

3.4.6 Comparison between detection of aneuploidy by ICM and FISH

The results of ICM DNA ploidy and FISH were compared to determine whether FISH had successfully detected the expected copy number and cell count to account for the total nuclear DNA content seen in the ploidy histograms. The total aneuploid cells detected by FISH ranged from 5% to 59%, and FISH detected fewer aneuploid cells from the aneuploid stem peak than ICM DNA ploidy in 8 cases. This data is shown in Table 3.8 together with the values of parameters acquired from ICM DNA ploidy analysis.

Table 3.8 Comparison between ICM DNA ploidy parameters and FISH on ICM DNA aneuploid
Comparison using the calculated aneuploid threshold of 15% copy number 3 or 4. The misclassified sample discussed below in section 3.4.7 is in red

Case no.	Diploid index of stem peak(s) on ICM	% epithelial cells in stem peak on ICM	% 5c exceeding frequency on ICM	Total % aneuploid epithelial cells on ICM	Total % aneuploid cells on FISH (all probes)	No. of FISH probes showing aneuploidy
S9	1.9 2.2	13 3*	1.00	17	33.7	10
S10	**1.88** **2.2**	**47** **8***	**4.0**	**59**	**5.0**	**0**
S11	1.1	29	0	29	6.7	4
S12	1.6	10	0.4	10.4	12.0	9
S13	1.8	42	3.1	45.1	27.4	10
S14	2.0	22	1.8	23.8	29.7	10
S15	3.5	87	11.1	87	47.4	10
S16	2.8	11	11.5	22.5	59.3	10
S17	1.8	44	8.9	52.9	10.7	6
S18	1.6	15	0.8	15.8	24.2	9
S19	2.18	51	11	62	19.6	9
S20	1.6	66	10.1	76.1	37.7	9

* peaks do not meet diagnostic threshold of 10% for diagnosis of aneuploidy alone, diagnosis based on larger peak.

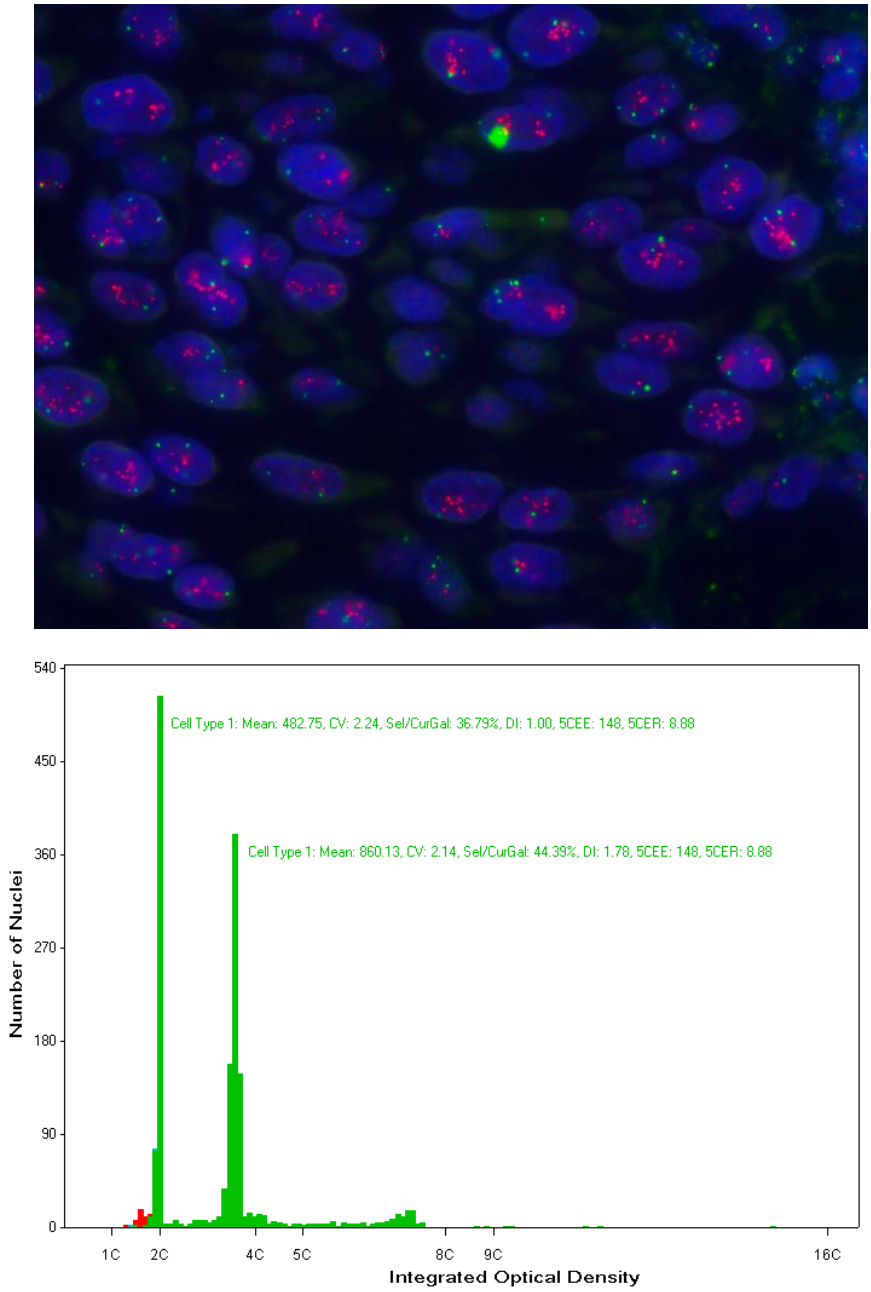

Figure 3.12 Example comparison between ICM DNA ploidy and FISH for sample S17. Ploidy histogram plotting number of nuclei against DNA content (as optical density) in lower panel; 2c indicates diploid DNA complement. An aneuploid peak comprising 44.4% of the epithelial nuclei is present at diploid index of 1.78 and there is a 5c-exceeding rate of 8.9% of the total epithelial nuclei, both of which individually define aneuploidy. FISH on the same sample (upper panel) shows CCND1 FISH signals (in red) ranging from 3 to 15 signals per nucleus, mean signals 8.57 (raw data shown in appendix).

3.4.7 Evaluation of FISH threshold value to discriminate diploid and aneuploid samples

When the calculated threshold of 15% of cells with copy number 3 or 4 was applied to the raw data, 8 cases were classified as diploid and 11 as aneuploid, misclassifying one aneuploid sample (S10) as diploid. All ICM DNA diploid samples were confirmed as diploid using all in situ probes so that the results were concordant between FISH and ICM in 18 out of 19 samples (94.7%, Table 3.9).

Table 3.9 Concordance between assessment of DNA ploidy by FISH and ICM
Concordance with ploidy status defined by threshold count of 3 and 4 of more than 15% for any one probe

		ICM (reference)		
		Aneuploid (+)	Diploid (-)	Total
FISH (test)	Aneuploid (+)	11	0	11
	Diploid (-)	1	7	8
	Total	12	7	19

Agreement 94.7%; κ value 0.89

When a 10% threshold limit was applied following ROC analysis (see Table 3.11 below) the ICM DNA aneuploid case misclassified as diploid by FISH using the 15% threshold was classified as aneuploid, in agreement with the reference test. However, one sample (S1) classified as diploid at the 15% threshold was classified as aneuploid by FISH.

Based on the calculated threshold of 15% (section 3.4.3), one ICM aneuploid sample (S10) did not show copy number imbalances at any of the chromosomal loci

investigated and had a borderline percentage of nuclei with 3 or more signals at 13% for the telomeric probe against chromosome 20 only (Table 3.10).

When the 10% threshold was applied, the sample S10 had 4 probes producing aneuploid results. Overall the data in Table 3.10 shows that ICM DNA aneuploid samples have high proportions of cells with FISH copy number 3 or more whichever threshold is applied.

Table 3.10 Percentage of nuclei showing copy number 3 or more on all probes for ICM aneuploid samples.
The misclassified sample S10 discussed below is shaded.

Sample	Cen3	TP63	Cen7	EGFR	Cen8	PTK2	Cen11	CCND	Tel 20p	MMP9
S9	45.5	42.5	28.0	32.0	47.5	34.0	29.5	33.0	41.5	47.5
S10	9.0	7.5	10.5	6.0	6.5	9.5	10.5	12.0	13.0	6.0
S11	5.0	6.0	21.5	17.5	15.5	15.5	6.5	7.5	3.5	2.0
S12	9.5	16.0	28.0	23.5	17.0	21.0	18.5	21.0	30.5	30.5
S13	57.3	51.5	34.5	37.5	21.5	45.0	17.5	64.0	40.0	49.5
S14	37.5	26.0	23.5	25.0	61.0	29.0	33.5	37.0	37.5	38.0
S15	36.5	32.0	39.5	34.5	72.5	41.5	31.5	64.0	71.0	50.5
S16	94.0	85.0	69.0	22.5	52.0	91.0	66.0	36.5	43.0	34.0
S17	15.5	10.0	38.0	6.0	10.0	13.0	28.2	72.9	61.5	18.5
S18	21.5	59.5	16.5	23.0	49.5	32.5	13.5	89.7	30.0	14.0
S19	25.7	16.4	25.0	18.5	17.0	19.5	11.5	21.0	24.5	17.5
S20	29.5	92.0	10.0	73.0	79.0	68.5	55.0	83.0	58.5	48.5

The 12 samples known to be aneuploid on ICM DNA ploidy analysis showed a range of copy number aberrations that varied between loci and chromosomes (Table 3.11). Five samples were consistently aneuploid for all targeted probes. Most were confirmed as aneuploid by more than one in situ probe but one (S10) proved to have a normal diploid copy number for all probes tested in all 3 areas assessed so that FISH failed to detect known aneuploidy in this one lesion. In 6 ICM aneuploid samples,

between 1 to 6 probes showed FISH diploid. The classification result by individual probe is shown in Table 3.11. The effect of applying the 10% ROC threshold is shown by highlighting the changed results in red.

Table 3.11 Application of the calculated threshold detection limit of 15%
Application of 15% threshold to determine FISH ploidy status for all samples using all 10 probes. The results changed to aneuploid by applying the 10% threshold are shown in red.

No	Chromosomes										Total probes		Dx
	Cen 3	3q28	Cen 7	7p11.2	Cen 8	8q24.3	Cen 11	11q13.3	Tel 20p	20q13.12	D	A	
S1	D	D	**D**	**D**	D	D	D	D	D	D	10	0	**D**
S2	D	D	D	D	D	D	D	D	D	D	10	0	D
S3	D	D	D	D	D	D	D	D	D	D	10	0	D
S4	D	D	D	D	D	D	D	D	D	D	10	0	D
S5	D	D	D	D	D	D	D	D	D	D	10	0	D
S6	D	D	D	D	D	D	D	D	D	D	10	0	D
S7	D	D	D	D	D	D	D	D	D	D	10	0	D
S9	A	A	A	A	A	A	A	A	A	A	0	10	A
S10	D	D	**D**	D	D	D	**D**	**D**	**D**	D	10	0	**D**
S11	D	D	A	A	A	A	D	D	D	D	6	4	A
S12	D	A	A	A	A	A	A	A	A	A	1	9	A
S13	A	A	A	A	A	A	A	A	A	A	0	10	A
S14	A	A	A	A	A	A	A	A	A	A	0	10	A
S15	A	A	A	A	A	A	A	A	A	A	0	10	A
S16	A	A	A	A	A	A	A	A	A	A	0	10	A
S17	A	D	A	D	D	D	A	A	A	A	4	6	A
S18	A	A	A	A	A	A	D	A	A	A	1	9	A
S19	A	A	A	A	A	A	D	A	A	A	1	9	A
S20	A	A	D	A	A	A	A	A	A	A	1	9	A
Total A	9	9	10	10	10	10	8	10	10	10	n/a	n/a	n/a

No: sample number; D diploid; A aneuploid; Dx overall diagnosis;
Cen: centromeric; Tel: telomeric

The ICM DNA ploidy histogram for the two borderline samples that give different results depending on the threshold cut off for counts of 3 and 4 are shown in Figure 3.13.

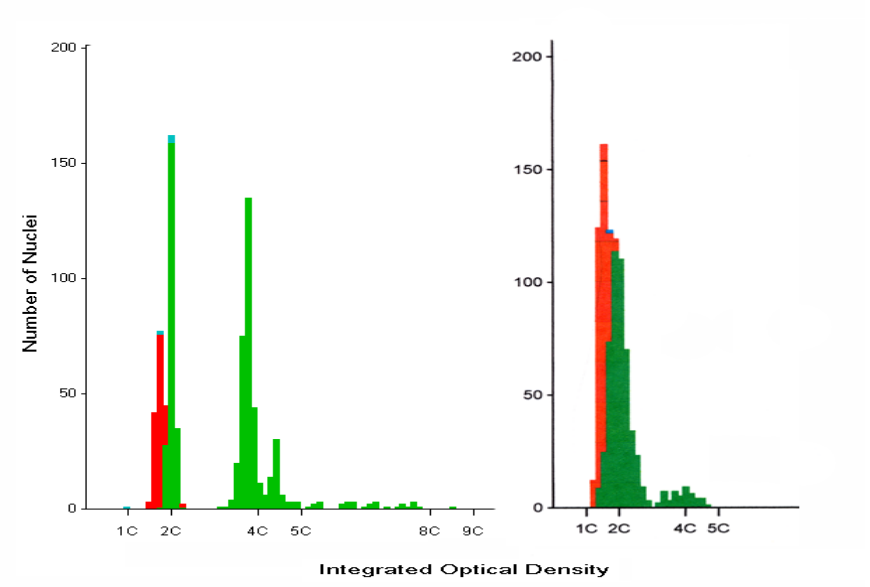

Figure 3.13 ICM DNA ploidy histograms for FISH misclassified samples
Sample S10 left, sample S1 right

Sample S10 has a good coefficient of variation of 2.98 for the diploid peak and a major aneuploid peak at diploid index of 1.88 containing 47% of the total of 610 nuclei classified, a minor peak at diploid index 2.2 containing 8.2% of nuclei and a 5c exceeding rate of 3.98. The ICM DNA ploidy classification is aneuploid based on both the presence of the major peak exceeding 10% and a 5c exceeding rate above 1%. This sample is clearly DNA aneuploid.

Sample S1 has a poor coefficient of variation of 9.9 for the diploid peak and a series of minor peaks in total comprising 9.98% of the total epithelial nuclei with an average diploid index of 1.95 and a 5c exceeding rate of 0. The high CV of the diploid peak is not accounted for by poor sample because the three minor peaks are well defined. This

histogram is therefore borderline for aneuploidy because the aneuploid cell total just fails to exceed 10% of the total.

3.4.8 Comparison between dysplasia and FISH results

The concordance between dysplasia grade and FISH results is shown in Table 3.12 and 3.13 in terms of the number of probes aneuploid and the final FISH diagnosis.

Table 3.12 Number of probes producing aneuploid results by dysplasia grade using the calculated threshold of 15% and the ROC threshold of 10%.

Dysplasia grade	Sample number	ICM DNA ploidy	Number of FISH probes showing aneuploidy at 15% threshold	FISH diagnosis at 15% threshold	Number of FISH probes showing aneuploidy at 10% threshold	FISH probes diagnosis at 10% threshold
Mild	S1	Diploid	0	D	2	A
Mild	S2	Diploid	0	D	0	D
Mild	S9	Aneuploid	10	A	10	A
Mild	S10	Aneuploid	0	D	4	A
Mild	S11	Aneuploid	4	A	4	A
Mild	S12	Aneuploid	9	A	9	A
Moderate	S3	Diploid	0	D	0	D
Moderate	S5	Diploid	0	D	0	D
Moderate	S6	Diploid	0	D	0	D
Moderate	S7	Diploid	0	D	0	D
Moderate	S13	Aneuploid	10	A	10	A
Moderate	S14	Aneuploid	10	A	10	A
Moderate	S15	Aneuploid	10	A	10	A
Moderate	S18	Aneuploid	9	A	9	A
Moderate	S19	Aneuploid	9	A	9	A
Moderate	S20	Aneuploid	9	A	9	A
Severe	S4	Diploid	0	D	0	D
Severe	S16	Aneuploid	10	A	10	A
Severe	S17	Aneuploid	6	A	6	A

A aneuploid; D diploid

Table 3.13 Compiled data for concordance between dysplasia grading and FISH defined by threshold count 3 and 4 of more than 15% for any probe

		FISH			Mean FISH aneuploid*
		Diploid	Aneuploid	Total	
Dysplasia grade	Mild	3	3	6	3.8
	Moderate	4	6	10	5.7
	Severe	1	2	3	5.3
	Total	8	11	19	n/a

* Mean number of FISH probes aneuploid per sample

Agreement 57.9%; κ value 0.06

3.5 Discussion

3.5.1 Samples

In this study, cases were selected to represent all grades of dysplasia. These samples are independent from the sets described in the other chapters and were initially selected as a pilot study or training set to evaluate FISH. Information on malignant transformation of all cases was not known.

3.5.2 Probes

Previous investigators in this area have traditionally focused on genes that are thought to play specific roles in malignant progression or in carcinoma. In this study a different approach has been taken to select chromosomal loci. We have selected chromosomal regions on the basis of amplification and not the genes located within them using data from a previous longitudinal analysis described in section 2.3.1 in combination with published data.

A total of the 5 most frequently amplified chromosomal locations suitable for FISH were selected from our wider panel (see Table 3.2) to produce our test set of 3q28, 7p11.2, 8q24.3, 11q13.3 and 20q13.12. The sequences within or adjacent to these regions selected for probe construction were within the following genes respectively; TP63, EGFR, PTK2, CCND1 and MMP9. All these genes are involved in the essential processes in development of cancer according to Hanahan and Weinberg (2011). However, these genes were chosen for their good characterisation and location rather than any putative role in malignant transformation of oral potentially malignant diseases.

While the genes for EGFR and CCND1 have been used in previous similar studies (Taoudi Benchekroun *et al.*, 2010; Poh *et al.*, 2012), the probes for 3q, 8q and 20q are

novel for this purpose. Two other studies have evaluated EGFR copy number using dual coloured FISH probe from Vysis, which have been used frequently in studies of other tumour types. These probes were incompatible with our fluorescence microscope photography system. However, results obtained with these probes should be comparable to our studies because probes are similarly sized (Vysis 303kb at 7p12; Cytocell 295kb at 7p11.2) though the sequences differ.

With each specific locus, a paired probe on the same chromosome was added in an attempt to determine whether amplifications detected reflected duplication of large pieces or whole chromosomes. Four were centromeric and one telomeric. Centromere-specific probes contain short repetitive sequences that are ideal to assess numerical aberrations in interphase analysis, but provide no data on presence of chromosome arms. Cross-hybridisation is a recognised problem with some centromeric probes (Kearney, 2001), thus for chromosome 20, a telomeric probe was selected. Although telomeres shorten with each cell division, as many as 90% of human cancer cells have telomeres of equivalent length to the adjacent normal tissues (Shay and Wright, 2011). Increase in centromeric probe copy number is normally considered to indicate chromosomal duplication, though this is an assumption (Werner *et al.*, 1997; Tibiletti, 2007).

3.5.3 Method

We have successfully carried out FISH, which follows the standard procedure commonly applied in a cytogenetic laboratory. Through a series of preliminary experiments, we optimized the duration of incubation in tissue pre-treatment solution reagent 1 (Cytocell, Cambridge UK) and enzyme digestion (section 3.3.3). These steps are critical for successful FISH on FFPE section to unmask the nucleic acids and allow

the probe to penetrate and hybridize to the target. It is highly dependent on the tissue types and formalin fixation times and optimization is necessary due to inter-laboratory variations on tissue handling (Chin *et al.*, 2003).

The recommended minimal number of cells scored should involve 100 nuclei (Summersgill *et al.*, 2008), which we have met and exceeded by evaluating 200 nuclei in this study. This is a common practice in the literature and this study has counted more cells than 2 previous studies of oral premalignant lesions (Taoudi Benchekroun *et al.*, 2010; Siebers *et al.*, 2013), and the same number as one (Poh *et al.*, 2012).

3.5.4 Results

One case failed in situ hybridisation after multiple attempts using probes targeting chromosomes 7 and 3. Possible reasons include tissue fixation using formalin and the age of the specimen. Tissue fixation might had been handled differently or the use of non-buffered formalin as fixative. Potential reasons for this are included in the discussion of DNA quality in section 2.5.1, QGPlex and qPCR chapter but the failure remains unexplained.

3.5.5 ICM DNA diploid samples

All samples had known ICM DNA status prior to FISH. ICM DNA diploid samples had FISH copy number counts consistent with this reference standard diploid status. Only a signal count of 5 or higher, which was not found, would be an absolute indicator of aneuploidy based on FISH alone. Whether copy numbers of 3 and 4 represent low copy number gain cannot be assessed by comparison with DNA ploidy data without risking a circular reasoning error. The proposed threshold for definition of aneuploidy is discussed in section 3.4.3.

3.5.6 ICM aneuploid samples

It is striking that aneuploid samples rarely showed copy number gains of five or higher. In this study, counts from 10 probes have been used and these results have to be compiled into single diagnoses of diploid or aneuploid to apply to a single dysplastic lesion. The multiple areas counted and multiple probes used increased the number of aneuploid cells detected and the additional loci gave added confidence to the categorization of each sample. Amplification involved several loci for all samples that were aneuploid except one, which has no counts above copy number 5.

Stem lines of aneuploid cells on ICM DNA ploidy show increases of 50% or more DNA content, and molecular analysis reveals this is amplification at multiple loci, so that it would be expected that there would be multiple chromosomes duplicated. In our experiments all aneuploid samples, apart from one, were revealed as aneuploid by multiple probes (see Table 3.11). Seven probes detected all 10 of these cases, two probes detected 9 and one 8. In 4 of the 5 paired sets of probes both the probe against the arm and centromere/telomere gave the same results. Only the chromosome 11 pair was not concordant and the discrepancy was only seen in 2 of 10 samples.

Siebers *et al.* (2013) using only two probes claimed equivalent predictive value to ICM DNA ploidy. If we had used only 2 probes against the same two loci at EGFR and centromeric 7 we would have achieved the same results and the same results could have been achieved with any 2 of 7 probes. If a reduced FISH panel were to be proposed to achieve the same result it would be logical to select the probes that reveal the highest copy number changes or gene amplification to increase the signal to noise ratio and allow smaller numbers of cells to be counted. In our experiments, the three probes giving the highest copy number variations were, in decreasing order

chromosome 20, 11, 3 and the two probes revealing gene amplification were CCND1 and EGFR. However, these latter probes only produced high copy number in a four cases.

The concordant results obtained with pairs of probes against the same chromosomes suggest that the karyotypic abnormality in these OPMD may well include duplication of whole chromosomes. This would be consistent with the suggestion that most chromosomal anomalies in cancer arise through non-disjunction, but amplification of smaller segments cannot be excluded. Further support for our suggestion of whole chromosome duplication was published by Taoudi Benchekroun *et al.* (2010), who, though they did not report the results for the single centromeric 7 probe separately from EGFR, did comment that counts of centromeric 7 and EGFR were usually balanced.

3.5.7 Gene amplification

Amplifications involved only EGFR and CCND1. Interestingly, the sites of EGFR amplification in the one affected sample did not correlate with the severe dysplastic changes seen on routine histology and the zone of amplification was sharply demarcated from adjacent nuclei with normal copy number. Moreover, of 3 tissue slices that comprised this sample, both the others were diploid throughout, including in the area of severe dysplasia. Distinctive patches of gene amplification were also seen for CCND1 in 4 samples. In this case the sites of the changes did correlate with the location of severe dysplasia.

These sharply demarcated zones of genetically distinct cells are probably a reflection of a clonal structure within the epithelial dysplasia. It is generally accepted that

the sharply defined edges of dysplasia in epithelium seen on routine histopathology reflect clonal boundaries but there is little molecular evidence for this. Heterogeneity in loss of heterozygosity within lesions has been shown very recently using multiple markers, but the study design was not able to reveal clonal structure (Gomes *et al.*, 2015). However, this clonal structure seems likely has previously been suggested to exist in oral dysplasia using X-linked histochemical methods (Seddon, 1993).

There are relatively few published studies on gene amplification in oral dysplasia (Taoudi Benchekroun *et al.*, 2010; Poh *et al.*, 2012). EGFR and CCND1 amplifications have been investigated in a retrospective study on 35 oral dysplastic lesions and high copy number was reported to be strongly associated with malignant transformation (Poh *et al.*, 2012). That study also showed amplification of EGFR and CCND1, but in fewer cases than in the present study. In another study, among 20 oral premalignant lesions that were FISH positive for EGFR, only one had gene amplification (Taoudi Benchekroun *et al.*, 2010).

3.5.8 Threshold evaluation

The few comparable published studies have used similar diagnostic criteria for aneuploidy to the present work. However, diagnostic criteria have not been standardised and the different approach taken to classify FISH aneuploid positive from negative cells and lesions in those studies reflect the lack of accepted standardised criteria. We have attempted to define a threshold criterion in this training dataset to be tested in a future study.

3.5.8.1 Low level copy number gain

All control known diploid nuclei in the connective tissue of all samples produced FISH copy number counts of 2 or less. However, ICM DNA diploid dysplasia samples produced varying numbers of cells with counts of 3 and 4. This supports the contention that the counts of 3 and 4 represent aneuploidy but with only low level copy number gain and that the division of samples into diploid and aneuploid by FISH might not be possible. We have attempted to determine whether a single threshold value for the percentage of these intermediate counts can distinguish ICM DNA aneuploid from diploid samples. This would rely on the percentage of cells with 3 or 4 signals being higher in low level copy number gain than in physiological copy number increase accounted for by cells in S and G2 phases. There is no evidence to support or refute this hypothesis. This is common in many studies of diagnosis by FISH and defining a threshold is the standard approach to devising a classification regime (Kearney, 2001).

Other workers have described copy number of 3 or 4 as low-level copy number gain (Poh *et al.*, 2012), trisomy and tetrasomy (Siebers *et al.*, 2013) and trisomy or polysomy (Taoudi Benchekroun *et al.*, 2010). Our copy number counts of 3 and 4, though lower than in our ICM DNA aneuploid samples were in general higher than in our ICM DNA diploid samples, in which a FISH copy number count of 4 was very infrequent (Table 3.4 and 3.5). Trisomy, tetrasomy and polysomy are states with multiples of complete chromosomal complement and our data supports Poh *et al.* (2012) in defining cases with copy number variation of 3 and 4 as having low copy number gain.

3.5.8.2 Mean + 3SD Threshold

We have attempted to calculate what percentage of cells with copy number 3 or with copy number 3 or 4 might be used as a definition of aneuploidy using ICM ploidy status as the reference standard. We applied a threshold calculated in two ways. The first was the maximum mean percentage of nuclei with signal counts of 3 or 4 plus 3SD as described in section 3.4.3. This approach has been established and used in various tumours by other workers (Bentz *et al.*, 1994; Qian *et al.*, 1996; Veltman *et al.*, 2000; Schwarz *et al.*, 2008). Using this classification threshold, cases were classified as aneuploid or diploid and the results are shown in Table 3.11. One incorrect classification was made, a case defined as aneuploid by DNA ICM was classified as diploid by FISH. Using the diagnostic criteria applied by Poh *et al.* (2012), this sample (S10) would have been classified as low copy number gain. Data from this case shows that copy number counts (Table 3.4 and 3.5) were low in comparison with all other ICM DNA aneuploid samples and with all probes.

In devising a threshold for a clinical test, it was the intention to ensure that no diploid cases were incorrectly diagnosed as aneuploid. This might lead to patient overtreatment. The threshold was therefore set at a high level based on the highest mean count found in any sample with any probe, with a generous margin of threefold SD and a counting error added (section 3.4.3). The threshold was calculated using counts of 3 and 3 or 4 but both calculations produced very similar thresholds and the higher value was selected.

3.5.8.3 Receiver Operating Characteristic analysis

The second approach was to apply ROC analysis, which is based on all signal counts of 3 or higher. Application of ROC to the present data risks bias because of

low sample numbers and the curves only apply to comparison with ICM DNA ploidy results as the reference standard. The power calculation showed that there was insufficient data to analyse by sample. Analysis was possible using single areas and the area under the curve is very high, indicating good discrimination of diploid and aneuploid areas by FISH, consistent with the predictive values. Analysis indicated a threshold value of 10% but applying this correctly classifies all ICM DNA aneuploid samples but generates one false positive, by reclassifying one ICM diploid sample as aneuploid. Larger numbers of cases are required to define the threshold more accurately but values in the range 10-15% can be tested in future studies. A threshold of 10% was used by Poh *et al.* (2012) without calculation, adopted from earlier studies in lung carcinoma. There are no published data on threshold calculations in other publications (Taoudi Benchekroun *et al.*, 2010; Siebers *et al.*, 2013). Overall the ROC analysis shows that the FISH assay has very good concordance with ICM DNA ploidy, good sensitivity and specificity.

Inspection of the DNA ploidy histograms for the two samples that were differently classified with the two thresholds (Figure 3.13) shows that one (S10) is a clear case of DNA aneuploidy with a predominant aneuploid peak, a minor aneuploid peak at DI and high 5c exceeding rate. The other sample (S1) was borderline and had been selected because of its borderline nature. A high CV for the diploid peak is often found in aneuploid cases and the internal constituent peaks cannot be separated at the threshold of detection of the system. This case had been diagnosed using the older camera but no tissue remained for re-analysis. The broad peak across the S phase region and extending to 5c comprises several small peaks. This suggests that there are several minor clones of aneuploid cells within the lesion. It is not surprising that this case is borderline on FISH

as well. No direct comparison between ICM DNA ploidy and FISH can be made because is not known whether the increased DNA content of the cells is accounted for by amplification of multiple chromosomes or a few chromosomes and only a small part of the sample has been subjected to FISH.

3.5.9 Comparison between ICM and FISH results

It was the intention of these experiments to develop a FISH panel to equal or better the predictive value of ICM DNA ploidy, taken as the reference test. The equivalent predictive value has been almost equalled using 5 targeted and 5 chromosomes specific. Although this panel of 10 probes falls slightly short of the sensitivity of DNA ICM, it exceeds that of conventional dysplasia grading on the basis of published literature (Mehanna *et al.*, 2009).

Analysis by FISH is always dependent on the counting technique used. In this study we have counted continuous runs of basal and supra-basal cells up to five cell layers from the basement membrane to include the stem cell compartment and transit amplifying population. Including several cell layers allows shorter lengths of epithelium to be assessed and has allowed demonstration of some internal clonal structure within dysplasias. Inclusion of prickle cells would have been possible but has disadvantages because their nuclei are larger and would be more prone to false negative counts caused by partial loss of nucleus on sectioning. Apoptotic cells are also a feature of dysplasia and it is possible that the most aneuploid cells undergo apoptosis in the basal layers, leaving more normal cells capable of maturation to form the upper layers. For these reasons only basal and parabasal cells were counted.

Recently, Siebers *et al.* (2013) assessed chromosomal instability using FISH with centromeric probes against chromosomes 1 and 7 and showed malignant transformation in 47.1% of FISH aneuploid leukoplakia, a similar predictive value to the 43.5% achieved by ICM in that centre. Using only two markers, agreement on ploidy status was only 63% compared to the present study at 92%, which also included a centromeric C7 probe. Data from the present study clearly shows the value of testing additional loci.

There is a mismatch between the results seen on ICM DNA ploidy and FISH (see Table 3.8). In DNA ploidy many cells seem to be aneuploid but FISH sometimes detects fewer, sometimes more. ICM DNA ploidy has an approximate 1% detection threshold for the total amount of DNA amplified or deleted providing the CV of the diploid peak is below 5% (manufacturer's data), a high degree of sensitivity. In our experiments, some ICM DNA aneuploid samples contained very large numbers of nuclei with large increases in DNA content that were not seen on FISH (S10, S11, S17; see Table 3.8). However, the two techniques are not directly comparable. ICM DNA ploidy analysis measures total nuclear DNA as a continuous variable. FISH counts discrete contributions towards the total DNA content based on specific loci. The amount of DNA amplified per signal may vary between samples, probes and possibly between cells depending on the karyotypic abnormality. It would be expected that FISH would always detect fewer cells than ICM, as it assesses a limited no of loci whereas ICM DNA ploidy detects all abnormal cells regardless of loci sites of amplification. It is possible that FISH might correlate better with ICM ploidy if only centromeric probes were used. Centromeric probe binding is likely to indicate larger duplications and amplifications than probes targeted to chromosome arms because

presence of a centromere usually indicates a whole or relatively intact chromosome and centromeric probes are widely used in cancer research to enumerate chromosomes (Manning *et al.*, 2014).

In all our samples, ICM DNA ploidy analysis has a high signal to noise ratio. Aneuploidy is easy to detect (Figure 3.12). The presence of peaks is obvious and large numbers of abnormal nuclei are present in samples of separated nuclei. It is possible that nuclear separation for ICM DNA ploidy enriches for abnormal nuclei, but this does not appear to have been investigated. Conversely, FISH detects very small numbers of abnormal cells in a smaller sample despite the fact that dysplastic lesions are considered to be clonal and every cell should show some degree of similarity in its karyotype. The problem of low copy number gain (refer to section 3.4.2) has more of an effect on classification in FISH whereas in ICM DNA ploidy it only affects sensitivity.

The method of tissue sampling may also account for part of the difference between techniques. In any tissue section for FISH, the nuclei will have been sectioned leading to loss of DNA so that the signals detected always reflect the minimum possible copy number. Section thickness was chosen to produce the minimum overlapping nuclei so that each signal could be confidently ascribed to one nucleus, but this has a cost in loss of nuclear material in the thinner sections. Only short sections of epithelium could be counted and these were selected based on dysplasia. However, it is recognised that there is an incomplete correlation between dysplasia and ICM DNA ploidy results (refer to ploidy chapter, Table 4.6) and in one of our samples we demonstrated EGFR amplification in an area without dysplasia. Sample preparation for ICM DNA ploidy uses thicker sections and much longer lengths of epithelium, usually 10mm or more and

up to 3000 cells can be assessed, providing a much more representative sample without the risk of selection bias.

Addition of further loci might be thought to increase the predictive value of the FISH panel but with diminishing returns, as the additional probes selected would target less frequently amplified loci. However, we have shown that almost all probes produce the same result in ICM DNA aneuploid samples (Table 3.11) and that the number of probes could be reduced without compromising the results. A similar suggestion was made by Siebers *et al.* (2013) despite the fact that the correlation in that two probe study was lower than in the present work. To increase predictive value, a better strategy would appear to be to reduce the panel but add probes deliberately targeted against less frequently amplified regions.

It is not possible to extrapolate from the data comparing dysplasia grade and FISH results shown in Table 3.12 and 3.13 because samples were selected to include a range of dysplasia grades and DNA ploidy status. The compiled results do not reflect the agreement found in our previous study (Sperandio *et al.*, 2013) for this reason. The number of probes producing aneuploid results per sample is similar in moderate and severe dysplasia but the marked differences between samples prevent any meaningful comparison. ICM DNA ploidy is a better predictor of FISH ploidy status than dysplasia grade.

3.5.10 Conclusion

In summary, using a panel of 10 FISH probes we have shown that the number of readily identifiable and definitely aneuploid cells within even grossly aneuploid epithelium is relatively small and high copy number gain at any individual locus is

relatively rare. The detected changes appear to represent relatively large chromosome duplications and the majority of ICM DNA aneuploid samples showed copy number gains for almost all probes. FISH was able to demonstrate sharply delineated areas within zones of epithelial dysplasia between which the copy number aberrations for individual loci differ, providing evidence of an internal clonal structure before the development of cancer.

This study has used the broadest panel of FISH probes for this purpose to date. We suggest that larger panels may not produce better results in terms of a clinical test to predict transformation, but the data has provided valuable novel data on the internal structure and genomic variation with in oral dysplastic lesions to inform design of future molecular diagnostic methods.

CHAPTER 4 : DNA Ploidy

4.1 Investigative plan for ICM DNA ploidy experiments

DNA ploidy alone has been proved as good as the best dysplasia grading reported in experiments performed previously in this laboratory. The aim of this section was to test tissue preparation using new DNA ploidy equipment (section 4.3.4) and perform a new part retrospective part prospective analysis of DNA ploidy analysis against outcome with a 10 year follow up period. Unlike the previous study (Sperandio *et al.*, 2013), that used a continuous series of low and high risk patients/lesions, the present work focused on clinically identified risk lesions (section 4.3.1.2) and, also unlike the previous study, DNA ploidy and dysplasia grading were performed on the same sample allowing calculation of combined predictive values (section 4.4.6).

In comparison with the previous study, ICM DNA ploidy produced a valid result in many more samples using the new methods (Figure 4.4) and the methods performed well (section 4.4.2) and both dysplasia grading (section 4.4.4) and DNA ploidy analysis (section 4.4.5) were confirmed as a good predictors of malignant transformation. It was possible in this study to calculate annual transformation rates (section 4.4.5.1). The same methods were also used to perform ICM DNA ploidy analysis for comparison with FISH analyses reported in chapter 3.

4.2 Background

4.2.1 The cell cycle and DNA content

Abnormally controlled cell proliferation resulting from deregulation of cell cycle control is a common feature of human cancers. The control mechanisms for cell cycle, cell proliferation, cell division and growth are highly conserved to ensure the fidelity of the genome at replication. The cell cycle has two principal stages, interphase and cell division (Figure 4.1). While cell division involves mitosis (M phase) generating two identical daughter cells, the interphase is a period of preparation for division, which includes G_1 (gap 1), S (synthesis) and G_2 (gap 2) phases. Most somatic cells are not in cycle and are said to be in phase G_0.

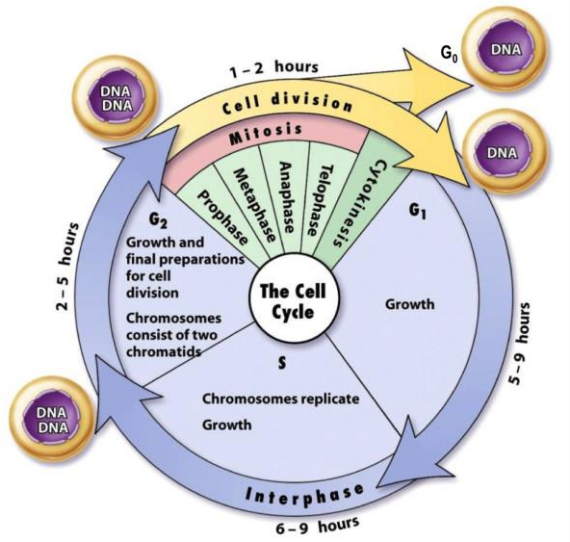

Figure 4.1 The cell cycle.
Source: Biology of humans, 2nd Edition 2007; Pearson Prentice Hall

With few exceptions, such as germ cells or multinucleate cells, the amount of DNA in each cell is uniform (Rabinovitch, 1994). In the resting G_0 phase, diploid cells contain 7.14 pg of DNA and enter the cell cycle through G_1, a gap period during which the cells are preparing themselves for DNA synthesis (Ross *et al.*, 2003). Cellular DNA content

continuously increases throughout S phase and becomes doubled to 14.28 pg per cell when the DNA duplication completes (Ross *et al.*, 2003). Cells continue to grow in G_2 phase whilst DNA damage and replication errors are repaired before entering the mitotic cycle. A normal cell in the G_0 or G_1 phase has 2N or 46 chromosomes while those in the G_2 and M phases have varying amounts with a maximum of 4N or 92 chromosomes (Figure 4.2). In multinucleate cells, such as muscle cells or osteoclasts each nucleus has a normal chromosome and DNA complement.

4.2.2 DNA histograms and ploidy analysis

Measurement of DNA content in individual cells provides information on DNA ploidy and for normal cells, indicates their position in particular phases of cell cycle (Darzynkiewicz, 2010). The principle of the analysis is the ability to accurately quantitate the DNA content of individuals cells by using dyes such as Feulgen stain, propidium iodine, cyanine dyes that bind DNA in a stoichiometric manner so that the amount of DNA within a cell can be inferred from the density of staining (Carey, 1994). Results from the analysis of nuclear DNA content are displayed as a frequency histogram of cell count versus the parameter measured (Figure 4.2). Two main techniques often used are image and flow cytometry that measure total dye binding through the parameters of integrated optical density (IOD) and fluorescence intensity respectively. Quantitation of nuclear DNA in image cytometry is conventionally scaled in 'c' units by comparison with DNA from reference cells (Haroske *et al.*, 2001), where c denotes the normal diploid chromosomal complement, equivalent to 2N. Though related to chromosomes, this is only a scaling convention indicating total DNA content, not true chromosomal status or chromosomal ploidy. Image based ploidy analysis is therefore best referred to as DNA ploidy analysis.

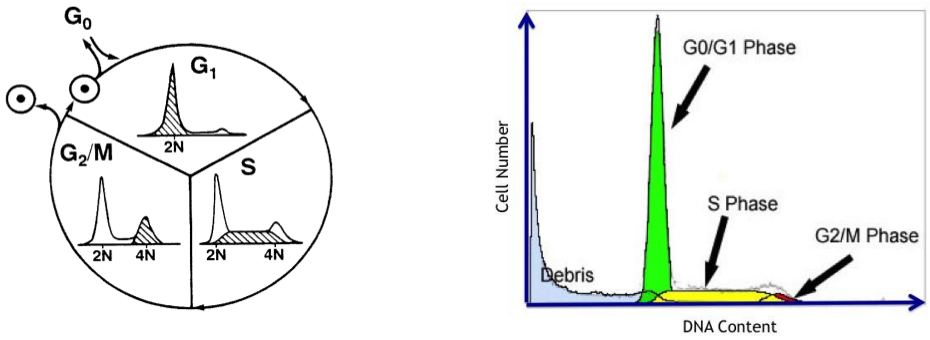

Figure 4.2 DNA content in the phases of cell cycle and DNA histogram
A schematic of DNA content throughout the phases of cell cycle (left panel). A typical DNA histogram (right panel) plotted from the measurement of DNA content by flow cytometry. Debris on the left side of the histogram, derived from damaged or fragmented nuclei, outside the G_1, S of G_2 windows. (Adapted from www.phoenixflow.com)

A DNA histogram is defined as DNA diploid when total DNA content clusters in the 2c or G_0/G_1 phases forming the main peak and the S, G_2M phases of cell population are relatively small. The 2c value used in image cytometry is determined by measurement of an internal reference standard, commonly lymphocytes (Carey, 1994). The majority of cells in a non-neoplastic tissue or low-grade neoplasms have a diploid chromosome number and show a peak at 2c or G_0/G_1 phases on a DNA histogram with up to approximately 15% of the cells in the S and G_2M phases. When another separate peak is found that differs substantially from the known diploid reference 2c or G_0/G_1 peak and cannot be accounted for by a 4c or G_2 peak, the histogram is defined as aneuploid. Aneuploidy is seen mostly in neoplasms but can also be found in occasional cells in apparently normal tissues.

DNA aneuploidy is also defined by the presence of abnormal cells at 5c or higher DNA content, having nuclear DNA content markedly higher than the cell population in G_2M phase (Haroske *et al.*, 2001). Such cells likely represent non-proliferating abnormal

cells with different chromosomal complements and abnormally high numbers of chromosomes (Haroske *et al.*, 2001).

DNA index (DI), a ratio of mean or mode of samples' DNA content in G_0/G_1 to the diploid reference has been described as a measure of the degree of DNA content abnormality (Shankey *et al.*, 1993). However, it reflects only the relative position of diploid and abnormal peaks on a histogram, higher values are not 'more aneuploid' as aneuploidy is not measured on a simple scale of DNA content but depends on the number of peaks and their relative size in addition. For normal tissue, the DI of cells in G_0/G_1 cell cycle is 1.0, cells in G_2M phase have DI = 2.0 and the DI of the S phase is between 1.0 and 2.0.

Variation in DNA binding between individual cells, sample preparation, presence of debris and instrument errors and precision all affect the accuracy of DNA content measurement. This variation is seen as the width of peaks in a histogram and is measured using the CV value, a measure of variation and the ratio between the standard deviation of the DNA content to the mean DNA content in a peak expressed as a percentage. The CV is used as a measure for the quality of a histogram and the associated experimental procedures and is measured on the G_0/G_1 cell population peak, as these normal cells have a predictable normal distribution (Rabinovitch, 1994). A high CV indicates a broad peak and the CV, as a measure of variation, determines the confidence with which two closely placed peaks can be confidently separated and hence the resolution of the instrument, method and experiment in detecting abnormal peaks.

4.2.3 DNA ploidy in OPMDs

In OPMDs, the role of DNA aneuploidy has been investigated in relation to its value as a predictor of malignant transformation (Torres-Rendon *et al.*, 2009; Bradley *et al.*, 2010; Bremmer *et al.*, 2011; Siebers *et al.*, 2013; Sperandio *et al.*, 2013), association with the dysplasia grade (Grässel-Pietrusky *et al.*, 1982; Saito *et al.*, 1995; Pentenero *et al.*, 2009; Donadini *et al.*, 2010; van Zyl *et al.*, 2012) and to a lesser extent its correlation with other clinical parameters (Islam *et al.*, 2010; Castagnola *et al.*, 2011).

Although the majority of the published studies have been retrospective involving a single cohort from a single centre, DNA aneuploidy has clearly been shown to be a potential marker of cancer progression from dysplastic epithelium (Table 4.1). More lesions that subsequently underwent malignant transformation were aneuploid compared to lesions that did not progress in all studies. In a study by Torres-Rendon *et al.*, 33.3% (14/42 cases) of progressing dysplastic lesions were aneuploid compared to only 11.3% (5/44 cases) of non-progressing dysplastic lesions ($p = 0.01$). A similar finding was reported in another study, 45% of dysplastic lesions that underwent malignant transformation had abnormal DNA content versus 12% that did not (Bradley *et al.*, 2010).

Increased risk of cancer progression in OPMD has been reported with a hazard ratio between 3 and 7.5 in four studies and the relationship remained significant after adjustment to other clinical parameters suggesting its utility as an independent predictor of cancer development (Table 4.1) (Bradley *et al.*, 2010; Bremmer *et al.*, 2011; Siebers *et al.*, 2013; Sperandio *et al.*, 2013). In all studies, aneuploid OPMDs transformed to carcinoma in a shorter time than any diploid lesions that did so. Only a few studies have defined the positive and negative predictive values and reported values range from 26%

- 74% and 58% - 90% respectively (Torres-Rendon *et al.*, 2009; Bremmer *et al.*, 2011; Sperandio *et al.*, 2013). These are relatively high values for such a predictive test for cancer.

The association between DNA ploidy and the presence and severity of dysplasia has been investigated using either image or flow cytometry on both formalin fixed and fresh frozen tissues (Grässel-Pietrusky *et al.*, 1982; Saito *et al.*, 1995; Pentenero *et al.*, 2009; Donadini *et al.*, 2010; van Zyl *et al.*, 2012). It has been shown that aneuploidy was more frequent in dysplastic than non-dysplastic OPMDs (Saito *et al.*, 1995; Pentenero *et al.*, 2009). Aneuploidy was significantly correlated with the degree of dysplasia as reported in one study (van Zyl *et al.*, 2012); 13 % of mild, 31 % of moderate, and 54 % of severe dysplasia lesions were aneuploid ($p=0.011$). The differences in ploidy status were more significant when grouping the dysplasia into low-risk and high-risk categories ($p = 0.008$) (van Zyl *et al.*, 2012).

As discussed in section 1.3.3.1, the anatomical site of OPMDs often correlates with the chances of finding epithelial dysplasia or malignant transition (Waldron and Shafer, 1975; Banoczy, 1977; Kramer *et al.*, 1978; Silverman *et al.*, 1984). High-risk locations include floor of the mouth, being the site with greatest risk, followed by tongue and soft palate. Based on the link between DNA ploidy and malignant transformation and grade of dysplasia as described above, a few studies have sought to associate DNA ploidy with the high risk oral subsites. Higher frequencies of aneuploidy were found in dysplastic lesions from lateral/ ventral tongue (85%), floor of the mouth (50%) and soft palate (44%) compared to the gingiva (22%) and lower lip (25%) ($p < 0.05$) (Islam *et al.*, 2010).

Table 4.1 Key studies on the association between DNA aneuploidy and malignant transformation in OPMD.
All studies used image-based or cell cytometric methods.

Studies	Findings	Sens	Spec	PPV	NPV	Hazard ratio (95% CI)		Time to progression for aneuploid samples
						Univariate	Multivariate	
Torres-Rendon *et al.* 2009	Aneuploidy was found in: 14/42 (33.3%) progressed OED 5/44 (11.3%) nonprogressed OED	33%	88%	74%	58%	-	-	Significantly shorter log rank, $p = 0.003$
Bradley *et al.* 2010	Aneuploidy was found in: 22/49 (45%) progressed OED 6/50 (12%) nonprogressed OED						3.3 (1.5 -7.4) p=0.003	Median = 49 months (95% CI: 34-86 months)
Bremmer *et al.* 2011	7/13 progressed lesions were aneuploid (5 dysplastic and 2 nondysplastic)	54%	60%	26%	83%	3.7 (1.1-13.0) p =0.04	7.1 (1.6 -30.5) p =0.008	Shorter time to progression log rank, p=0.0001
Siebers *et al.* 2013	Cases underwent malignant transformation: 10/23 (43.5%) were aneuploid 6/79 (7.6%) were diploid					7.2 (2.61-20.03) $p < 0.001$	5.4 (1.82-15.77) p =0.002	Shorter survival
Sperandio *et al.* 2013	Cases underwent malignant transformation: 20/59 (34%) aneuploid 10/161 (6%) diploid 2/53 (4%) tetraploid	65%	75%	39%	90%	[a] 7.4 (3.4 -15.9) $p< 0.001$ [b] 5.1 (1.8 -14.2) p =0.002		Transformed more rapidly log rank: $x^2 = 44.25$ df = 2, $p < 0.0001$

Sens: sensitivity; Spec: specificity

PPV: positive predictive value; NPV: negative predictive value

[a] Analysis included malignant transformation within 6 months of the index biopsy

[b] Analysis excluded transformation less than 6 months of the index lesions

There appear to be differences in the equipment and software used for DNA ploidy analysis as revealed by their predictive values. It seems all systems can identify aneuploidy and show a relationship to malignant transformation. However, the negative predictive values differ widely. Using one system (Bradley *et al.*, 2010) the association between aneuploidy and carcinoma development was clear but the negative predictive value of a diploid result was not high enough to propose DNA ploidy as a clinical test because eventually almost all diploid and tetraploid cases underwent malignant transformation in a follow up period of 12 years. The best predictive values for use in a clinical context are reported by Sperandio *et al.* (2013), in which the transformation rate for diploid and tetraploid cases was only 5%. This high negative predictive value is achieved at the cost of a slightly reduced positive predictive value for aneuploid lesions in comparison with the study of Bradley *et al.* (2010). However, the requirement for a clinically valid test is the widest possible difference between negative and positive values. Discrepancies between studies most likely reflect methodological differences, though the study populations may also account for part of the difference because the overall transformation rate in the study by Bradley *et al.* (2010) was higher. These differences also raise the possibility that techniques suitable for clinical use could be too sensitive and identify low levels of aneuploidy that do not affect transformation. The diagnostic criteria need to be better defined against outcome. Currently, all studies have used standard diagnostic criteria for image cytometry and not defined any specific parameters for analysis of OPMD.

4.3 Materials and Methods

4.3.1 Cases and tissue samples

4.3.1.1 Search Strategy

Pathology reports and original request forms for specimens submitted between the year 2004 and 2007 were searched by hand from the archive of the Department of Oral Pathology, King's College London. Supplementary reports of ploidy analysis were also obtained when available.

4.3.1.2 Inclusion Criteria

Inclusion criteria during the search were cases with diagnosis confirmed histopathologically and with a clinical description provided by the clinician indicating clinically defined high risk of transformation, as detailed in information included in the pathology requests and reports detailed in Table 4.2. Reports with the diagnosis of normal tissue from any oral subsite were also retrieved for use as controls.

Table 4.2 Inclusion Criteria.
Only cases with matching clinical and pathological criteria were included

Pathological Diagnosis	Clinical Description
Keratosis/atrophy with dysplasia	Leukoplakia or Erythroplakia or White patch/lesion or Red patch/lesion
Keratosis/atrophy with no dysplasia	Leukoplakia or Erythroplakia or White patch/lesion or Red patch/lesion
Keratosis with or without dysplasia	Proliferative verrucous leukoplakia

4.3.1.3 Exclusion criteria

Patients with prior history or histological signs of squamous cell carcinoma were excluded. Similarly, patients were excluded if the cancer database record showed that they had had cancer less than 2 weeks from the date of biopsy in the histopathogical

report. Cases with likely diagnosis of actinic cheilitis, Epstein Barr virus infection and candidosis or affecting the oropharynx or lip vermillion were excluded. When the wax blocks were irretrievable or no tissue was left in the wax blocks, they were also excluded.

4.3.2 Data collection

The following baseline data gathered from the reports were documented; date of birth, gender, date of biopsy, clinical description, site of lesions, absence or presence of oral epithelial dysplasia including the grade and ploidy status.

Longitudinal follow-up data was acquired from cancer registrations and causes of death data from the Health and Social Care Information Centre records for 1990 – 2014 by matching the subjects' name, date of birth and gender or National Health Service (NHS) registration number with address and postcode. Data included for analysis were the cause and date of death and the type, site and date of cancer registration. Ethics approval to hold and analyse this data without individual patient consent was obtained under Section 60 of the Health and Social Care Act 2001 from the Patient Information Advisory Group (subsequently transferred to the National Information Governance Board for Health and Social Care) under reference PIAG 4-09(f)/2003 and to analyse tissue samples from the Guy's Research Ethics Committee under reference 02/10/14. These approvals also covered the experiments reported in other chapters in this thesis.

4.3.3 Samples and blocks specimens

Wax block specimens for cases identified from the archival report but for which ploidy status was unknown were retrieved. H&E stained slides were reviewed for histological diagnosis and areas for ploidy analysis showing the worst areas of dysplasia

were outlined. Based on the size of tissue seen on H&E, cases were subgrouped into specimens that were suitable for routine conventional or a novel method of monolayer preparation. However, the final decision on whether ploidy could be performed for each case was dependent upon visual inspection of sufficient amount of tissue available on wax blocks. Multiple sections of 50μm thick equivalent to at least 50mm epithelial length were cut and placed into a 15ml graduated labelled polypropylene centrifuge tube using a microtome (Jung RM2055, Leica).

4.3.4 Preparation of Monolayers

4.3.4.1 Conventional method

To remove the paraffin wax, tissues were incubated twice for 30 minutes in 4ml of xylene. This was followed by rehydration in a series of aqueous ethanol solutions of decreasing concentration; two washes of 5 minutes immersion in 4ml absolute ethanol and sequential incubation for 10 minutes each in 96%, 85%, 74% and 50% ethanol. After washing in 4ml cold PBS for 5 minutes, enzyme digestion was performed by incubating with 2mls 0.05% protease type XXIV (Sigma) in a 37°C high speed shaking water bath at 250 rpm for 90 minutes. Tubes were then transferred to crushed ice, 2ml of cold PBS was added and tissue pellets were briefly re-suspended using a disposable 1ml pastette. Precipitated disintegrated cells and large debris were segregated from remaining nuclei by filtration through 60mesh nylon gauze into fresh 5ml polystyrene Falcon tubes. After 10 minutes of 3300rpm centrifugation (Immufuge II), the supernatant was carefully removed, and re-suspended in 0.5 to 2ml PBS depending on the size of the pellet. To disperse a monolayer of separated nuclei onto a glass microscope slide, 200ul of the cell suspension was spun for 5 minutes at 600rpm in a cytospin (Thermo Shandon Cytospin 4). Nuclear concentration was established under a

light microscope (Zeiss). Ideally monolayers contained between 10 and 15 nuclei per x40 field and, failing this, a new monolayer was made from residual suspension adjusted accordingly. The attached nuclei were then fixed in 4% buffered formalin overnight in a fume cupboard.

4.3.4.2 Modified protocol

To increase nuclear yield, a modified protocol was used. Paraffin wax was removed by incubation of tissues twice in 4 ml xylene for 15 minutes each and rehydrated as in the conventional method. Tubes were centrifuged at 1000rpm for 10 minutes, supernatant decanted and replaced with 8ml of cold PBS. Samples were again centrifuged at 2200 rpm for 10 minutes before enzyme treatment with 1ml 0.5mg/ml protease solution (Bacillus licheniformis type VIII, Sigma). Using micro-magnetic stirring bars 5 x 2 mm immersed in the protease, the enzyme incubation was performed at room temperature on a magnetic stirrer at 600rpm, constantly whirling the fleas inside the tube. After 90 minutes, 8ml of cold PBS was added to each sample and it was filtered through 60 mesh nylon gauze into a new 5ml polystyrene Falcon tube as in the conventional method. After 20 minutes centrifugation at 2500 rpm, the tissue pellet was re-suspended in 0.5 to 2ml of cold PBS and monolayers prepared as for the conventional method.

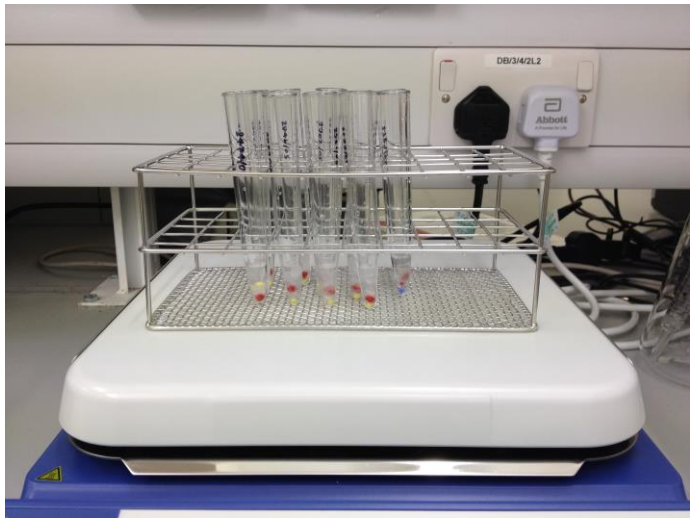

Figure 4.3 Modified method for nuclear extraction in progress.
Enzyme incubation was performed using micro-magnetic stirring bars rotating continuously at 600rpm on a stirrer for 90 minutes at room temperature.

4.3.5 Feulgen Staining

Fixed monolayers were washed in distilled water for 2 minutes. Acid hydrolysis to remove the purine bases of DNA was carried out in 5N HCl for 1 hour at room temperature. After washing for 2 minutes in distilled water, nuclei were stained in Schiff's reagent in the dark for 2 hours followed by three changes of sodium bisulphate solution for a total of 30 minutes. Slides were gently rinsed in tap water followed by distilled water, dehydrated through a series of graded alcohols to xylene for 5 minutes each, and mounted with DPX mounting medium with coverslip and dried flat in an oven at 60^{o}C for 30 minutes.

4.3.6 Measurement of DNA content

Nuclear DNA content was measured using a PWS (Ploidy Work Station) Grabber system (Room4, Sussex UK). The system consists of an automated scanning Zeiss Axioplan II microscope (Zeiss) equipped with a 546 nm green barrier filter. Images

were captured with a black and AxioCam MRm digital camera (Zeiss) with 40x lens providing a resolution for analysis of 162 nm per pixel.

Optical density and nuclear area of each nucleus were measured and corrected to the background optical density. Integrated optical density (IOD) was calculated automatically by integrating the measured optical density of each pixel across the area of each nucleus. A maximum of 3000 nuclei including lymphocytes and fibroblasts were automatically scanned and images were collected and grouped into different galleries for nuclei of interest, reference and discarded nuclei. The galleries were edited using PWS Classifier (Room 4, Sussex UK) to discard cut, overlapped and pyknotic nuclei. Cases with less than 300 nuclei of interest were repeated when possible or excluded. PWS Classifier created the DNA ploidy histograms from IOD of the nuclei using the lymphocytes and fibroblasts (reference nuclei) as internal diploid control. All galleries were edited and all histograms were diagnosed by ZZ and diagnosis confirmed by supervisor EWO.

4.3.7 DNA ploidy diagnostic criteria

Histograms were classified according to previous criteria (Sperandio *et al.*, 2013). A lesion was classified as DNA diploid if only one 2c peak (G_0/G_1) formed by epithelial nuclei was present, the number of nuclei at 4c peak (G_2) did not exceed 10% of the total number of epithelial nuclei and the number of nuclei with DNA content more than 5c did not exceed 1%. A lesion was defined as tetraploid if a 4c peak (DI 1.9–2.1; 3.8c-4.2c) exceeding 10% of the total nuclei was present with no other abnormality. Aneuploid lesions were characterized by the presence of one or more peak(s) containing more than 10% of the epithelial nuclei outside the range of the normal or tetraploid peaks, that is outside DI 0.9-1.1 (1.8 – 2.2c) for the diploid peak and DI 1.8-2.2 (3.6 –

4.4c) for the G2 peak or when the number of nuclei with a DNA content above 5c exceeded 1% of the total number of epithelial nuclei. At least 300 epithelial nuclei were assessed and samples with a diploid peak coefficient variation greater than 5% were excluded.

4.3.8 Statistical analyses

4.3.8.1 Comparison of enzyme digestion methods

To evaluate reproducibility of DNA ploidy analysis using a modified enzyme digestion method, an independent set of 10 samples diagnosed in the year 2014 was selected. Comparison between conventional and novel methods were made on following parameters; the mean number of nuclei in each gallery, the total number of nuclei acquired, percentage of cells rejected from analysis and CV of the diploid peak using the Wilcoxon signed rank test because the data distributions were skewed and the sample was small (n=10). The reproducibility of DNA ploidy diagnosis was evaluated by using Cohen's kappa coefficient. *P*-values < 0.05 were regarded as statistically significant.

4.3.8.2 Malignant transformation

The unit of analysis for malignant transformation was the patient. For univariate and multivariate analysis, when a patient had multiple biopsies or specimens, the earliest diagnosis with the most abnormal result was used as the index lesion for analysis ('first-worst' dysplasia and 'first-worst' ploidy). When no dysplasia or DNA ploidy abnormality was found, the earliest lesion was taken as the index lesion.

A single patient was excluded from the dysplasia analysis because the worst grade of dysplasia was diagnosed at the same time as the carcinoma. However, lower grades of

dysplasia and DNA aneuploidy preceded the carcinoma allowing the case to be included in the univariate analysis of DNA ploidy. Patients were grouped for separate analysis into those who developed a carcinoma after and those who developed carcinoma within 6 months of their index lesion.

The endpoint date was defined as one of four outcomes: the date carcinoma developed, the last follow-up date when no progression had occurred, the date of death if the patient had died of oral carcinoma or the date of death from any other cause.

The association between ploidy diagnosis and dysplasia grade was calculated using the Pearson chi-square test. Kaplan-Meier methods were used to estimate the time to progression and percentage of patients who underwent malignant transformation over the period of follow-up by dysplasia and ploidy diagnoses. Survival curves were compared using the log rank test. Cox regression methods were used to investigate the main independent predictors of malignant transformation. Adjusting for age and gender, each dysplasia grade and ploidy result category was assessed separately in a univariate Cox proportional hazard model. In the multivariate model, adjustment involved age, sex and mutual adjustment between dysplasia grade and ploidy status. Hazard ratios (HR) with 95% confidence interval (95% CI) and p values were reported and $p < 0.05$ was considered statistically significant. Positive and negative predictive values, sensitivity and specificity were calculated from 2x2 tables with malignant transformation as reference. Annual malignant transformation rates were calculated based on actual person-years of follow up in order to take into account the time to transformation.

4.4 Results

4.4.1 Patient characteristics and follow-up

A total of 259 cases of OPMD were identified from the archive. The follow up data on malignant transformation of 7 patients were not traceable, 8 patients had prior history of cancer and 2 patients were diagnosed with cancer less than two weeks after biopsy. In two cases the cancer diagnosis returned by central UK cancer registration was miscoded as cancer when the original diagnosis submitted by our laboratory to the local registry had been carcinoma in situ. These diagnoses were corrected on the basis of date of diagnosis.

Ploidy analysis could not be carried out on 7 cases due to lack of tissue left after previous use or an irretrievable specimen. Insufficient nuclei resulted in failed analyses of ploidy on 3 cases. A total of 228 patients remained to be included in this analysis and Table 4.3 shows the demographic details, histological diagnosis and ploidy diagnosis for all patients. A STARD diagram for the studies is shown in Figure 4.4.

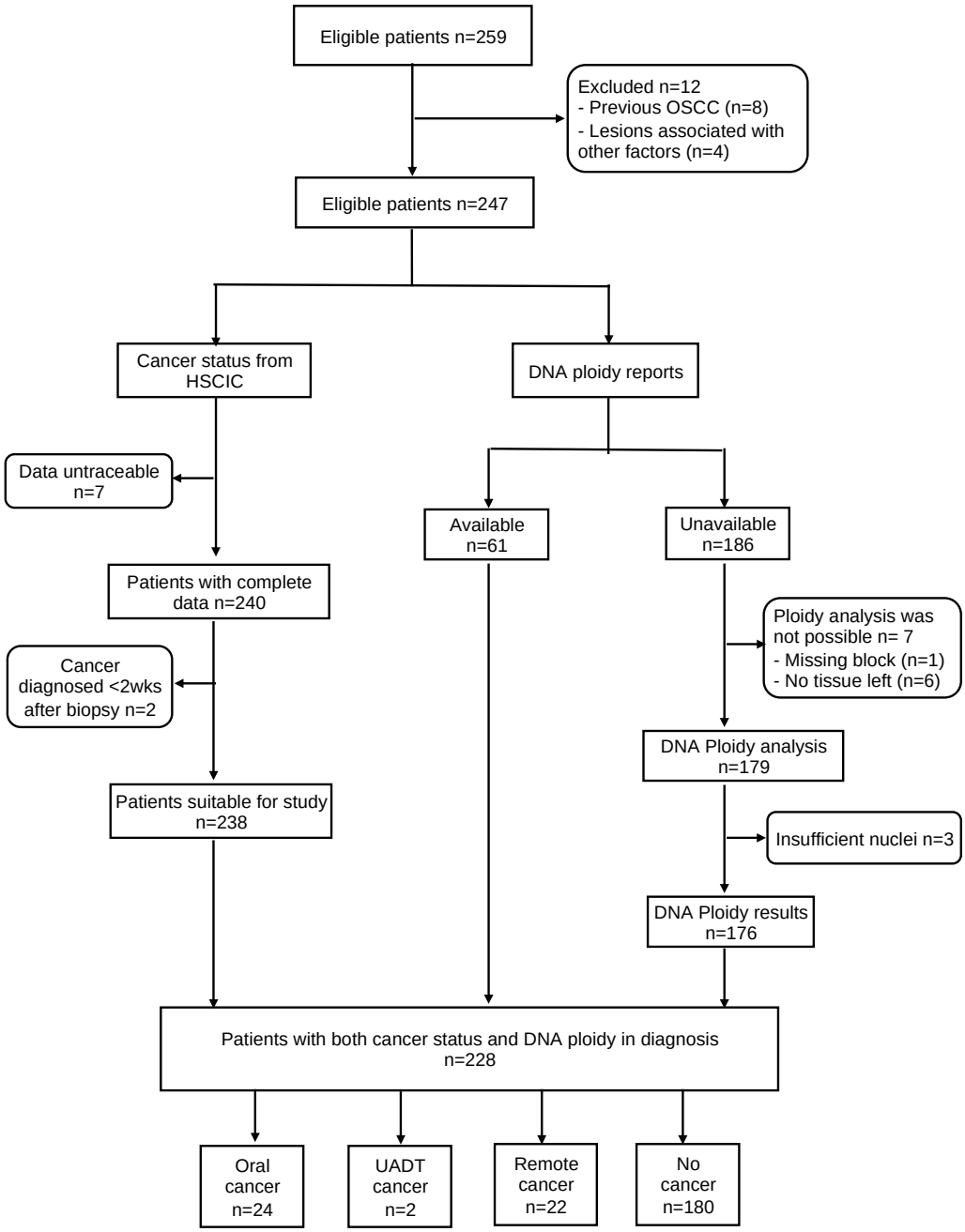

Figure 4.4 STARD diagram showing recruitment of patients for this study.
UADT is upper aerodigestive tract.

The mean age of the patients at time of diagnosis of the index lesion was 55 years (SD 13.9 years) and the male patients (53.5%) were slightly greater in number than female patients. The follow up period ranged from 5 to 9.6 years (mean = 7.61, SD = 2.69). Nine patients developed carcinoma less than 6 months from index specimen and this group was excluded for a second analysis (Table 4.4).

Table 4.3 Characteristics of all patients and samples including those with malignant transformation less than 6 months from index lesion

	Number (%)	Malignant transformation	
		Yes (%)	No (%)
Total patients	228	24 (10.5)	204 (89.5)
Age in years			
Mean (SD)	55 (13.9)	60.4 (10.4)	54.2 (14.2)
Gender			
Male	122 (53.5)	11 (45.8)	111 (54.4)
Female	106 (46.5)	13 (54.2)	93 (45.6)
Dysplasia grade			
No	121 (53.1)	1 (4.2)	120 (58.8)
Mild	47 (20.6)	2 (8.3)	45 (22.1)
Moderate	32 (14.0)	7 (29.2)	25 (12.2)
Severe	28 (12.3)	14 (58.3)	14 (6.9)
DNA Ploidy			
Diploid	183 (80.3)	10 (41.7)	173 (84.8)
Tetraploid	3 (1.3)	0 (0)	3 (1.5)
Aneuploid	42 (18.4)	14 (58.3)	28 (13.7)

Table 4.4 Characteristics of all patients and samples excluding those with malignant transformation less than 6 months from index lesion

	Number (%)	Malignant transformation	
		Yes (%)	No (%)
Total patients	219	15 (6.9)	204 (93.1)
Age in years			
Mean (SD)	55 (14.1)	62.2 (11.6)	54.2 (14.2)
Gender			
Male	118 (53.9)	7 (46.7)	111 (54.4)
Female	101 (46.1)	8 (53.3)	93 (45.6)
Dysplasia grade			
No	121 (55.3)	1 (6.7)	120 (58.8)
Mild	47 (21.5)	2 (13.3)	45 (22.1)
Moderate	30 (13.7)	5 (33.3)	25 (12.2)
Severe	21 (9.5)	7 (46.7)	14 (6.9)
DNA Ploidy			
Diploid	180 (82.2)	7 (46.7)	173 (84.8)
Tetraploid	3 (1.4)	0 (0)	3 (1.5)
Aneuploid	36 (16.4)	8 (53.3)	28 (13.7)

4.4.2 Comparison between conventional and modified methods for extraction of nuclei

There were 8 diploid and 2 aneuploid cases included in the comparison. The agreement between DNA ploidy diagnosis when applying conventional and modified novel protocols was 100% (**K** value = 1.00) indicating complete agreement so that no difference between the methods was evident in terms of final outcome.

The mean total number of nuclei isolated by the conventional method was 3150 (median 3075) compared to the modified protocol of 3792 (median 3696, see Table 4.5). The CVs were significantly different between these two protocols ($p = 0.007$) with lower values obtained from the routine method. Using the modified method, a statistically greater number of lymphocytes as reference cells was acquired in software galleries 1 and 2 with $p = 0.01$ and 0.005 respectively. However, fibroblast nuclei were isolated more frequently using the routine method ($p = 0.03$). There was no difference between the numbers of nuclei that were edited out as defective between both protocols

Table 4.5 Comparison between the number of nuclei collected and ploidy histogram parameters between the two different nuclear extraction methods

	Nuclei extraction method	Mean	Median	Standard deviation	*p* value
Total nuclei acquired before cleaning	Routine	3149.8	3075.0	146.81	0.14
	Modified	3792.2	3695.5	1541.24	
Total epithelial nuclei	Routine	2196.9	2377.5	363.5	0.06
	Modified	1892.5	2208.5	528.2	
Total small lymphocyte nuclei	Routine	3.8	1.5	5.6	0.01*
	Modified	28.0	13.0	45.9	
Total large lymphocyte/monocyte /neutrophil nuclei	Routine	94.7	49.0	106.5	0.005*
	Modified	106.5	575.5	988.9	
Total fibroblast nuclei	Routine	5.7	4.5	6.0	0.03*
	Modified	2.2	1.5	1.9	
Total defective nuclei nuclei	Routine	849.3	676.5	389.3	0.22
	Modified	1009.1	839.5	555.1	
CV of 2c DNA stemline	Routine	2.13	2.14	0.73	0.007*
	Modified	2.65	2.61	0.76	
% of nuclei cleaned	Routine	26.66	20.97	11.37	0.96
	Modified	27.19	25.17	8.62	

*statistically significant $p < 0.05$

4.4.3 DNA ploidy and dysplasia

Of the 228 samples, 42 (18.4%) were aneuploid, 3 (1.3%) tetraploid and 183 (80.3%) diploid (Table 4.6). DNA aneuploidy was diagnosed mainly in lesions with moderate (36%) and severe (38%) epithelial dysplasia. The majority of non-dysplastic lesions (65.6%) were diploid (Table 4.6).

There was a significant association between grade of dysplasia and DNA ploidy status (Pearson x^2= 73.3, df = 3, $p < 0.001$). Sixteen of 28 cases with severe dysplasia were aneuploid (57.1%) and the remainders were diploid (12/28 = 42.9%). Approximately three quarters of the mildly dysplastic epithelial lesions (74.5%) were diploid. No non-dysplastic epithelial lesions showed abnormal DNA content.

Table 4.6 Distribution of DNA ploidy by degree of dysplasia in all samples.
Upper table shows % of total with each DNA ploidy result and lower table % of each dysplasia grade.

DNA ploidy	Dysplasia n (%)				Total n (%)
	None	Mild	Moderate	Severe	
Diploid	120 (65.6)	35 (19.1)	16 (8.7)	12 (6.6)	183 (100.0)
Tetraploid	1 (33.3)	1 (33.3)	1 (33.3)	0 (0.0)	3 (100.0)
Aneuploid	0 (0.0)	11 (26.2)	15 (35.7)	16 (38.1)	42 (100.0)
Total n (%)	121 (53.1)	47 (20.6)	32 (14.0)	28 (12.3)	228 (100.0)

DNA ploidy	Dysplasia n (%)				Total n (%)
	None	Mild	Moderate	Severe	
Diploid	120 (99.2)	35 (74.5)	16 (50.0)	12 (42.9)	183 (80.26)
Tetraploid	1 (0.8)	1 (2.13)	1 (3.1)	0 (0.0)	3 (1.32)
Aneuploid	0 (0.0)	11 (23.40)	15 (46.9)	16 (57.1)	42 (18.4)
Total n (%)	121 (100.0)	47 (100.0)	32 (100.0)	28 (100.0)	228 (100.0)

Representative examples of ploidy histograms are shown in Figure 4.5. Lymphocytes appear slightly left of the diploid peak because of high nuclear density and refraction of light around the periphery.

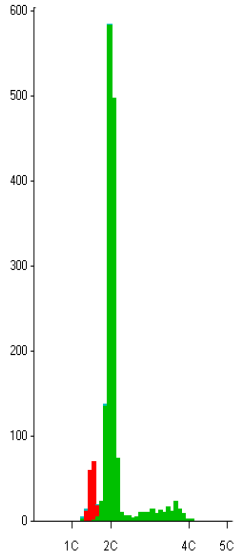

Diploid peak only, 505 nuclei, CV 3.6, small S phase/G2 phase
Diagnosis: Diploid

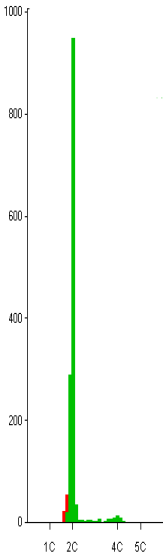

Diploid peak only, 1238 nuclei, CV 2.8
Diagnosis: Diploid

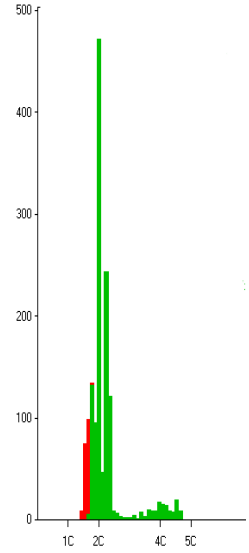

Diploid peak 120 nuclei, CV2.6, 2 aneuploid peaks at diploid index 1.14 and 1.29. No nuclei >5C. **Diagnosis**: Aneuploid on basis of stem line peaks

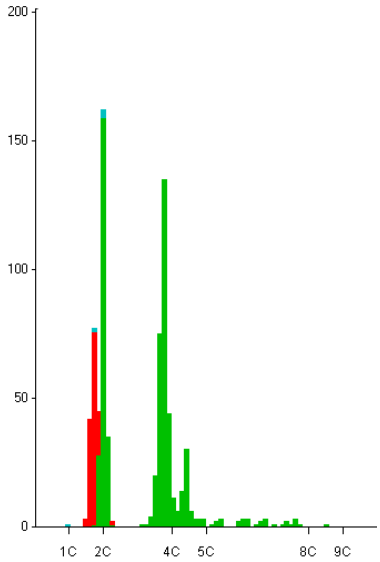

Diploid peak 220 nuclei, CV 2.9, Aneuploid peak at diploid index 1.88 of 46.7% nuclei and at 2.2 with 8.2% of nuclei.
5C exceeding rate 3.98%
Diagnosis: Aneuploid on basis of stem line peaks & 5C exceeding rate

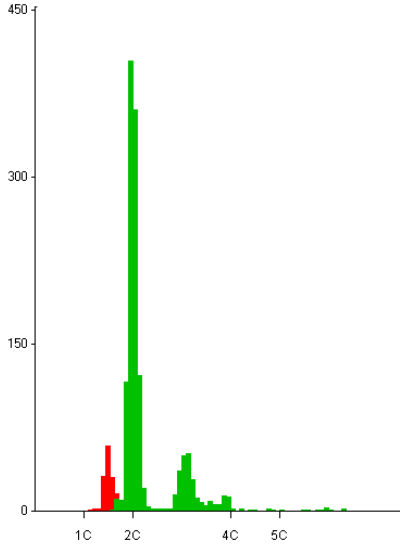

Diploid peak CV 4, 550 nuclei. Aneuploid peak at diploid index 1.55 containing 15% of epithelial nuclei. 5C exceeding rate 0.75%.
Diagnosis: Aneuploid on basis of stem line peak

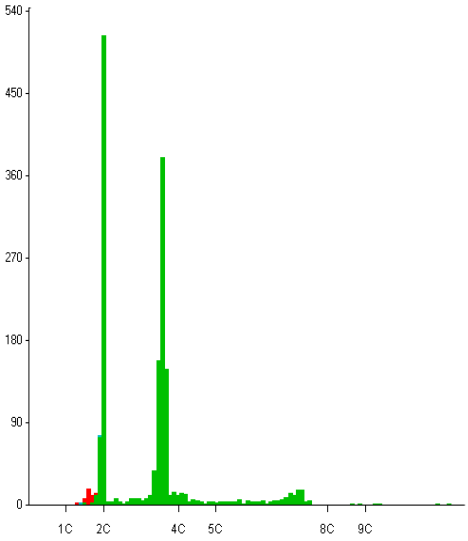

Diploid peak CV 2.4, 482 nuclei. Aneuploid peak at diploid index 1.78 containing 44% of epithelial nuclei. 5C exceeding rate 8.9%. A small peak at 7C probably represents a G2 phase for the aneuploid cell line.
Diagnosis: Aneuploid on basis of stem line peak and 5C exceeding rate

Figure 4.5 Example ICM DNA ploidy histograms from this study.
All x axes show integrated optical density on a scale of DNA content per nucleus. 2C diploid peak. Histogram descriptive parameters are shown below each graph, together with ploidy diagnostic category and reasons for categorisation. Green, epithelial nuclei, red lymphocytes internal diploid control.

4.4.4 Dysplasia and malignant transformation

4.4.4.1 Analysis including early transformation

Among the 24 (10.5%) of 228 patients who developed carcinoma including those with transformation less than 6 months from index lesion, more than half (58.3%) had severe dysplasia (Table 4.3). The mean transformation time was 1.95 year (SD = 2.09).

One case was excluded in the Kaplan-Meier and Cox regression analyses because the worst dysplasia was on the day carcinoma developed but prior biopsies had been aneuploid 8 months before transformation. Adjusting for age and sex, Kaplan-Meier curves of progression-free estimates in Figure 4.5 shows that the time to malignant transformation was significantly shorter in the severely dysplastic group (log rank: x^2= 76.25, df = 3, $p < 0.0001$).

Hazard ratios were highly significant ($p < 0.001$) implying the risk of a severely dysplastic lesion on developing carcinoma was 81.8 (95% CI: 10.5, 635.9) times higher than for a non-dysplastic lesion (Table 4.7). Multivariate analysis was conducted incorporating all grades of dysplasia and ploidy adjusted for age and gender, and showed that the HR for severe dysplasia was lower at 54.25 (CI: 6.6, 448.2) but remained highly significant ($p < 0.001$).

The percentage estimates of transformation after 2, 5 and 9 years were detailed in Table 4.8. An increasing trend in cumulative malignant transformation incidence was observed in relation to the length of follow-up. No further transformations were detected after 5 years for mild and moderate dysplasia. The proportion of patients with severe dysplasia who progressed to carcinoma in 5 years was 45% (95% CI: 28.3, 65.1) compared to 23% (95% CI: 11.7, 42.6) for moderate dysplasia.

Table 4.7 Cox proportional hazards model on association of dysplasia grade and ploidy status with malignant progression including transformation within 6 months

	N	Univariate		Multivariate	
		HR (95% CI)	*P* value	HR (95% CI)	*P* value
Total patients	228				
Dysplasia					
No	121	1.00	-	1.00	-
Mild	47	5.13 (0.46, 56.6)	0.182	3.81 (0.33, 43.96)	0.284
Moderate	32	29.64 (3.6, 243.6)	0.002	18.78 (2.1, 167.9)	0.009
Severe	28	81.82 (10.5, 635.9)	0.000	54.25 (6.6, 448.2)	0.000
DNA Ploidy					
Diploid	183	1.00	-	1.00	-
Aneuploid	42	7.92 (3.45, 18.17)	0.000	2.41(0.89, 6.52)	0.083

HR: hazard ratio
Univariate: adjusted for age, sex
Multivariate: adjusted for age, sex and mutually adjusted

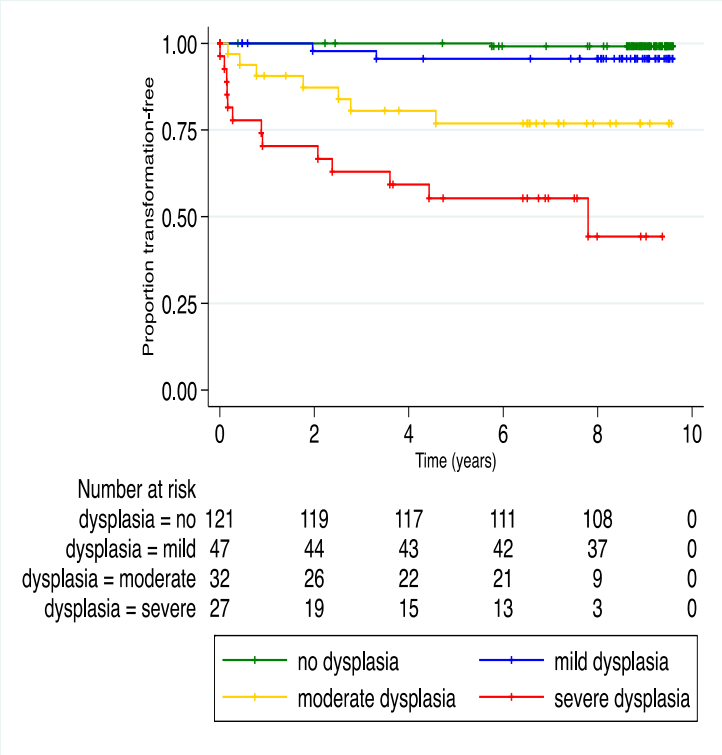

Figure 4.6 Kaplan Meier curves of progression-free proportion by dysplasia grades including transformation within 6 months.
The number of patients who were still at risk at selected time points (*x*-axis) is shown below. The difference in time to progression for different grades were statistically significant, log rank test p=0.000.

Table 4.8 Cumulative incidence of malignant transformation at 2, 5 and 9 years interval including progression within 6 months of index lesion

	N	Malignant transformation estimate			
		2 year *n*; %(CI)	**5 year** *n*; %(CI)	**9 year** *n*; %(CI)	**Test for trend**
Dysplasia					
No	121	0	0	1; 0.86 (0.12,5.96)	
Mild	47	1; 2.22(0.32, 14.7)	2; 4.44(1.13, 16.6)	2; 4.44(1.13, 16.6)	x^2 = 76.25 df=3 *P* = 0.0000
Moderate	32	4; 12.73 (4.97, 30.5)	7; 23.11 (11.7, 42.6)	7; 23.11 (11.7, 42.6)	
Severe	28	8; 29.63 (16.1, 50.6)	12; 44.69 (28.3, 65.1)	13; 55.75 (33.8, 80.0)	
Overall	227	13; 5.78(3.4, 9.74)	21; 9.45(6.27, 14.1)	23; 10.5(7.08, 15.4)	x^2= 397.8 df=1 *P* = 0.0000
DNA Ploidy					
Diploid	183	6; 3.33(1.51, 7.27)	9; 5.05 (2.66, 9.49)	10; 5.64 (3.07, 10.23)	x^2 = 33.15 df=2 *P* = 0.0000
Tetraploid	3	0	0	0	
Aneuploid	42	8; 19.25 (10.1, 34.8)	13; 31.48 (19.6, 47.9)	14; 37.19 (22.9, 56.3)	
Overall	228	14; 6.21(3.73, 10.3)	22; 9.87(6.61, 14.6)	24; 10.9(7.43, 15.8)	x^2= 398.4 df=1 *P* = 0.0000

4.4.4.2 Analysis excluding early transformation

Excluding patients with transformation within 6 months of the index biopsy (n = 219), the number of cases that underwent malignant transformation was reduced to 15 in a mean time of 3.03 years (SD = 1.96). One patient (6.7%) with a nondysplastic lesion and 2 (13.3%), 5 (33.3%), 7 (46.7%) patients with mild, moderate and severely dysplastic epithelium respectively had undergone malignant transition.

Patients with a higher grade of dysplasia developed carcinoma more rapidly (log rank: x^2= 40.28, df = 3, p < 0.0001, Figure 4.6). Although the hazard ratios for moderate and severe dysplasia were decreased to 21.6 (2.49, 186.8) and 45.8 (5.52, 379.6) respectively when compared to univariate analysis that included early transformation, they remained highly significant with p-value ≤ 0.005 (Table 4.9).

Multivariate analysis incorporating all grades of dysplasia and ploidy, adjusted for age and gender showed that the hazard ratio for severe dysplasia was lower at 30.56 (3.37, 277.4). The p value was slightly higher than in the univariate analysis, however still significant (p < 0.05).

The transformation rate estimate at 9 years was 43.11% (95%CI 20.2, 75.6), at 5 years 28.89% (95%CI: 14.1, 53.4) and 2 years for severe dysplasia 9.52% (95%CI: 2.47, 33.0) (Table 4.10). Progression to carcinoma from mild and moderately dysplastic epithelium occurred in the first five years duration from the index biopsies.

Table 4.9 Cox proportional hazards model on association of dysplasia grade and ploidy status with malignant progression excluding transformation within 6 months

	N	Univariate		Multivariate	
		HR (95% CI)	*P* value	HR (95% CI)	*P* value
Total patients	219				
Dysplasia grade					
No	121	1.00	-	1.00	-
Mild	47	5.03 (0.46, 55.7)	0.187	3.90 (0.33, 45.4)	0.278
Moderate	30	21.57 (2.49, 186.8)	0.005	14.11 (1.45, 137.3)	0.023
Severe	21	45.79 (5.52, 379.6)	0.000	30.56 (3.37, 277.4)	0.002
DNA Ploidy					
Diploid	180	1.00	-	1.00	-
Aneuploid	36	6.79 (2.56, 17.9)	0.000	2.39(0.72, 7.98)	0.155

HR = hazard ratio
Univariate: adjusted for age, sex
Multivariate: adjusted for age, sex and mutually adjusted

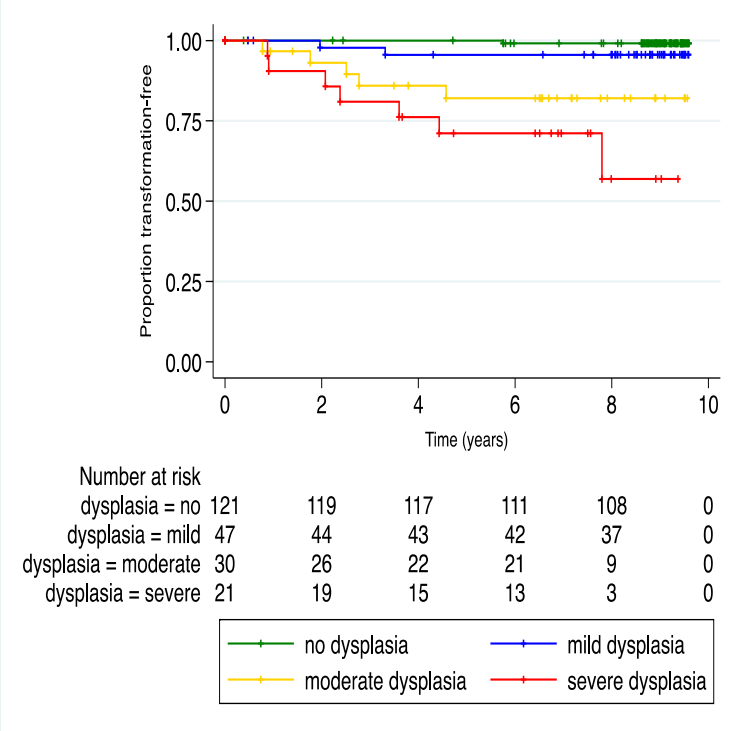

Figure 4.7 Kaplan Meier curves of progression-free proportion by dysplasia grades including transformation within 6 months.
The number of patients still at risk at selected time points (*x*-axis) is shown below. The difference in time to progression for different grades were statistically significant, log rank test p=0.000.

Table 4.10 Cumulative incidence of malignant transformation at 2, 5 and 9 years interval excluding progression within 6 months of index lesion

	n	Malignant transformation estimate			
		2 year *n*; %(CI)	**5 year** *n*; %(CI)	**9 year** *n*; %(CI)	**Test for trend**
Dysplasia					
No	121	0	0	1; 0.86 (0.12,5.96)	x^2 = 40.28 df=3 *P* = 0.0000
Mild	47	1; 2.22 (0.32, 14.7)	2; 4.44 (1.13, 16.6)	2; 4.44 (1.13, 16.6)	
Moderate	30	2; 6.91 (1.77, 24.9)	5; 17.98 (7.88, 38.03)	5; 17.98 (7.88, 38.03)	
Severe	21	2; 9.52 (2.47, 33.0)	6; 28.89 (14.1, 53.4)	7; 43.11 (20.2, 75.6)	
Overall	219	5; 2.33(0.98, 5.52)	13; 6.14(3.61,10.3)	15; 7.21(4.4, 11.7)	x^2=377.9 df=1 *P* = 0.0000
DNA Ploidy					
Diploid	183	3; 1.71 (0.55, 5.2)	6; 3.46 (1.57, 7.54)	7; 4.06 (1.95, 8.32)	x^2 = 17.88 df=2 *P* = 0.0001
Tetraploid	3	0	0	0	
Aneuploid	36	2; 5.71 (1.46, 20.9)	7; 20.0 (10.1, 37.4)	8; 26.67 (13.4, 48.7)	
Overall	219	5; 2.34(0.98, 5.52)	13; 6.15(3.62, 10.4)	15; 7.21(4.4, 11.7)	x^2=377.6 df=1 *P* = 0.0000

4.4.5 DNA ploidy and malignant transformation

Including malignant transformation within 6 months of the index biopsy, 14 (58.3%) aneuploid and 10 (41.7%) diploid lesions progressed to carcinoma (Table 4.3) in a mean time of 2.05 years (SD = 2.01). The risk of cancer transition was 7.92 times higher (CI: 3.45, 18.17) in aneuploid than diploid lesions ($p < 0.001$) (Table 4.7). Patients with aneuploid lesions developed cancer more rapidly than those with diploid (log rank: $x^2 = 33.15$, df = 2, $p < 0.0001$) (Figure 4.7). At year 2, 5 and 9, the transformation estimates for aneuploid lesions were 19.25% (CI: 10.1, 34.8), 31.48% (CI: 19.6, 47.9) and 37.19% (CI: 22.9, 56.3) respectively (Table 4.8). At nine years follow up the proportion of aneuploid lesions that underwent malignant transformation was significantly higher 37.19% compared to 4.06% for diploid lesions.

Excluding patients with transformation within 6 months of the index biopsy (n = 219), 8 (53.3%) patients with aneuploid and 7 (46.7%) diploid lesions underwent malignant transformation (Table 4.5). The mean transformation time was 3.05 year (SD = 1.93). The hazard ratio for a patient with aneuploid was 6.79 (CI: 2.56, 17.9) and was highly significant ($p < 0.001$) compared to patients with diploid lesions (Table 4.9). Patients with aneuploid index lesions developed carcinoma in a shorter time than diploid (log rank: $x^2 = 17.88$, df = 2, $p = 0.0001$) (Figure 4.9). Over a 5-year period, the transformation rate estimate was 20.0% (CI: 10.1, 37.4) for aneuploid compared to diploid at 3.46% (CI: 1.57, 7.54).

In multivariate analysis, the hazard ratio for patients with aneuploid lesions was 2.41(CI: 0.89, 6.52) and 2.39 (CI: 0.72, 7.98) when transformation of less than 6 months was included and excluded in the analysis, respectively (Table 4.7 and 4.9). However these were not statistically significantly different.

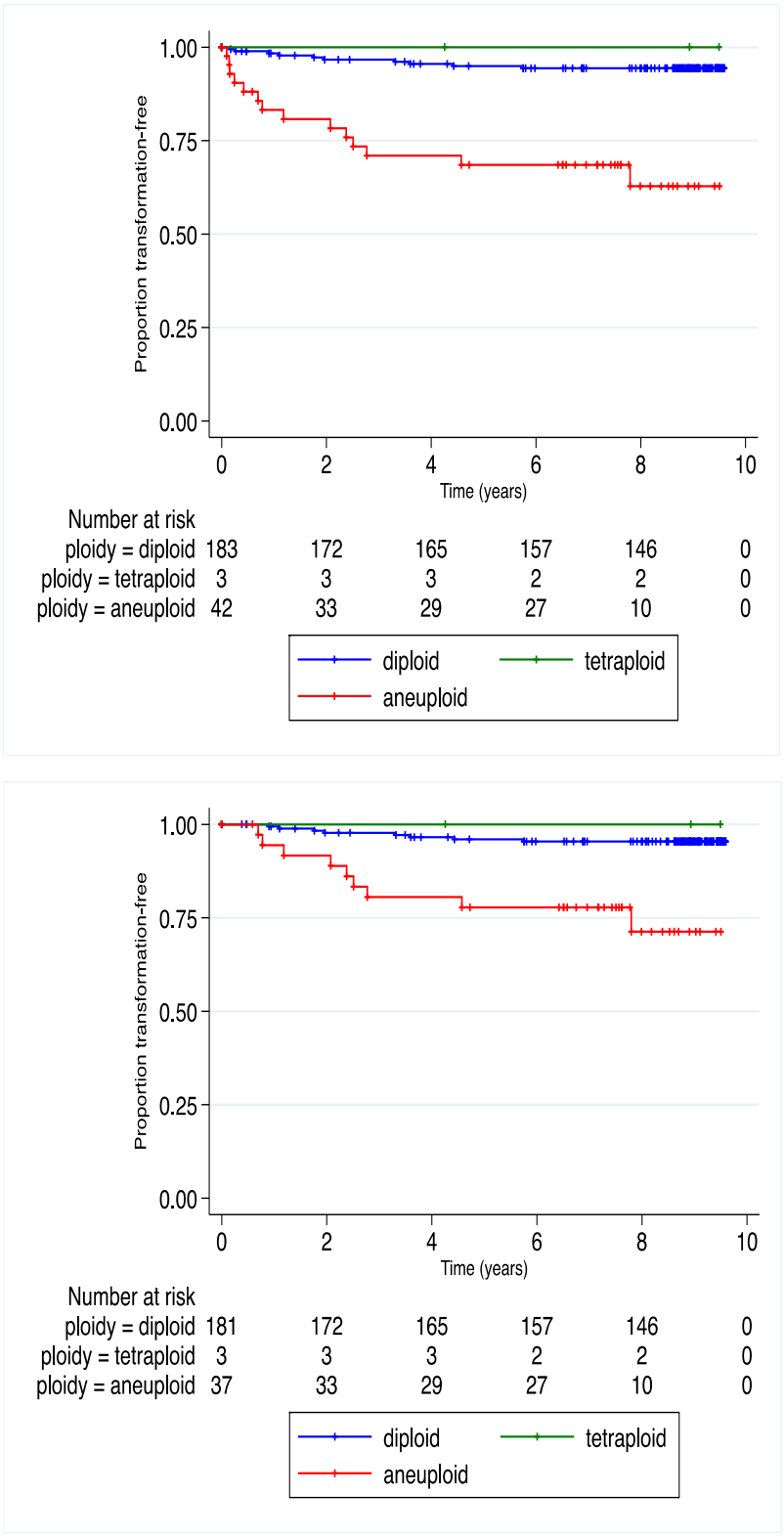

Figure 4.8 Kaplan Meier survival curves including (upper panel) and excluding (lower panel) within 6 months transformation by DNA ploidy.
Number of patients still at risk at selected time points (shown on *x*-axis) is shown below.

4.4.5.1 Annual transformation rate

Annual malignant transformation rates based on dysplasia grading and DNA aneuploidy are shown in Table 4.11 to 4.13. For dysplasia grade, total person-year of follow up was 1733.07 and 1731.64 when transformation within 6 months was included and excluded yielding an annual rate of 1.32% and 0.87% respectively. Transformation rates increased with the severity of dysplasia. When transformation within 6 months of index lesion was excluded, the rates were 0.09% for the non-dysplastic lesion, 0.53% for mild, 2.68% moderate and 5.77% for severe dysplasia. Annual malignant transformation rates for ploidy calculated with inclusion and exclusion of within 6 months malignant transformation were 1.38% and 0.87% cases per year respectively. By analyzing cases of dysplasia only (Table 4.13), the transformation rate was slightly higher at 3.2% and 2.04% cases per year when early transformation was included and excluded respectively.

Table 4.11 Dysplasia grade- and DNA ploidy-specific annual transformation rates including malignant transformation within 6 months of index biopsy

	N	***n* malignant**	**Person-years follow up**	**Annual transformation rate (%)**	**95% CI**
Dysplasia grade					
No	121	1	1045.02	0.09	0.01 – 0.68
Mild	47	2	378.85	0.53	0.13 – 2.11
Moderate	32	7	187.08	3.74	1.78 – 7.85
Severe	28	13	122.13	10.64	6.18 – 18.33
Overall	228	23	1733.07	1.32	0.88 – 1.99
DNA Ploidy					
Diploid	183	10	1478.24	0.68	0.36 – 1.26
Tetraploid	3	0	22.68	0	-
Aneuploid	42	14	234.31	5.97	3.54 – 10.1
Overall	228	24	1735.23	1.38	0.93 – 2.06

Table 4.12 Dysplasia grade- and DNA ploidy-specific annual transformation rates excluding malignant transformation within 6 months of index biopsy

	N	*n* malignant	Person-years follow up	Annual transformation rate (%)	95% CI
Dysplasia grade					
No	121	1	1045.02	0.09	0.01 – 0.68
Mild	47	2	378.85	0.53	0.13 – 2.11
Moderate	30	5	186.49	2.68	1.11 – 6.44
Severe	21	7	121.29	5.77	2.75 – 12.11
Overall	219	15	1731.64	0.87	0.52 – 1.44
DNA Ploidy					
Diploid	180	7	1476.69	0.47	0.23 – 0.99
Tetraploid	3	0	22.68	0	-
Aneuploid	36	8	232.55	3.44	1.72 – 6.88
Overall	219	15	1731.93	0.87	0.52 – 1.44

Table 4.13 The annual transformation rates of dysplasia grade determined by omitting the non-dysplastic samples

	N	*n* malignant	Person-years follow up	Annual transformation rate (%)	95% CI
Dysplasia grade					
			Including 6 months		
Mild	47	2	378.85	0.53	0.13 – 2.11
Moderate	32	7	187.08	3.74	1.78 – 7.85
Severe	27	13	122.13	10.64	6.18 – 18.33
Overall	106	22	688.06	3.20	2.10 – 4.86
			Excluding 6 months		
Mild	47	2	378.85	0.53	0.13 – 2.11
Moderate	30	5	186.48	2.68	1.11 – 6.44
Severe	21	7	121.29	5.77	2.75 – 12.1
Overall	98	14	686.63	2.04	1.21 – 3.44

4.4.6 Predictive values for dysplasia grading combined with DNA ploidy

The number of patients in the tetraploid group was too small for analysis, therefore predictive values were calculated combining diploid and tetraploid groups, justified on the basis our previous analysis (Sperandio *et al.*, 2013).

Including malignant transformation less than 6 months from index lesion (Table 4.14), the positive predictive value (PPV) for severe dysplasia was 50% (CI: 31.5, 68.5) and 33.3% (CI: 19.0, 47.6) for aneuploid lesions. When lesions with both DNA aneuploidy and severe dysplasia were combined, the PPV was increased to 56.3% (31.9, 80.6). Diploid or tetraploid and non-dysplastic lesions had high negative predictive values (NPV) of 94.6% (CI: 91.4, 97.8) and 99.17 % (97.4, 100.8) respectively.

Excluding cases with transformation within 6 months of index lesion (Table 4.15), the PPV was reduced to 33.3% (CI: 13.1, 53.5) and 22.2% (CI: 8.6, 35.8) for severe dysplasia and DNA aneuploidy respectively. When lesions with both DNA aneuploidy and severe dysplasia were combined, the PPV was slightly increased to 36.4% (7.9, 64.8). The NPV of diploid or tetraploid was 96% (CI: 93.4, 99.0) and 99% (CI: 97.4, 100.8) for non-dysplastic lesions.

Table 4.14 Positive and negative predictive value of dysplasia grading and DNA ploidy including malignant transformation within 6 months of index biopsy

			PPV %(95 CI)	NPV %(95 CI)
Total patients			*N* = 228	
Dysplasia grade				
Severe			50.0 (31.5, 68.5)	50.0 (31.5, 68.5)
Moderate			21.88 (7.5, 36.1)	78.12 (63.8, 92.4)
Mild			4.26 (-1.5, 9.9)	95.74 (89.9, 101.5)
No			0.83 (-0.8, 2.4)	99.17 (97.4, 100.8)
DNA Ploidy				
Aneuploid			33.33 (19.0, 47.6)	66.67 (59.9, 73.5)
Diploid or Tetraploid			5.38 (2.1, 8.5)	94.62 (91.4, 97.8)
Combinations				
DNA ploidy	**Operator**	**Dysplasia**		
Aneuploid	AND	Severe	56.3 (31.9, 80.6)	-
Aneuploid	AND	Severe OR moderate	45.2 (27.6, 62.7)	-
Aneuploid	AND	Any grade	33.3 (19.1, 47.6)	-
Aneuploid	OR	Severe	35.2 (22.4, 47.9)	-
Aneuploid	OR	Severe OR moderate	29.2 (18.7, 39.7)	-
Aneuploid	OR	Any grade	21.5 (13.7, 29.3)	-
Diploid or Tetraploid	AND	No dysplasia	-	99.2 (97.6, 100.8)
Diploid or Tetraploid	AND	No dysplasia OR mild dysplasia	-	98.1 (95.9, 100.2)
Diploid or Tetraploid	AND	Any grade	-	94.6 (91.4, 97.9)
Diploid or Tetraploid	OR	No dysplasia	-	94.6 (91.4, 97.9)
Diploid or Tetraploid	OR	No dysplasia OR mild dysplasia	-	94.9 (91.9, 98.0)
Diploid or Tetraploid	OR	Any grade	-	89.5 (85.5, 93.5)

PPV positive predictive value; NPV negative predictive value

Table 4.15 Positive and negative predictive value of dysplasia grading and DNA ploidy excluding malignant transformation within 6 months of index biopsy

			PPV %(95 CI)	NPV %(95 CI)
Total patients			*N* = 219	
Dysplasia grade				
Severe			33.33 (13.1, 53.5)	66.67 (46.5, 86.9)
Moderate			16.67 (3.4, 30.0)	83.33 (70.0, 96.6)
Mild			4.26 (-1.5, 9.9)	95.74 (89.9, 101.5)
No			0.83 (-0.8, 2.4)	99.17 (97.4, 100.8)
DNA Ploidy				
Aneuploid			22.22 (8.6, 35.8)	77.78 (64.2, 91.4)
Diploid or Tetraploid			3.83 (1.0, 6.6)	96.17 (93.4, 99.0)
Combinations				
DNA ploidy	**Operator**	**Dysplasia**		
Aneuploid	AND	Severe	36.4 (7.9, 64.8)	-
Aneuploid	AND	Severe OR moderate	32.0 (13.7, 50.3)	-
Aneuploid	AND	Any grade	22.2 (8.6, 35.8)	-
Aneuploid	OR	Severe	23.9 (11.6, 36.2)	-
Aneuploid	OR	Severe OR moderate	19.4 (9.5, 29.2)	-
Aneuploid	OR	Any grade	14.3 (7.4, 21.2)	-
Diploid or Tetraploid	AND	No dysplasia	-	99.2 (97.6, 100.8)
Diploid or Tetraploid	AND	No dysplasia OR mild dysplasia	-	98.1 (95.9, 100.2)
Diploid or Tetraploid	AND	Any grade	-	96.2 (93.4, 99.0)
Diploid or Tetraploid	OR	No dysplasia	-	96.2 (93.4, 99.0)
Diploid or Tetraploid	OR	No dysplasia OR mild dysplasia	-	96.4 (93.8, 99.0)
Diploid or Tetraploid	OR	Any grade	-	93.2 (89.8, 96.5)

PPV positive predictive value; NPV negative predictive value

4.5 Discussion

4.5.1 Methods

In this study, a novel nuclear separation technique was applied that required only half as much tissue as the conventional protocol (section 4.3.4). OPMDs tissues mainly derive from small biopsies and it is not always feasible to obtain the 50mm epithelial length required to yield 3000 nuclei for DNA ploidy analysis using the conventional separation method. The proportion of nuclei exceeding 5c and 9c can be determined more precisely when at least 1000 nuclei remain after editing and included in the analysis (Pradhan *et al.*, 2006). Total nuclei obtained by the modified protocol were more numerous than the routine method (section 4.4.2), overall similar numbers being isolated form samples half the size used conventionally. Interestingly, more lymphocytes were acquired by the modified method ($p < 0.001$). Although there was no statistical difference between these methods in the CVs of the diploid peak on analysis, the routine method produced lower CV values.

We have analysed outcomes for dysplasia grades and DNA ploidy diagnoses with and without early transformation. Most studies have applied a 6-month cut off for exclusion of early transformation in their analyses. The reason is that most investigators are intending to define transformation rates in OPMD and must ensure carcinomas are not included in error. Transformation within 6 months of biopsy is assumed to result from sampling error at the stage of biopsy and to indicate that the carcinoma was already present at the time. However, in clinical practice it would be required that a test could identify the risk of concurrent as well as subsequent carcinoma. In addition, the experiments might reveal diagnostic information capable of identifying lesions with a risk of early transformation. In order to reduce the risk that any samples comprised

carcinoma, we excluded cases where a carcinoma was diagnosed at the site within 2 weeks of the index biopsy. Our study in general has showed that early transformations often found in moderately or severely dysplastic lesions that were aneuploid (refer to Table 4.8 and 4.10) as in the previous study from our laboratory (Sperandio *et al.*, 2013). It is not possible to comment on whether these early transforming cases did have concurrent carcinoma, but if so it was not appreciated clinically.

4.5.2 Samples

The samples selected in these experiments were from a sequential series of patients who had lesions considered at high risk of malignant transformation on the basis of both clinical description and pathological diagnosis (Table 4.2). This study population differs from that in the study published previously by our group (Sperandio *et al.*, 2013) in which all red and white lesions were included and low risk lesions were included, a much larger population. Other studies that used DNA image cytometry have selected samples confirmed histologically as dysplastic in a case-control design (Torres-Rendon *et al.*, 2009; Bradley *et al.*, 2010) while two others included only cases of leukoplakia (Bremmer *et al.*, 2011; Siebers *et al.*, 2013). The intention of this study was to provide an evaluation of ploidy analysis and dysplasia grading on a more focused group of risk patients to evaluate the predictive value of the test when used in a hospital referral population and in routine pathology diagnosis. This and our previous study have approximately the same size sample, but the present cases were selected from a shorter time period. This was possible because experience in ICM DNA ploidy and the new sample method allowed a higher proportion of eligible cases to be successfully analysed.

Follow-up data on 240 patients was obtained for this study. We were surprised to discover that some carcinoma-in-situ codes had been miscoded as carcinoma at the

national registry but were able to confidently exclude these as non-invasive dysplasia on the basis of dates of diagnosis matching exactly those in our local pathology database that are transferred to the cancer registry, lack of subsequent cancer codes and outcome. It is unclear at what stage of cancer registration the miscoding occurred. Miscoding is an issue in all cancer registration and in one audit of a UK central cancer registry, a miscoding rate of 2.4% was found after data cleaning for primary skin squamous carcinoma (Maudsley and Williams, 1999), similar to our findings. *In situ* carcinoma is considered synonymous with severe dysplasia in the WHO classification and by the pathologists reporting cases for this study. However, the term causes problems in cancer registration. The Office for National Statistics defines carcinoma in situ as "the cancer is in its earliest stages (not yet spread from the surface layer of cells in an organ or other tissue) and is usually curable" implying that the *in situ* stage is a cancer (Office for National Statistics).

In every case where nuclear suspensions were obtainable, a DNA ploidy analysis result could be produced. Three samples that were very thin and small with size of less than 3mm in length yielded insufficient nuclei and were excluded from analysis (section 4.4.1). Excluded samples and cases were few in number and would appear to carry little risk of sample bias (refer to Figure 4.4). Excluded cases comprised 1 patient without dysplasia, 3 with mild and 4 with moderate or severe dysplasia.

The distributions of age and gender, grades of dysplasia and presence of aneuploidy are comparable to other similar studies. The mean age of this study population is similar to Bremmer *et al.* (2011) and Sperandio *et al.* (2013). Comparing to studies that evaluated OPMDs without DNA ploidy analysis, the mean age is also similar (Napier *et al.*, 2003; Brouns *et al.*, 2014; Dost *et al.*, 2014). When all patients were grouped into

those who had undergone malignant transformation and those who had not, the mean age was slightly higher in the former group. This pattern is seen in both sets of analyses regardless of whether transformation in less than 6 months was included or excluded (Table 4.3 and 4.4). Nevertheless, the mean age of population that had malignant transformation in this study is consistent with previous similar studies (Torres-Rendon *et al.*, 2009; Bradley *et al.*, 2010; Siebers *et al.*, 2013).

The male to female ratio follows most Western population studies with higher numbers of male than female patients (Torres-Rendon *et al.*, 2009; Bradley *et al.*, 2010; Siebers *et al.*, 2013) though there is no consensus on the expected ratio and others have reported the opposite (Napier *et al.*, 2003; Bremmer *et al.*, 2011). A low male to female ratio in the subgroup who developed carcinoma is also consistent with previous studies (Napier *et al.*, 2003; Warnakulasuriya *et al.*, 2011; Brouns *et al.*, 2014) though this has also not been consistent in the literature and differs from others with similar experimental designs using selected patients rather than sequential series (Torres-Rendon *et al.*, 2009; Bradley *et al.*, 2010; Bremmer *et al.*, 2011; Siebers *et al.*, 2013).

4.5.3 Dysplasia and DNA ploidy

Our data shows that, of the clinically suspicious lesions, almost half had a histological diagnosis of dysplasia. This is similar to previous dysplasia-ploidy studies (Bremmer *et al.*, 2011; Siebers *et al.*, 2013). Again, there is no consensus on the expected prevalence of dysplasia in such series. Some have shown dysplasia to be relatively infrequent in high-risk lesions in population-based studies (Banoczy, 1977; Silverman *et al.*, 1984; Cowan *et al.*, 2001). A study in Northern Ireland (Cowan *et al.*, 2001) revealed that only 12% of 'worrying' intra-oral mucosal lesions selected for biopsy were dysplastic. These differences highlight that study design and sample size and selection

can bias studies by altering the proportion of high risk cases and number with dysplasia. The features of our study population are supported as representative by data from a 10-year follow-up study in the South-East London population (Warnakulasuriya *et al.*, 2011), the source of most of samples diagnosed in this institution.

Surprisingly, in view of different case inclusion criteria, we have found similar proportions of DNA ploidy abnormalities in our study population as in our previous study (Sperandio *et al.*, 2013). Approximately 20% of cases showed aneuploidy in both studies. Tetraploidy was reported more frequently in the earlier study and this may be a result of poorer preparation quality, a lower number of nuclei included in the analysis and acceptance of a higher diploid peak CV in the diagnostic criteria.

A significant correlation between DNA ploidy and dysplasia grade shown in this study was consistent with previous reports (Saito *et al.*, 1995; Pentenero *et al.*, 2009; Torres-Rendon *et al.*, 2009; Bradley *et al.*, 2010; Sperandio *et al.*, 2013). Among the aneuploid lesions, approximately 40% were severely dysplastic and the proportions decreased with lower degree of dysplasia (refer to Table 4.6). None of our non-dysplastic lesions were aneuploid. As in the previous studies cited above, diploid status was found in 43% of severely dysplastic lesions and half of moderately dysplastic lesions and 23% of mild dysplasia lesions harboured aneuploidy. As the positive predictive value of dysplasia exceeds that of aneuploidy alone, it can be concluded that severe dysplasia does transform when ICM DNA diploid and this raises the possibility of whether diagnostic criteria or higher definition techniques might identify these extra cases at risk. It can also be concluded that ICM DNA ploidy has value in identifying high risk lesions from among apparently low risk cases with mild dysplasia.

4.5.4 Dysplasia and malignant transformation

As noted in the introduction, most studies have failed to show a good correlation between dysplasia grade and malignant transformation. Among the recent studies that reported lack of association between dysplasia grade and malignant transformation, the approach taken by Dost *et al.* (2014) to model a 'real-world' setting appears attractive because it uses the original diagnostic report. This approach accepts that diagnosis in routine practice is less standardized that it would be in a research setting or with a consensus diagnosis. In the present study and previous study (Sperandio *et al.*, 2013) we also opted to use the original diagnostic dysplasia grade, which according to local protocol at the time of diagnosis was a consensus of two pathologists views, with a third opinion sought in the event of disagreement. This approach has recently been suggested as best practice for research studies (Speight *et al.*, 2015).

Without re-diagnosing any cases in this study, we applied a prospective research design and found a significantly higher risk of malignant transformation with higher grade of dysplasia (Table 4.7 and 4.9). Each grade remains statistically significant even when DNA ploidy was considered simultaneously and was true whether or not early transformation was included, which concurs with the findings of our previous study on cases from the previous decade (Sperandio *et al.*, 2013). These results support that dysplasia grade is a strong independent indicator of malignant transformation. Bremmer *et al.* (2011) grouped mild or no dysplasia together and moderate or severe dysplasia together as a second group and showed a significant association with risk of progression. These combinations may be in keeping with recently recommended binary classification but we show a statistically significant trend between dysplasia grades, which justifies distinguishing three grades. Our results are supported by a meta-analysis

on 14 follow-up studies of oral dysplasia that demonstrated a clear distinction in transformation rates between all three grades (Mehanna *et al.*, 2009).

In this series, carcinomas arising in mild and moderate dysplasia arose in the first 2 years of follow up, while those arising in severe dysplasia continued to develop throughout the 9.6 years study duration (Table 4.8 and 4.10). Our findings concur with other studies showing that malignant transformation in all grades was greatest in the first 5 years of follow up and decreased thereafter, though risk remained (Pindborg *et al.*, 1968; Silverman *et al.*, 1984; Lind, 1987; Schepman *et al.*, 1998). One reason why the few diploid samples that progressed transformed early could be sampling error. Areas of moderate or severe dysplasia might have been present in adjacent mucosa but not sampled, resulting in an erroneously mild grade of dysplasia. Alternatively, this may just be random clustering of a small number of events.

Our group has shown that oral epithelial dysplasia indicates a 10-year risk of developing carcinoma (Warnakulasuriya *et al.*, 2011; Sperandio *et al.*, 2013). A 20-year population-based follow-up study has demonstrated that the proportion of transformation in dysplastic lesions for the first and second 10-year periods was similar (Cowan *et al.*, 2001). Moreover, the author of a systematic review on follow up studies of oral dysplasia concluded that the time to transformation range from 0.5 to 16 years (Mehanna *et al.*, 2009) and it seems likely that cases would continue to transform in a longer follow-up period.

4.5.5 DNA ploidy

The quality of DNA ploidy histograms obtained from the samples was very good and better than in our previous studies. This might be due to the use of samples that

had been stored for fewer years than those used by Sperandio *et al.* (2013), though considerably more experience has been gained in the analysis since that study was completed. An upgraded camera and improved cell sorting software was used in the current experiments. In the present work, the CV of the diploid peak was often very low around 1-2%, providing the system with high resolution to detect minor aneuploid peaks and matching the CV obtained in high resolution ultraviolet flow cytometry (Brouns *et al.*, 2012). Diagnostic criteria require a CV less than 5% and our much lower CVs lend confidence to the accuracy of the present data. The number of nuclei retrieved, a mean of 3150 nuclei per sample, was much higher than in previous studies, which report counts ranging from 1000 to 2000 (Torres-Rendon *et al.*, 2009; Bremmer *et al.*, 2011; Siebers *et al.*, 2013). The higher the number of nuclei the better the coefficient of variation would be expected to be.

The ploidy diagnostic criteria used in these experiments are the same as used previously (Sperandio *et al.*, 2013) and the same as in routine diagnostic use in our pathology service. These were originally validated by the Oslo group on other tissues, but are also used in general ploidy research by others. They differ from those used by Bradley *et al.* (2010) in which the cytology of the nuclei is also incorporated into the result by a diagnostic cytologist, though in an undefined way. The Oslo diagnostic criteria have proved effective in our previous work (Sperandio *et al.*, 2013) and have also been adopted by others (Torres-Rendon *et al.*, 2009; Siebers *et al.*, 2013). Using these criteria we were able to classify all ploidy histograms.

In agreement with our previous studies (Sperandio *et al.*, 2013) we have shown that DNA ploidy analysis predicts malignant transformation (Table 4.7). Outcomes for aneuploid and diploid lesions were statistically significantly different and, like dysplasia,

indicated a long-term risk of malignant transformation whether or not early transformation was excluded from the analysis. One similar study (Siebers *et al.*, 2013) analysed excluding early transformation produced a similar risk of transformation to the present study including early transformation. This difference is most likely to be due to differences in sample selection as discussed above (section 4.5.2). In a study of randomly selected patients presented with leukoplakia, Bremmer *et al.* (2011) found a lower hazard ratio.

We found that the statistical significance of DNA aneuploidy was lost when dysplasia grade was considered simultaneously in multivariate analysis (Table 4.7 and 4.9). This has not been shown by others (Bradley *et al.*, 2010; Bremmer *et al.*, 2011; Siebers *et al.*, 2013). However, those analyses were performed on smaller case series (Bremmer *et al.*, 2011), using different DNA ploidy analysis system (Bradley *et al.*, 2010), and incorporating only aneuploid lesions that were dysplastic (Bradley *et al.*, 2010; Bremmer *et al.*, 2011; Siebers *et al.*, 2013). Conclusions on the predictive superiority of DNA ploidy over traditional dysplasia for malignant transformation should therefore be made with caution. Our data suggests that ploidy results should be considered along with other established parameters when predicting the outcome of OPMDs and possible combinations of results are discussed below.

4.5.6 Malignant transformation

No follow up study has yet reported patterns of malignant transformation for DNA ploidy diagnoses over such a long period. In this study, the proportion of cases that underwent malignant transformation in the ICM DNA aneuploid group was greatest in the first 5 years, similar to rates for lesions with severe dysplasia (Table 4.11 to 4.13). This similarity was expected, as most aneuploid lesions were also severely dysplastic. All

cases that transformed in the ICM DNA diploid group developed carcinoma during the first 6 years of follow up.

There is significant variation in the literature regarding the transformation rate of dysplasia, as discussed earlier (see section 1.2.7). Disparities in the literature often arise following simplistic calculations of the proportion of cases in a study population that developed carcinoma without taking into account differences in follow up period between subjects (Warnakulasuriya *et al.*, 2011). We have calculated rates taking time to transformation for each individual into account and the annual transformation rates for oral epithelial dysplasia in our series were 1.32% and 0.87%, including and excluding transformation within 6 months of index lesions respectively. These results are in keeping with the rates reported by previous studies calculating results correctly (Dost *et al.*, 2014). Higher rates were observed with greater severity of dysplasia (see Table 4.11 to 4.13). A lower annual malignant transformation rate for ICM DNA aneuploid lesions (5.97%) was observed than was found for severe dysplasia (10.64%).

Non-dysplastic samples from oral leukoplakia and other OPMD have been included in the majority of published studies on malignant transformation. There are however, a few studies that have focused on lesions with epithelial dysplasia only and these have reported that 13.2% (Banoczy and Csiba, 1976), 6.6% (Pindborg *et al.*, 1977), 36% (Lumerman *et al.*, 1995), 22% (Ho *et al.*, 2012) (Ho et al) and 4.7% (Dost *et al.*, 2014) of their cases underwent malignant transformation. This is a very broad range and the variation is probably accounted for by the factors discussed above such as case selection and risk habits. When we limited our analysis to the lesions with dysplasia only, the proportion of cases that developed carcinoma was 21% and 14%, when early transformation was included and excluded respectively (Table 4.13). These figures are

within the reported range, but the correctly calculated transformation rates provide more meaningful data and would be a more comparable statistic to compare different studies, as pointed out by Warnakulasuriya *et al.* (2011).

4.5.7 Predictive values compared

We have shown that severe dysplasia but not moderate dysplasia is a better predictor of malignant transformation than ICM DNA aneuploidy (Table 4.14 and 4.15). Both absence of dysplasia and ICM DNA diploid had an equivalent positive and negative predictive value. This is true whether or not early transformation is included in the analysis. This appears to suggest that ICM DNA ploidy analysis has no added advantage for clinical practice. However, it is noteworthy that only this work and our previous published studies show good correlation between dysplasia and malignant transformation. Therefore, in other centres where dysplasia grading is less predictive, DNA ploidy analysis would appear to have great potential. Even in our present study DNA ploidy analysis has identified aneuploidy in almost a quarter of cases that showed only mild dysplasia (Table 4.6).

It was not possible to combine the results of ICM DNA ploidy analysis with dysplasia grade in our previous study (Sperandio *et al.*, 2013) because the two analyses were performed on different study populations. In the present work, we have been able to combine the two sets of results in a more meaningful fashion. As shown in previous study (Sperandio *et al.*, 2013) the predictive values of ICM DNA diploidy and tetraploidy were not significantly different, and so they were combined for this analysis (see Table 1.14). The combination of severe dysplasia and ICM DNA aneuploidy has increased predictive value over both aneuploidy and severe dysplasia alone and a similar relationship holds with moderate dysplasia. In contrast, adding diploid or tetraploid to

the absence of dysplasia showed no benefit to the negative predictive value. These predictive values of combined results are the basis to derive a clinical diagnostic algorithm for implementation of ICM DNA ploidy analysis in routine diagnosis that will form part of future work.

4.5.8 Conclusion

In conclusion, the results of this study provide support for the hypothesis that ICM DNA ploidy analysis is a good predictor of malignant transformation in OPMD when applied to oral lesions assessed as having a risk of transformation on clinical grounds. The results also complement the sparse data supporting the efficacy of dysplasia grading to predict malignant transformation in routine clinical practice. The highest predictive values are produced by combinations of the two techniques and the predictive values reported here exceed those from published studies to date.

CHAPTER 5 : Conclusions and Future Work

5.1 Summary and conclusion

The aims of this study were to improve the diagnosis and predictive tests for patients with OPMD. We set out to evaluate ICM DNA ploidy analysis to predict malignant transformation and compare the results to dysplasia grading, and to assess FISH, QGPlex and qPCR as alternative methods to detect aneuploidy, using DNA ploidy as the reference test.

The main conclusions of this work are that DNA image-based ploidy analysis proved to be an effective technique for routine clinical analysis of archival paraffin embedded samples. Compared to other techniques it was rapid, gave control of tissue localisation and used internal controls. We have shown ICM DNA ploidy analysis to have a positive predictive value of 33% for development of cancer in a large referral series of 228 patients. This was not as high as severe dysplasia grading in our studies but considerably higher than in other published studies. The combination of aneuploidy and severe dysplasia had a PPV of 56%. We suggest that ICM DNA ploidy merits further evaluation as a routine clinical test with potential patient benefit.

The advantages of FISH were no requirement for reference gene or intact DNA and tissue localisation and FISH proved successful. We have demonstrated that copy number increase at 10 amplified loci in OPMD and shown that that even small numbers of probes would be sufficient to identify aneuploidy. Only a very small number of aneuploid cells were detected in any lesion. FISH also revealed clonal patterns and gene amplification in a minority of samples. However, FISH proved to have high cost

requiring special equipment, and was labour intensive and time consuming to produce data, making it unsuitable for routine diagnostic use.

The theoretical potential advantages of QuantiGenePlex included high signal amplification, ability to analyse degraded DNA and multiplexing. Conversely, requirement for costly special equipment makes it less suitable for routine used across laboratories. Though our ability to perform this assay sufficient times limited the results, we identified problems with selection of reference genes and possibly sample quality and sample enrichment. We showed that the technique was insufficiently reproducible for clinical work without further optimisation of sample preparation.

Real time qPCR is the method of choice for rapid high throughput genetic testing in many laboratories. However, the accuracy of results obtained from qPCR has always been a concern when performed on genomic DNA extracted from formalin fixed tissue. The inconsistencies seen in our results were likely attributable to fragmentation and cross-linking of genomic DNA isolated from fixation in formalin. We had insufficient matched samples to compare qPCR and QGPlex in this study.

5.2 Recommendations for future work

- Further work to validate the QGP technique for OPMD and optimize the process is merited as the technique appears potentially useful.
- QPCR has insufficient accuracy and reliability to detect copy number variation and no further work is suggested pending evaluation of QGP.
- Both QPCR and QGP are dependent on control genes and calibrator but it is difficult to propose a stable unaffected gene for future work.
- FISH merits further work using a reduced target panel, automated staining and simplified counting method suitable for routine clinical application using colorimetric ISH.
- ICM DNA ploidy analysis remains the best predictor of malignant transformation in OPMD but requires further work to improve diagnostic criteria
- Predictive values of ICM and DNA ploidy should be used to define a clinically applicable treatment algorithm.

Bibliography

Abbey LM, Kaugars GE, Gunsolley JC, Burns JC, Page DG *et al.* (1995). Intraexaminer and interexaminer reliability in the diagnosis of oral epithelial dysplasia. *Oral Surg Oral Med Oral Pathol Oral Radiol Endod* 80(2)*:*188-191.

Amagasa T, Yamashiro M, Ishikawa H (2006). Oral leukoplakia related to malignant transformation. *Oral Science International* 3(2)*:*45-55.

Arduino PG, Bagan J, El-Naggar AK, Carrozzo M (2013). Urban legends series: oral leukoplakia. *Oral Dis* 19(7)*:*642-659.

Arora S, Kaur J, Sharma C, Mathur M, Bahadur S *et al.* (2005). Stromelysin 3, Ets-1, and vascular endothelial growth factor expression in oral precancerous and cancerous lesions: correlation with microvessel density, progression, and prognosis. *Clin Cancer Res* 11(6)*:*2272-2284.

Awan K, Yang Y, Morgan P, Warnakulasuriya S (2012). Utility of toluidine blue as a diagnostic adjunct in the detection of potentially malignant disorders of the oral cavity--a clinical and histological assessment. *Oral Dis* 18(8)*:*728-733.

Awan KH, Morgan PR, Warnakulasuriya S (2011). Evaluation of an autofluorescence based imaging system (VELscope™) in the detection of oral potentially malignant disorders and benign keratoses. *Oral Oncol* 47(4)*:*274-277.

Banoczy J, Sugar L (1972). Longitudinal studies in oral leukoplakias. *J Oral Pathol* 1(6)*:*265-272.

Banoczy J, Sugar L (1975). Progressive and regressive changes in Hungarian oral leukoplakias in the course of longitudinal studies. *Community Dent Oral Epidemiol* 3(4)*:*194-197.

Banoczy J, Csiba A (1976). Occurrence of epithelial dysplasia in oral leukoplakia. Analysis and follow-up study of 12 cases. *Oral surgery, oral medicine, and oral pathology* 42(6)*:*766-774.

Banoczy J (1977). Follow-up studies in oral leukoplakia. *J Maxillofac Surg* 5(1)*:*69-75.

Banoczy J, Rigo O (1991). Prevalence study of oral precancerous lesions within a complex screening system in Hungary. *Community Dent Oral Epidemiol* 19(5)*:*265-267.

Barnes L, World Health Organization., International Agency for Research on Cancer. (2005). Pathology and genetics of head and neck tumours Lyon: IARC Press.

Bayani J, Selvarajah S, Maire G, Vukovic B, Al-Romaih K *et al.* (2007). Genomic mechanisms and measurement of structural and numerical instability in cancer cells. *Seminars in cancer biology* 17(1)*:*5-18.

Bediaga NG, Alfonso-Sanchez MA, de Renobales M, Rocandio AM, Arroyo M *et al.* (2008). GSTT1 and GSTM1 gene copy number analysis in paraffin-embedded tissue using quantitative real-time PCR. *Analytical biochemistry* 378(2)*:*221-223.

Bentz M, Cabot G, Moos M, Speicher MR, Ganser A *et al.* (1994). Detection of chimeric BCR-ABL genes on bone marrow samples and blood smears in chronic myeloid and acute lymphoblastic leukemia by in situ hybridization. *Blood* 83(7)*:*1922-1928.

Bhargava K, Smith LW, Mani NJ, Silverman S, Jr., Malaowalla AM *et al.* (1975). A follow up study of oral cancer and precancerous lesions in 57,518 industrial workers of Gujarat, India. *Indian journal of cancer* 12(2)*:*124-129.

Bhattacharya A, Roy R, Snijders AM, Hamilton G, Paquette J *et al.* (2011). Two distinct routes to oral cancer differing in genome instability and risk for cervical node metastasis. *Clin Cancer Res* 17(22)*:*7024-7034.

Bortoluzzi MC, Yurgel LS, Dekker NP, Jordan RC, Regezi JA (2004). Assessment of p63 expression in oral squamous cell carcinomas and dysplasias. *Oral Surg Oral Med Oral Pathol Oral Radiol Endod* 98(6)*:*698-704.

Bouquot JE, Gorlin RJ (1986). Leukoplakia, lichen planus, and other oral keratoses in 23,616 white Americans over the age of 35 years. *Oral surgery, oral medicine, and oral pathology* 61(4)*:*373-381.

Bouquot JE, Speight PM, Farthing PM (2006). Epithelial dysplasia of the oral mucosa - Diagnostic problems and prognostic features. *Current Diagnostic Pathology* 12(11-21.

Boyle JO, Hakim J, Koch W, van der Riet P, Hruban RH *et al.* (1993). The incidence of p53 mutations increases with progression of head and neck cancer. *Cancer Res* 53(19)*:*4477-4480.

Bradley G, Odell EW, Raphael S, Ho J, Le LW *et al.* (2010). Abnormal DNA content in oral epithelial dysplasia is associated with increased risk of progression to carcinoma. *Br J Cancer* 103(9)*:*1432-1442.

Bremmer JF, Brakenhoff RH, Broeckaert MA, Beliën JA, Leemans CR *et al.* (2011). Prognostic value of DNA ploidy status in patients with oral leukoplakia. *Oral Oncol* 47(10)*:*956-960.

Brennan M, Migliorati CA, Lockhart PB, Wray D, Al-Hashimi I *et al.* (2007). Management of oral epithelial dysplasia: a review. *Oral Surg Oral Med Oral Pathol Oral Radiol Endod* 103 Suppl(S19.e11-12.

Brennan PA, Conroy B, Spedding AV (2000). Expression of inducible nitric oxide synthase and p53 in oral epithelial dysplasia. *Oral Surg Oral Med Oral Pathol Oral Radiol Endod* 90(5)*:*624-629.

Brouns E, Baart J, Karagozoglu K, Aartman I, Bloemena E *et al.* (2014). Malignant transformation of oral leukoplakia in a well-defined cohort of 144 patients. *Oral Dis* 20(3)*:*e19-24.

Brouns ER, Bloemena E, Belien JA, Broeckaert MA, Aartman IH *et al.* (2012). DNA ploidy measurement in oral leukoplakia: different results between flow and image cytometry. *Oral Oncol* 48(7)*:*636-640.

Cabay RJ, Morton TH, Jr., Epstein JB (2007). Proliferative verrucous leukoplakia and its progression to oral carcinoma: a review of the literature. *J Oral Pathol Med* 36(5)*:*255-261.

Califano J, van der Riet P, Westra W, Nawroz H, Clayman G *et al.* (1996). Genetic progression model for head and neck cancer: implications for field cancerization. *Cancer Res* 56(11)*:*2488-2492.

Campo-Trapero J, Cano-Sánchez J, Palacios-Sánchez B, Sánchez-Gutierrez JJ, González-Moles MA *et al.* (2008). Update on molecular pathology in oral cancer and precancer. *Anticancer Res* 28(2B)*:*1197-1205.

Cancer Research UK. Cancer Research UK 2014 [cited 2015; Available from: http://cruk.org/cancerstats.

Carey FA (1994). Measurement of nuclear DNA content in histological and cytological specimens: principles and applications. *J Pathol* 172(4)*:*307-312.

Carter SL, Eklund AC, Kohane IS, Harris LN, Szallasi Z (2006). A signature of chromosomal instability inferred from gene expression profiles predicts clinical outcome in multiple human cancers. *Nature genetics* 38(9):1043-1048.

Castagnola P, Malacarne D, Scaruffi P, Maffei M, Donadini A *et al.* (2011). Chromosomal aberrations and aneuploidy in oral potentially malignant lesions: distinctive features for tongue. *BMC Cancer* 11(445.

Cebeci AR, Gulsahi A, Kamburoglu K, Orhan BK, Oztas B (2009). Prevalence and distribution of oral mucosal lesions in an adult Turkish population. *Med Oral Patol Oral Cir Bucal* 14(6):E272-277.

Cervigne NK, Reis PP, Machado J, Sadikovic B, Bradley G *et al.* (2009). Identification of a microRNA signature associated with progression of leukoplakia to oral carcinoma. *Hum Mol Genet* 18(24):4818-4829.

Cha JD, Kim HJ, Cha IH (2011). Genetic alterations in oral squamous cell carcinoma progression detected by combining array-based comparative genomic hybridization and multiplex ligation-dependent probe amplification. *Oral Surg Oral Med Oral Pathol Oral Radiol Endod* 111(5):594-607.

Chaw YF, Crane LE, Lange P, Shapiro R (1980). Isolation and identification of cross-links from formaldehyde-treated nucleic acids. *Biochemistry* 19(24):5525-5531.

Chen GK, Chang X, Curtis C, Wang K (2013). Precise inference of copy number alterations in tumor samples from SNP arrays. *Bioinformatics* 29(23):2964-2970.

Chen YK, Hsue SS, Lin LM (2004). p73 expression for human buccal epithelial dysplasia and squamous cell carcinoma: does it correlate with nodal status of carcinoma and is there a relationship with malignant change of epithelial dysplasia? *Head Neck* 26(11):945-952.

Cheong SC, Chandramouli GV, Saleh A, Zain RB, Lau SH *et al.* (2009). Gene expression in human oral squamous cell carcinoma is influenced by risk factor exposure. *Oral Oncol* 45(8):712-719.

Chibon F, Lagarde P, Salas S, Perot G, Brouste V *et al.* (2010). Validated prediction of clinical outcome in sarcomas and multiple types of cancer on the basis of a gene expression signature related to genome complexity. *Nature medicine* 16(7):781-787.

Chin SF, Daigo Y, Huang HE, Iyer NG, Callagy G *et al.* (2003). A simple and reliable pretreatment protocol facilitates fluorescent in situ hybridisation on tissue microarrays of paraffin wax embedded tumour samples. *Molecular pathology : MP* 56(5)*:*275-279.

Choi S, Myers JN (2008). Molecular pathogenesis of oral squamous cell carcinoma: implications for therapy. *J Dent Res* 87(1)*:*14-32.

Collins ML, Irvine B, Tyner D, Fine E, Zayati C *et al.* (1997). A branched DNA signal amplification assay for quantification of nucleic acid targets below 100 molecules/ml. *Nucleic acids research* 25(15)*:*2979-2984.

Cowan CG, Gregg TA, Napier SS, McKenna SM, Kee F (2001). Potentially malignant oral lesions in northern Ireland: a 20-year population-based perspective of malignant transformation. *Oral Dis* 7(1)*:*18-24.

Crisan D, Mattson JC (1993). Retrospective DNA analysis using fixed tissue specimens. *DNA and cell biology* 12(5)*:*455-464.

Cruz IB, Snijders PJ, Meijer CJ, Braakhuis BJ, Snow GB *et al.* (1998). p53 expression above the basal cell layer in oral mucosa is an early event of malignant transformation and has predictive value for developing oral squamous cell carcinoma. *J Pathol* 184(4)*:*360-368.

Cukier HN, Pericak-Vance MA, Gilbert JR, Hedges DJ (2009). Sample degradation leads to false-positive copy number variation calls in multiplex real-time polymerase chain reaction assays. *Analytical biochemistry* 386(2)*:*288-290.

D'Haene B, Vandesompele J, Hellemans J (2010). Accurate and objective copy number profiling using real-time quantitative PCR. *Methods* 50(4)*:*262-270.

da Silva SD, Ferlito A, Takes RP, Brakenhoff RH, Valentin MD *et al.* (2011). Advances and applications of oral cancer basic research. *Oral Oncol* 47(9)*:*783-791.

Darzynkiewicz Z (2010). Critical aspects in analysis of cellular DNA content. *Curr Protoc Cytom* Chapter 7(Unit7 2.

de Carvalho Fraga CA, Farias LC, de Oliveira MV, Domingos PL, Pereira CS *et al.* (2014). Increased VEGFR2 and MMP9 protein levels are associated with epithelial dysplasia grading. *Pathol Res Pract* 210(12)*:*959-964.

de Vicente JC, Rodrigo JP, Rodriguez-Santamarta T, Lequerica-Fernandez P, Allonca E *et al.* (2013). Podoplanin expression in oral leukoplakia: tumorigenic role. *Oral Oncol* 49(6):598-603.

Dietrich T, Reichart PA, Scheifele C (2004). Clinical risk factors of oral leukoplakia in a representative sample of the US population. *Oral Oncol* 40(2):158-163.

Dionne KR, Warnakulasuriya S, Zain RB, Cheong SC (2015). Potentially malignant disorders of the oral cavity: current practice and future directions in the clinic and laboratory. *Int J Cancer* 136(3):503-515.

Donadini A, Maffei M, Cavallero A, Pentenero M, Malacarne D *et al.* (2010). Oral cancer genesis and progression: DNA near-diploid aneuploidization and endoreduplication by high resolution flow cytometry. *Cell Oncol* 32(5-6):373-383.

Dost F, Le Cao K, Ford PJ, Ades C, Farah CS (2014). Malignant transformation of oral epithelial dysplasia: a real-world evaluation of histopathologic grading. *Oral Surg Oral Med Oral Pathol Oral Radiol* 117(3):343-352.

Dunbar SA (2006). Applications of Luminex xMAP technology for rapid, high-throughput multiplexed nucleic acid detection. *Clinica chimica acta; international journal of clinical chemistry* 363(1-2):71-82.

Dutt A, Beroukhim R (2007). Single nucleotide polymorphism array analysis of cancer. *Curr Opin Oncol* 19(1):43-49.

Epstein JB, Guneri P (2009). The adjunctive role of toluidine blue in detection of oral premalignant and malignant lesions. *Curr Opin Otolaryngol Head Neck Surg* 17(2):79-87.

Farah CS, McIntosh L, Georgiou A, McCullough MJ (2012). Efficacy of tissue autofluorescence imaging (VELScope) in the visualization of oral mucosal lesions. *Head Neck* 34(6):856-862.

Ferlay J, Shin HR, Bray F, Forman D, Mathers C *et al.* (2010). Estimates of worldwide burden of cancer in 2008: GLOBOCAN 2008. *Int J Cancer* 127(12):2893-2917.

Ferlay J, Soerjomataram I, Dikshit R, Eser S, Mathers C *et al.* (2015). Cancer incidence and mortality worldwide: sources, methods and major patterns in GLOBOCAN 2012. *Int J Cancer* 136(5):E359-386.

Feuk L, Carson AR, Scherer SW (2006). Structural variation in the human genome. *Nat Rev Genet* 7(2):85-97.

Fischer DJ, Epstein JB, Morton TH, Schwartz SM (2004). Interobserver reliability in the histopathologic diagnosis of oral pre-malignant and malignant lesions. *J Oral Pathol Med* 33(2):65-70.

Flagella M, Bui S, Zheng Z, Nguyen CT, Zhang A *et al.* (2006). A multiplex branched DNA assay for parallel quantitative gene expression profiling. *Analytical biochemistry* 352(1):50-60.

Fornatora M, Jones AC, Kerpel S, Freedman P (1996). Human papillomavirus-associated oral epithelial dysplasia (koilocytic dysplasia): an entity of unknown biologic potential. *Oral Surg Oral Med Oral Pathol Oral Radiol Endod* 82(1):47-56.

Fraga CA, de Oliveira MV, de Oliveira ES, Barros LO, Santos FB *et al.* (2012). A high HIF-1alpha expression genotype is associated with poor prognosis of upper aerodigestive tract carcinoma patients. *Oral Oncol* 48(2):130-135.

Garnis C, Coe BP, Ishkanian A, Zhang L, Rosin MP *et al.* (2004a). Novel regions of amplification on 8q distinct from the MYC locus and frequently altered in oral dysplasia and cancer. *Genes Chromosomes Cancer* 39(1):93-98.

Garnis C, Coe BP, Zhang L, Rosin MP, Lam WL (2004b). Overexpression of LRP12, a gene contained within an 8q22 amplicon identified by high-resolution array CGH analysis of oral squamous cell carcinomas. *Oncogene* 23(14):2582-2586.

Garnis C, Chari R, Buys TP, Zhang L, Ng RT *et al.* (2009). Genomic imbalances in precancerous tissues signal oral cancer risk. *Mol Cancer* 8(50.

Giaretti W, Maffei M, Pentenero M, Scaruffi P, Donadini A *et al.* (2012). Genomic aberrations in normal appearing mucosa fields distal from oral potentially malignant lesions. *Cell Oncol (Dordr)* 35(1):43-52.

Gillison ML, Koch WM, Capone RB, Spafford M, Westra WH *et al.* (2000). Evidence for a causal association between human papillomavirus and a subset of head and neck cancers. *J Natl Cancer Inst* 92(9):709-720.

Gillison ML (2007). Current topics in the epidemiology of oral cavity and oropharyngeal cancers. *Head Neck* 29(8):779-792.

Ginzinger DG (2002). Gene quantification using real-time quantitative PCR: an emerging technology hits the mainstream. *Experimental hematology* 30(6)*:*503-512.

Gollin SM (2005). Mechanisms leading to chromosomal instability. *Seminars in cancer biology* 15(1)*:*33-42.

Gomes CC, Fonseca-Silva T, Galvao CF, Friedman E, De Marco L *et al.* (2015). Inter- and intra-lesional molecular heterogeneity of oral leukoplakia. *Oral Oncol* 51(2)*:*178-181.

Grandis JR, Tweardy DJ (1993). Elevated levels of transforming growth factor alpha and epidermal growth factor receptor messenger RNA are early markers of carcinogenesis in head and neck cancer. *Cancer Res* 53(15)*:*3579-3584.

Grässel-Pietrusky R, Deinlein E, Hornstein OP (1982). DNA-ploidy rates in oral leukoplakias determined by flow-cytometry. *J Oral Pathol* 11(6)*:*434-438.

Gresham D, Dunham MJ, Botstein D (2008). Comparing whole genomes using DNA microarrays. *Nat Rev Genet* 9(4)*:*291-302.

Gupta PC, Mehta FS, Daftary DK, Pindborg JJ, Bhonsle RB *et al.* (1980). Incidence rates of oral cancer and natural history of oral precancerous lesions in a 10-year follow-up study of Indian villagers. *Community Dent Oral Epidemiol* 8(6)*:*283-333.

Gupta PC (1984a). Epidemiologic study of the association between alcohol habits and oral leukoplakia. *Community Dent Oral Epidemiol* 12(1)*:*47-50.

Gupta PC (1984b). A study of dose-response relationship between tobacco habits and oral leukoplakia. *Br J Cancer* 50(4)*:*527-531.

Gupta PC, Murti PR, Bhonsle RB, Mehta FS, Pindborg JJ (1995). Effect of cessation of tobacco use on the incidence of oral mucosal lesions in a 10-yr follow-up study of 12,212 users. *Oral Dis* 1(1)*:*54-58.

Ha PK, Califano JA (2006). Promoter methylation and inactivation of tumour-suppressor genes in oral squamous-cell carcinoma. *The lancet oncology* 7(1)*:*77-82.

Hall GL, Shaw RJ, Field EA, Rogers SN, Sutton DN *et al.* (2008). p16 Promoter methylation is a potential predictor of malignant transformation in oral epithelial dysplasia. *Cancer Epidemiol Biomarkers Prev* 17(8)*:*2174-2179.

Hanahan D, Weinberg RA (2000). The hallmarks of cancer. *Cell* 100(1)*:*57-70.

Hanahan D, Weinberg RA (2011). Hallmarks of cancer: the next generation. *Cell* 144(5)*:*646-674.

Haroske G, Baak JP, Danielsen H, Giroud F, Gschwendtner A *et al.* (2001). Fourth updated ESACP consensus report on diagnostic DNA image cytometry. *Anal Cell Pathol* 23(2)*:*89-95.

Hicks DG, Tubbs RR (2005). Assessment of the HER2 status in breast cancer by fluorescence in situ hybridization: a technical review with interpretive guidelines. *Human pathology* 36(3)*:*250-261.

Ho MW, Risk JM, Woolgar JA, Field EA, Field JK *et al.* (2012). The clinical determinants of malignant transformation in oral epithelial dysplasia. *Oral Oncol* 48(10)*:*969-976.

Hogewind WF, van der Waal I (1988). Prevalence study of oral leukoplakia in a selected population of 1000 patients from The Netherlands. *Community Dent Oral Epidemiol* 16(5)*:*302-305.

Högmo A, Lindskog S, Lindholm J, Kuylenstierna R, Auer G *et al.* (1998). Preneoplastic oral lesions: the clinical value of image cytometry DNA analysis, p53 and p21/WAF1 expression. *Anticancer Res* 18(5B)*:*3645-3650.

Holmstrup P, Vedtofte P, Reibel J, Stoltze K (2006). Long-term treatment outcome of oral premalignant lesions. *Oral Oncol* 42(5)*:*461-474.

Horn T, Chang CA, Urdea MS (1997). Chemical synthesis and characterization of branched oligodeoxyribonucleotides (bDNA) for use as signal amplifiers in nucleic acid quantification assays. *Nucleic acids research* 25(23)*:*4842-4849.

Inoue H, Miyazaki Y, Kikuchi K, Yoshida N, Ide F *et al.* (2012). Podoplanin expression during dysplasia-carcinoma sequence in the oral cavity. *Tumour Biol* 33(1)*:*183-194.

Islam MN, Kornberg L, Veenker E, Cohen DM, Bhattacharyya I (2010). Anatomic site based ploidy analysis of oral premalignant lesions. *Head Neck Pathol* 4(1)*:*10-14.

Jaber MA, Porter SR, Speight P, Eveson JW, Scully C (2003). Oral epithelial dysplasia: clinical characteristics of western European residents. *Oral Oncol* 39(6)*:*589-596.

Jaber MA (2010). Oral epithelial dysplasia in non-users of tobacco and alcohol: an analysis of clinicopathologic characteristics and treatment outcome. *J Oral Sci* 52(1)*:*13-21.

Jayaprakash V, Reid M, Hatton E, Merzianu M, Rigual N *et al.* (2011). Human papillomavirus types 16 and 18 in epithelial dysplasia of oral cavity and oropharynx: a meta-analysis, 1985-2010. *Oral Oncol* 47(11)*:*1048-1054.

Jemal A, Bray F, Center MM, Ferlay J, Ward E *et al.* (2011). Global cancer statistics. *CA: a cancer journal for clinicians* 61(2)*:*69-90.

Jiang WW, Fujii H, Shirai T, Mega H, Takagi M (2001). Accumulative increase of loss of heterozygosity from leukoplakia to foci of early cancerization in leukoplakia of the oral cavity. *Cancer* 92(9)*:*2349-2356.

Jordan RC, Macabeo-Ong M, Shiboski CH, Dekker N, Ginzinger DG *et al.* (2004). Overexpression of matrix metalloproteinase-1 and -9 mRNA is associated with progression of oral dysplasia to cancer. *Clin Cancer Res* 10(19)*:*6460-6465.

Kalyankrishna S, Grandis JR (2006). Epidermal growth factor receptor biology in head and neck cancer. *J Clin Oncol* 24(17)*:*2666-2672.

Karabulut A, Reibel J, Therkildsen MH, Praetorius F, Nielsen HW *et al.* (1995). Observer variability in the histologic assessment of oral premalignant lesions. *J Oral Pathol Med* 24(5)*:*198-200.

Kawaguchi H, El-Naggar AK, Papadimitrakopoulou V, Ren H, Fan YH *et al.* (2008). Podoplanin: a novel marker for oral cancer risk in patients with oral premalignancy. *J Clin Oncol* 26(3)*:*354-360.

Kearney L (2001). Molecular cytogenetics. *Best Pract Res Clin Haematol* 14(3)*:*645-669.

Kerr AR, Sirois DA, Epstein JB (2006). Clinical evaluation of chemiluminescent lighting: an adjunct for oral mucosal examinations. *J Clin Dent* 17(3)*:*59-63.

Kovesi G, Szende B (2006). Prognostic value of cyclin D1, p27, and p63 in oral leukoplakia. *J Oral Pathol Med* 35(5):274-277.

Kramer IR, El-Labban N, Lee KW (1978). The clinical features and risk of malignant transformation in sublingual keratosis. *Br Dent J* 144(6):171-180.

Kreppel M, Kreppel B, Drebber U, Wedemayer I, Rothamel D *et al.* (2012). Podoplanin expression in oral leukoplakia: prognostic value and clinicopathological implications. *Oral Dis* 18(7):692-699.

Kubista M, Andrade JM, Bengtsson M, Forootan A, Jonak J *et al.* (2006). The real-time polymerase chain reaction. *Molecular aspects of medicine* 27(2-3):95-125.

Kujan O, Oliver R, Roz L, Sozzi G, Ribeiro N *et al.* (2006a). Fragile histidine triad expression in oral squamous cell carcinoma and precursor lesions. *Clin Cancer Res* 12(22):6723-6729.

Kujan O, Oliver RJ, Khattab A, Roberts SA, Thakker N *et al.* (2006b). Evaluation of a new binary system of grading oral epithelial dysplasia for prediction of malignant transformation. *Oral Oncol* 42(10):987-993.

Kuo MY, Cheng SJ, Chen HM, Kok SH, Hahn LJ *et al.* (1998). Expression of CD44s, CD44v5, CD44v6 and CD44v7-8 in betel quid chewing-associated oral premalignant lesions and squamous cell carcinomas in Taiwan. *J Oral Pathol Med* 27(9):428-433.

Kyzas PA, Stefanou D, Batistatou A, Agnantis NJ (2005). Prognostic significance of VEGF immunohistochemical expression and tumor angiogenesis in head and neck squamous cell carcinoma. *J Cancer Res Clin Oncol* 131(9):624-630.

LaFramboise T (2009). Single nucleotide polymorphism arrays: a decade of biological, computational and technological advances. *Nucleic acids research* 37(13):4181-4193.

Lane PM, Gilhuly T, Whitehead P, Zeng H, Poh CF *et al.* (2006). Simple device for the direct visualization of oral-cavity tissue fluorescence. *J Biomed Opt* 11(2):024006.

Laurikkala J, Mikkola ML, James M, Tummers M, Mills AA *et al.* (2006). p63 regulates multiple signalling pathways required for ectodermal organogenesis and differentiation. *Development* 133(8):1553-1563.

Lee CH, Ko YC, Huang HL, Chao YY, Tsai CC *et al.* (2003). The precancer risk of betel quid chewing, tobacco use and alcohol consumption in oral leukoplakia and oral submucous fibrosis in southern Taiwan. *Br J Cancer* 88(3):366-372.

Lee JJ, Hong WK, Hittelman WN, Mao L, Lotan R *et al.* (2000). Predicting cancer development in oral leukoplakia: ten years of translational research. *Clin Cancer Res* 6(5):1702-1710.

Leemans CR, Braakhuis BJ, Brakenhoff RH (2011). The molecular biology of head and neck cancer. *Nat Rev Cancer* 11(1):9-22.

Lehmann U, Kreipe H (2001). Real-time PCR analysis of DNA and RNA extracted from formalin-fixed and paraffin-embedded biopsies. *Methods* 25(4):409-418.

Lengauer C, Kinzler KW, Vogelstein B (1997). Genetic instability in colorectal cancers. *Nature* 386(6625):623-627.

Lim K, Moles DR, Downer MC, Speight PM (2003). Opportunistic screening for oral cancer and precancer in general dental practice: results of a demonstration study. *Br Dent J* 194(9):497-502; discussion 493.

Lind PO (1987). Malignant transformation in oral leukoplakia. *Scandinavian journal of dental research* 95(6):449-455.

Lingen MW, Kalmar JR, Karrison T, Speight PM (2008). Critical evaluation of diagnostic aids for the detection of oral cancer. *Oral Oncol* 44(1):10-22.

Lingen MW, Pinto A, Mendes RA, Franchini R, Czerninski R *et al.* (2011). Genetics/epigenetics of oral premalignancy: current status and future research. *Oral Dis* 17 Suppl 1(7-22.

Liu W, Wang YF, Zhou HW, Shi P, Zhou ZT *et al.* (2010). Malignant transformation of oral leukoplakia: a retrospective cohort study of 218 Chinese patients. *BMC Cancer* 10(685.

Liu W, Bao ZX, Shi LJ, Tang GY, Zhou ZT (2011). Malignant transformation of oral epithelial dysplasia: clinicopathological risk factors and outcome analysis in a retrospective cohort of 138 cases. *Histopathology*.

Livak KJ, Schmittgen TD (2001). Analysis of relative gene expression data using real-time quantitative PCR and the 2(-Delta Delta C(T)) Method. *Methods* 25(4)*:*402-408.

Lo Muzio L, Pannone G, Leonardi R, Staibano S, Mignogna MD *et al.* (2003). Survivin, a potential early predictor of tumor progression in the oral mucosa. *J Dent Res* 82(11)*:*923-928.

López M, Aguirre JM, Cuevas N, Anzola M, Videgain J *et al.* (2003). Gene promoter hypermethylation in oral rinses of leukoplakia patients--a diagnostic and/or prognostic tool? *Eur J Cancer* 39(16)*:*2306-2309.

Lorch JH, Posner MR, Wirth LJ, Haddad RI (2009). Seeking alternative biological therapies: the future of targeted molecular treatment. *Oral Oncol* 45(4-5)*:*447-453.

Lumerman H, Freedman P, Kerpel S (1995). Oral epithelial dysplasia and the development of invasive squamous cell carcinoma. *Oral Surg Oral Med Oral Pathol Oral Radiol Endod* 79(3)*:*321-329.

Lupski JR (1998). Genomic disorders: structural features of the genome can lead to DNA rearrangements and human disease traits. *Trends Genet* 14(10)*:*417-422.

Lupski JR (2007). Genomic rearrangements and sporadic disease. *Nature genetics* 39(7 Suppl)*:*S43-47.

Macdonald DG, Rennie JS (1975). Oral epithelial atypia in denture induced hyperplasia, lichen planus and squamous cell papilloma. *International journal of oral surgery* 4(1)*:*40-45.

Manning AL, Benes C, Dyson NJ (2014). Whole chromosome instability resulting from the synergistic effects of pRB and p53 inactivation. *Oncogene* 33(19)*:*2487-2494.

Mao L, Lee JS, Fan YH, Ro JY, Batsakis JG *et al.* (1996). Frequent microsatellite alterations at chromosomes 9p21 and 3p14 in oral premalignant lesions and their value in cancer risk assessment. *Nature medicine* 2(6)*:*682-685.

Maserejian NN, Joshipura KJ, Rosner BA, Giovannucci E, Zavras AI (2006). Prospective study of alcohol consumption and risk of oral premalignant lesions in men. *Cancer Epidemiol Biomarkers Prev* 15(4)*:*774-781.

Matsubara R, Kawano S, Kiyosue T, Goto Y, Hirano M *et al.* (2011). Increased DeltaNp63 expression is predictive of malignant transformation in oral epithelial dysplasia and poor prognosis in oral squamous cell carcinoma. *Int J Oncol* 39(6)*:*1391-1399.

Maudsley G, Williams EM (1999). What lessons can be learned for cancer registration quality assurance from data users? Skin cancer as an example. *International journal of epidemiology* 28(5)*:*809-815.

McGranahan N, Burrell RA, Endesfelder D, Novelli MR, Swanton C (2012). Cancer chromosomal instability: therapeutic and diagnostic challenges. *EMBO Rep* 13(6)*:*528-538.

McIntosh L, McCullough MJ, Farah CS (2009). The assessment of diffused light illumination and acetic acid rinse (Microlux/DL) in the visualisation of oral mucosal lesions. *Oral Oncol* 45(12)*:*e227-231.

McSherry EA, McGoldrick A, Kay EW, Hopkins AM, Gallagher WM *et al.* (2007). Formalin-fixed paraffin-embedded clinical tissues show spurious copy number changes in array-CGH profiles. *Clin Genet* 72(5)*:*441-447.

Mehanna HM, Rattay T, Smith J, McConkey CC (2009). Treatment and follow-up of oral dysplasia - a systematic review and meta-analysis. *Head Neck* 31(12)*:*1600-1609.

Mehrotra R, Singh M, Thomas S, Nair P, Pandya S *et al.* (2010). A cross-sectional study evaluating chemiluminescence and autofluorescence in the detection of clinically innocuous precancerous and cancerous oral lesions. *J Am Dent Assoc* 141(2)*:*151-156.

Mehta FS, Shroff BC, Gupta PC, Daftary DK (1972). Oral leukoplakia in relation to tobacco habits. A ten-year follow-up study of Bombay policemen. *Oral surgery, oral medicine, and oral pathology* 34(3)*:*426-433.

Mettu RK, Wan YW, Habermann JK, Ried T, Guo NL (2010). A 12-gene genomic instability signature predicts clinical outcomes in multiple cancer types. *The International journal of biological markers* 25(4)*:*219-228.

Mincer HH, Coleman SA, Hopkins KP (1972). Observations on the clinical characteristics of oral lesions showing histologic epithelial dysplasia. *Oral surgery, oral medicine, and oral pathology* 33(3)*:*389-399.

Mulshine JL, Atkinson JC, Greer RO, Papadimitrakopoulou VA, Van Waes C *et al.* (2004). Randomized, double-blind, placebo-controlled phase IIb trial of the cyclooxygenase inhibitor ketorolac as an oral rinse in oropharyngeal leukoplakia. *Clin Cancer Res* 10(5):1565-1573.

Murti PR, Warnakulasuriya KA, Johnson NW, Bhonsle RB, Gupta PC *et al.* (1998). p53 expression in oral precancer as a marker for malignant potential. *J Oral Pathol Med* 27(5):191-196.

Nankivell P, Mehanna H (2011). Oral dysplasia: biomarkers, treatment, and follow-up. *Curr Oncol Rep* 13(2):145-152.

Nankivell P, Williams H, Matthews P, Suortamo S, Snead D *et al.* (2013). The binary oral dysplasia grading system: validity testing and suggested improvement. *Oral Surg Oral Med Oral Pathol Oral Radiol* 115(1):87-94.

Napier SS, Cowan CG, Gregg TA, Stevenson M, Lamey PJ *et al.* (2003). Potentially malignant oral lesions in Northern Ireland: size (extent) matters. *Oral Dis* 9(3):129-137.

Napier SS, Speight PM (2008). Natural history of potentially malignant oral lesions and conditions: an overview of the literature. *J Oral Pathol Med* 37(1):1-10.

Negrini S, Gorgoulis VG, Halazonetis TD (2010). Genomic instability--an evolving hallmark of cancer. *Nature reviews Molecular cell biology* 11(3):220-228.

Noutomi Y, Oga A, Uchida K, Okafuji M, Ita M *et al.* (2006). Comparative genomic hybridization reveals genetic progression of oral squamous cell carcinoma from dysplasia via two different tumourigenic pathways. *J Pathol* 210(1):67-74.

Office for National Statistics. Cancer Registration Statistics, England 2011 26 June 2013 [cited 2015; Available from: http://www.ons.gov.uk.

Ohkura S, Kondoh N, Hada A, Arai M, Yamazaki Y *et al.* (2005). Differential expression of the keratin-4, -13, -14, -17 and transglutaminase 3 genes during the development of oral squamous cell carcinoma from leukoplakia. *Oral Oncol* 41(6):607-613.

Papadimitrakopoulou VA, William WN, Jr., Dannenberg AJ, Lippman SM, Lee JJ *et al.* (2008). Pilot randomized phase II study of celecoxib in oral premalignant lesions. *Clin Cancer Res* 14(7)*:*2095-2101.

Partridge M, Emilion G, Pateromichelakis S, A'Hern R, Phillips E *et al.* (1998). Allelic imbalance at chromosomal loci implicated in the pathogenesis of oral precancer, cumulative loss and its relationship with progression to cancer. *Oral Oncol* 34(2)*:*77-83.

Partridge M, Pateromichelakis S, Phillips E, Emilion GG, A'Hern RP *et al.* (2000). A case-control study confirms that microsatellite assay can identify patients at risk of developing oral squamous cell carcinoma within a field of cancerization. *Cancer Res* 60(14)*:*3893-3898.

Pentenero M, Giaretti W, Navone R, Demurtas A, Rostan I *et al.* (2009). DNA aneuploidy and dysplasia in oral potentially malignant disorders: association with cigarette smoking and site. *Oral Oncol* 45(10)*:*887-890.

Pentenero M, Donadini A, Di Nallo E, Maffei M, Marino R *et al.* (2012). Field effect in oral precancer as assessed by DNA flow cytometry and array-CGH. *J Oral Pathol Med* 41(2)*:*119-123.

Petti S (2003). Pooled estimate of world leukoplakia prevalence: a systematic review. *Oral Oncol* 39(8)*:*770-780.

Pikor L, Thu K, Vucic E, Lam W (2013). The detection and implication of genome instability in cancer. *Cancer Metastasis Rev* 32(3-4)*:*341-352.

Pindborg JJ, Renstrup G, Poulsen HE, Silverman S, Jr. (1963). Studies in Oral Leukoplakias. V. Clinical and Histologic Signs of Malignancy. *Acta odontologica Scandinavica* 21(407-414.

Pindborg JJ, Jolst O, Renstrup G, Roed-Petersen B (1968). Studies in oral leukoplakia: a preliminary report on the period pervalence of malignant transformation in leukoplakia based on a follow-up study of 248 patients. *J Am Dent Assoc* 76(4)*:*767-771.

Pindborg JJ, Daftary DK, Mehta FS (1977). A follow-up study of sixty-one oral dysplastic precancerous lesions in Indian villagers. *Oral surgery, oral medicine, and oral pathology* 43(3)*:*383-390.

Pitiyage G, Tilakaratne WM, Tavassoli M, Warnakulasuriya S (2009). Molecular markers in oral epithelial dysplasia: review. *J Oral Pathol Med* 38(10):737-752.

Poh CF, Zhu Y, Chen E, Berean KW, Wu L *et al.* (2012). Unique FISH patterns associated with cancer progression of oral dysplasia. *J Dent Res* 91(1):52-57.

Pradhan M, Abeler VM, Danielsen HE, Trope CG, Risberg BA (2006). Image cytometry DNA ploidy correlates with histological subtypes in endometrial carcinomas. *Modern pathology : an official journal of the United States and Canadian Academy of Pathology, Inc* 19(9):1227-1235.

Public Health England. Cross-Contaminated & Misidentified Cell Lines [cited 2015; Available from: http://www.phe-culturecollections.org.uk/services/celllineidentity verification/misidentifiedcelllines.jsp.

Qian J, Bostwick DG, Takahashi S, Borell TJ, Brown JA *et al.* (1996). Comparison of fluorescence in situ hybridization analysis of isolated nuclei and routine histological sections from paraffin-embedded prostatic adenocarcinoma specimens. *Am J Pathol* 149(4):1193-1199.

Rabinovitch PS (1994). DNA content histogram and cell-cycle analysis. *Methods Cell Biol* 41(263-296.

Radonic A, Thulke S, Mackay IM, Landt O, Siegert W *et al.* (2004). Guideline to reference gene selection for quantitative real-time PCR. *Biochemical and biophysical research communications* 313(4):856-862.

Rajcan-Separovic E (2012). Chromosome microarrays in human reproduction. *Hum Reprod Update* 18(5):555-567.

Raju B, Mehrotra R, Oijordsbakken G, Al-Sharabi AK, Vasstrand EN *et al.* (2005). Expression of p53, cyclin D1 and Ki-67 in pre-malignant and malignant oral lesions: association with clinicopathological parameters. *Anticancer Res* 25(6C):4699-4706.

Ram S, Siar CH (2005). Chemiluminescence as a diagnostic aid in the detection of oral cancer and potentially malignant epithelial lesions. *Int J Oral Maxillofac Surg* 34(5):521-527.

Rashid A, Warnakulasuriya S (2015). The use of light-based (optical) detection systems as adjuncts in the detection of oral cancer and oral potentially malignant disorders: a systematic review. *J Oral Pathol Med* 44(5)*:*307-328.

Reibel J (2003). Prognosis of oral pre-malignant lesions: significance of clinical, histopathological, and molecular biological characteristics. *Crit Rev Oral Biol Med* 14(1)*:*47-62.

Reuter CW, Morgan MA, Eckardt A (2007). Targeting EGF-receptor-signalling in squamous cell carcinomas of the head and neck. *Br J Cancer* 96(3)*:*408-416.

Roed-Petersen B (1982). Effect on oral leukoplakia of reducing or ceasing tobacco smoking. *Acta Derm Venereol* 62(2)*:*164-167.

Romano RA, Ortt K, Birkaya B, Smalley K, Sinha S (2009). An active role of the DeltaN isoform of p63 in regulating basal keratin genes K5 and K14 and directing epidermal cell fate. *PLoS One* 4(5)*:*e5623.

Roosaar A, Yin L, Johansson AL, Sandborgh-Englund G, Nyren O *et al.* (2007). A long-term follow-up study on the natural course of oral leukoplakia in a Swedish population-based sample. *J Oral Pathol Med* 36(2)*:*78-82.

Rosin MP, Cheng X, Poh C, Lam WL, Huang Y *et al.* (2000). Use of allelic loss to predict malignant risk for low-grade oral epithelial dysplasia. *Clin Cancer Res* 6(2)*:*357-362.

Ross JS, Linette GP, Stec J, Ross MS, Anwar S *et al.* (2003). DNA ploidy and cell cycle analysis in breast cancer. *American journal of clinical pathology* 120 Suppl(S72-84.

Rothenberg SM, Mohapatra G, Rivera MN, Winokur D, Greninger P *et al.* (2010). A genome-wide screen for microdeletions reveals disruption of polarity complex genes in diverse human cancers. *Cancer Res* 70(6)*:*2158-2164.

Roz L, Wu CL, Porter S, Scully C, Speight P *et al.* (1996). Allelic imbalance on chromosome 3p in oral dysplastic lesions: an early event in oral carcinogenesis. *Cancer Res* 56(6)*:*1228-1231.

Saintigny P, El-Naggar AK, Papadimitrakopoulou V, Ren H, Fan YH *et al.* (2009). DeltaNp63 overexpression, alone and in combination with other biomarkers, predicts the development of oral cancer in patients with leukoplakia. *Clin Cancer Res* 15(19)*:*6284-6291.

Saito T, Yamashita T, Notani K, Fukuda H, Mizuno S *et al.* (1995). Flow cytometric analysis of nuclear DNA content in oral leukoplakia: relation to clinicopathologic findings. *Int J Oral Maxillofac Surg* 24(1 Pt 1)*:*44-47.

Saito T, Sugiura C, Hirai A, Notani K, Totsuka Y *et al.* (2001). Development of squamous cell carcinoma from pre-existent oral leukoplakia: with respect to treatment modality. *Int J Oral Maxillofac Surg* 30(1)*:*49-53.

Schepman KP, van der Meij EH, Smeele LE, van der Waal I (1998). Malignant transformation of oral leukoplakia: a follow-up study of a hospital-based population of 166 patients with oral leukoplakia from The Netherlands. *Oral Oncol* 34(4)*:*270-275.

Schepman KP, Bezemer PD, van der Meij EH, Smeele LE, van der Waal I (2001). Tobacco usage in relation to the anatomical site of oral leukoplakia. *Oral Dis* 7(1)*:*25-27.

Schoelch ML, Le QT, Silverman S, Jr., McMillan A, Dekker NP *et al.* (1999). Apoptosis-associated proteins and the development of oral squamous cell carcinoma. *Oral Oncol* 35(1)*:*77-85.

Schwarz S, Bier J, Driemel O, Reichert TE, Hauke S *et al.* (2008). Losses of 3p14 and 9p21 as shown by fluorescence in situ hybridization are early events in tumorigenesis of oral squamous cell carcinoma and already occur in simple keratosis. *Cytometry A* 73(4)*:*305-311.

Seddon SV (1993). An investigation of the clonal organisation of normal and neoplastic oral epithelium using x-linked histochemistry, Cardiff University.

Shah NG, Trivedi TI, Tankshali RA, Goswami JA, Shah JS *et al.* (2007). Molecular alterations in oral carcinogenesis: significant risk predictors in malignant transformation and tumor progression. *The International journal of biological markers* 22(2)*:*132-143.

Shankey TV, Rabinovitch PS, Bagwell B, Bauer KD, Duque RE *et al.* (1993). Guidelines for implementation of clinical DNA cytometry. International Society for Analytical Cytology. *Cytometry* 14(5)*:*472-477.

Shay JW, Wright WE (2011). Role of telomeres and telomerase in cancer. *Seminars in cancer biology* 21(6)*:*349-353.

Shen Z (2011). Genomic instability and cancer: an introduction. *J Mol Cell Biol* 3(1)*:*1-3.

Shin DM, Ro JY, Hong WK, Hittelman WN (1994). Dysregulation of epidermal growth factor receptor expression in premalignant lesions during head and neck tumorigenesis. *Cancer Res* 54(12)*:*3153-3159.

Shinawi M, Cheung SW (2008). The array CGH and its clinical applications. *Drug Discov Today* 13(17-18)*:*760-770.

Siebers TJ, Bergshoeff VE, Otte-Holler I, Kremer B, Speel EJ *et al.* (2013). Chromosome instability predicts the progression of premalignant oral lesions. *Oral Oncol* 49(12)*:*1121-1128.

Silverman S, Bhargava K, Smith LW, Malaowalla AM (1976). Malignant transformation and natural history of oral leukoplakia in 57,518 industrial workers of Gujarat, India. *Cancer* 38(4)*:*1790-1795.

Silverman S, Jr., Gorsky M, Lozada F (1984). Oral leukoplakia and malignant transformation. A follow-up study of 257 patients. *Cancer* 53(3)*:*563-568.

Silverman S, Jr., Gorsky M (1997). Proliferative verrucous leukoplakia: a follow-up study of 54 cases. *Oral Surg Oral Med Oral Pathol Oral Radiol Endod* 84(2)*:*154-157.

Smith J, Rattay T, McConkey C, Helliwell T, Mehanna H (2009). Biomarkers in dysplasia of the oral cavity: a systematic review. *Oral Oncol* 45(8)*:*647-653.

Smith LW, Bhargava K, Mani NJ, Malaowalla AM, Silverman S, Jr. (1975). Oral cancer and precancerous lesions in 57,518 industrial workers of Gujarat, India. *Indian journal of cancer* 12(2)*:*118-123.

Sonnenschein C, Soto AM (2013). The aging of the 2000 and 2011 Hallmarks of Cancer reviews: a critique. *J Biosci* 38(3)*:*651-663.

Speicher MR, Carter NP (2005). The new cytogenetics: blurring the boundaries with molecular biology. *Nat Rev Genet* 6(10)*:*782-792.

Speight PM (2007). Update on oral epithelial dysplasia and progression to cancer. *Head Neck Pathol* 1(1)*:*61-66.

Speight PM, Abram TJ, Floriano PN, James R, Vick J *et al.* (2015). Interobserver agreement in dysplasia grading: toward an enhanced gold standard for clinical pathology trials. *Oral Surg Oral Med Oral Pathol Oral Radiol.*

Sperandio M, Brown AL, Lock C, Morgan PR, Coupland VH *et al.* (2013). Predictive value of dysplasia grading and DNA ploidy in malignant transformation of oral potentially malignant disorders. *Cancer Prev Res (Phila)* 6(8)*:*822-831.

Srinivasan M, Jewell SD (2001). Evaluation of TGF-alpha and EGFR expression in oral leukoplakia and oral submucous fibrosis by quantitative immunohistochemistry. *Oncology* 61(4)*:*284-292.

Stokes A, Drozdov I, Guerra E, Ouzounis CA, Warnakulasuriya S *et al.* (2011). Copy number and loss of heterozygosity detected by SNP array of formalin-fixed tissues using whole-genome amplification. *PLoS One* 6(9)*:*e24503.

Suh YE, Raulf N, Gaken J, Lawler K, Urbano TG *et al.* (2014). MicroRNA-196a promotes an oncogenic effect in head and neck cancer cells by suppressing annexin A1 and enhancing radioresistance. *Int J Cancer.*

Summersgill B, Clark J, Shipley J (2008). Fluorescence and chromogenic in situ hybridization to detect genetic aberrations in formalin-fixed paraffin embedded material, including tissue microarrays. *Nat Protoc* 3(2)*:*220-234.

Sunaga H, Fujieda S, Tsuzuki H, Asamoto K, Fukuda M *et al.* (2001). Expression of granulocyte colony-stimulating factor receptor and platelet-derived endothelial cell growth factor in oral and oropharyngeal precancerous lesions. *Anticancer Res* 21(4B)*:*2901-2906.

Swain N, Kumar SV, Routray S, Pathak J, Patel S (2014). Podoplanin--a novel marker in oral carcinogenesis. *Tumour Biol* 35(9)*:*8407-8413.

Syrjanen S, Lodi G, von Bultzingslowen I, Aliko A, Arduino P *et al.* (2011). Human papillomaviruses in oral carcinoma and oral potentially malignant disorders: a systematic review. *Oral Dis* 17 Suppl 1(58-72.

Tang YC, Amon A (2013). Gene copy-number alterations: a cost-benefit analysis. *Cell* 152(3)*:*394-405.

Tanimoto K, Hayashi S, Tsuchiya E, Tokuchi Y, Kobayashi Y *et al.* (2000). Abnormalities of the FHIT gene in human oral carcinogenesis. *Br J Cancer* 82(4)*:*838-843.

Taoudi Benchekroun M, Saintigny P, Thomas SM, El-Naggar AK, Papadimitrakopoulou V *et al.* (2010). Epidermal growth factor receptor expression and gene copy number in the risk of oral cancer. *Cancer Prev Res (Phila)* 3(7)*:*800-809.

Tibiletti MG (2007). Interphase FISH as a new tool in tumor pathology. *Cytogenet Genome Res* 118(2-4)*:*229-236.

Tomar SL, Winn DM, Swango PA, Giovino GA, Kleinman DV (1997). Oral mucosal smokeless tobacco lesions among adolescents in the United States. *J Dent Res* 76(6)*:*1277-1286.

Torres-Rendon A, Stewart R, Craig GT, Wells M, Speight PM (2009). DNA ploidy analysis by image cytometry helps to identify oral epithelial dysplasias with a high risk of malignant progression. *Oral Oncol* 45(6)*:*468-473.

Toruner GA, Ulger C, Alkan M, Galante AT, Rinaggio J *et al.* (2004). Association between gene expression profile and tumor invasion in oral squamous cell carcinoma. *Cancer Genet Cytogenet* 154(1)*:*27-35.

Tsongalis GJ (2006). Branched DNA technology in molecular diagnostics. *American journal of clinical pathology* 126(3)*:*448-453.

Tsui IF, Rosin MP, Zhang L, Ng RT, Lam WL (2008). Multiple aberrations of chromosome 3p detected in oral premalignant lesions. *Cancer Prev Res (Phila)* 1(6)*:*424-429.

Tsui IF, Poh CF, Garnis C, Rosin MP, Zhang L *et al.* (2009). Multiple pathways in the FGF signaling network are frequently deregulated by gene amplification in oral dysplasias. *Int J Cancer* 125(9)*:*2219-2228.

van der Riet P, Nawroz H, Hruban RH, Corio R, Tokino K *et al.* (1994). Frequent loss of chromosome 9p21-22 early in head and neck cancer progression. *Cancer Res* 54(5)*:*1156-1158.

van der Waal I, Reichart PA (2008). Oral proliferative verrucous leukoplakia revisited. *Oral Oncol* 44(8)*:*719-721.

van der Waal I (2009). Potentially malignant disorders of the oral and oropharyngeal mucosa; terminology, classification and present concepts of management. *Oral Oncol* 45(4-5)*:*317-323.

van der Waal I (2010). Potentially malignant disorders of the oral and oropharyngeal mucosa; present concepts of management. *Oral Oncol* 46(6)*:*423-425.

van Zyl AW, van Heerden MB, Langenegger E, van Heerden WF (2012). Correlation between dysplasia and ploidy status in oral leukoplakia. *Head Neck Pathol* 6(3)*:*322-327.

Vandesompele J, De Preter K, Pattyn F, Poppe B, Van Roy N *et al.* (2002). Accurate normalization of real-time quantitative RT-PCR data by geometric averaging of multiple internal control genes. *Genome biology* 3(7)*:*RESEARCH0034.

Varella-Garcia M, Diebold J, Eberhard DA, Geenen K, Hirschmann A *et al.* (2009). EGFR fluorescence in situ hybridisation assay: guidelines for application to non-small-cell lung cancer. *J Clin Pathol* 62(11)*:*970-977.

Veltman JA, Bot FJ, Huynen FC, Ramaekers FC, Manni JJ *et al.* (2000). Chromosome instability as an indicator of malignant progression in laryngeal mucosa. *J Clin Oncol* 18(8)*:*1644-1651.

Vered M, Allon I, Dayan D (2009). Maspin, p53, p63, and Ki-67 in epithelial lesions of the tongue: from hyperplasia through dysplasia to carcinoma. *J Oral Pathol Med* 38(3)*:*314-320.

Vergeer MR, Doornaert PA, Rietveld DH, Leemans CR, Slotman BJ *et al.* (2009). Intensity-modulated radiotherapy reduces radiation-induced morbidity and improves health-related quality of life: results of a nonrandomized prospective study using a standardized follow-up program. *International journal of radiation oncology, biology, physics* 74(1)*:*1-8.

Vousden KH, Lane DP (2007). p53 in health and disease. *Nature reviews Molecular cell biology* 8(4)*:*275-283.

Waldron CA, Shafer WG (1975). Leukoplakia revisited. A clinicopathologic study 3256 oral leukoplakias. *Cancer* 36(4)*:*1386-1392.

Warnakulasuriya S, Johnson NW, van der Waal I (2007). Nomenclature and classification of potentially malignant disorders of the oral mucosa. *J Oral Pathol Med* 36(10)*:*575-580.

Warnakulasuriya S (2009). Global epidemiology of oral and oropharyngeal cancer. *Oral Oncol* 45(4-5)*:*309-316.

Warnakulasuriya S (2010). Living with oral cancer: epidemiology with particular reference to prevalence and life-style changes that influence survival. *Oral Oncol* 46(6)*:*407-410.

Warnakulasuriya S, Kovacevic T, Madden P, Coupland VH, Sperandio M *et al.* (2011). Factors predicting malignant transformation in oral potentially malignant disorders among patients accrued over a 10-year period in South East England. *J Oral Pathol Med* 40(9)*:*677-683.

Werner M, Wilkens L, Aubele M, Nolte M, Zitzelsberger H *et al.* (1997). Interphase cytogenetics in pathology: principles, methods, and applications of fluorescence in situ hybridization (FISH). *Histochem Cell Biol* 108(4-5)*:*381-390.

Winn DM (2001). Tobacco use and oral disease. *J Dent Educ* 65(4)*:*306-312.

Woo SB, Cashman EC, Lerman MA (2013). Human papillomavirus-associated oral intraepithelial neoplasia. *Modern pathology : an official journal of the United States and Canadian Academy of Pathology, Inc* 26(10)*:*1288-1297.

Wu L, Patten N, Yamashiro CT, Chui B (2002). Extraction and amplification of DNA from formalin-fixed, paraffin-embedded tissues. *Applied immunohistochemistry & molecular morphology : AIMM / official publication of the Society for Applied Immunohistochemistry* 10(3)*:*269-274.

Yang W, Maqsodi B, Ma Y, Bui S, Crawford KL *et al.* (2006). Direct quantification of gene expression in homogenates of formalin-fixed, paraffin-embedded tissues. *BioTechniques* 40(4)*:*481-486.

Zhang L, Cheung KJ, Lam WL, Cheng X, Poh C *et al.* (2001). Increased genetic damage in oral leukoplakia from high risk sites: potential impact on staging and clinical management. *Cancer* 91(11)*:*2148-2155.

Zhang L, Rosin MP (2001). Loss of heterozygosity: a potential tool in management of oral premalignant lesions? *J Oral Pathol Med* 30(9)*:*513-520.

Zhang L, Poh CF, Williams M, Laronde DM, Berean K *et al.* (2012). Loss of heterozygosity (LOH) profiles--validated risk predictors for progression to oral cancer. *Cancer Prev Res (Phila)* 5(9):1081-1089.